Modulating the Immune System by Amino Acid Depletion – IDO and Beyond

Laura Vallius

Merton College

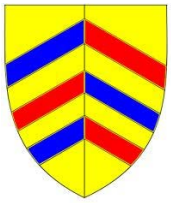

Thesis submitted for the degree of Doctor of Philosophy

Tumour Immunology Programme

Weatherall Institute of Molecular Medicine

Medical Sciences Division

University of Oxford

Trinity Term 2011

Dedicated to my mum who sadly passed away during the completion of this degree.

You were always there for me.

Acknowledgements

First I would like to thank my supervisor Professor Vincenzo Cerundolo for the opportunity and privilege to work in his lab and for his support and understanding throughout the four years it took to complete this degree. It has been a wonderful learning experience for me.

I am also eternally grateful to Jonathan Silk and Uzi Gileadi for all the practical help I have been given during my time in the lab. I have learnt a lot from you guys and would have often been in trouble without your advice. Many thanks also to everyone else in the level 7 lab for all the help and advice I have been given, and of course for the often colourful lunchtime discussions! The days would have been so much greyer without them. Although we seem to live separate lives in different parts of the hospital complex, thank you also to the other half of the Cerundolo lab for help and discussions whenever I have popped by. It was great to be a part of a large lab where there was rarely a shortage of knowledge in any scientific area.

I must also thank our collaborators, particularly Jasmin Mecinovic and Ed Batchelar in Professor Christopher Schofield's lab in the Department of Chemistry, Oxford for their help with the initial inhibitor screening for IDO. I am also grateful to Thomas Bowden in the Structural Biology Group for his help and patience with my lack of computing prowess when we were doing molecular modelling with the IDO inhibitors.

The biggest thanks have to go to Ioannis who has supported me throughout the many difficult moments I have had during this project. There are no words to describe how thankful I am for his belief in me and the loyalty and support he has given me for as long as I have known him. You are the best. I am also forever grateful to my family in Finland, my mum, my dad and my brother for giving me the support and opportunity to get where I am now.

Abstract

Amino acid availability plays an important role in modulating the activity of T-cells. One of the pathways employed by T-cells to sense nutrient levels is the "mammalian target of rapamycin" (mTOR) pathway that is inhibited in response to nutrient depletion. Indoleamine 2,3-dioxygenase (IDO) is the first and rate-limiting enzyme along the tryptophan catabolising kynurenine pathway. T-cells are very sensitive to lack of this essential amino acid in their microenvironment and this confers strong immunomodulatory properties to cells expressing active IDO. It therefore has a significant physiological role as a homeostatic mechanism used in mammalian organisms to dampen excessive activation of the immune system but is also used as an immune evasion mechanism by many cancers.

In this study, we investigated the IDO inhibitory properties and mechanism of action of the tryptophan metabolite 3-hydroxyanthranilic acid (3-HAA) that potentially forms a negative feedback loop in the kynurenine pathway. We studied the molecule in enzymatic assays, in live cells and *in vivo* and discovered that it inhibits IDO in an indirect way via the formation of hydrogen peroxide. Secondly, we looked at the effects of tryptophan and its metabolites on T-cell proliferation and mTOR activity, and discovered a metabolite that inhibits T-cell proliferation. Lastly we examined mechanisms of T-cell suppression employed by myeloid derived suppressor cells (MDSCs), focusing on their ability to deplete amino acids from their microenvironment. We were able to exclude tryptophan consumption as a suppressive mechanism and established that by manipulating extracellular concentrations of several amino acids other than arginine and cysteine – that are known to be utilised by MDSCs - we were able to reduce their inhibitory properties.

In summary, we have described in detail how 3-HAA inhibits IDO in *in vitro* assays, outlined how some tryptophan metabolites can inhibit T-cell proliferation, and clarified aspects of suppressive mechanism employed by MDSCs.

Contents

ACKNOWLEDGEMENTS **2**

ABSTRACT **3**

CHAPTER 1: INTRODUCTION **9**

1.1 MAIN COMPONENTS OF THE IMMUNE SYSTEM 10

1.1.1 Complement *11*
1.1.2 Macrophages *13*
1.1.3 Neutrophils *14*
1.1.4 Natural killer -cells *14*
1.1.5 T and B-cells *15*
1.1.6 Regulatory T-cells *16*
1.1.7 Dendritic cells *18*

1.2 IMMUNITY TO TUMOURS 20

1.2.1 Cancer immunosurveillance and immune evasion *20*
1.2.2 Myeloid derived suppressor cells *27*
1.2.3 Indoleamine 2,3-dioxygenase (IDO) *28*
1.2.4 The mTOR pathway and nutrient deprivation *33*
1.2.5 The GCN2 pathway *39*
1.2.6 Tryptophan transport in IDO-mediated immunosuppression *40*

1.3 AIMS 41

CHAPTER 2: IDO INHIBITOR SCREEN AND PROPERTIES OF 3-HYDROXYANTHRANILIC ACID AS AN IDO INHIBITOR **42**

2.1 INTRODUCTION 43

2.2 MATERIALS AND METHODS 45

2.2.1 Mice and inhibitor screen compounds *45*
2.2.2 Cell culture *45*
2.2.3 Recombinant human IDO in pET21b vector *46*
2.2.4 Cloning of IDO into pET15b vector *46*

2.2.5 Expression and purification of recombinant human IDO *47*
2.2.6 Measurement of IDO activity *48*
2.2.7 Crystallisation of recombinant human IDO in the presence or absence of inhibitors *49*
2.2.8 Induction and measurement of IDO activity in vivo *50*
2.2.9 Measurement of H_2O_2 concentration in a reaction containing 3-HAA *51*
2.2.10 Molecular modelling studies of IDO inhibitors *51*

2.3 RESULTS 52

2.3.1 1-methyl tryptophan (L) inhibits IDO but is a weak substrate in tryptophan-free conditions *52*
2.3.2 Inhibitor screen with recombinant human IDO *53*
2.3.3 IDO enzyme kinetics in the presence of 3-HAA *54*
2.3.4 3-HAA activity in cellular assays *55*
2.3.5 IDO inhibition by 3-HAA possibly mediated by H_2O_2 production *57*
2.3.6 IDO in THP1 cells is inhibited by 3-HAA via radical oxygen species *58*
2.3.7 In vivo activity of 3-HAA *60*
2.3.8 Purification and crystallisation of IDO *62*

2.4 DISCUSSION 64

2.5 FIGURES 68

Figure 1 ..... *68*
Figure 2 ..... *69*
Figure 3 ..... *70*
Figure 4 ..... *71*
Figure 5 ..... *72*
Figure 6 ..... *73*
Figure 7 ..... *74*
Figure 8 ..... *75*
Figure 9 ..... *76*
Figure 10 ..... *77*
Figure 11 ..... *78*
Figure 12 ..... *79*
Figure 13 ..... *80*

CHAPTER 3: EFFECTS OF TRYPTOPHAN METABOLITES ON MTOR IN T-CELLS AND ON T-CELL PROLIFERATION 81

3.1 INTRODUCTION 82

3.2 MATERIALS AND METHODS 83

3.2.1 Mice *83*
3.2.2 Cell culture media *83*
3.2.3 Amplification of kynurenine pathway enzymes from human tumour cell lines by PCR *84*
3.2.4 Western blotting for phospho-S6, phospho-eIF2 and β-tubulin *86*
3.2.5 Splenocyte preparation from whole spleen *86*
3.2.6 Carboxyfluorescein succinimidyl ester (CFSE) -staining for cell proliferation assays *87*
3.2.7 Cell Tracker Orange (CTO) –staining *87*
3.2.8 Cell surface staining protocol *87*
3.2.9 Intracellular/intranuclear staining protocol *88*
3.2.10 T-cell proliferation assays and FACS-based mTOR assays *89*

3.3 RESULTS 90

3.3.1 IDO activity in tumour cells inhibits CD8+ T cell proliferation and additional tryptophan can rescue it *90*
3.3.2 CD8+ T cell proliferation is strongly dependent on available nutrient levels but less so on tryptophan only (FCS Trp titration) *91*
3.3.3 Kynurenine pathway enzyme expression in human tumour cell lines *91*
3.3.4 At optimal nutrient levels, tryptophan metabolites have no significant effect on CD8+ T-cell proliferation *93*
3.3.5 In starvation or moderate starvation conditions 3-HK and 3-HAA mildly inhibit CD8+ T-cell proliferation *93*
3.3.6 Only 3-hydroxykynurenine of all tested kynurenines inhibits CD4+ T-cell proliferation. *94*
3.3.7 3-hydroxykynurenine increases CD25+ Foxp3+ T_{reg} numbers whereas other kynurenines do not affect them *95*
3.3.8 mTOR activity is dependent on tryptophan concentration *95*
3.3.9 Kynurenines enhance eIF2α activity in EG7 cells *97*
3.3.10 Kynurenines do not affect mTOR activity of CD8+ T cells at low stimulation level *98*
3.3.11 3-hydroxykynurenine inhibits mTOR activity at moderate stimulation level after 24h but the effect is lost after strong stimulation *98*

3.4 DISCUSSION 100

3.5 FIGURES 105

Figure 1 ..... *105*
Figure 2 ..... *106*
Figure 3 ..... *107*
Figure 4 ..... *108*
Figure 5 ..... *109*
Figure 6 ..... *110*

Figure 7 ..... *111*
Figure 8 ..... *112*
Figure 9 ..... *113*
Figure 10 ..... *114*
Figure 11 ..... *115*
Figure 12 ..... *116*
Figure 13 ..... *117*

CHAPTER 4: THE IMMUNOREGULATORY ROLE OF MYELOID DERIVED SUPPRESSOR CELLS AND THE EFFECT OF AMINO ACIDS ON THEIR FUNCTION 118

4.1 INTRODUCTION 119

4.2 MATERIALS AND METHODS 121

4.2.1 Mice *121*
4.2.2 Making of bone marrow -derived dendritic cells *121*
4.2.3 Making and purification of myeloid derived suppressor cells *121*
4.2.4 CFSE-staining of splenocytes *122*
4.2.5 Purification of CD8+ T-cells from mixed splenocytes *122*
4.2.6 Arginase activity assay (colorimetric measurement) *123*
4.2.7 Arginase protein expression by western blot *124*
4.2.8 IDO expression in MDSC by western blot *124*
4.2.9 T-cell proliferation assays *125*
4.2.10 Quantitative PCR for IDO and SLC16A4 ..... *125*
4.2.11 Kynurenine pathway expression in MDSC by PCR *126*

4.3 RESULTS 128

4.3.1 Myeloid –derived suppressor cells (MDSCs) can inhibit CD8+ T-cell proliferation in vitro in response to cognate peptide presented either by matured bone marrow –derived dendritic cells (BMDCs) or by splenic antigen presenting cells *128*
4.3.2 Inhibition of CD8+ and CD4+ T-cells by MDSCs is enhanced by additional IFNγ *129*
4.3.3 MDSC –mediated CD8+ T –cell inhibition is proportional to the strength of T-cell stimulation *130*
4.3.4 MDSCs utilise arginase and iNOS as a method to inhibit CD8+ T –cell proliferation by depleting arginine *130*
4.3.5 IDO is expressed functionally by HeLa cells in response to IFNγ and a putative alternative tryptophan transporter SLC16A4 is up-regulated on tryptophan depletion *131*
4.3.6 IDO is up-regulated in MDSCs after IFNγ treatment at the mRNA level but not functionally, and they do not express the alternative Trp transporter *133*

4.3.7 The kynurenine pathway of IFNγ-treated MDSCs is expressed all the way to NAD+ synthesis and they may result in excess 3-hydroxykynurenine production ... *134*
4.3.8 Some essential amino acids can partially rescue CD8+ T -cell proliferation in the presence of MDSCs ... *135*
4.3.9 Arginine, cystine, valine, leucine and phenylalanine do not appear to rescue CD4+ T-cell proliferation in response to anti-CD3 and anti-CD28 in the presence of MDSCs ... *136*
4.3.10 MDSCs inhibit mTOR activity in CD8+ T –cells marginally after 24h but enhance it after 48h in the remaining CD8+ T –cells ... *137*

4.4 DISCUSSION ... 139

4.5 FIGURES ... 145

Figure 1 ... *145*
Figure 2 ... *146*
Figure 3 ... *147*
Figure 4 ... *148*
Figure 5 ... *149*
Figure 6 ... *150*
Figure 7 ... *151*
Figure 8 ... *152*
Figure 9 ... *153*
Figure 10 ... *154*

CHAPTER 5: CONCLUDING REMARKS AND FUTURE DIRECTIONS ... **155**

APPENDICES ... **159**

BIBLIOGRAPHY ... **160**

Chapter 1: Introduction

1.1 Main components of the immune system

The human immune system can be broadly thought of as consisting of two divisions, innate and adaptive. The innate immune system is the 'first line of defense' against invading pathogens.[1] In addition to mechanical, chemical, and microbiological barriers such as tight junctions between epithelial cells, antibacterial peptides and the normal microbial flora on the skin and gut, respectively, innate immunity employs the complement system, professional phagocytes and natural killer cells that can directly destroy pathogens.

These components are able to distinguish microbial non-self organisms from non-pathogenic commensal flora and self molecules via the recognition of Pathogen Associated Molecular Patterns (PAMPs) such as conserved polysaccharides and polynucleotides specific to certain pathogens.[2,3,4] The recognition molecules for these patterns can be cell-associated or soluble molecules (called Pattern Recognition Receptors, PRRs). Soluble molecules include the mannose-binding lectin (MBL) that can activate the lectin pathway of the complement system and ficolins that recognise patterns of acetyl groups and may be involved in disposal of altered cells and the initiation of inflammatory responses.[2] Cell-bound receptors include scavenger and Toll-like receptors (TLR). Scavenger receptors consist of a structurally diverse group of PRRs that recognise low density lipoprotein lipopolysaccharide (LPS) and lipotechoic acid of Gram-negative and Gram-positive bacteria and one such receptor, the macrophage-associated SR-A1 I/II, has been shown to directly bind *S. aureus* and *E. coli.*[5] TLRs were the first PRRs that were identified and they are either membrane bound or associated with intracellular vesicles.[6] There are ten identified TLR types in human each of which detects a distinct PAMP from viruses, bacteria, mycobacteria, parasites and fungi. TLR1, TLR2 and TLR6 recognise lipoproteins, TLR3 double-stranded RNA, TLR4 LPS, TLR5 flagellin, TLR7 and TLR8 single-stranded RNA and TLR9 DNA.[6] TLR11 recognises the *Toxoplasma gondii* profilin-like molecule. TLRs recruit adaptor molecules which results in the initiation of a downstream signalling cascade that can lead to activation of macrophages and recruitment of neutrophils and thus to

direct killing of pathogens.[6] TLRs are also links to the adaptive immune system as their stimulation leads to maturation of dendritic cells (DC), which can then induce the adaptive system.

1.1.1 Complement

The complement system is a mixture of the two PRR types as it consists of a large number of different membrane-bound and soluble plasma proteins that both opsonise pathogens leading to their removal by other immune cells, and induce inflammatory responses.[7] There are three main activation pathways: "classical", lectin and "alternative" (Figure 1). As mentioned earlier the lectin pathway is activated on binding of MBL or one of the ficolins to acetylated residues or specific carbohydrate surfaces. The classical pathway is activated upon binding of the soluble PRR C1q to either IgG or IgM that are bound to antigen. The alternative pathway is induced when C3, a central part of the complement is either auto-activated on a microbial surface or by different proteases such as thrombin or kallikrein.[7,8] Each pathway culminates in the formation of convertases that create the opsonin C3b and the anaphylatoxin C3a from C3.[7] C3b is attached to C4bC2a or C3bBb and can then cleave C5 to create another anaphylatoxin C5a and C5b, a keystone molecule that drives the formation of the membrane attack complex which when fully formed perforates the cell membrane. C3a and C5a can recruit immune cells of both the innate and adaptive systems to the activation site.[7] It is therefore a vital system that both sides of the immune system utilise to effectively monitor and protect the extracellular space.

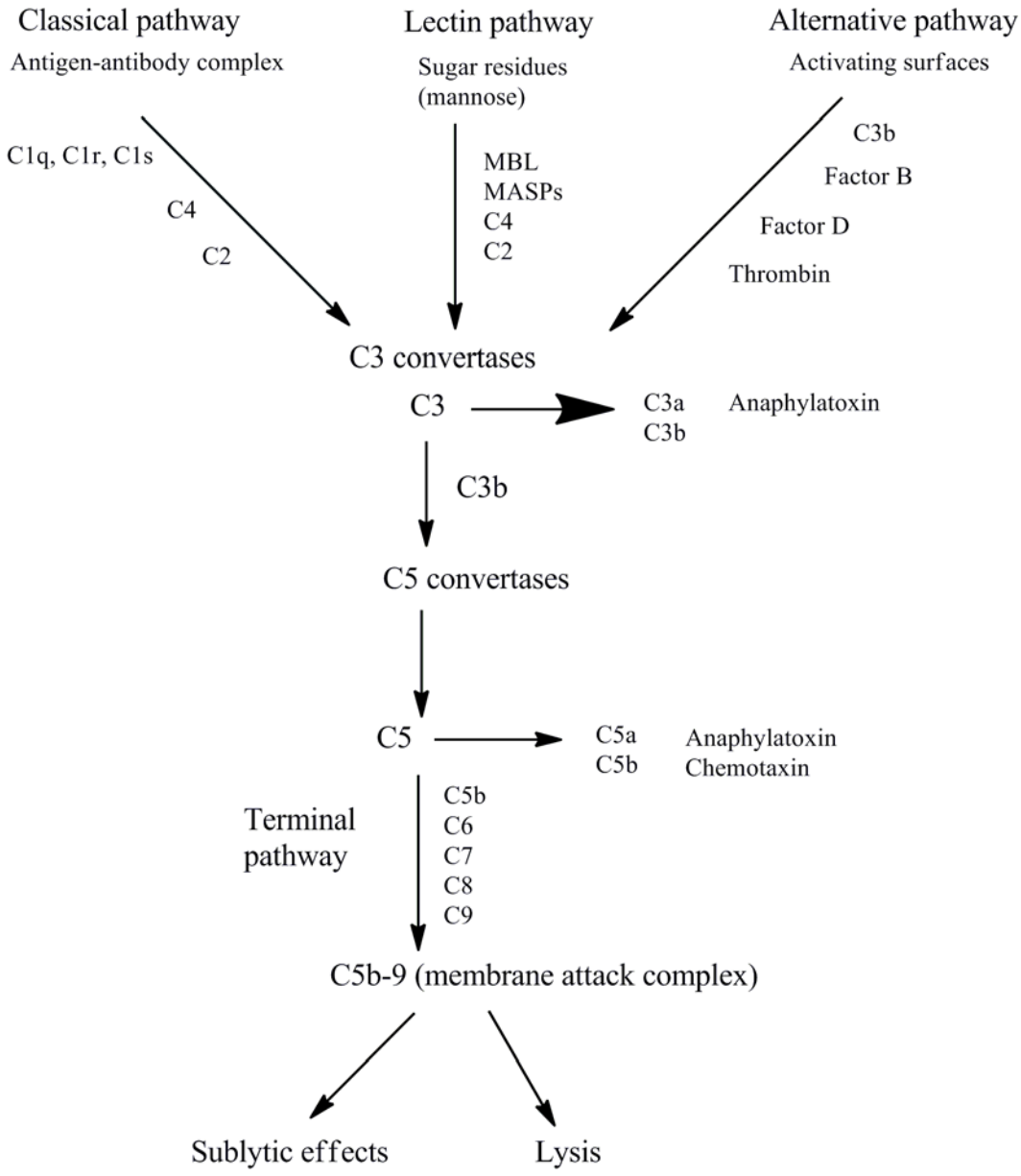

Figure 1. A simplified diagram of the complement system pathways. Adapted from Cook, HT and Botto, M. (2006) *Nature Clinical Practice Rheumatology*, **2**, 330-337.

1.1.2 Macrophages

Phagocytic macrophages continuously develop from monocytes by leaving the circulation and migrating into tissues where they exist mainly in one of three states.[1] When the tissue is not under threat the cells are slowly proliferating and collecting dead cell debris. On response to the cytokine IFNγ, they convert into a primed, activated, state and become antigen presenting cells by up-regulating MHC class II. When macrophages bind to mannose or LPS, both common cell wall components of many bacteria, they become hyperactivated and can start directly killing other cells by secreting the cytokine tumour necrosis factor (TNF). Macrophages are, however, a heterogeneous cell population and their microenvironment and the type of monocyte the macrophage was prior to maturation, may affect the specific functional properties of the macrophage.[9,10,11] Mature macrophages are broadly classified into M1 and M2 macrophages. M1 macrophages are microbicidal and inflammatory post-infection, and are induced by LPS and other microbial products. They express TLR2 and TLR4, which recognize bacterial lipoproteins and LPS, respectively.[12] They also express the arginine depleting enzyme iNOS that produces reactive oxygen and nitrogen species (ROS, RNS), thus enabling the macrophage to directly kill pathogens. M2 macrophages are weakly microbicidal and more anti-inflammatory due to e.g. their production of the anti-inflammatory cytokine IL-10 and glucocorticoid hormones.[12] They also express arginase that produces urea rather than ROS or RNS. This differentiation is not, however, terminal, and the macrophages can change 'type' according to what is required in their local microenvironment. [13] Although macrophages are generally able to kill tumour cells when appropriately stimulated, there is a group of tumour-associated macrophages (TAMs or M2) that have been shown to have no cytotoxic activity and, in fact, have actively pro-tumour properties.[14,15,16,17] They are therefore an important group of cells that can contribute to tumour evasion.

1.1.3 Neutrophils

Another type of phagocyte, the neutrophil, expresses a vast array of PRRs, including all TLRs except TLR3, FPR1 that recognises formylated proteins found in bacteria and mitochondria, C-type lectin, sensors of ribonucleic acid in the cytoplasm (RIG-I and MDA5), ficolins, and PTX3 that activates the classical complement pathway.[18] Sensing via these PRRs together with signals from lymphoid cells activate the neutrophils to produce reactive oxygen species, lytic enzymes, antimicrobial peptides and cytokines such as IL-6, IFNγ and IL-17A leading to a pro-inflammatory response.[18] Neutrophils are not only important as reservoirs for PRRs but important in harnessing DCs by inducing maturation of monocyte-derived dendritic cells via DC-SIGN in vitro, although the neutrophil-DC crosstalk does not always lead to DC activation.[18] Via this cross-talk, neutrophils can therefore have an effect on the adaptive immune system as mature DCs can induce T-cell proliferation and polarisation to the cytotoxic T helper cell type (T_h1).[19] Neutrophils are also important modulators of natural killer -cell (NK) activation status as they can enhance the NK-cell IFNγ production, and regulate their proliferation and cell survival. In return, NK-cells produce soluble factors such as granulocyte macrophage colony-stimulating factor (GM-CSF) and IFNγ that promote neutrophil survival.[18] Neutrophils can also have, while normally an anti-tumour, a pro-tumour phenotype N2 driven by transforming growth factor-β (TGF-β) in the tumour microenvironment.[20]

1.1.4 Natural killer -cells

Natural killer (NK) -cells are bone marrow –derived granular lymphocytes that detect infection via a limited number of germline-encoded PRRs, which, when engaged, allow NK-cells to directly kill infected cells and produce proinflammatory cytokines and mediators.[21] NK-cells destroy infected cells by a directed release of lytic granules that contain perforin, granzymes and Fas -ligand (which induces apoptosis when bound to its receptor).[22] The killing ability of NK-cells can be either activated or inhibited

depending on which receptors are occupied. Activating receptors include CD16, 2B4, NKG2D and LFA-1, and their engagement promotes target cell adhesion. Cell adhesion can be abrogated for instance via the co-binding of NKG2A by its ligand HLA-E present on the target cell.[22] NK-cells can be considered to be at the interface of the innate and adaptive immune systems. Although they are traditionally classified as cells of the innate system due to their ability for rapid response against infected cells without prior sensitisation, new evidence suggests that they share many characteristics with lymphocytes of the adaptive immune system such as CD8+ cells, which are considered later (reviewed in [23]).

NK-cells are members of the lymphocyte lineage but lack a unique antigen recognition receptor and cannot rearrange their receptor genes like B and T- cells.[23] Recent evidence suggests, however, that NK-cells can be 'educated' against self-reactivity by contact between the major histocompatibility complex (MHC) class I and its receptor on NK-cells.[24] NK-cells have also been shown to have memory in hypersensitivity experiments where the mice lacked B and T-cells, although the specific receptor that recognised the antigen has not been identified.[25] Similar memory has been shown with response against cytomegalovirus in an adoptive transfer experiment.[26] NK-cells are an important anti-tumour cell type since they are able to kill cells directly, but they also have an indirect tumour-promoting role whereby the IFNγ they secrete drives the tumour cells via IL-1β and TNFα to produce CCL22, a chemokine that attracts immunosuppressive regulatory T- cells (T_{regs}).[27]

1.1.5 T and B-cells

The adaptive immune system is characterised by its ability to recognise and remember specific pathogens and to differentiate between self and non-self molecules during antigen presentation. Its main components are B and T-lymphocytes. Both are derived from multipotent haematopoietic stem cells in the bone marrow and, unless activated, look morphologically similar. B-cells are involved in the humoral immune response, i.e. they produce antibodies whereas T-cells are involved in cell-mediated immunity and

complete their maturation in the thymus. T-cells as a group recognise antigens presented to them via the T-cell receptor (TCR). TCRs (and B-cell receptors) have a highly diverse pool of configurations allowing them to distinguish and bind a wide range of antigens. This is achieved during thymocyte development by the rearrangement of the variable, diversity and joining genes of the TCR in a process called V(D)J recombination.[28]

T-cells are classified broadly as CD8+ (cytotoxic) or CD4+ (helper) T-cells based on expression of the respective co-receptor. In recent years there has been a rapid expansion in the amount of research describing further functional and phenotypic subdivisions, not all of which have gained universal acceptance as there is increasing evidence that there is a certain amount of overlap and plasticity. Nevertheless, commonly accepted subgroups include naïve, memory, effector and regulatory T-cells with numerous more or less well-defined subcategories.

In addition to these main groups natural killer T-cells (NKT) and γδ T-cells have been characterised and found to have specific roles in the immune system. NKTs appear to be involved in lipid recognition and γδ T-cells appear to recognise non-protein phosphoantigens.[29,30]

1.1.6 Regulatory T-cells

The regulatory T-cell subgroup of T-cells (T_{regs}) has an essential role in the maintenance of self-tolerance and the development of cancer. They are characterised by the expression of the transcription factor forkhead box P3 (FOXP3) gene, an indispensable marker, which, if mutated, results in fatal autoimmune disease and immunopathology.[31] Most of FOXP3+ T_{reg} cells are also CD4+ and CD25+ and their regular function is to suppress the activation, proliferation and effector functions of, among other things, CD4+, CD8+ T-cells, and NK and B-cells but due to this function they also inhibit antitumour immune responses and therefore favour tumour progression.[32] Therefore a

decreased ratio of CD8+ T-cells to FOXP3+CD25+CD4+ T_{regs} can correlate with poor prognosis for cancer patients.[33]

T_{regs} can be either natural or induced, the former of which are cells made in the thymus and are suppressive when they leave the organ. Induced T_{regs} are produced from naive CD4+ T-cells when the right signals are present. These include TGB-β and retinoic acid.[34] The role and real *in vivo* suppressive function of induced T_{regs} is still under investigation as they show little suppressive function in humans after differentiation with TGF-β and TCR stimulation, indicating that other stimuli may be needed for induction of suppressive function or the cells do not have a significant role *in vivo*.[35,36] However, a few studies have shown that human T_{reg} need to be activated through their TCR to exert functional suppressive activity in vitro.[37,38,39,40,41]

Surprisingly human T_{regs} do not have to be viable to be suppressive as paraformaldehyde-fixed cells as well as apoptotic T_{regs} are still inhibitory.[42] What does matter to the extent of T_{reg} -mediated suppression is the strength of T-cell stimulation. When effector T-cells receive strong co-stimulation, the T_{regs} lose their efficacy as suppressors but in the presence of low stimulation their suppressive activity is restored.[37,42] Both mouse and human T_{regs} express FOXP3 (humans express two isoforms) and various other markers depending on their differentiation status and current function (naive, effector or terminal effector T_{reg}), including CD45RA, CD95, CTLA4, CD69, CC-chemokine receptor 4 (CCR4), CCR6, CCR9 and IL-1R.[32]

In mice many suppressive mechanisms employed by T_{regs} have been elucidated. They can suppress by both a contact-dependent and a cytokine-mediated mechanism. The former includes CTLA4 on T_{reg} downregulating the co-stimulatory function of APCs, CD73-CD39 hydrolysing inflammatory extracellular ATP, LAG3 inducing inhibitory signalling via MHC class II molecules, granzyme A (human) and B (mouse) lysing conventional T-cells, and CD95-CD95 ligand inducing lysis of conventional T-cells.[32] The cytokine-mediated suppression takes place via secretion of TGF-β and LAP, which induce FOXP3 expression in conventional T-cells, IL-10 which attenuates DC function and converts conventional T-cells into T_R1 cells, galectin 1 that causes cell cycle arrest

and apoptosis of conventional T-cells, and CD25 that enhances adsorption of IL-2 by the T_{reg}.[32]

Research efforts have focused on finding cell surface markers that are specific for T_{regs} and which could be targeted for T_{reg} depletion in the treatment of cancer. So far anti-CD25 depleting antibodies, anti-CTLA4 blocking antibodies, and agonistic anti-OX40 and anti-GITR antibodies have enhanced tumour-specific immunity in mice.[32] In humans a CTLA4-specific monoclonal antibody is in clinical trials to treat advanced cancer, however, a combination of these antibodies is more likely to give preferential results than a single antibody type since these molecules are also expressed on the cell surface of activated T-cells. These combinations can then be modified according to the requirements of the illness, i.e. whether more suppression or more enhancement of T-cell activity is needed.

1.1.7 Dendritic cells

Dendritic cells (DCs) are professional antigen-presenting cells (APCs) and are critical in the priming phase of the immune response, bridging the innate and adaptive immune systems. They are traditionally classified as either conventional DCs (derived from common DC progenitors) or non-conventional DCs (plasmacytoid and monocyte-derived).[43] DCs are distributed across various organs and have multiple subtypes. The main types of DC include the Langerhans cells (skin), CD103+ dermal DC, and CD11b+ classic dermal DCs which are of the migratory type but can be found in lymph nodes at steady state.[44] There are also splenic DCs that can also be found in lymph nodes; these include CD4- CD8- DCs, CD4+ DCs, CD8+ DCs and plasmacytoid DCs. In addition there are DCs that are rapidly generated from monocytes during inflammation.[44] There are many more markers on different subtypes of DCs but they fall outside the scope this introduction.

Immature DCs are characterised by high endocytic and phagocytic activity as they sample the environment using TLRs and PRRs on their surface, making them an integral part of the innate immune system. However, once TLR signalling has started, the DCs mature and migrate to lymph nodes where they activate the adaptive immune system by functioning as antigen presenting cells.[45] At the same time they express the co-stimulatory molecules CD40, CD80 and CD86, the first binding to CD40L on T-helper cells, and the latter two to CD28 on the responding lymphocytes. This co-stimulation is required for successful activation of lymphocytes during antigen presentation.[46]

DCs present antigens via two molecules; the major histocompatibility complex I (MHC class I) and MHC class II. MHC class I presents peptides derived from the cytosol - this process is also called the endogenous antigen-presenting pathway. These molecules are found on every nucleated cell of the body but only certain cells present antigens "professionally". MHC class I presentation leads to the activation of cytotoxic CD8+ T-cells. MHC class II molecules are found on APCs such as DCs, macrophages and B-cells. The MHC class II molecule associates with protein fragments of extracellular origin that have been endocytosed, digested in the lysosome and loaded on the class II molecule then transported to the cell surface. Class II presentation activates naive CD4+ T-cells into T-helper cells.[47] Activated DCs, under certain circumstances produce IL-12 that drives naïve T-helper cells to develop into the T_H1 subtype that secretes IFNγ and TNF-β. These cytokines promote cytotoxic activities by CD8+ T-cells and macrophages. Under different conditions DCs can alternatively secrete IL-4 that promotes differentiation of T-helper cells into the T_H2 subtype; these in turn secrete more IL-4 and IL-5, IL-13 and IL-10 driving B-cell proliferation and antibody production.[48]

1.2 Immunity to tumours

1.2.1 Cancer immunosurveillance and immune evasion

Having established the main components of the immune system, the focus will now be on how tumour cells escape the detection by these various components. The idea that the immune system controls the growth of tumour cells via a process later described as "immunosurveillance" was first coined by Paul Erlich at the beginning of the 20th century when he hypothesised that without the immune system, carcinomas would appear with high frequency.[49] This idea was slowly gaining traction until it was challenged in the 1970's when studies by Stutman *et al*. demonstrated that athymic mice had the same amount of tumours as immunocompetent mice.[50] This discovery did not take into account the fact that the innate immune system could also play a part in the surveillance. As more anti-tumour lymphocyte types such as NKT-cells and γδ T-cells were discovered and further evidence of the importance of molecules such as IFNγ and perforin in tumour development was found, the idea of surveillance was revived.[51] An important tool in the tumour surveillance studies has been identification of recombinase activating gene RAG-2. The gene has enabled studies with mice that lack the gene and cannot rearrange their antigen receptors, which leads to a failure to form functional T-cells, B-cells, NKT-cells and γδ T-cells.[52] These mice developed tumours faster than mice with an intact immune system. IFNγ has also been shown to be crucial for anti-tumour effects.[53]

The immune system has various mechanisms to recognise tumour cells. It can detect mutated or inappropriately expressed tumour antigens presented on MHC class I molecules to CD8+ T-cells either by the tumour cell itself or by APCs. If an APC presents the antigen, the act is called 'cross-priming'. This is thought to enhance the immune response against the tumour. Examples of tumour antigens that have arisen from the differentiation of the tumour include Melan-A, gp-100 and tyrosinase.[54,55] Antigens that are products of a mutation include abnormal p53, over-expressed antigens include HER-2/neu, and viral antigens such as human papilloma virus antigens and cancer-

testis antigen NY-ESO-1 can all be presented on MHC class I by APCs resulting in CD8+ T-cell activation.[54,56,57]

Another mechanism by which the immune system becomes aware of the tumour is the presence of danger signals such as uric acid, which is released from dying cells and this has been shown to enhance cytotoxic T-cell priming when presented by a mature DCs.[58] Other signals include the MHC class I chain-related proteins A and B (MICA/B) that are normally only expressed in the gut epithelium but are highly expressed in many primary carcinomas such as lung, kidney and colon and they stimulate killing activity in CD8+ T-cells and activated NK cells. [59,60]

Tumour escape mechanisms

Despite the control mechanisms, tumours can and do escape detection and/or destruction by the immune system. Cancer development is a multifactorial process; through accumulation of genetic and epigenetic changes cells assume a phenotype that allows them to bypass normal growth controls. Although neoplastic cells are antigenic, they are often only weakly immunogenic resulting in a lack of capacity to mount a sufficiently pro-inflammatory environment to allow full T-cell activation. Although other APCs such as B-cells, monocytes and macrophages express tumour associated antigens (TAAs) through exogenous and endogenous pathways, it is dendritic cells that are mainly responsible for the initiation of an immune response and therefore crucial in the development of an immunosuppressive tumour microenvironment. Their role is to prime the effector functions in antigen-specific T-cells but they may fail to do so for various reasons. In order to activate an effector T-cell, the cell requires presentation of both the TAA on an MHC molecule by the DC, and engagement of a co-stimulatory molecule CD80 and CD86 (both of the B7 family of ligands) in the presence of pro-inflammatory cytokines such as IL-12.[61] This environment is not always present around tumours but instead consists of immature DCs in the presence of more tolerogenic mediators. These DCs are incapable of providing a full activation signal to the effector T-cell making them susceptible to anergy, turning into T_{regs} or staying naive.[62,63] CD8+ T-

cells can also become tolerogenic in a conducive environment and ignore or become tolerant of TAAs.[64,65] CD8+ T-cells can also exhibit split anergy whereby if they don't receive a co-stimulatory signal, the T-cells cannot produce IL-2 even though they are still cytotoxic.[66] This results in inefficient effector function. Therefore some aspects of CD8+ T-cell effector functions can be impaired with incomplete priming while they can still have partial effector functionality. So, how does a cancer cell create a microenvironment that is so favourable to tolerance and leads to the inefficient priming of effector T-cells? The main mechanisms can be broadly divided into two categories: tumour cell contact-dependent mechanisms and tumour cell contact-independent mechanisms.

Cell contact-dependent mechanisms

There are three main methods that tumours employ to achieve their escape through contact-dependent means. They can down-regulate or lose cell-surface molecules that are critical for adhesion or immune recognition and activation. They can also adversely affect receptor ligand interactions by expressing surface molecules that result in inhibition of T-cell activation. Alternatively the tumour cells may acquire genetic or epigenetic modifications that enhance the cells' resistance to apoptosis.

A common tactic by cancer cells is to interfere with the TAA presentation via the MHC complex. They achieve this by mutating the assembly pathway of the MHC complex leading to misprocessing or mispresentation of the TAAs.[67] This results in the formation of incomplete MHC complexes due to e.g. mutation and down-regulation of parts of its components such as the transporter associated with antigen processing (TAP1 and TAP2) proteins and the immunoproteasome. The tumour cells also either do not express or down-regulate the expression of the co-stimulatory molecules CD80 and CD86 making them very poor APCs.[68,69] T-cell signalling can also be affected by the decreased expression of the TCR components such as the CD3ζ-chain and tyrosine kinases $p56^{lck}$ and $p59^{fyn}$.[70] Although the mechanisms used by tumour cells to achieve

this are not yet fully understood, there is evidence that at least depletion of the amino acids arginine and tryptophan by the tumour cells can induce the effect.[71,72]

A method that tumour cells also employ to inhibit T-cell activation is the use of CTLA-4, a natural component of a cell whose function, when engaged by CD86 (B7-2), is to inhibit lymphocyte proliferation and activation. Several studies have found that if CTLA-4 is blocked it can lead to enhanced tumour rejection *in vivo*.[73,74,75] Tumour cells can also directly regulate the cytokine production and proliferation of T-cells by expressing the ligands for programmed death receptor-1 (PD-1), which itself is expressed on many immune cells, notably on mature T and B-cells and thymocytes.[76,77] PD-ligand 1 (PD-L1, aka B7-H1) particularly is strongly expressed on many tumours and is a crucial escape mechanism for a tumour type that is normally highly immunogenic but still manages to form lethal tumour masses.[78] PD-L1 is normally expressed in both nonlymphoid organs such as the lung, heart and placenta in humans and mice but also in human monocytes, dendritic cells and keratinocytes to balance T-cell activation and suboptimal priming by CD28-mediated costimulation.[79] Both PD-L1 and its homolog PD-L2 when bound to PD-1 inhibit T-cell proliferation by blocking cell cycle progression at G_0/G_1 in activated T-cells but they do not increase cell death.[79] Both are induced by IFNγ, presumably to control the resulting pro-inflammatory environment in response to the cytokine. However, it appears that the expression level of PD-1 in activated T-cells is strongest when the TCR signal is weak, possibly to avoid the proliferation of suboptimally activated T-cells.[79] Therefore tumours that only weakly activate T-cells and express PD-L1 and PD-L2 are in a strong position to dampen even a weak response to them.

Another member of the B7 family, B7-H4 (aka VTCN1) has also been described as having a similar effect on T-cell proliferation as PD-L1.[80] It is expressed in myeloid and lymphoid cells and its engagement results in cell cycle arrest and inhibition of cytokine production, particularly IL-2, and inhibition of the development of cytotoxicity in T-cells.[80] Its receptor is not yet known but there is evidence that it blocks T-cell proliferation by interfering with activation of ERK, JNK and AKT signalling.[81] B7-H4 is expressed by many tumour types including ovarian, renal and breast carcinomas and is

blockade can enhance tumour regression indicating that the tumours derive a benefit by expressing it.[82,83]

Apoptosis is another mechanism tumours exploit to escape destruction by the immune system. Following findings of lower numbers of circulating CD8+ T-cells in some patients, tumour cells were identified as able to induce apoptosis of T-cells in certain cancers.[84,85] It has been suggested that they do this by expressing Fas ligand (FasL) that on engagement with Fas on the T-cell surface initiates programmed cell death in the T-cell.[85] Tumours can also release soluble FasL in microvesicles in the tumour microenvironment or in the circulation thus avoiding contact with T-cells and helping to create an "immunoprivileged" site for the tumour.[86]

While causing apoptosis to T-cells, tumour cells are often resistant to it themselves. The resistance pathways can be broadly defined as either intrinsic (or mitochondrial) or extrinsic (or death receptor) to the induction of apoptosis. The intrinsic pathway begins within the cell as a reaction to stimuli such as hypoxia, irreparable DNA damage, high oxidative stress and extremely high cytosolic Ca^{2+} concentration.[87] Each of these stimuli increases the permeability of the mitochondria resulting in the release of pro-apoptotic molecules such as cytochrome-c into the cytoplasm.[88] The pathway is regulated by proteins of the Bcl-2 (derived from B-cell lymphoma 2) family that is divided into pro-apoptotic (e.g. Bax, Bak, Bcl-Xs) and anti-apoptotic (e.g. Bcl-2, Bcl-X_L, Bcl-W) proteins. It is the balance of these proteins that determines whether apoptosis is initiated or not. Ultimately the release of cytochrome-c leads to the induction of caspase 3 via the complex of apoptosome.[87] In cancer these proteins can be unbalanced whereby pro-apoptotic proteins are underexpressed and anti-apoptotic proteins are over-expressed. This was evident in studies by Raffo *et al*. and Fulda *et al*. who found that overexpression of Bcl-2 increased the survival of prostate cancer by protecting the cells from apoptosis and that it lead to the inhibition of TRAIL-induced apoptosis in neuroblastoma, glioblastoma and mammary carcinoma cells.[89,90] In colorectal cancers the bax gene has undergone frameshift mutations leading to impaired apoptosis whereas in chronic lymphocytic leukaemia the malignant cells have high levels of the anti-apoptotic Bcl-2 and low levels of Bax.[91,92] The p53 tumour protein is another well

known suppressor of tumours but also a cause for unregulated growth when it is mutated. It is involved in the induction of apoptosis, cell cycle regulation, development, differentiation, DNA recombination and chromosomal segregation, making it a critical protein in many areas of a cell's life. It is therefore not surprising that defects in it have been found in more than 50% of human cancers.[87]

In the case of increased resistance to extrinsic cell death, a crucial receptor is the Fas. It can be either down-regulated itself or there might be defects downstream in caspase activation or overexpression of anti-apoptotic proteins such as FLICE-inhibitory protein (FLIP).[93,94,95] There are also inhibitors of apoptosis proteins (IAPs) that regulate apoptosis, cytokinesis and signal transduction. They are endogenous inhibitors of caspases by binding into their active site which promotes the enzyme's degradation or prevents it from binding its substrates.[96] Dysregulated IAPs have been found in many human cancers such as pancreatic cancer, melanoma and lymphoma and the abnormal expression of these proteins correlated with the malignant cells' resistance to chemotherapy, particularly in pancreatic cancer.[97,98,99]

Fas downregulation remains as one of the most important mechanisms in tumour progression. It has been found in many human malignancies[95,100,101] and for a host immune system that relies on Fas-mediated cytotoxicity, the emergence of a Fas-resistant (Fas^{lo}) tumour variant can prove even more lethal. These variants have been shown to exhibit enhanced tumour growth and higher resistance to CTL-based immunotherapy in a mouse lung cancer model.[102,103] Studies have also shown that the development of these variants can be due to selective pressure from the host system which, through the elimination of Fas^{hi} populations, allows the more aggressive Fas^{lo} variants to escape.[102] As these cells are also more refractory to CTL-based immunotherapy, they are an important target to study for better therapies.

Cell contact-independent mechanisms

These mechanisms can be broadly divided into tumour-derived factors (TDFs) and immunosuppressive subsets of cells that contribute to tumour escape. TDFs can have

pro-apoptotic or immune suppressive properties. These include transforming growth factor-β (TGF-β), vascular endothelial factor (VEGF), IL-10, prostaglandin PGE_2, reactive oxygen species (ROS) and indoleamine 2,3-dioxygenase (IDO). Many of these, such as IL-10 and TGF-β, can act on lymphocytes directly but several (e.g. VEGF, PGE_2, GM-CSF) have indirect effect through APCs such as DCs and macrophages making the lymphocytes tolerogenic or non-stimulatory. Malignant cells are able to produce these factors by having constitutive STAT3 activity, which results in a reduced pro-inflammatory microenvironment around the tumour hampering proper DC maturation.[104] The TDFs are also able to induce endogenous STAT3 activity in DCs, therefore impairing both innate and adaptive immunity against the tumour.[105] It is not only lymphocytes and DCs that are adversely affected by TDFs, but their actions can create pro-tumour cell populations such as stromal fibroblasts and tumour-associated macrophages (TAMs).[15] These cells can then enable tumour vascularisation by producing angiogenic factors such as VEGF. TAMs are often recruited by the TDF colony-stimulating factor-1 (CSF-1) and PGE_2 produced by the tumour stroma. TGF-β is a crucial TDF for tumour progression. Its actions abrogate T-cell differentiation, proliferation and effector function via the loss of IL-12 production and lytic activity.[106] Stromal cells that have been exposed to TGF-β can produce IL-4 and IL-10 skewing the immune response towards type 2 response (humoral-mediated immunity), which hampers effective cytotoxic activity against the tumour.[107] TGF-β affects DCs directly by downregulating the expression levels of MHC class I and II molecules on the APC.[108] Many TDFs not only promote tumour progression by affecting the surrounding cells but they also enhance the tumour cells' own survival. TGF-β, PGE_2 and VEGF can up-regulate additional angiogenic activators such as matrix metalloproteinase-2 and anti-apoptotic genes such as c-FLIP and Bcl-x_L, which are key factors enabling tumour escape and progression.[109,110,111]

These potent TDFs can induce immunosuppressive subsets within lymphoid and myeloid cells. Well known immunosuppressive cell populations include T_{regs}, myeloid-derived suppressor cells (MDSCs), IDO+ DC subsets and macrophages, and CD1-restricted NKT-cells, the last of which downregulate host immune responses via the production of IL-13 and recruitment of MDSCs.[112,113]

For the purposes of this project we focused on two tumour immune evasion mechanisms that appear to involve depletion of amino acids from the environment: the recruitment of myeloid derived suppressor cells and the expression of the enzyme indoleamine 2,3-dioxygenase.

1.2.2 Myeloid derived suppressor cells

Myeloid derived suppressor cells (MDSCs) are a heterogeneous group of immature myeloid cells. These are progenitor cells that in a healthy individual would quickly differentiate into DCs, macrophages and mature granulocytes, but under pathological conditions do not undergo full differentiation. They have an important immunoregulatory role in both innate and adaptive immunity, and as they are often implicated in tumour evasion[114] are further described here. It has been suggested that MDSCs play an important role in the non-pathological setting by preventing the immune system from excessive activation and resulting tissue damage.[115,116] They also accumulate in bacterial and parasitic infections, inflammation, trauma and autoimmunity but one of their most notable adverse effects is the inhibition of immunosurveillance that can contribute to tumour progression.[114]

Cell surface markers of human and mouse MDSCs differ from each other and for the purposes of this thesis, the mouse MDSCs are further explained. Mouse MDSCs can be divided into two subsets according to which epitope the Gr1 marker on MDSCs binds, and their mechanism for T-cell suppression is different from one another. $CD11b^{+}$ $LY6G^{+}LY6C^{low}$ MDSCs have a granulocytic morphology whereas $CD11b^{+}LY6G^{-}LY6C^{hi}$ have a more monocytic appearance.[117,118,119] Monocytic MDSCs also have the ability to mature into DCs and macrophages *in vitro*. MDSC expansion can be induced by cyclooxygenase 2, prostaglandins, stem-cell factor (SCF), IL-6 and GM-CSF.[118,120] These factors trigger signalling pathways that lead to the transcription factor STAT3 (signal transducer and activator of transcription 3), which is the main transcription factor regulating the expansion of MDSCs. In addition to the factors regulating expansion, the MDSCs have to be activated in order to be suppressive. IFNγ, TLR ligands, IL-4, IL-13

and IL-1β can all trigger signalling pathways that lead to the upregulation of arginase 1, inducible nitric oxide synthase (iNOS), the suppressive cytokine TGFβ, and enhanced reactive oxygen species production, all major mechanisms of MDSC-mediated T-cell suppression.[118]

Arginine depletion has historically been considered as one of the main mechanisms that MDSCs utilise for their suppressive activity. Two enzymes that use arginine as a substrate have been shown to be expressed in MDSCs: Arginase 1 - leading to the production of urea and L-ornithine - and inducible Nitric Oxide Synthase (iNOS). The resulting depletion of arginine leads to the down-regulation of the T-cell CD3 ζ-chain and prevention of the up-regulation of cell cycle regulator cyclin D3 and cyclin-dependent kinase 4.[121,122] Nitric oxide induces the inhibition of JAK3/STAT5 signalling in T-cells and inhibits MHC class II expression.[123,124] MDSCs also produce reactive oxygen species (ROS) that have been shown to be critical to their inhibitory activity[125] and peroxynitrite that causes the nitration of the T-cell receptor and CD8 molecules, altering the specific peptide binding in the T-cell making the cells unresponsive to stimulation with their natural cognate antigen.[126] A new mechanism involving the depletion of cystine/cysteine by MDSC that results in T-cells being deprived of cysteine has also recently been described.[127] This results in reduced T-cell activation. These mechanisms are used to a different extent by the two types of MDSC whereby the granulocytic type expresses high levels of ROS and low levels of NO, and the monocytic type the opposite. Both types express arginase 1 although the granulocytic type depends on it more than the monocytic type which relies more on iNOS. [117,128] MDSCs are also important inducers of regulatory T-cells.[129]

1.2.3 Indoleamine 2,3-dioxygenase (IDO)

IDO is the first and rate-limiting enzyme of the kynurenine pathway that breaks down tryptophan, although this function can also be performed by a functionally similar but structurally different enzyme, tryptophan 2,3-dioxygenase (TDO).[130,131] TDO is liver-specific and is constitutively expressed while IDO is interferon-gamma (IFNγ)-inducible

in many cell types, including cells of epithelial and monocytic lineages.[132,133] It is also expressed in pDCs and certain other DCs.[134] Both enzymes are cytosolic. The activity of IDO was first described in 1975 in the rabbit intestine but advances in molecular biology allowed its cloning and sequencing from human and mouse fibroblasts and rectal cancer line CMT-93, respectively, in the early 1990's. [130,135,136,137] IDO is located on chromosome 8 in both human and mouse, and they both encode a protein of 40kDa in size. The human and mouse IDO peptide sequences share 61% identity (Appendix I). IDO belongs to the family of heme-containing dioxygenases that catalyze the incorporation of molecular oxygen (O_2) into their substrates. IDO catalyses the cleavage of the 2,3-double bond in the indole moiety of tryptophan by a dioxygen bound to the reduced heme-iron (Fe^{2+}) to produce N-formylkynurenine along the kynurenine pathway (Figure 2).[138]

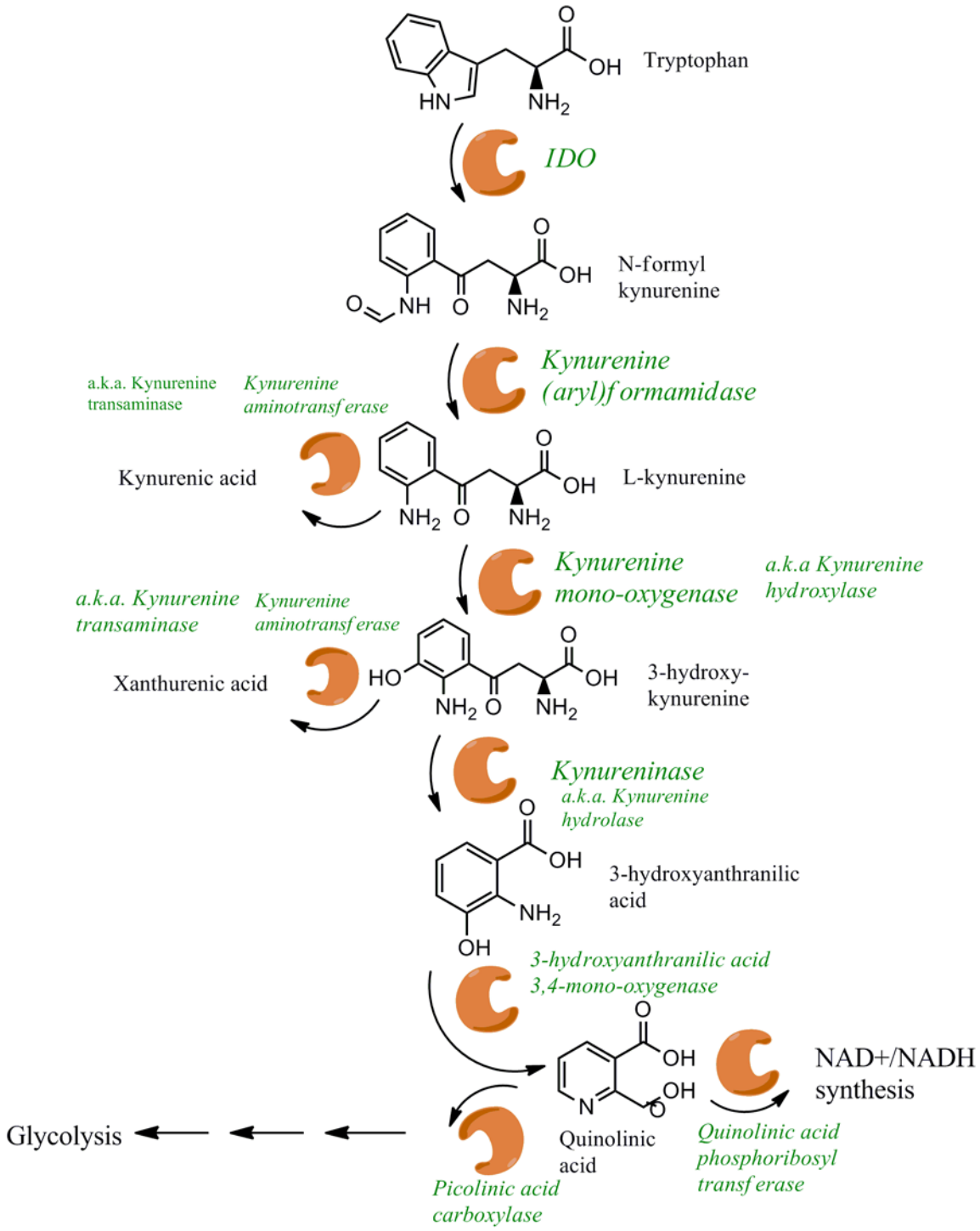

Figure 2. Kynurenine pathway with main enzymes (in green) and metabolites (in black).

The structure of IDO has been solved with the non-competitive inhibitor 4-phenylimidazole bound to its active site, and this has helped in the analysis of its catalytic mechanism and aided computer modelling-based screening for IDO inhibitors.[139,138,140] The latter has yielded a few new nanomolar inhibitors and identified 1-methyl tryptophan as a substrate, in addition to the known substrates tryptophan (L and D), serotonin and tryptamine.[140,138,141] The structure of IDO revealed by Sugimoto *et al*. in 2006 reveals the monomeric enzyme to have two domains labelled as "small" and "large" (Figure 3).[139] The large domain is made up solely of helices (13 α and two 3_{10} helices) and the heme containing active site is in this domain. The molecular oxygen sits on the heme iron and is cleaved from here when it is incorporated into the substrate. The small domain consists of six α -helices, two β -sheets and three 3_{10} helices, and the contact between the domains is extensive at around 3100 $Å^2$. The way in which the heme in IDO is reduced is not entirely clear but cytochrome b5 has been suggested as a candidate by Vottero *et al*. but the authors also suggest that due to the partial redundancy of cytochrome b5, IDO may be able to auto-oxidise or use NADPH-cytochrome P-450 oxidoreductase or superoxide dismutase as electron sources.[142]

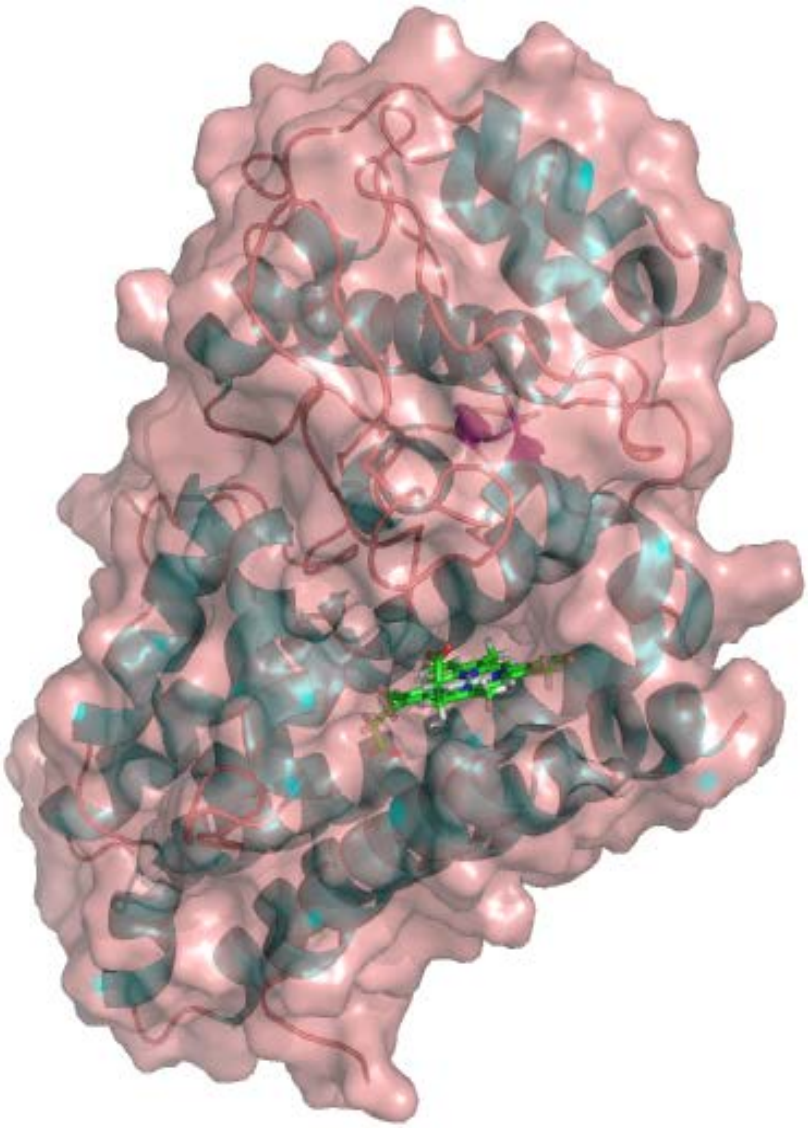

Figure 3. Crystal structure of IDO with heme prosthetic group that forms part of the enzyme active site. PDB file: 2D0T

Various lines of evidence have revealed an important role for IDO-dependent tryptophan metabolism in regulating immunity. The IDO-dependent kynurenine pathway was first thought to be only involved in antibacterial innate immunity, because depletion of intracellular tryptophan inhibits the replication of invading microorganisms.[143] It was then found that placental IDO expression prevents maternal

immune responses to foetal antigens, the first line of evidence suggesting a role for IDO in regulation of adaptive immunity.[144,145] Other groups showed that loss of IDO expression or function shortened graft survival[146,147], and exacerbated autoimmune diseases, such as experimental allergic encephalomyelitis.[148,149] In addition, inhibition of IDO activity in HIV-1 encephalitis enhanced the generation of HIV-1 -specific cytotoxic lymphocytes, thus eliminating HIV-1 –infected macrophages.[150] In the cancer context IDO was initially thought to be tumouricidal due to the depletion of tryptophan[151], however the finding that IDO is crucial in establishing materno-foetal tolerance brought up the possibility that IDO expression in APCs in the tumour-draining lymph nodes may be beneficial to the tumour rather than harmful.[145]

The role of IDO in cancer was raised in studies by Uyttenhove *et al*. who reported that most human tumours express IDO.[152] Recently it has become evident that the reason many tumours express IDO suggesting is that they derive a benefit from its expression by e.g. causing a proliferation arrest in the T-cells in their microenvironment and the generation of T_{regs}.[152,153] This benefit is thought to be a combination of the effect of tryptophan depletion and the accumulation of certain tryptophan metabolites through the kynurenine pathway. The metabolites have been implicated in neurological disorders such as Parkinson's disease[154], Huntington's disease[155] and schizophrenia[156] but also in chronic inflammatory bowel disease[157] and chronic renal insufficiency[158]. There are also indications that some of them are specifically toxic to CD8+ T-cells and some drive the conversion of naive CD4+ cells into T_{regs}.[159,160]

1.2.4 The mTOR pathway and nutrient deprivation

At least one of the mechanisms how cells detect amino acids is by mTOR. The mTOR pathway is a central regulator of cell growth, metabolism, proliferation and survival. The mTOR protein is a serine-threonine kinase of 289kDa and belongs to the phospho-inositide 3-kinase family.[161] Structurally and functionally it appears as part of two distinct multiprotein complexes: mTOR complex 1 (mTORC1) and mTOR complex 2

(mTORC2) (Figure 4). mTORC1 consists of five components: the catalytic subunit (mTOR), regulatory associated protein of mTOR (Raptor), mammalian lethal with Sec13 protein 8 (mLST8 or GβL), proline-rich AKT substrate 40kDa (PRAS40) and DEP-domain-containing mTOR-interacting protein (Deptor).[161,162] The exact role of each component in the complex is not entirely clear but it has been proposed that PRAS40 and Deptor are inhibitors of mTOR kinase activity.[163]

mTORC2 is a complex made up of six proteins: mTOR, rapamycin-insensitive companion of mTOR (Rictor), mammalian stress-activated protein kinase interacting protein (mSIN1), protein observed with Rictor-1 (Protor-1), mLST8 and Deptor. As with mTORC1, Deptor also inhibits mTORC2 and is the only known direct physiological inhibitor of this complex.

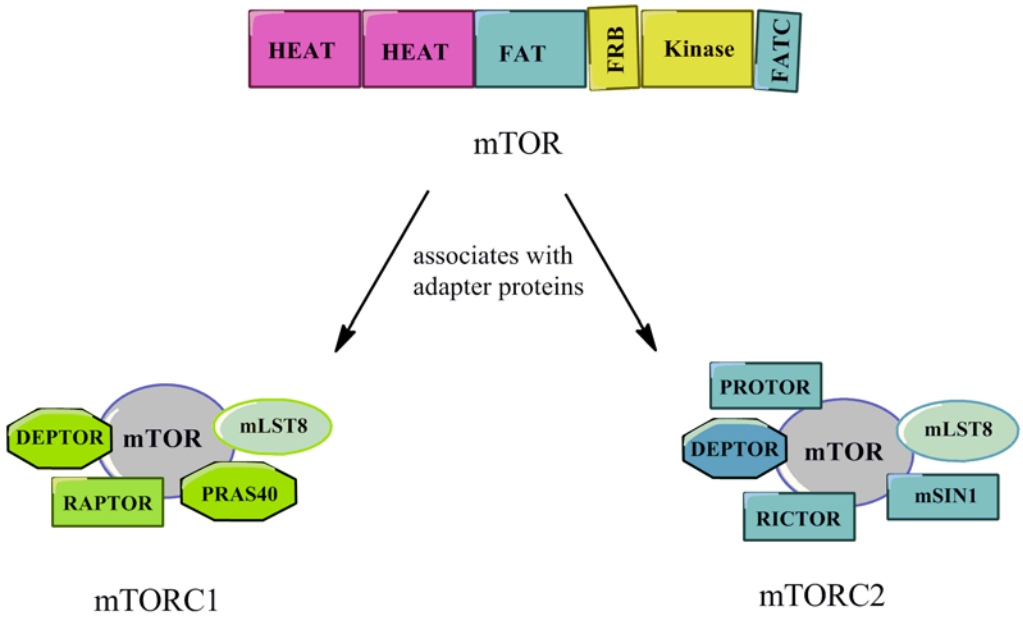

Figure 4. Composition of mTOR complexes. Adapted from Powell, JD. et al. (2012) *Annu. Rev. Immunol*. **30**, 39-68.

The name of the mTOR kinase is derived from the bacterial macrolide rapamycin that is a well-characterised and very specific inhibitor of mTORC1 activity, although there is evidence that chronic exposure to rapamycin can prevent mTORC2 assembly and inhibit it this way.[161,164] Relatively little is known about the physiological role of mTORC2 apart from its regulatory role in cytoskeletal organisation but its signalling pathways are still largely unknown.[165,161]

The physiological role of mTORC1 has been studied more exhaustively. It is a positive regulator of protein synthesis by phosphorylating the eukaryotic initiation factor 4E (eIF4E)-binding protein 1 (4E-BP1) and the p70 ribosomal S6 kinase (S6K1) which in turn phosphorylates the ribosomal protein S6 that is often used as a read-out for mTOR activity (Figure 5). mTORC1 is important in the initiation of autophagy in nutrient-poor conditions when its normal role in repressing autophagy-related proteins unc-51-like kinase 1 (ULK1), autophagy-related gene 13 (ATG13) and focal adhesion kinase family-interacting protein of 200kDa (FIP200), is inhibited.[166] This is an important mechanism that allows the cell to sustain its metabolic processes through controlled protein turnover and organelle degradation.

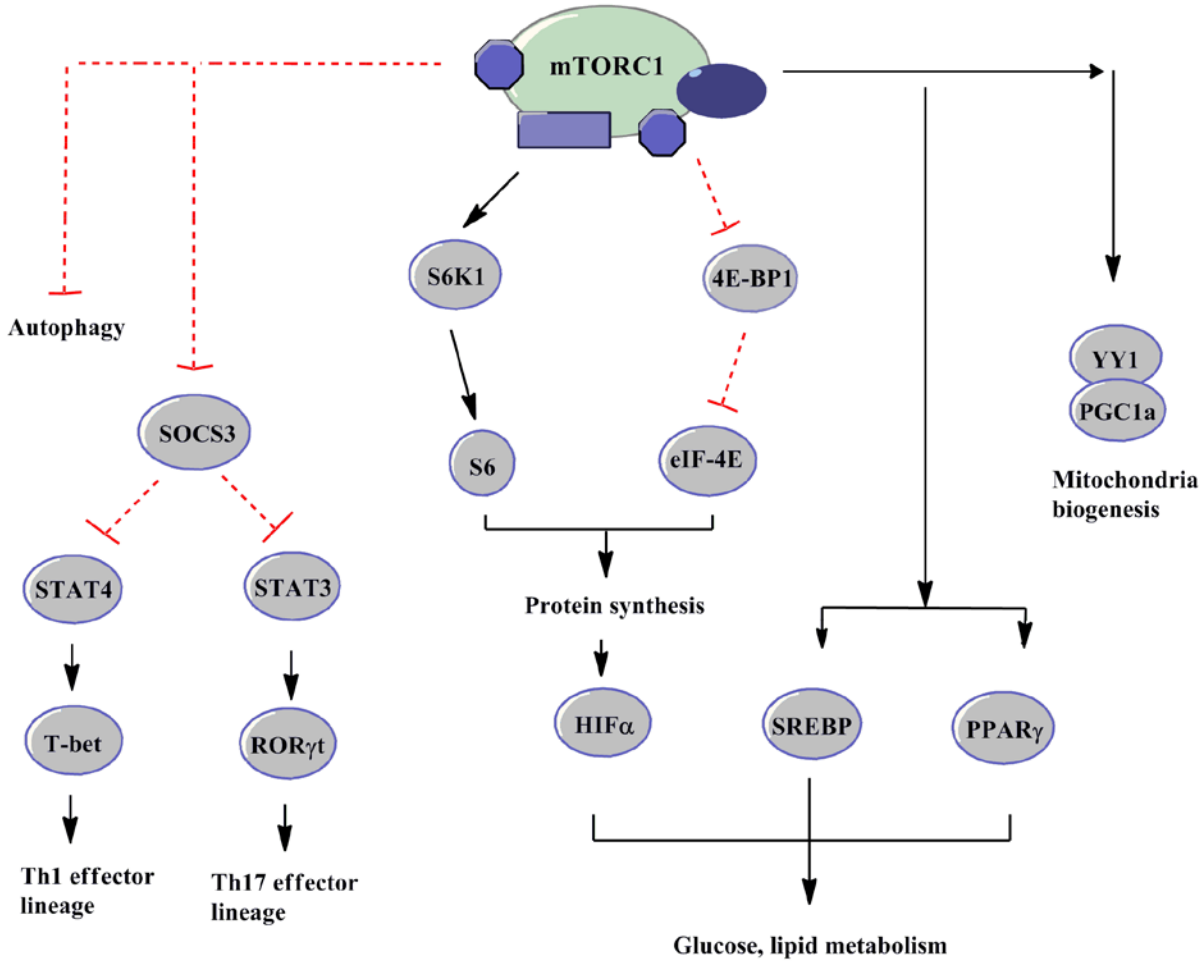

Figure 5. Downstream signalling of mTOR. Adapted from Powell, JD. et al. (2012) *Annu. Rev. Immunol*. **30**, 39-68.

mTORC1 has a major role in integrating signals for growth factors, and availability of energy sources, oxygen and amino acid as well as receiving input from cellular stress and DNA damage pathways (Figure 6). mTORC1 is stimulated by growth factors via the canonical insulin and Ras signalling pathways. Cellular energy status is signalled through the AMP-activated protein kinase pathways while oxygen availability is detected through regulation of the "DNA damage response 1" (REDD1) pathway.[167] Amino acids are strong activators of mTOR. Under amino-acid starvation conditions it is impossible to maximally activate mTOR even in the presence of strong alternative

stimulation.[168] Although the exact details still remain to be elucidated, it has recently been shown that an as-yet-to-be-discovered amino acid concentration sensing mechanism is linked to mTORC1 by four related Rag proteins (GTPases) that bind to Raptor and induce relocalisation of mTORC1 to the perinuclear region where it associates with its activator Rheb.[169]

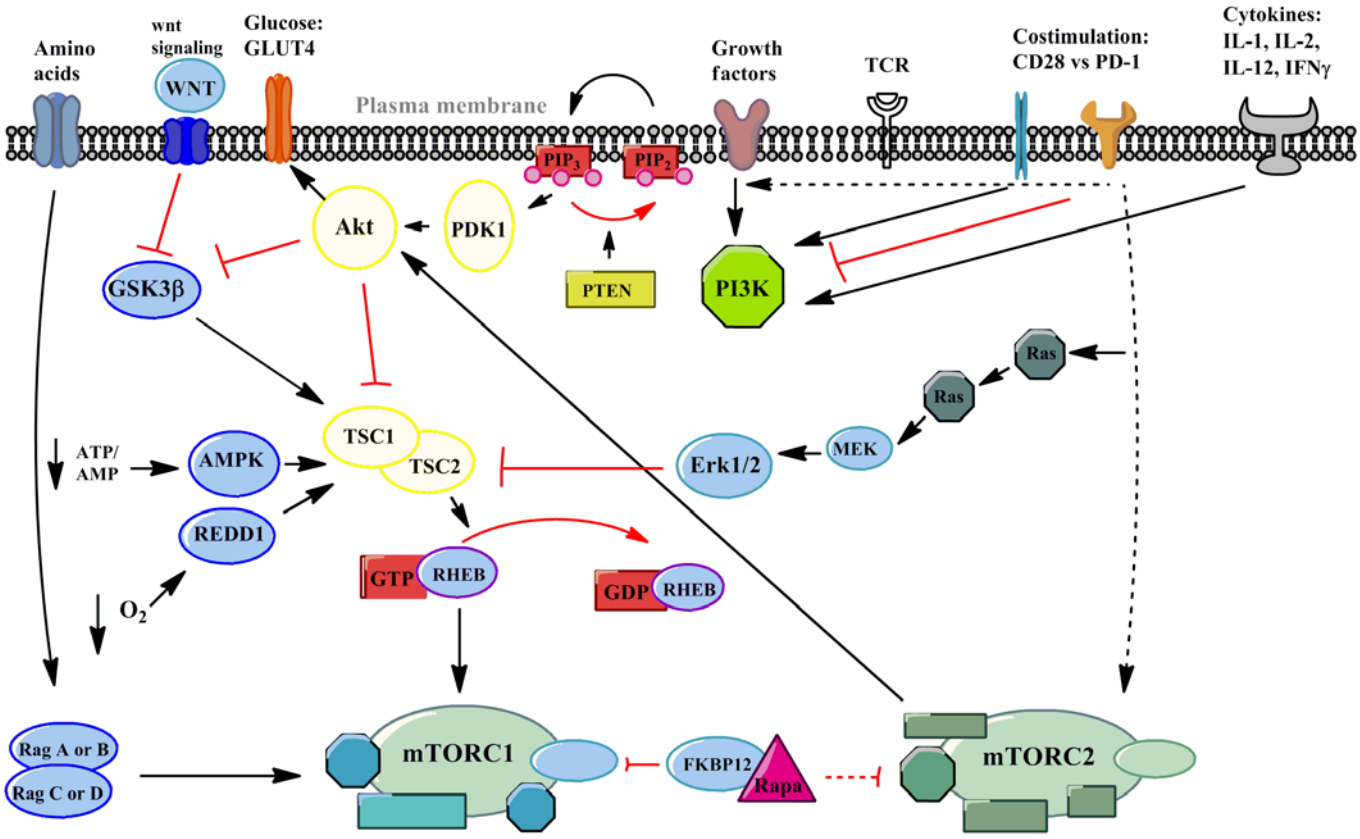

Figure 6. Upstream signalling cascade leading to mTOR activation. Adapted from Powell, JD. et al. (2012) *Annu. Rev. Immunol*. **30**, 39-68.

Due to the critical role of mTOR in cell growth, a lot of attention has been given to mTOR inhibition as a target for anti-cancer therapy. Around 50% of all human malignancies including colorectal cancer and acute myelogenous leukaemia (AML), have been

reported to have heightened mTOR activity.[170,171,172] This is due to many growth promoting signalling pathways commonly upregulated in cancers, such as AKT, HER2/neu and epidermal growth factor receptor (EGFR) being directly linked to mTOR and possibly mediating some of their pro-tumour properties through effectors downstream of mTOR.[173]

Although from a logical point of view mTOR inhibition appears to be a good target for cancer therapies, mTOR inhibition with rapamycin analogs has only been shown to be moderately effective against a few types of cancer such as mantle cell lymphoma (a type of non-Hodgkin's lymphoma), endometrial cancer and renal cell carcinoma.[174] This has been attributed to the fact that the inhibitors only inhibit mTORC1 while concomitant inhibition of mTORC2 appears to be important for success in the therapy.[175] Because of this problem a new strategy for mTOR inhibition is focussing on inhibition at the ATP-binding site of the mTOR kinase. This site is required for activity for both mTORC1 and mTORC2 and would therefore encompass the problem of inhibiting both complexes.

As understanding of the role of mTOR in the adaptive immune system has grown, one issue that has come to the fore is the potential for mTOR inhibitors in cancer to be counterproductive by weakening immune surveillance.[172] It is becoming increasingly clear that blockade of mTORC1 activity can have a profound effect on the differentiation fate of naive lymphocytes. In some cases this may have potentially beneficial effects – mTORC1 blockade appears to result in increased CD8+ memory T-cell generation rather than cytotoxic effector T-cell[176] , and this effect could be harnessed for the development of, for example, better tumour vaccines. At the same time, however, mTORC1 inhibition clearly inhibits direct cytotoxic activity and more worryingly has been shown to result in significantly increased rates of conversion of naive CD4+ T-cells upon stimulation to immunosuppressive T_{regs}.[177] It would not be surprising if this effect is exploited by tumour cells and some of the experiments carried out as part of this project suggest that this may indeed be the case.

1.2.5 The GCN2 pathway

In addition to mTOR, the general control non-derepressible-2 (GCN2) kinase also detects amino acid depletion. It is one of four kinases in mammals involved in the phosphorylation of eukaryotic Initiation Factor 2α (eIF2α) in response to amino acid levels and environmental stresses.[178] The main function of the kinases is to control proteins synthesis levels and the expression levels of genes involved in, amongst other things, amino acid biosynthesis. During low amino acid levels the GCN2 kinase physically senses the uncharged tRNA via its regulatory domain turning it into the active form able to phosphorylate eIF2α.[178] eIF2 binds either GDP or GTP but it is only when bound to GTP when it is able to attach methionyl- tRNA to the ribosome and transfer it to the 40S ribosomal subunit. When the attachment to the 40S subunit has taken place, the GTP is hydrolysed to GDP and inorganic phosphate. Phosphorylated eIF2α inhibits the reversal of GDP to GTP, which results in a reduction of protein synthesis.[178] In yeast during GCN2 activation a transcriptional activator GCN4 has also been identified, which keeps residual amino acid synthesis during starvation enabling survival in adverse conditions.[179]

There is no mammalian ortholog of the *GCN4* gene but the expression of a related basic leucine zipper transcriptional regulator *ATF4* is increased during amino acid starvation.[180] This gene induces a cascade of transcriptional regulators involved in cellular metabolism, redox status and apoptosis, and it has recently been shown that *ATF4* is translationally upregulated in nutrient deprived conditions in which it upregulates amino acid biosynthetic pathways and is closely linked to eIF2α phosphorylation by GCN2.[180] Since GCN2 can, at least in plants, be activated, in addition to amino acid starvation, by other stimuli such as salicylic acid, purine analogue 8-azaadenine, UV-B, wounding and cold-shock[181], it would be interesting to see whether amino acid metabolites, such as kynurenines produced by tryptophan metabolism, can activate the GCN2 pathway, therefore collaborating with mTOR in the inhibition of protein synthesis and induction of apoptosis. If a tumour cell can cause the depletion of amino acids from its microenvironment via e.g. IDO or iNOS, and if the GCN2 pathway can get activated with their metabolites too, this would be an additional method by

which the tumour cell can wreak havoc in the surrounding effector T-cells. The GCN2-ATF4 pathway has been shown to be crucial for tumour progression in mouse and human tumours enabling them to survive in nutrient deprived conditions.[180] It would therefore be interesting to study whether T-cells are more susceptible to nutrient depletion because of deficient ATF4 upregulation. If there are differences between the induction of tumour and T-cell GCN2-ATF4 pathways, it would provide a great target for new cancer therapy since tumour cells could be targeted specifically.

1.2.6 Tryptophan transport in IDO-mediated immunosuppression

Another emerging aspect of IDO activity in a tumour setting relates to the varying ability of different cell types to extract tryptophan. T-cells are very sensitive to the tryptophan concentration in their microenvironment; on the other hand tumour cells appear to be more resistant and it is not currently known why. One possible explanation would be that tumour cells are able to express higher affinity transport systems when tryptophan levels are low, outcompeting cells without that ability.

Tryptophan, like other amino acids, is taken up by a substrate-specific transmembrane transporter. System L is a ubiquitously expressed heterodimeric transporter that, in addition to tryptophan, transports other large hydrophobic amino acids.[182,183] Its function is sodium-independent. It consists of a common heavy chain –also known as CD98 -accompanied by a catalytic light chain –either LAT1 or LAT2.[184,185] It is possible that tumour cells would increase the expression of System L in low tryptophan conditions, but a recent finding by Silk *et al*. identified a possible alternative transporter that is resistant to the System L inhibitor 2-aminobicyclo-(2,2,1)-heptane-2-carboxylic acid (BCH).[186] In their study both human and mouse tumour cell lines upregulated the new transporter when transfected with IDO or treated with IFNγ that induces IDO expression.

This would indicate that upregulation of the new transporter system could help tumour cells survive in an IDO positive, tryptophan-depleted environment. T-cells do not appear to have the ability to upregulate the same transporter (unpublished observations) and would therefore be at a significant disadvantage in an IDO-positive tumour environment even if tryptophan levels were not completely depleted.

This finding has significant clinical implications as small-molecule inhibitors against the new transporter could specifically affect the tumour cells by reducing their tryptophan uptake, making them more susceptible to tryptophan shortage and likely forcing them to either downregulate IDO or face significant growth penalties thus removing their advantage against T-cells.

1.3 Aims

This project has focused on investigating different aspects of immunomodulatory mechanisms employed by cancer cells that rely on modifying amino-acid availability to cells of the immune system. As expression of IDO and recruitment of MDSCs were two of the better described mechanisms we decided to investigate their mechanics more closely aiming to identify ways these could be counteracted in a clinical setting.

We specifically selected to employ various biochemical and immunological assays to study the principles underlying IDO expression and function, and explore potential avenues for its inhibition, and attempted to clarify the nature and importance of the inhibitory mechanisms used by MDSCs; in particular the role amino-acid depletion played.

In the first chapter our aim was to identify an IDO inhibitor with in vivo activity and potential for clinical application. In the second chapter, we attempted to clarify whether catabolic products of tryptophan rather than its depletion alone affected T-cell activity and if so, to what extent and under which circumstances. In the final results chapter we investigated potential mechanisms of T-cell suppression employed by MDSCs and their relative importance.

Chapter 2: IDO inhibitor screen and properties of 3-hydroxyanthranilic acid as an IDO inhibitor

2.1 Introduction

The potential of IDO inhibition as anti-cancer therapy has become apparent since the discovery that many tumours express IDO and that its expression is correlated with a poor prognosis.[187,188,189,190] This has indicated that therapeutic intervention in IDO activity may have clinical value in the treatment of cancer. Supporting this hypothesis were studies that have described significantly more frequent tumour regressions when IDO inhibitors were used in conjunction with conventional chemotherapeutic agents compared to single-agent therapy.[191,192,193]

For many years, the most well known IDO inhibitors were tryptophan derivatives and β-carbolines, which have inhibition constants in the micromolar range.[194,195] Of these, 1-methyl tryptophan (1-MT) has been widely used as a standard IDO inhibitor and it is currently undergoing clinical trials.[196] There is, however, uncertainty as to which stereoisomer is more relevant as they display different activities in different systems; 1-MT (L) inhibits the pure enzyme better than 1-MT (D) which has stronger inhibitory activity in cellular assays; however, its activity depends on the cell type.[150,191,197,198] 1-MT also has the added disadvantage of inhibiting the transport system L that is responsible for tryptophan transport through the cell membrane in many cell types, decreasing the cell's ability to take up this essential amino acid.[199] Despite these conflicting effects on intracellular tryptophan availability, it has nevertheless be shown to have some activity *in vivo* resulting in tumour regression when it has been given in combination with different chemotherapeutic agents, with a metabolic enzyme inhibitor or as a vaccine in which it was conjugated to a tumour antigen peptide.[200,191,201] The latest findings with 1-MT (D), however, also indicate to its potential in up-regulating IDO1 mRNA via p38 MAPK and JNK signalling. [202] This is worrying for the ongoing trials with 1-MT (D) and definitely leaves a window open for more potent and specific inhibitors of which a few have been described in recent years.

The first nanomolar inhibitors were described in 2006 when two groups isolated molecules from marine organisms that were structurally unrelated to tryptophan.[203,204] Exiguamine A had a K_i ranging from 41nM to 210nM but it has so far only been tested *in*

vitro with the recombinant IDO thus providing no information of its usefulness in whole cells.[203,205] Annulin B and C were another group of marine organism-derived molecules with K_i values in the 100 nM range using recombinant IDO, however they were unable to cross the cell wall in a yeast-based assay.[204] These molecules did, nonetheless, give a template to guide the design of new IDO inhibitors and in 2008 Kumar *et al*. published naphthoquinone inhibitors based on the annulin B core that induced tumour regressions *in vivo* in mice when administered together with the chemotherapeutic agent paclitaxel.[206] Exiguamine A also provided a base for the synthesis of simpler tryptaminequinone analogues that were active in the submicromolar range *in vitro*, however these have not yet been tested in cellular assays.[205]

The most recent and promising competitive IDO inhibitor was discovered independently of the above and is based on a hydroxyamidine scaffold.[207] It showed activity in assays with recombinant IDO (IC50 67nM) but more importantly also inhibited endogenous IDO in assays with HeLa cells (IC50 19nM). Furthermore, it also inhibited kynurenine production and suppressed melanoma growth in C57BL/6 mice, making it the most promising inhibitor to date.[207] Additionally, the efficacy of hydroxyamidine-based inhibitors has been further studied in non-rodent species and in colon and pancreatic carcinoma models, in which the inhibitor suppresses kynurenine production in plasma, tumours and lymph nodes without apparent toxicity to the animal.[208] Although these inhibitors appear the most potent so far, we decided to look for IDO inhibitors within compounds that are already produced in the cell.

Given the similar structures of many of the intermediates in the kynurenine pathway[209], and the mode of binding of 4-phenylimidazole in the IDO active site as revealed by crystallographic analyses[139], our strategy was to screen for potential IDO inhibitors including the downstream metabolites of tryptophan. If any were identified, they may guide the design of new inhibitors and give information on possible inhibitory feedback mechanisms within the cell. In this chapter I will describe the IDO inhibitory properties of the tryptophan metabolite 3-hydroxyanthranilic acid (3-HAA) *in vitro* and *in vivo* and reveal that 1-methyl tryptophan can function as a substrate for IDO in addition to its inhibitory properties.

2.2 Materials and methods

2.2.1 Mice and inhibitor screen compounds

C57BL/6 mice were bred in the Biomedical Services Unit, John Radcliffe Hospital, and used for *in vivo* experiments under the authority of a U.K. Home Office Project Licence.

Antibodies (anti-mouse CD4, CD8 and CD3) were from eBioscience; flow cytometry was performed on a FACScalibur device using CellQuestPro software. 3-hydroxyanthranilic acid (3-HAA), *L*-tryptophan, *D*-tryptophan and 1-MT (*D*, *L* and *D*/*L*) were from Sigma Aldrich. The Zorbax SB-C18 column used for HPLC was from Agilent Technologies, USA.

The other tested compounds were obtained from Sigma-Aldrich (2,4,5,10,12,19,22,23), Alfa Aesar (1,3,7,8,9,11,13,14,17,21,24,25,26,27,28,29), TCI Europe NV (6), Acros Organics (15), Maybridge (18), and Apollo Scientific (20). Compound 16 was synthesized from 3-carbomethoxy-1,2,3,4-tetrahydroisoquinoline-1,4-dione. Ethyl ester 3-HAA, monoacetylated 3-HAA and diacetylated 3-HAA were synthesized from commercially available 3-HAA (by Jasmin Mecinovic, University of Oxford).

2.2.2 Cell culture

The mouse T cell lymphoma line EG7 had been made in our laboratory by transfecting EL4 cells with a complete copy of the chicken ovalbumin (OVA) mRNA and the neomycin (G418) resistance gene. The EG7 cells constitutively synthesise and secrete OVA and are therefore useful in being able to activate cells that recognise the protein. This ability was used in later chapters where T-cells from OT-I mice that are transgenic for the OVA peptide 257-264 were stimulated by EG7 cells. EL4 cells by comparison are unable to stimulate the T-cells and were used as negative controls.

The EG7 cells were maintained in complete RPMI 1640 medium (Sigma) (containing 10% foetal calf serum (FCS, from Sigma), 2-mercaptoethanol (50 μM), 50 U/ml penicillin and 50 μg/ml streptomycin) and 0.4mg/ml G-418. Where appropriate, the

EG7 cells were cultured in tryptophan-free RPMI 1640 (HyClone) containing the same additives as above. The human cervical cancer cell line HeLa was maintained in complete MEM (containing 10% FCS, 50 U/ml penicillin and 50 μg/ml streptomycin and non-essential amino acids (1% v/v). The human acute monocytic leukaemia cell line THP-1 was maintained in RPMI 1640 medium supplemented with 10% FCS, 50 U/ml penicillin and 50 μg/ml streptomycin, 1% v/v non-essential amino acids, and 1mM sodium pyruvate. The mouse monocytic leukaemia cell line RAW was maintained in RPMI 1640 + 10% FCS + 50 U/ml penicillin and 50 μg/ml streptomycin.

2.2.3 Recombinant human IDO in pET21b vector

Full-length human IDO cDNA had been cloned earlier into pET21b expression vector by Samira Lakhal (University of Oxford). The cDNA had been amplified from IFN-γ -treated THP-1 with the following oligonucleotides:

Forward: 5' AAT GAT CAC CAC CAT GCA CAC GCT ATG G 3'

Reverse: 5' GCC TCG AGT TAA CCT TCC TTC AAA AGG GAT TTC 3'

and for ligation to the vector, digested overnight at 37°C with XhoI and NheI restriction enzymes (NEB).

2.2.4 Cloning of IDO into pET15b vector

Full-length IDO cDNA was amplified from pET21b-IDO plasmid with the following primers both containing an XhoI restriction site:

Forward: 5'- GAA AAC TCG AGA TGG CAC ACG CTA TGG AA

Reverse: 5'- GAA AAC TCG AGT TAA CCT TCC TTC AAA AGG G

A proofreading DNA polymerase was used (Phusion, Finnzymes) and the cycling conditions were as follows: 2 min at 95 ^{o}C, [30s at 95 ^{o}C, 15s at 57 ^{o}C, 30s at 72 ^{o}C] x30, 5 min at 72 ^{o}C.

The pET15b plasmid was digested with XhoI (New England Biolabs) together with shrimp alkaline phosphatase (SuperSAP, USB) to prevent vector self-ligation. Ligation was done with a 1:14 ratio of vector and insert, respectively, at room temperature for 3 hours.

To check the orientation and identity of products, PCR was performed with the following vector- and insert-specific primers:

Vector-specific (FWD): 5'- GAA GGA GAT ATA CCA TGG

Insert-specific (REV): 5'- CCA GTT TCT TGG AGA GTT GGC

Finally, for identity confirmation positive samples were sequenced by the DNA sequencing service in the WIMM, University of Oxford.

2.2.5 Expression and purification of recombinant human IDO

IDO in both vectors was expressed in BL21 cells. Cultures were grown until optical density reached 0.6 at which point the production of IDO was induced with 500μM of Isopropyl β-D-1-thiogalactopyranoside (IPTG). In addition the heme precursor 5-aminolevulinic acid was added at 500μM. The induced cultures were then grown overnight. To purify IDO from the bacterial cells, the cultures were spun at 3500 rpm for 30 min. The pellets were resuspended in 10mM imidazole containing 1 tablet of EDTA-free protease inhibitor (Roche) and 1mg of DNase I (Sigma). The suspension was then sonicated to break the bacterial cells. The suspension was then centrifuged at 10 000g for 30 min and the supernatant injected into a HisTrap column (both plasmids contain a histidine tag). The nickel column-purified IDO was then further purified by FPLC (HiLoad 26/60, Superdex 75 column) and the fractions run on 12% SDS-PAGE.

2.2.6 Measurement of IDO activity

2.2.6.1 IDO activity in cell culture

Tryptophan and kynurenine concentrations in cell supernatants were measured by HPLC. Briefly, supernatants were treated with 30% (w/v) trichloroacetic acid and centrifuged at 10000 g for 30 minutes before injecting into a Zorbax SB-C18 column (Agilent Technologies, USA) on an HPLC system with variable wavelength detector. Kynurenine was detected at a wavelength of 365 nm and tryptophan at 280 nm.

2.2.6.2 IDO activity in cell lysate

$1x10^6$ cells were lysed by freeze/thawing and spun at 10000g for 10 min and the clear lysate was mixed with incubation medium (100 mM potassium phosphate buffer pH 6.5, 40 mM ascorbic acid, 20 μM methylene blue, 200 units/ml catalase and with/without different concentrations of tryptophan) and kept at 37^oC for 1 hour before addition of 30% (w/v) Trichloroacetic acid (TCA). The samples were then incubated for 30 minutes at 50 ^0C. The concentration of kynurenine was measured as previously described. Concentrations were normalized to protein concentration in lysate (as measured by Nanodrop, Thermo Scientific, USA).

2.2.6.3 Recombinant human IDO activity

To measure the catalytic activity of recombinant human IDO, 200 ng of the purified protein was added to 100 μl of the incubation medium containing tryptophan and assayed as described above. To assess the effect of different compounds on IDO activity they were added at 1 mM. IDO enzyme kinetics was done over 3 minutes when less than 25% of substrate had been used. For 3-HAA inhibition curves tryptophan was used at 5, 10, 20, 50, 100, 250 and 400 μM and 3-HAA at 0, 10, 50, 100 and 400 μM. For Michaelis-Menten curves with 1-MT (L), 1-MT (D), L-Trp and D-Trp, they were used at

0, 5, 20, 50, 100, 200 and 400 μM. IDO activity is shown as specific activity (μmole kynurenine/mg IDO/hour or μmole kynurenine/mg IDO/min).

2.2.7 Crystallisation of recombinant human IDO in the presence or absence of inhibitors

Crystal screening was attempted with both plasmids as follows:

pET21b-IDO:

- His-tag cleaved with carboxypeptidase, 12 mg/ml. (Screens **1** (Hampton CS1 and CS2), **2** (Wizard I and II), **3** (Hampton PEG/Ion, P6k, AmSoI), **4** (Hampton Natrix, CS Cryo), **5** (P/Li, NaCl, MPD, Quik), Index and a custom screen). These were co-crystal screens with either 3-HAA or 1-MT (L).
- Uncleaved, 10.5 mg/ml in 10 mM MES, 25 mM NaCl pH 6.5. Screens 1, 3, P, Index and custom. Co-crystal screens with either 3-HAA or 1-MT (L) and one with protein only (custom screen)
- Uncleaved, 9.1 mg/ml in MOPS 25 mM, 25 mM NaCl, pH 7.5. Screens 1,2,3,4,5, SRX, P, Index. Co-crystal screens with 1-MT (L), 1-MT (L)+3-HAA, or protein on its own.
- Uncleaved, 12.5 mg/ml in 25 mM MOPS, 25 mM NaCl, pH 7.5. Optimisation screen from a condition previously found to have formed a potential crystal. IDO on its own.

pET15b-IDO:

- Cleaved with thrombin, 8 mg/ml in 50mM Tris-HCl, 10mM $CaCl_2$, pH 8. Screens 1,2,3,4,5, and Index. Co-crystal screening with 3-HAA+"Incubation media" and protein only.

2.2.8 Induction and measurement of IDO activity *in vivo*

Effects of 3-HAA on thymocytes: Mice were immunised intraperitoneally (i.p.) with different doses of 3-HAA daily over 4 days and weighed. At the end of the experiment thymocytes and splenocytes were stained with antibodies against CD4, CD3 and CD8 and analyzed by flow cytometry, gating on propidium iodide negative (live) cells.

Kynurenine measurement in the sera of mice injected with LPS: C57BL/6 mice were injected intraperitoneally (i.p.) with a vehicle (6 mice) or 3mg/mouse of 3-HAA pH 8 (6 mice) on day -1. On day 0, 3 mice were given a vehicle injection, 3 mice LPS (20μg/mouse), 3 mice 3-HAA (3mg/mouse), and 3 mice were injected with both LPS and 3-HAA at the above concentrations. On day 1 the mice were bled and sacrificed and their spleens removed. The sera were measured for kynurenine and tryptophan levels. The serum was treated with 30% w/v TCA before injecting into the HPLC. We also counted and stained the splenocytes for maturation marker CD86 and B-cell marker B220 and saw that LPS had induced upregulation of CD86 and that 3-HAA did not affect the maturation on its own or with LPS (data not shown).

EG7 tumour experiment with 3-HAA injection for kynurenine detection: C57BL/6 were injected subcutaneously with $5x10^5$ cells with either EG7 OVA wt (6 mice), EG7 OVA GFP (6 mice) or EG7 OVA IDO+ (6 mice). The tumours were grown for ten days and their sizes were measured regularly. On day 10 three mice in each group received an injection of PBS and the other three mice 3-HAA (3 mg/mouse i.p.). On the same day, prior to the injections, the 6 mice in each group were bled for serum kynurenine and tryptophan measurements (these are “before injection” measurements in Figure 12). The mice were bled for serum kynurenine and tryptophan measurements by HPLC analysis prior to and one day after injection.

2.2.9 Measurement of H_2O_2 concentration in a reaction containing 3-HAA

Hydrogen peroxide produced in either cell culture supernatant, cell lysate supernatant or assay buffer for the recombinant IDO was measured with an H_2O_2 fluorimetric detection kit from Assay Designs/Stressgen according to the instructions. In the recombinant IDO assay buffer, 3-HAA (and 1-MT (L) as a control) was titrated at 0 μM, 10 μM, 40 μM, 100 μM, 200 μM, 500 μM and 800 μM. Volumes of PBS, DMSO, and incubation media were kept constant in each sample, as at least PBS can affect the fluorescence readings. The samples were incubated for 1 hour at 37°C after which the H_2O_2 was measured as per kit instructions.

2.2.10 Molecular modelling studies of IDO inhibitors

Targeting a 10Å radius sphere on top of the heme iron in the IDO active site, the programme Genetic Optimization for Ligand Docking (GOLD)[210] was used to dock IDO ligands. 3D coordinates (SYBYL mol2 files) of these ligands were generated using the PRODRG server.[211] Hydrogen atoms were written out for accurate ligand docking. The Goldscore or ASP scoring function was used to evaluate and rank the efficacy of docking. To validate these results, docking of phenylimidazole was also performed and compared with the known co-crystal structure of IDO (PDB ID: 2d0t).

2.3 Results

2.3.1 1-methyl tryptophan (L) inhibits IDO but is a weak substrate in tryptophan-free conditions

To date 1-methyl tryptophan (L) is mostly known as a competitive IDO inhibitor with a K_i of 19 μM in assays with recombinant IDO.[191] We confirmed this by performing an *in vitro* inhibition assay with recombinant human IDO. The assay was run for 3 minutes after which the kynurenine produced was measured and the results plotted in GraphPad Prism. Of all available curve fitting methods for enzyme inhibition, the best was achieved with the competitive inhibition model, agreeing with published data. [195] To confirm the results, the data was also plotted into a Lineweaver-Burk double reciprocal plot, which shows the characteristic fit for a competitive inhibitor (each inhibitor concentration curve converging at the y-axis, Figure 1B). The lowest tryptophan concentrations (5 and 10 μM) were omitted from the double-reciprocal plot due to the insensitivity of the HPLC-based detection method at measuring very low kynurenine levels which subsequently results in skewing of the results. In our hands 1-MT (L) gave a K_i value of 73 μM which is higher than published values[191] (Figure 1 A and B).

Due to noticing kynurenine production in a control enzyme assay with 1-MT (L) and no tryptophan, we wanted to investigate the possibility that 1-MT (L) is also an IDO substrate. 1-MT (L) was subsequently found to be a weak substrate for IDO in Trp-deficient conditions (Figure 1C). The conversion rate was too slow to allow reliable enzyme kinetic measurements. The results shown here represent conversion of 1-MT (L) into kynurenine over one hour. Further examination of IDO kinetics with 1-MT (L) as the substrate were hindered by the stock 1-MT (L) containing a considerable amount of tryptophan (Figure 1D). The amount of tryptophan is roughly 20% of the stock 1-MT (L). This may have been due to spontaneous conversion of 1-MT (L) into tryptophan over time or contamination during production. Therefore any experiment done with 1-MT (L) as an IDO substrate had to be done with purified 1-MT (L). The purification procedure was performed by Katalin di Gleria (WIMM, University of Oxford) by liquid

chromatography-mass spectrometry (HPLC-MS). The purified 1-MT (L) had to be used instantly as we noticed conversion of 1-MT (L) into tryptophan even after freezing the sample in -20 ^{o}C (data not shown). The results shown in Figure 1C were obtained with pure 1-MT (L) and the absence of tryptophan was confirmed by HPLC.

2.3.2 Inhibitor screen with recombinant human IDO

Since 1-MT (L) is not a very efficient IDO inhibitor, we focussed on screening a small library of inhibitors similar to tryptophan and its metabolites for potential IDO inhibition. Previously in our laboratory, 3-hydroxyanthranilic acid (3-HAA) had been found to be a 5-8-fold stronger inhibitor than 1-methyl tryptophan (L) in assays with purified IDO (DPhil thesis, Samira Lakhal). Considering that 3-HAA is a downstream metabolite of tryptophan, we screened other metabolites of the kynurenine pathway for inhibition and possible feedback loops - picolinic acid (1), quinolinic acid (2), kynurenic acid (12), and xanthurenic acid (13) (Figure 3). Other molecules similar to their structures were also included. In order to identify which chemical group(s) of 3-HAA is important for its inhibitory activity compounds 20-23 were included in the screen. Structures of all the screened molecules are listed in Figure 3.

Only 3-HAA (compound 19) and methyl 2-aminopyridine-4-carboxylic acid (MAPC, compound 14) showed potent activity at 1mM (Figure 2A). Consequently the screen was further extended to include six MAPC -like molecules to identify important groups for its activity (compounds 24-29, Figure 2B). Of this screen only compound 29 showed any significant activity and was taken to cellular assays together with 3-HAA and MAPC. It also revealed the potential importance of the hydroxyl and amine group position in 3-HAA since none of the modified molecules showed similar activity.

2.3.3 IDO enzyme kinetics in the presence of 3-HAA

As 3-HAA emerged as the strongest inhibitor candidate, further characterisation of its mode of inhibition was performed. To identify the optimal pH for IDO activity, a pH screen with and without catalase was performed. Catalase is a component of the media that is used to keep IDO in an active state in *in vitro* assays by providing it with O_2 and removing H_2O_2 that has IDO inhibitory properties.[212] pH 6-6.5 was found to be optimal for IDO activity and this range was used in all experiments (Figure 4A). A 3 minute time point was chosen for the kinetic experiments as it was still practical, and it was the point by which only 25% of the lowest concentration of substrate (5μM) had been used, making it unlikely that tryptophan would be limiting and skewing the results (Figure 4B). To identify how 3-HAA inhibits IDO, inhibition assays were performed.

After trying out all the available curve fittings, the best fit is achieved with a mixed-model of inhibition, even though non-competitive and uncompetitive models fit almost as well as measured with GraphPad Prism 5.0 (Figure 4C illustrates the mixed model fitting but the other two options showed a similar fitting). When these data were plotted in the double-reciprocal Lineweaver-Burk plot, the results indicate irreversible binding as it is the only option for a fitting where none of the lines converge in a single point but rather criss-cross each other (Figure 4D).

To further examine whether the binding of 3-HAA to IDO is irreversible, a competition assay was performed where IDO and 3-HAA were first incubated together for 10 min at room temperature followed by the addition of tryptophan in the incubation media (1 hour in 37 ^{o}C). If the binding was reversible, the added tryptophan should displace the bound 3-HAA and result in increase of kynurenine compared to no tryptophan or lower tryptophan concentrations. There was, however, no increase in kynurenine with higher concentrations of tryptophan, indicating that the binding is indeed irreversible (Figure 4E).

2.3.4 3-HAA activity in cellular assays

Cellular assays with 3-HAA were run alongside the kinetic experiments. First, we wanted to examine the effect of 3-HAA, MAPC and compound 29 on the kynurenine production in IDO+ cells. EG7 OVA IDO+ cells were incubated for 48h starting with $5x10^5$ cells. In the case of measurements from the supernatants, the cells were incubated in the presence of 500 μM of inhibitor and after 48h the supernatant was analysed on HPLC. The lysate assay was performed similarly with the exception that there was no inhibitor present during the 48h cell incubation but it was added after the lysis of the cells together with the incubation media. In this case 1 mM of each inhibitor was used.

When the inhibition is measured by the amount of kynurenine in the supernatants, 1-MT (L) inhibits kynurenine production by 50% and 3-HAA and MAPC about 30%. The inhibition by 3-HAA was not as strong, however, as previously reported (80%, from DPhil thesis by Samira Lakhal), but it was still statistically significant. Compound 29 does not have an effect (Figure 5A). In the cell lysate –based assay 3-HAA and compound 29 inhibit better, both around 60% and MAPC even more (80%, Figure 5B). 1-MT (L) inhibits IDO activity around 40%. Because compound 29 did not have an effect on the kynurenine levels in the supernatant, further characterisation was not pursued. MAPC was further analysed in kinetic assays with rhIDO but it proved a very weak inhibitor with 40% inhibition seen only at 400 μM (data not shown). For this reason, MAPC was also left out of further testing.

As 3-HAA was still the strongest inhibitor we had found, we wanted to see whether the inhibitory effect of 3-HAA in mouse and human whole cells and cell lysates is dose-dependent. The cells for the supernatant measurement were treated for 48h with 3-HAA concentrations ranging from 10-400 μM. To take into account the possibility that 3-HAA does not get into the cells to exert its effect, the cells for the lysate assay were now co-incubated for 48h with the inhibitor. After 48h the washed cells were lysed and

the reaction started with the addition of incubation media without any additional inhibitor. If any inhibition was seen, it should therefore have been caused by the inhibitor inside the cell. The assays were started with $5x10^5$ cells/well in the case of HeLa cells and $1x10^6$/well with EG7 cells.

There was no inhibition of kynurenine production in either EG7 or HeLa supernatants (Figure 6A and B). In the EG7 lysates, the inhibition by 3-HAA is dose-dependent, but there is no inhibition in the HeLa lysates (Figure 6C and D). Surprisingly, in the EG7 lysates, 1-MT (L) causes an increase in kynurenine concentration, which is unexpected considering that it is a well-known IDO inhibitor. A possible reason for this could tryptophan transport inhibition by 1-MT (L), which has been observed in our laboratory by others. This could then cause accumulation of kynurenine inside the cells that is then released on cell lysis. HeLa wild type cells were also treated with IFNγ to see if 3-HAA has an effect on the induced endogenous IDO. There was only around 40% inhibition at 400μM, indicating that 3-HAA is no more effective against endogenous IDO (Figure 6E). To investigate the discrepancy between the results from the whole cell assay and the lysate assay, we investigated the possibility that 3-HAA cannot get into the cell from the culture medium. To do that, EG7 cells were incubated with various concentrations of 3-HAA for 48h and then lysed and the 3-HAA concentrations measured from the lysates. The 3-HAA concentration inside the cells is measurable, even though the levels are considerably lower than what was initially added (Figure 6F). This indicates that 3-HAA can cross the cell membrane suggesting that the lack of inhibition in the whole cell assay cannot be attributed to the inaccessibility of 3-HAA to the cytoplasm.

Due to the discrepancy between the results from the assays with the pure recombinant enzyme and the whole cell assays, we wanted to investigate the possibility that 3-HAA is not in high enough levels inside the cells to inhibit IDO. To facilitate a more efficient crossing of the cell membrane, more hydrophobic versions of 3-HAA were examined. Ethyl ester 3-HAA, monoacetyl 3-HAA and diacetyl 3-HAA were synthesised from commercial 3-HAA by Jasmin Mecinovic for us (Department of Chemistry, University of

Oxford). EG7 cells were incubated for 48h in the presence of the inhibitors, which were added at 500 μM. Ethyl ester 3-HAA was added at 100 μM because of its toxicity to cells at higher concentrations (data not shown). Both mono- and diacetyl 3-HAA molecules showed significant activity in cell lysates and the reduction of kynurenine levels was also measurable in the supernatants suggesting that these molecules may be worth investigating more (Figure 7A and B). They also inhibited the recombinant human IDO significantly, but not as well as 3-HAA (Figure 7D).

2.3.5 IDO inhibition by 3-HAA possibly mediated by H_2O_2 production

Although it is possible that the lack of IDO inhibition by 3-HAA in the whole cell assays was due to its limited ability to cross the cell membrane, we wanted to further examine its inhibitory mechanism. To investigate the possible irreversible binding of 3-HAA into IDO, a mass spectrometry analysis was performed with MALDI-TOF and electrospray ionisation (Katalin di Gleria, University of Oxford). The samples were also trypsin-digested in an attempt to identify the location of the binding. There were, however, no differences in the sizes of the fragments between the pure enzyme and the enzyme treated with 3-HAA, indicating that irreversible binding does not occur (data not shown). The enzyme was also analysed undigested and again no differences were found. Furthermore there was no difference in size in the prosthetic heme group between the enzyme only and the enzyme+3-HAA samples. These results suggest that there must be an alternative explanation as to the variable IDO inhibition 3-HAA displays in different assays. We looked at the possibility of 3-HAA down-regulating IDO expression at mRNA level, but this was not the case (Figure 8A).

An online search for chemical reactions involving 3-HAA revealed that on reacting with O_2, 3-HAA can auto-oxidise to produce H_2O_2 as a by-product (EMBL-EBI, e.g. reaction RHEA: 17246). This has also been reported by Dykens *et al*.[213] Hydrogen peroxide is a known inhibitor of IDO[212] so we wanted to investigate whether this could be the cause for the IDO inhibition in assays with the pure enzyme and cell lysates. It is plausible as both of these assays involve the use of the IDO activating incubation media where

molecular oxygen is produced from H_2O_2 by catalase. H_2O_2 in turn is produced by the reaction between ascorbic acid and methylene blue.[214] IDO is functional at the H_2O_2 concentration that is produced from that reaction but if excess H_2O_2 is introduced as a by-product of 3-HAA, it is possible that the turnover rate of catalase is not sufficient to prevent H_2O_2 from blocking IDO activity. This IDO inhibition can then appear as irreversible because the catalase is limiting.

The first experiment to see whether H_2O_2 is indeed the "inhibitor", involved titrating catalase into cell culture containing 3-HAA at a concentration known to kill at least 50% of the cells. If the cells survive and the death percentage is smaller with catalase, the death is likely to be caused by H_2O_2, which is now broken down by catalase. Indeed, the percentage of live cells doubled at both 3-HAA concentrations (500 μM and 1 mM) when catalase was introduced (Figure 8B). The introduction of catalase also improved the ability of the cells to proliferate and this was clearly seen at the lower 3-HAA concentration where the cells without catalase would not proliferate significantly (assay was started with $5x10^5$ cells) but would if catalase was present (Figure 8C). In order to get a definite answer as to the presence of H_2O_2 in the assays involving the incubation media, the concentration of H_2O_2 was directly measured in an assay with rhIDO. The presence of IDO did not have an effect on the amount of H_2O_2 present as expected (not shown), and catalase decreased it by a small amount (Figure 8D). It is clear, however, that there is a large amount of H_2O_2 produced when 3-HAA is present, making it very likely that it is H_2O_2 that causes the inhibition of IDO and not 3-HAA directly.

2.3.6 IDO in THP1 cells is inhibited by 3-HAA via radical oxygen species

Following the finding that 3-HAA potentially reacts with components of the incubation media, and in particular O_2, we wanted to study the possibility that 3-HAA could inhibit IDO in cells that produce radical oxygen species, such as O_2^- when activated. Therefore we decided to study its effects on IDO in macrophages, using the monocytic leukaemia cell line THP1 as the human model and the mouse equivalent cell line RAW as the mouse model. First we wanted to establish which maturation cocktail produced the

highest IDO activation when measured by kynurenine production. THP1 cells produced the highest amount of kynurenine when matured with 1000 u/ml of IFNγ and 200 ng/ml LPS (Figure 9A). In order to make sure that the immature THP1 cells were completely matured so as to produce radical oxygen species, we chose to use the combination of IFNγ, LPS and phorbol myristate acetate (PMA, 16 nM) as the maturation cocktail in the future experiments. That produced a high enough kynurenine concentration to measure for potential inhibition. The mouse RAW cells did not produce any kynurenine before or after the addition of IFNγ and LPS, so those cells could not be studied further (Figure 9B).

THP1 cells were then further examined with a range of 3-HAA concentrations. Kynurenine production in THP1 cells that had been stimulated with only IFNγ and LPS was unaffected by all 3-HAA concentrations (Figure 9C). There was, however, a small reduction in the kynurenine concentration in THP1 cells that had received IFNγ, LPS and PMA treatment, and 3-HAA at 200 μM. This was a positive indication that the ROS produced by mature THP1 can interact with 3-HAA and form H_2O_2 which then inhibits IDO. This was further studied by increasing the 3-HAA concentrations, which dose-dependently reduced the kynurenine concentrations in the media (Figure 9D). 3-HAA is, however, known to be toxic to the cells from around 200 μM upwards, making it necessary to ascertain whether the kynurenine reduction was due to cell death. The effect of 3-HAA on the cells was visible under the microscope where the normally plate-bound mature macrophages, started floating when 3-HAA was added at high enough concentrations. The floating cells were collected and stained with trypan blue to determine whether they were dead or alive. The floating cells in the sample with activated THP1 but no 3-HAA, the floating portion was predominantly dead cells (Figure 9E). In the samples containing 3-HAA, this portion consisted around 50% or more of live cells, suggesting that 3-HAA at least had a significant effect on the phenotype of the THP-1 cells, so that, even if they were not dead or dying, their kynurenine production capacity may have been adversely affected.

2.3.7 *In vivo* activity of 3-HAA

Considering that 3-HAA may inhibit IDO in the presence of ROS –producing macrophages, we wanted to investigate whether it was possible to measure kynurenine in the mouse sera after LPS injection or with IDO+ tumours, and whether exogenous 3-HAA would affect its levels. Previously it had been reported that 3-HAA (and other tryptophan metabolites from within the kynurenine pathway such as quinolinic acid) are toxic to thymocytes *in vitro* and *in vivo*.[215] We injected C57BL/6 mice with 20 or 200 mg/kg 3-HAA intraperitoneally (i.p.) once a day for 4 days. The lower dose was similar to that reported previously.[215]

The weight of the mice did not change during the course of the experiment (Figure 10D). On day 5, thymocytes and splenocytes from the mice were counted and stained with antibodies against CD4, CD8 and CD3, then analyzed by flow cytometry, gating on propidium iodide negative (live) cells (Figure 10A and B). The proportions of $CD4^+$, $CD8^+$ or double positive thymocytes in each group were similar, indicating little effect by 3-HAA on thymocytes (Figure 10B). Similar data were seen with splenocytes (Figure 10A). These data contrast with a 45% reduction in $CD4^+/CD8^+$ thymocytes previously reported.[215] In our study, little effect was seen in the total thymic cell numbers with either dose of 3-HAA compared with the vehicle group (Figure 10C), compared with the 75% reduction previously reported.[215] A small reduction in the number of splenocytes was observed with the highest dose of 3-HAA (Figure 10C). These data suggest that, at least by i.p. injection, administration of 3-HAA does not have a deleterious effect on naïve lymphocytes *in vivo.*

After establishing that 3-HAA is not as toxic to thymocytes *in vivo* as reported, we wanted to see whether a reduction by 3-HAA in the serum kynurenine levels could be measured when endogenous IDO was induced in LPS matured DCs *in vivo*. There was an increase in kynurenine levels in the sera in mice injected with LPS, but no reduction when 3-HAA was used in conjunction with LPS (Figure 11A). Tryptophan levels did not vary considerably between the groups. We also tried measuring 3-HAA in the sera but

due to its similar retention time in the C18 HPLC column with an unknown component in the serum, we were unable to measure its concentration reliably.

We then went on to study whether a significant increase could be detected in the serum kynurenine levels in mice that had been injected with IDO+ tumour cells. If detectable, it would enable us to test the efficacy of 3-HAA and/or other inhibitors on these tumours and on the kynurenine levels in the serum. C57BL/6 mice were injected subcutaneously with $5x10^5$ cells of EG7 OVA wt, EG7 OVA GFP-transfected or EG7 OVA IDO-transfected cells and the tumours were grown for 7 days. On day 8 the sera were run on the HPLC. There was a significant increase in kynurenine levels in the sera of mice with IDO+ tumours (Figure 11B) and tryptophan levels did not change significantly between the groups.

Following the finding that IDO+ tumours produce a measurable increase in the kynurenine levels in the sera compared to IDO- tumours, we tried to see whether we could see a reduction in kynurenine levels when the mice had IDO+ tumours and were given 3-HAA. In addition to the difficulties in detecting 3-HAA in the serum, the tumours did not grow consistently within the groups (Figure 12A). Tumours that did not grow were GFP+PBS (GFP 3 in Figure 12A), GFP+ 3-HAA (GFP 4), IDO^+ +3-HAA (IDO+ 2), and IDO^+ +PBS (IDO+ 4 and 5) and these were left out of the analysis to prevent false negative/positive results. We were, nonetheless, able to measure kynurenine and tryptophan levels in the blood of the tumour-bearing mice before and after PBS and 3-HAA injections.

The levels of kynurenine in mice injected with IDO+ tumour cells were significantly higher than in mice injected with IDO- tumours, therefore agreeing with our previous results (Figure 11B). There was, however, no reduction in kynurenine levels in mice with IDO+ tumours injected with 3-HAA, indicating that any inhibition by 3-HAA cannot be seen with this method. Tryptophan levels did not vary significantly between the groups. Overall, IDO+ tumours increase the levels of kynurenine in the serum consistently but the addition of 3-HAA does not decrease them. As we cannot, however, be certain of the levels of 3-HAA in the serum because of the difficulties with measuring

it, we cannot be sure whether it has reached the bloodstream in high enough concentration to have any effect on IDO.

2.3.8 Purification and crystallisation of IDO

The premise that 3-HAA is a potent IDO inhibitor warranted structural work with IDO. All this was done prior to the finding that IDO inhibition by 3-HAA may be mediated by H_2O_2. We tried crystallisation with IDO in both pET21b and pET15b vectors. In both cases, the protein was expressed in BL21 cells and was purified successfully (Figure 13A and B). The full length human IDO had initially been cloned into a pET21b vector and this was used for initial crystal screening. Only one possible protein crystal was obtained from these screens, which included co-crystallisation with 3-HAA and/or 1-MT (L) or the enzyme alone. The possible crystal was IDO only in a reservoir solution containing 20% w/v PEG 6000, 100 mM MES pH6 and 10 mM ZiCl. No inhibitor was present. The needle crystal was, however, too small for diffraction studies and further attempts with similar conditions failed to produce more crystals. The pET21b vector did not contain a specific a cleavage site for the histidine tag and therefore all screens were performed with the uncleaved protein. In order to cleave the His-tag off and to emulate the conditions in which IDO has previously been crystallised in, it was cloned into the pET15b vector, which contains a thrombin site for his-tag cleavage. One attempt has been made with the cleaved IDO from this construct but no protein crystals were formed. We attempted co-crystals with 3-HAA and crystals with apo-enzyme.

As we have not been able to get diffractive crystals of IDO alone or with either 3-HAA or 1-MT (L), we went on to do *in silico* modelling using the available crystal structure of IDO and these molecules. This was done with the generous help from Thomas Bowden of the Structural Biology group at the University of Oxford. We docked the already co-crystallised inhibitor 4-phenylimidazole as the control and modelled tryptophan and 1-MT (L) binding similarly. The molecules docked in the active site perfectly but as we could not co-crystallise IDO with 1-MT (L), the binding cannot be confirmed. 3-HAA also docked in the active site but this is probably not its real position considering that it does

not inhibit IDO directly. Although, it may be feasible that 3-HAA was in the active site and the H_2O_2 was formed while it was there reacting with the molecular oxygen bound to the heme group. This would have to be confirmed with a co-crystal of IDO and 3-HAA which we unfortunately were not successful in obtaining.

2.4 Discussion

In this chapter we have studied the characteristics of the tryptophan metabolite 3-hydroxyanthranilic acid (3-HAA) as an IDO inhibitor. 1-methyl tryptophan in its racemic mix or as the L-isomer is the most well known and used IDO inhibitor. It is not, however, very potent with a published K_i of 19 μM for L-isomer and 35 μM for the racemic mix.[191] It also has the added problem of inhibiting tryptophan transport in the cell, thus interfering with the essential amino acid's normal uptake into the cell.[199] We have also discovered that 1-MT (L) is a slow IDO substrate further highlighting the need for better IDO inhibitors. The fact that 1-MT (L) is an IDO substrate was concurrently with our work discovered and published by Chauhan *et al*. who calculated a K_m of 150 μM with the purified 1-MT (L) using human recombinant IDO.[138] In our experiments we could not calculate a K_m as the production of (methyl-)kynurenine did not reach a plateau in our setting. We were able to measure the K_m of tryptophan which was 5-fold lower than that of 1-MT (L) at 29 μM so Chauhan et al. results with 1-MT (L) seem plausible, however they succeeded in reaching a plateau between 400-600 μM 1-MT (L) whereas in our assay the product formed linearly up to 2 mM, which was our highest 1-MT (L) concentration.

There are various IDO inhibitors available whose K_i are in the nanomolar or even picomolar range, but these have either limited usability in whole cells because of problems crossing the cell membrane, or they are complex to extract and have not been tested further yet.[203] Therefore we were interested in looking at IDO metabolites and their derivatives for potential in IDO inhibition. 3-HAA had been previously identified in our laboratory by Samira Lakhal in her thesis as a candidate but we wanted to examine its inhibitory characteristics more closely. With the knowledge that 3-HAA inhibited recombinant human IDO, we compiled a screen that included compounds similar in structure. Some of them are other tryptophan metabolites. The idea that 3-HAA would be a potent IDO inhibitor raised the interesting possibility that the tryptophan metabolites would be able to form a negative feedback loop regulating tryptophan consumption. The premise was good and we went on to look at the kinetics of 3-HAA – mediated inhibition more closely. Previously in preliminary kinetic assay, 3-HAA had

been identified as a competitive inhibitor (DPhil thesis, Samira Lakhal). In our assays, we increased the selection of 3-HAA concentrations and tryptophan concentrations in order to maximise the accuracy of the results. We also identified an appropriate time point for the kinetic assay so as to prevent the lowest substrate concentrations from becoming limiting. We were able to analyse the kinetics and after many repeats and curve fittings, we came to the conclusion that the inhibition mode that 3-HAA displays is not competitive or reversible. This was evident from the Lineweaver-Burke plots that indicated irreversible-type binding and which was confirmed by an assay where excess tryptophan failed to displace 3-HAA and restore IDO activity when it was added in excess after 3-HAA.

The irreversible binding was investigated further by mass spectrometry but we could not locate either an amino acid residue or heme as a position that 3-HAA would have been bound to. Also the inconsistent results from cellular assays in which the inhibition was either mild or non-existent (whole cells) while strong in lysates left us puzzled. This inconsistency was not found to be a cell membrane crossing- related either as we were able to measure 3-HAA inside the cells that had been previously incubated with 3-HAA. The possibility that 3-HAA might react with molecular oxygen forming hydrogen peroxide was raised following an extensive online search for reactions that 3-HAA might be involved in under conditions found in our assay. The possibility was confirmed by research by Morita *et al*.[159] H_2O_2 is a known IDO inhibitor[212] so we decided to look into this possibility.

The media composition for lysate assays and assays with recombinant IDO requires an excess of molecular oxygen to be available along with other co-factors to ensure IDO activation in vitro. The availability of excess O_2 in the in vitro assays therefore made it possible that 3-HAA would react with it and form H_2O_2 resulting in the IDO inhibition we observed. We had also noticed that 3-HAA is toxic to the cells in culture at concentrations above 200 μM. We decided to check whether this toxicity was H_2O_2 - related too. Catalase breaks down H_2O_2 into water and oxygen so it was added to the cell culture media containing otherwise toxic effects of 3-HAA up to 500 μM in terms of number of live cells but also of cell proliferation. At the higher 3-HAA concentrations the

cells survived better but did not proliferate. It is therefore possible that the 3-HAA toxicity is due to the quenching of oxygen and the subsequent accumulation of toxic amounts of H_2O_2. Why this formed H_2O_2 does not result in IDO inhibition inside the cells is not clear, but it could be that it does not get into the cell at high enough concentration to inhibit IDO in the cytosol. When the concentration of H_2O_2 was measured in the assay buffer for lysate and recombinant IDO assays following the addition of 3-HAA, it was clear that there was a dose-dependent increase in the concentration of H_2O_2 which did not happen with 1-MT (L). The formation of H_2O_2 seemed to taper off when more than 200 μM of 3-HAA was added but this may have been due to detection limits.

Even though we had not seen IDO inhibition in the whole cells, we went on to study cells that naturally produce reactive oxygen species on activation, and hypothesised that maybe IDO in these cells could be inhibited by H_2O_2 that is formed by the reaction of superoxide with 3-HAA. These cells maybe more resistant to the effects of H_2O_2 and may allow H_2O_2 to be inside the cell or let it in, where it would then have a chance to inhibit IDO. We were able to see a dose-dependent decrease in kynurenine production by mature THP1 cells that seems to confirm this hypothesis. As mentioned earlier however, 3-HAA is toxic to cells above 200 μM and it is possible that the reduction is due to dying cells. 3-HAA causes the otherwise adherent mature THP1 to float so we counted the number of live and dead cells in the portion. Approximately half of them are alive by trypan blue staining so the reduction in kynurenine may not be due to cell death, even though it is possible that these floating cells are dying and do not have active IDO anymore.

We also studied the effect of 3-HAA in vivo early on. IDO has been reported toxic *in vivo* by earlier studies[215] but we did not notice cell death at the same level with the same dose they used (around 0.3 mg/mouse) or with a 10-fold higher one. We were able to get clear measurements of kynurenine in the bloodstream of mice injected with LPS or mice that had a palpable IDO+ tumour. This provided a good basis for testing the efficacy of 3-HAA *in vivo*. We grew IDO+ tumours in mice and injected them with 3-HAA a day before taking blood and measuring it for kynurenine. We could not see any reduction in kynurenine levels, which could be due to blood-taking so close to the 3-

HAA administration. Alternatively, in the light of the results from the in vitro assays and the discovery of the link with H_2O_2, 3-HAA may not be a sufficiently potent inhibitor and will not reduce kynurenine levels when administered systemically in vivo. It is an immunomodulatory molecule[216,159,215] so any therapy with 3-HAA will have to take those effects into account. The effect of 3-HAA on IDO has now been discovered by others[217] too but the mechanism for the inhibition that we have discovered elucidates the reasons for its inconsistent potency in different systems, and also potentially why Lopez *et al*. saw IDO inhibitory activity with 3-HAA in macrophages but not in monocytes.

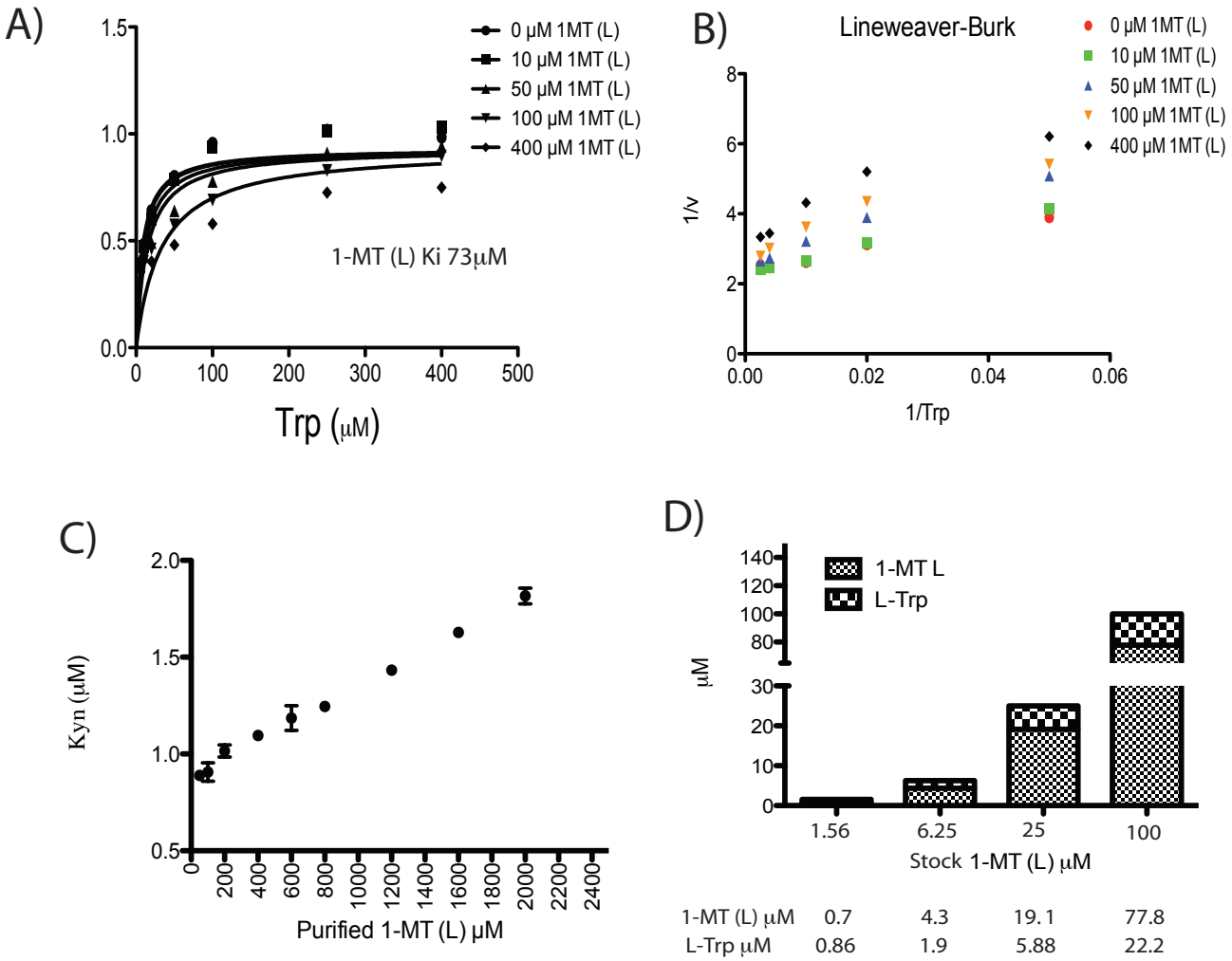

Figure 1. 1-methyl tryptophan is an IDO inhibitor but also a weak IDO substrate. A) Recombinant human IDO was incubated with tryptophan for 3 minutes at 37 Celsius. The conversion of Trp into kynurenine was measured by HPLC. Error bars represent standard deviations of duplicate samples. Ki for 1-MT (L) was 73µM. Km for tryptophan was also calculated to be 29µM when 1-MT (L) was absent. **B)** Figure A data represented as a Lineweaver-Burke plot. **C)** Kynurenine produced when purified 1-MT (L) was used as substrate for rhIDO. Assay performed for 1 hour at 37 Celsius.
D) 1-MT (L) stock contains approx. 23% tryptophan as a contaminant so 1-MT (L) has to be purified prior to any assay that uses it as an IDO substrate. The numbers below show the amount of 1-MT (L) and tryptophan in each "1-MT (L)" -sample.

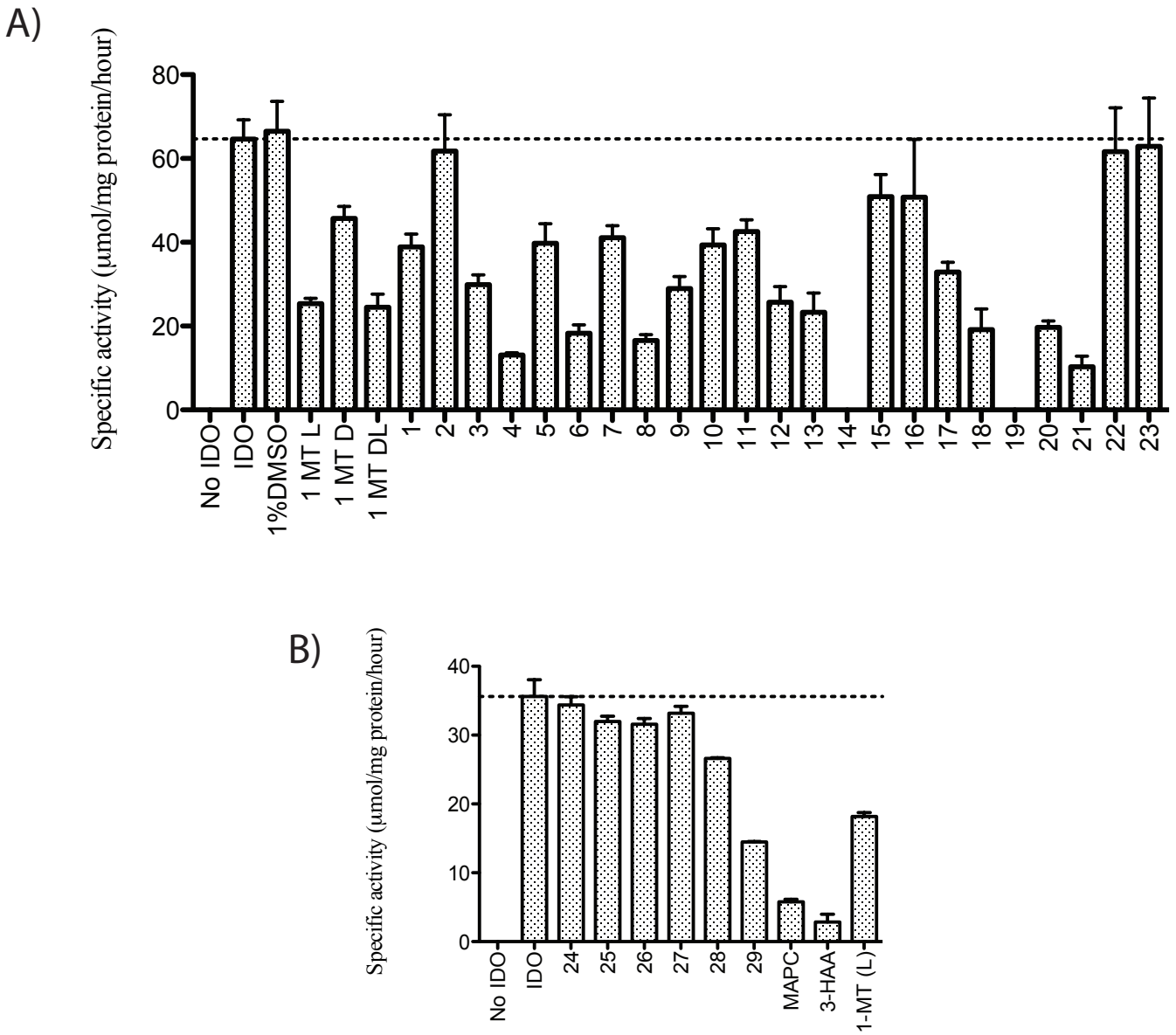

Figure 2. Inhibitor screen for IDO inhibition. A) Initial screen with 23 new candidates and B) smaller screen with compounds similar to compound 14. Each compound was added at 1mM and the enzyme reaction run for 1 hour at 37 Celsius. Error bars represent standard deviations of triplicate samples.

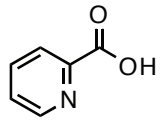

1. Picolinic acid

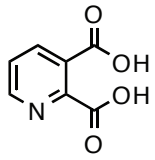

2. Quinolinic acid

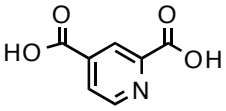

3. 2,4-pyridinedicarboxylic acid

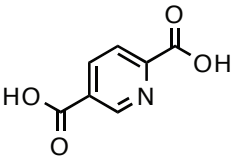

4. 2,5-pyridinedicarboxylic acid

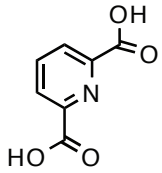

5. 2,6-pyridinedicarboxylic acid

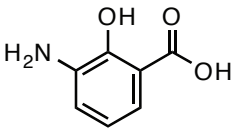

6. 3-aminosalicylic acid

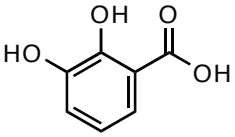

7. 2,3-dihydroxybenzoic acid

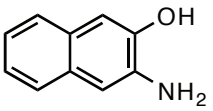

8. 3-amino-2-naphthol

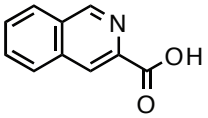

9. 3-isoquinolinecarboxylic acid

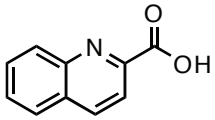

10. Quinaldic acid

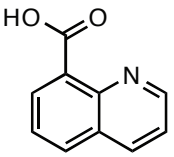

11. Quinoline-8-carboxylic acid

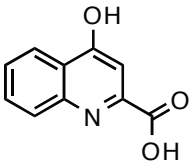

12. Kynurenic acid

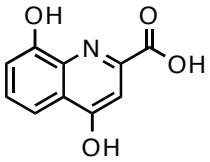

13. Xanthurenic acid

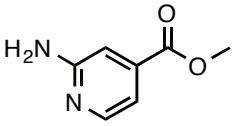

14. Methyl 2-aminopyridine-4-carboxylic acid

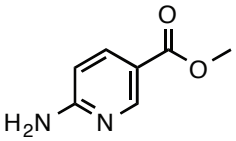

15. 6-aminonicotinic acid methyl ester

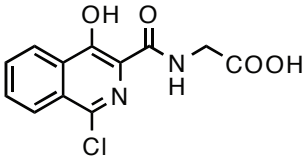

16. FG2216

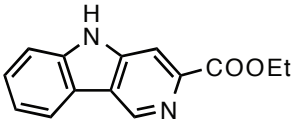

17. Ethyl 9H-pyrido[3,4-b]-indole-3-carboxylate

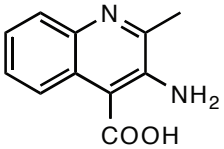

18. 3-amino-2-metylquinoline-4-carboxylic acid

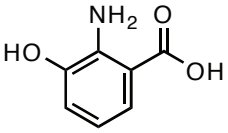

19. 3-hydroxyanthranilic acid

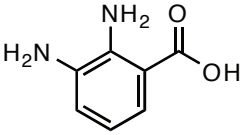

20. 2,3-diaminobenzoic acid

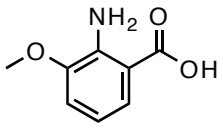

21. 2-amino-3-methoxybenzoic acid

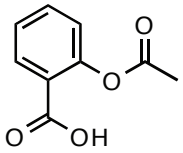

22. Acetylsalicylic acid

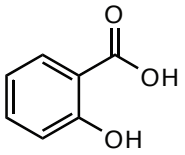

23. Salicylic acid

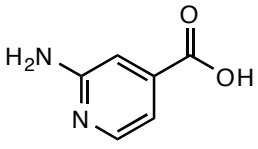

24. 2-aminopyridine-4-carboxylic acid

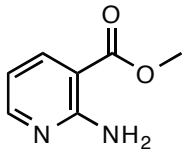

25. 2-aminonicotinic acid methyl ester

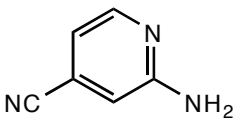

26. 2-amino-4-cyanopyridine

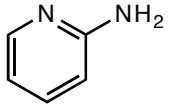

27. 2-aminopyridine

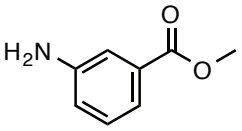

28. Methyl aminobenzoate

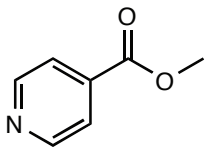

29. Methyl isonicotinate

Figure 3. List of compounds screened for IDO inhibition.

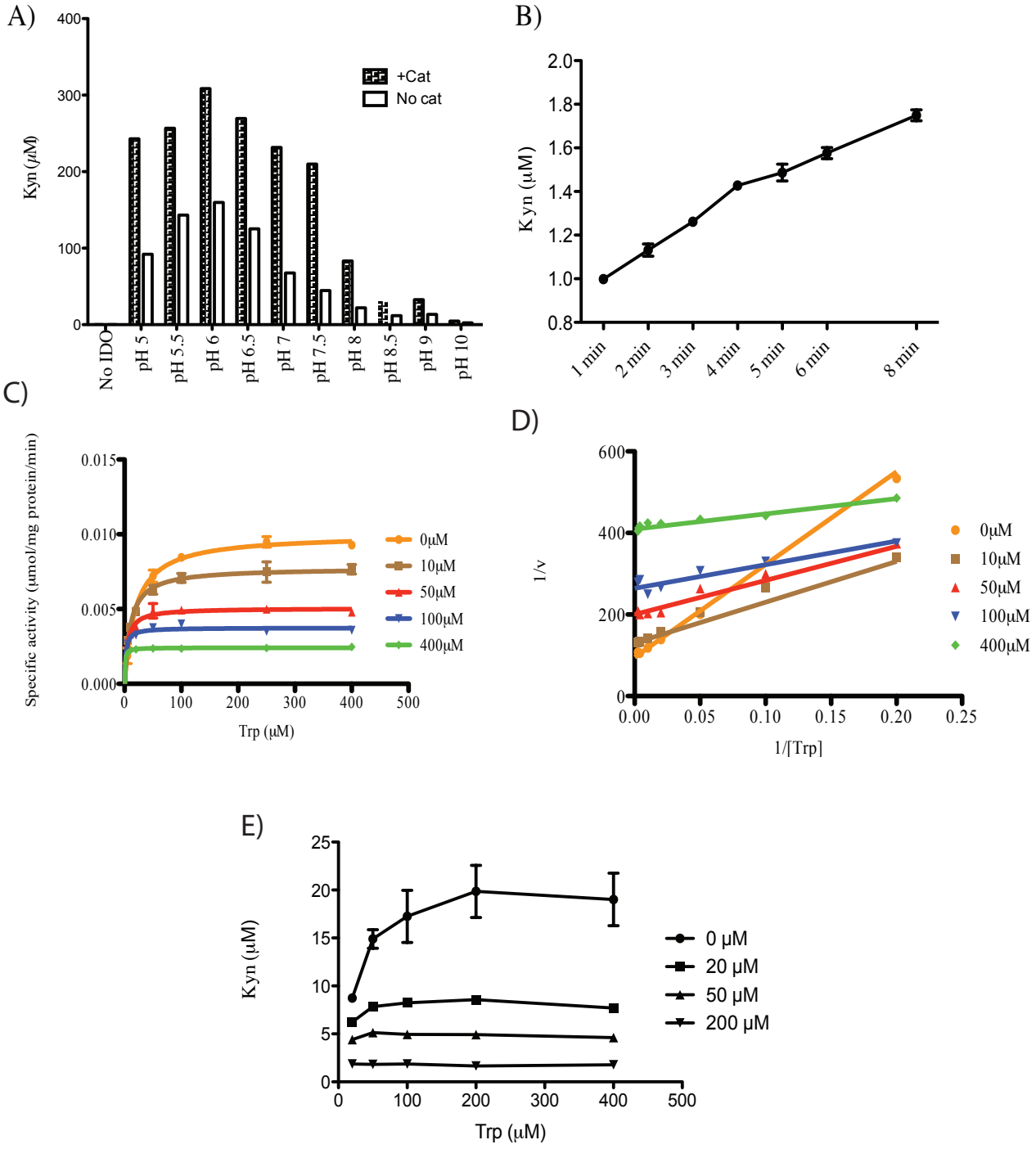

Figure 4. IDO enzyme kinetics with 3-HAA. A) A pH curve with and without catalase in the incubation media that activates IDO. B) Time-course curve with 5μM of Trp to establish an appropriate time point to use in the kinetic experiments (3 min was chosen). C) Inhibition curve for 3-HAA with mixed inhibition curve fitting at various concentrations of 3-HAA. D) Lineweaver-Burke plot of the same data as in C showing a characteristic fitting for an irreversible inhibitor. E) 3-HAA is possibly an irreversible inhibitor. IDO was pre-incubated with various concentrations of 3-HAA for 10 min followed by the addition of tryptophan. The increasing levels of Trp did not rescue enzymatic activity indicating irreversible inhibition by 3-HAA. All error bars represent standard deviations.

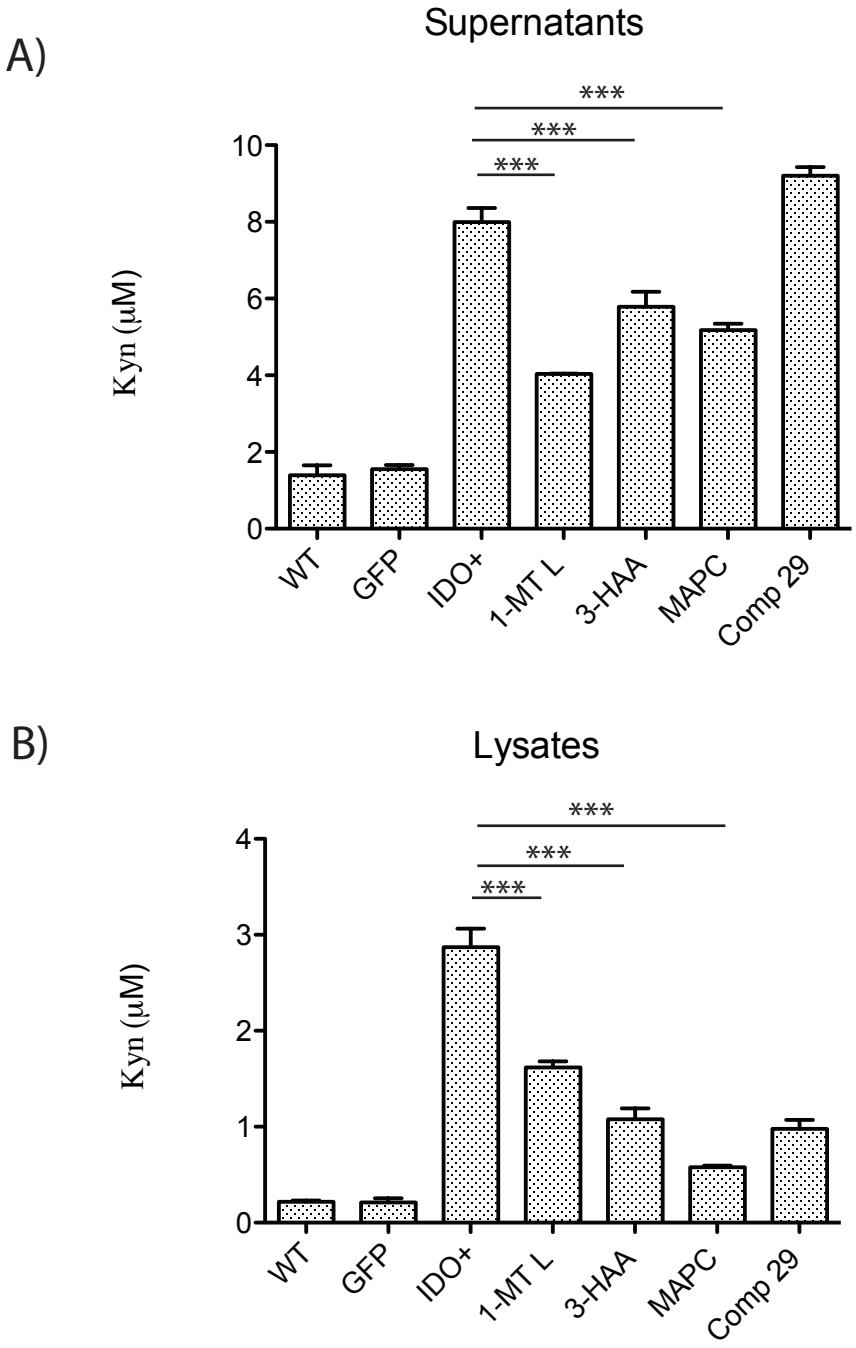

Figure 5. 3-HAA inhibits IDO in cell lysates and variably in whole cells. A) EG7 cells were incubated for 48h in R10 in the presence of the inhibitor at 500μM and the supernatant measured for kynurenine by HPLC. B) The lysate assay was done with identical numbers of lysed EG7 cells and the assay run for 1 hour at 37 C in the presence of 1mM of inhibitor. The statistical analysis was done with 1-way ANOVA ($p<0.05$). Errors bars are standard deviations.

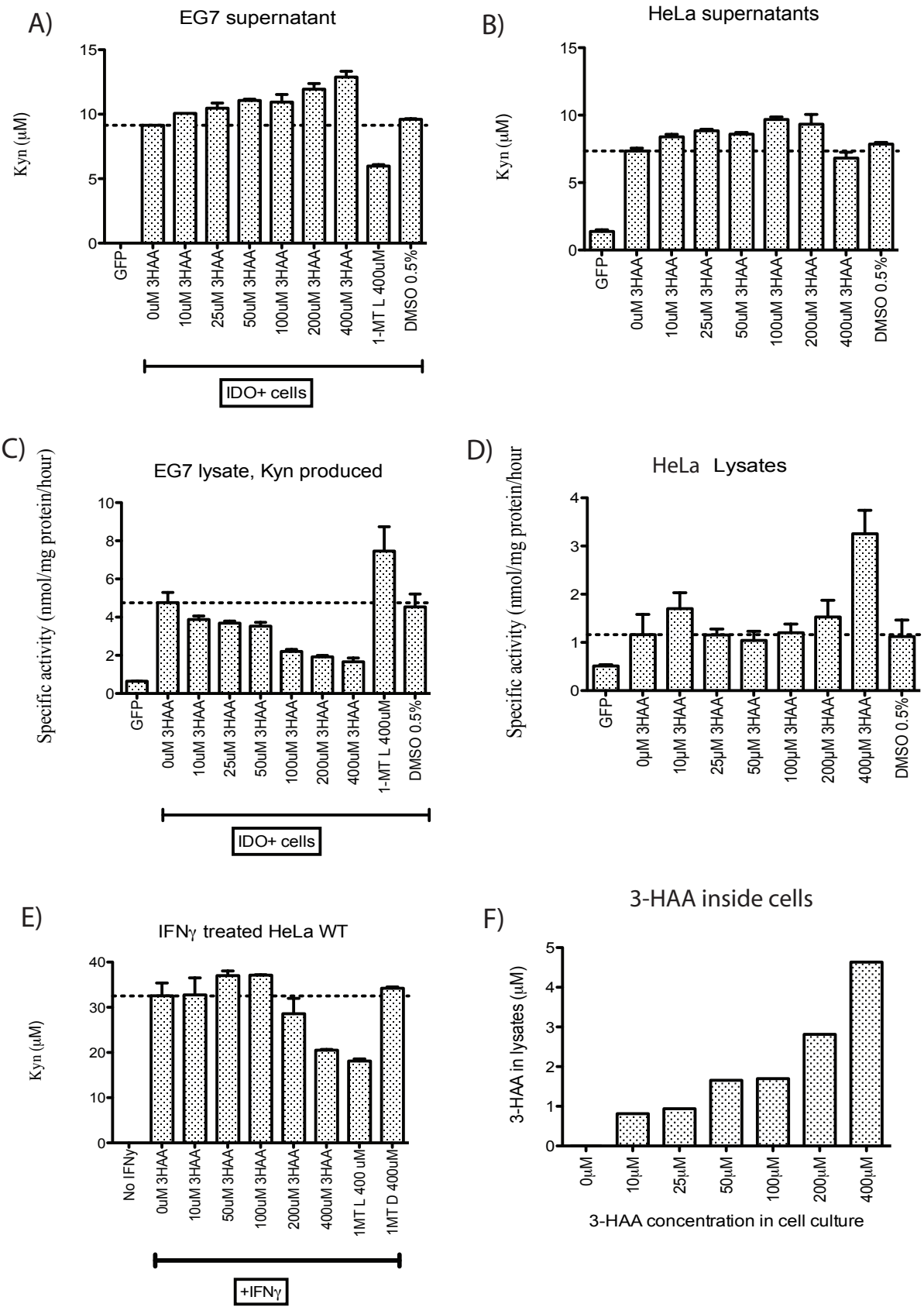

Figure 6. 3-HAA inhibits IDO in EG7 lysates but not in whole cells. 3-HAA in EG7 and HeLa cells after 48h. A) EG7 supernatant. B) HeLa supernatant. C) EG7 lysates. D) HeLa lysates. E) HeLa wt cells treated with 1000u/ml IFNγ for 48h. Supernatant measured. F) 3-HAA concentration in EG7 lysates after 48h incubation of cells. All error bars are standard deviations.

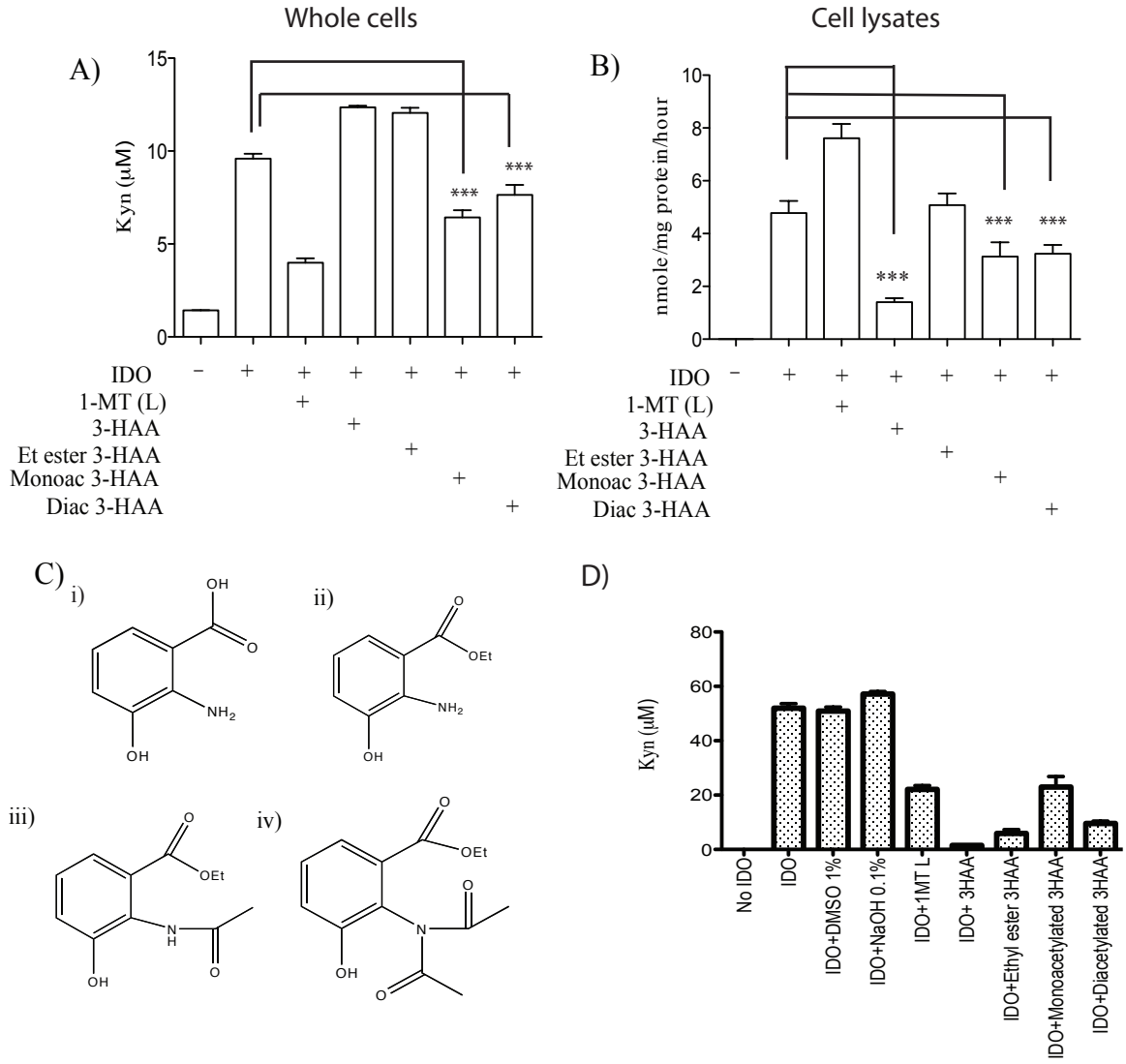

Figure 7. 3-HAA derivatives inhibit rhIDO activity and IDO in whole cells and lysates.
A) Inhibition of IDO activity in whole cells. Assay run for 48h with 500μM of inhibitor except for ethyl ester 3-HAA which was at 100μM due to toxicity. B) Inhibition of IDO in cell lysates. Inhibitors at 1mM. C) Structures of the 3-HAA derivatives, i) 3-HAA, ii) ethyl ester 3-HAA, iii) monoacetylated 3-HAA, iv) diacetylated 3-HAA. D) IDO inhibition in an rhIDO assay, inhibitors at 1mM. Statistical analysis 1-way ANOVA $p<0.05$. Errors are standard deviations.

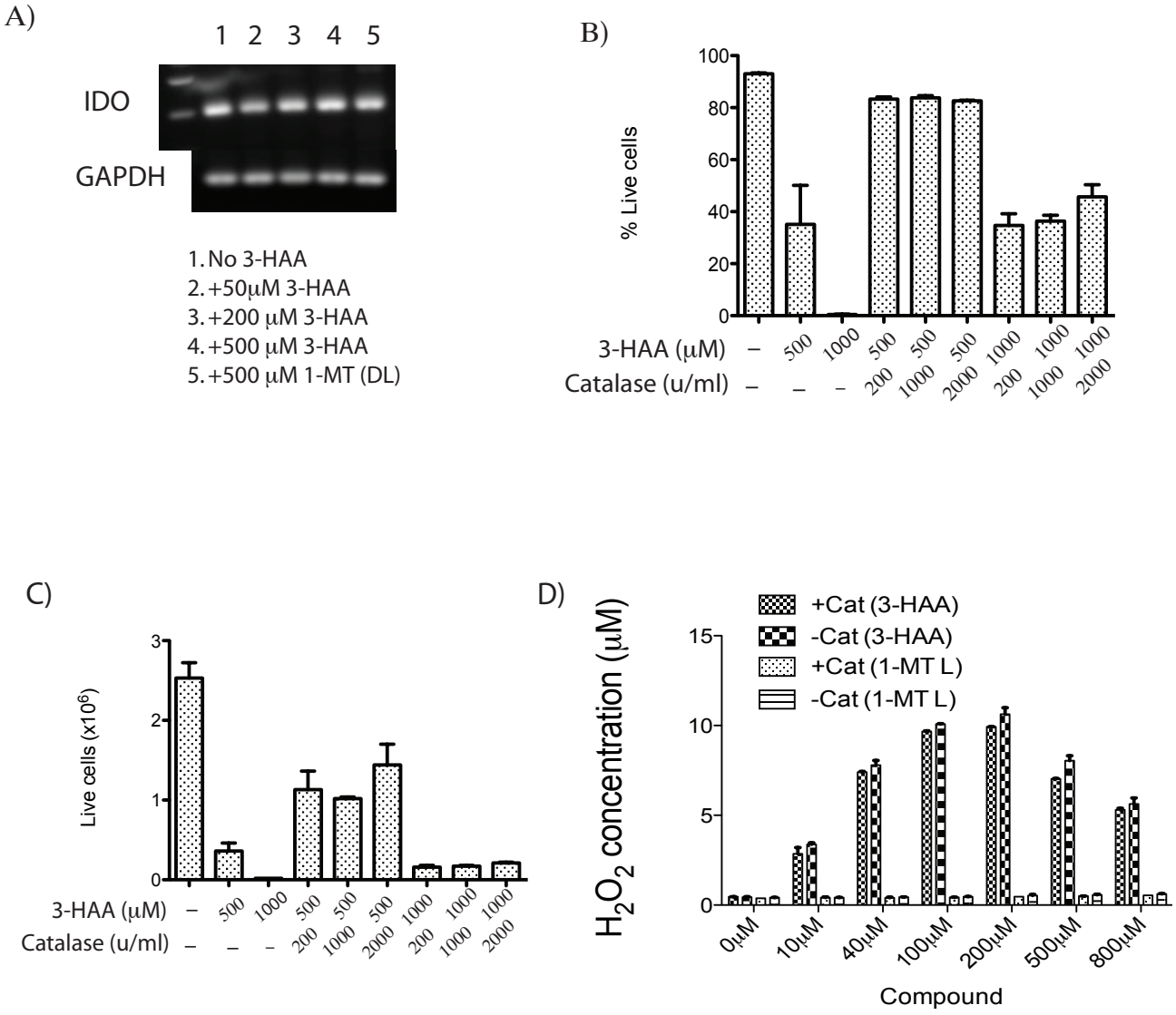

Figure 8. **3-HAA produces H2O2 in assays but its toxic effects can be reduced with the addition of catalase.** A) Effect of 3-HAA on IDO expression by PCR. B) Percentage of live cells when 3-HAA is at 500μM or 1mM and catalase at 200 u/ml, 1000 u/ml or 2000 u/ml. C) Total cell numbers after 48h in culture. Assay was started with 500 000 cells. D) Hydrogen peroxide concentration in assay media after the introduction of various amounts of 3-HAA. Error bars represent standard deviations.

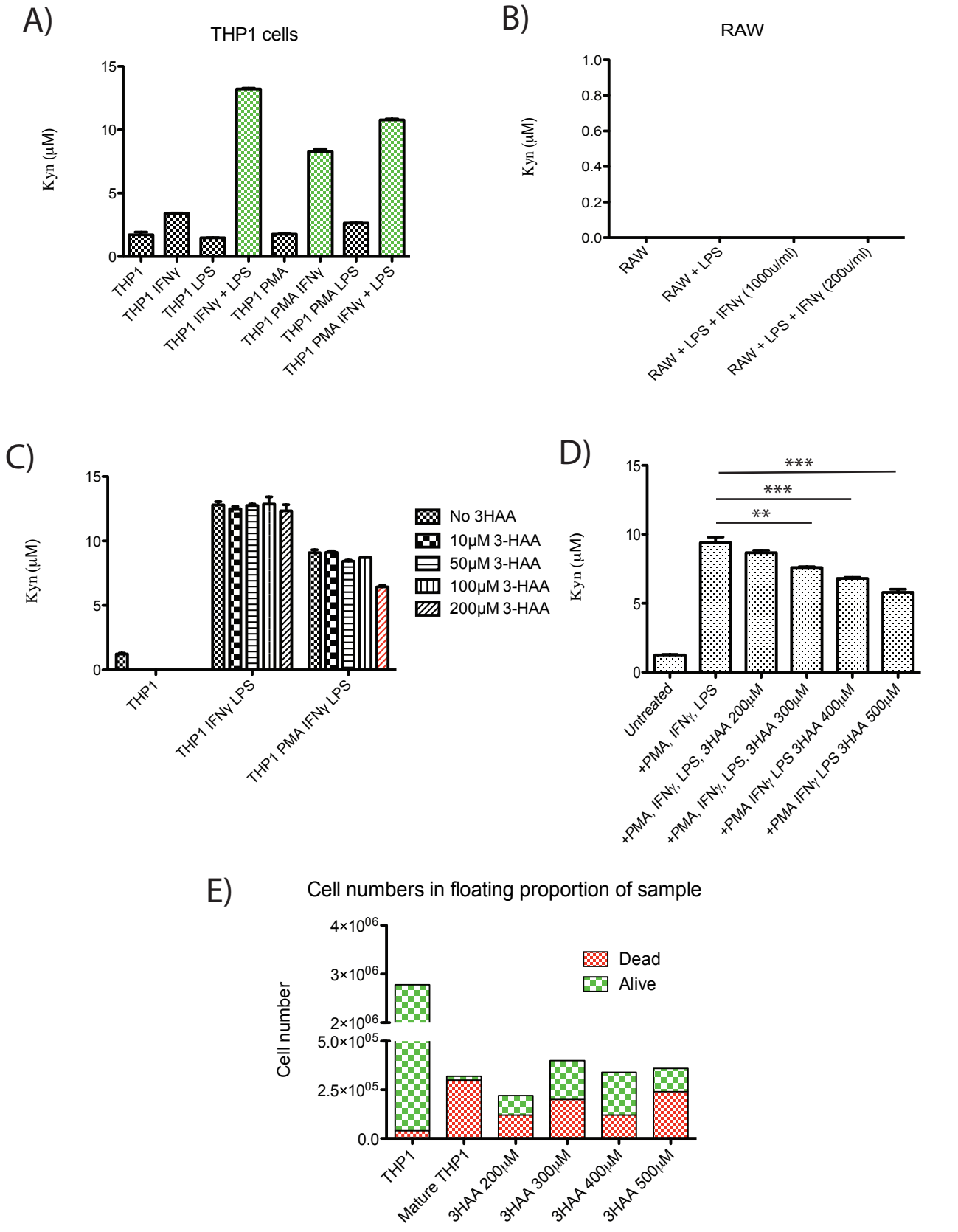

Figure 9. 3-HAA reduces IDO activity in activated THP1 cells. A) An appropriate maturation cocktail was seleceted for maximum IDO activity in THP1 cells. IFNγ 1000u/ml, LPS 20µg/ml, PMA 16nM. B) No IDO activity in RAW cells was detected after maturation. C) Lower range 3-HAA titration in shows inhibition with 200µM of 3-HAA. D) Higher range of 3-HAA concentrations shows a dose-dependent inhibition of kynurenine production. E) 3-HAA causes normally adherent mature THP1 to float and this panel shows the proportions of live and dead cells in the floating portion. Statistics: 1-way ANOVA $p<0.05$, error bars are standard deviations.

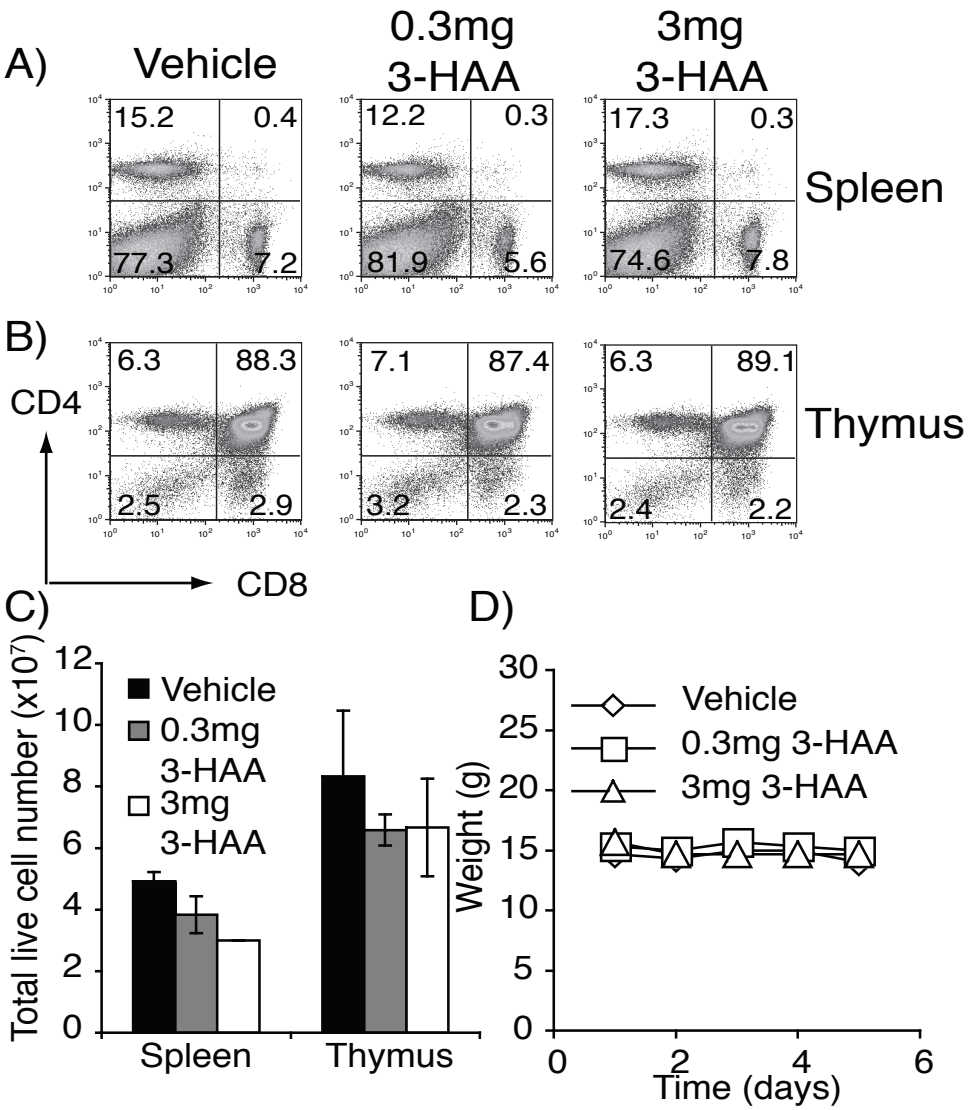

Figure 10. **T-cell apoptosis in vivo by 3-HAA**. A) Effect of 3-HAA on splenocytes and B) thymocytes after 5 days and four injections of 3-HAA (once a day). C) Total cell numbers in the spleen and thymus after 5 days. D) Weights of the mice throughout the experiment. Error bars are standard deviations.

-

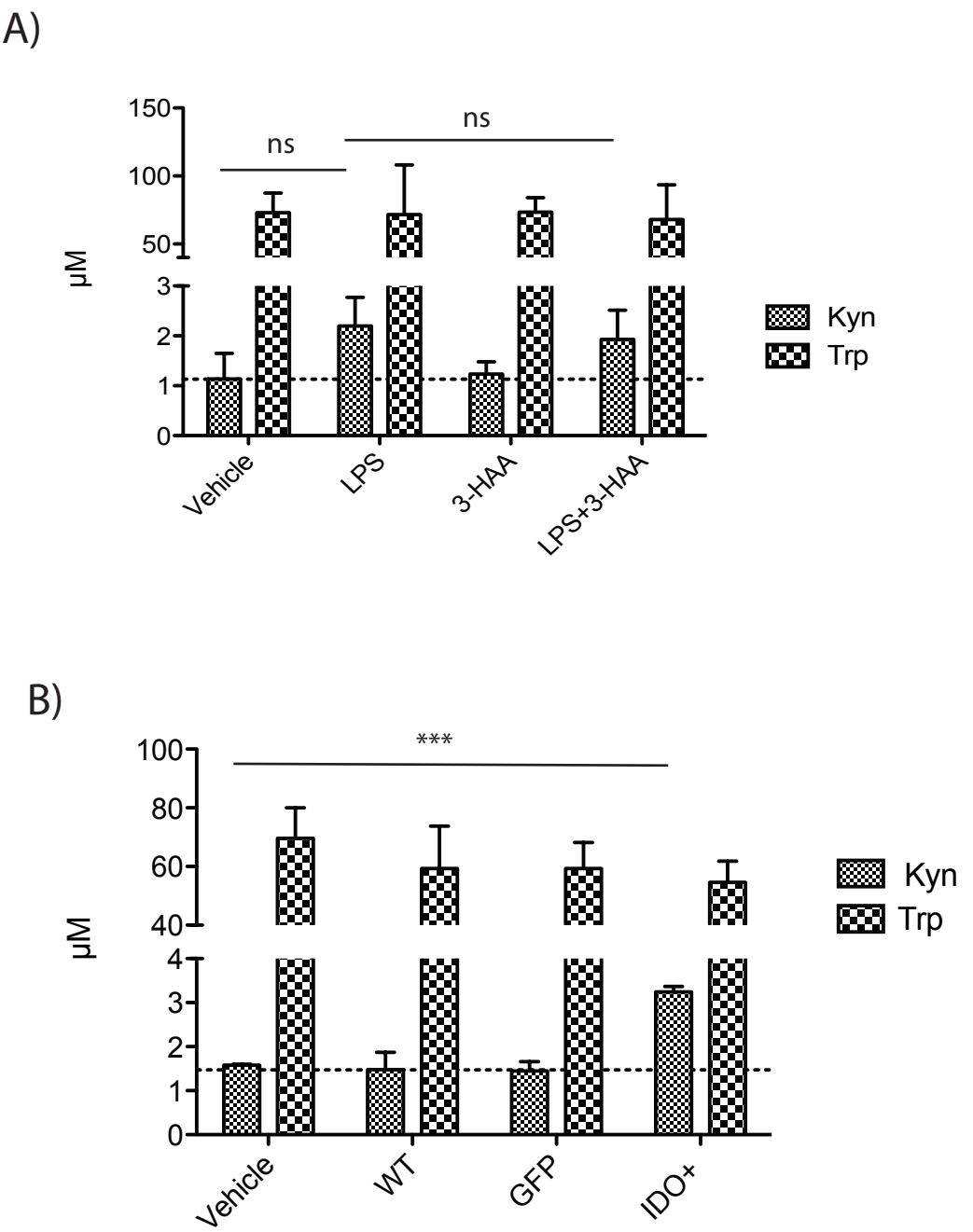

Figure 11. Kynurenine can be measured in mouse serum 24h after LPS injection or when an IDO+ tumour is present. A) Kynurenine and tryptophan levels in C57BL/6 mouse sera at 24h after injection (i.p.). LPS raises serum kynurenine levels but not significantly and injection of 3-HAA does not reduce the levels. B) IDO+ tumour increases serum kynurenine levels significantly. Statistics: 1-way ANOVA $p<0.05$, triplicate samples, errors standard deviations. Average splenocyte number in A) Vehicle: 56 000 000, LPS: 44 000 000, 3-HAA: 69 000 000, 3-HAA+LPS: 44 000 000.

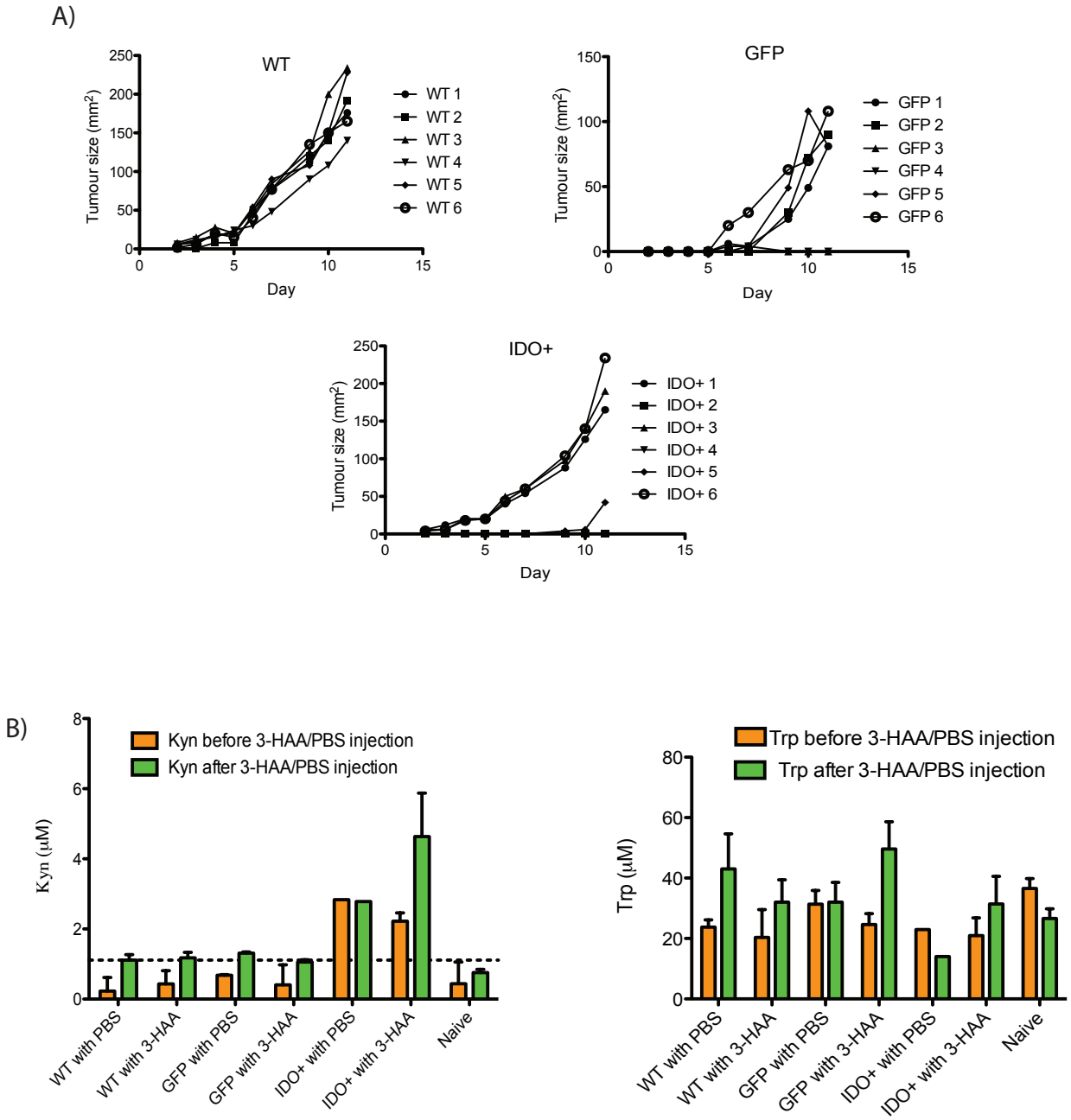

Figure 12. Effect of 3-HAA on blood kynurenine levels when IDO- and IDO+ tumours are present. A) Growth of EG7 tumours in BL6 mice. Only mice that grew tumours were used for measurement of kynurenine and tryptophan levels after 3-HAA and PBS injection. B) Blood levels of kynurenine and tryptophan before and after 3-HAA or PBS injection. Error bars are standard deviations.

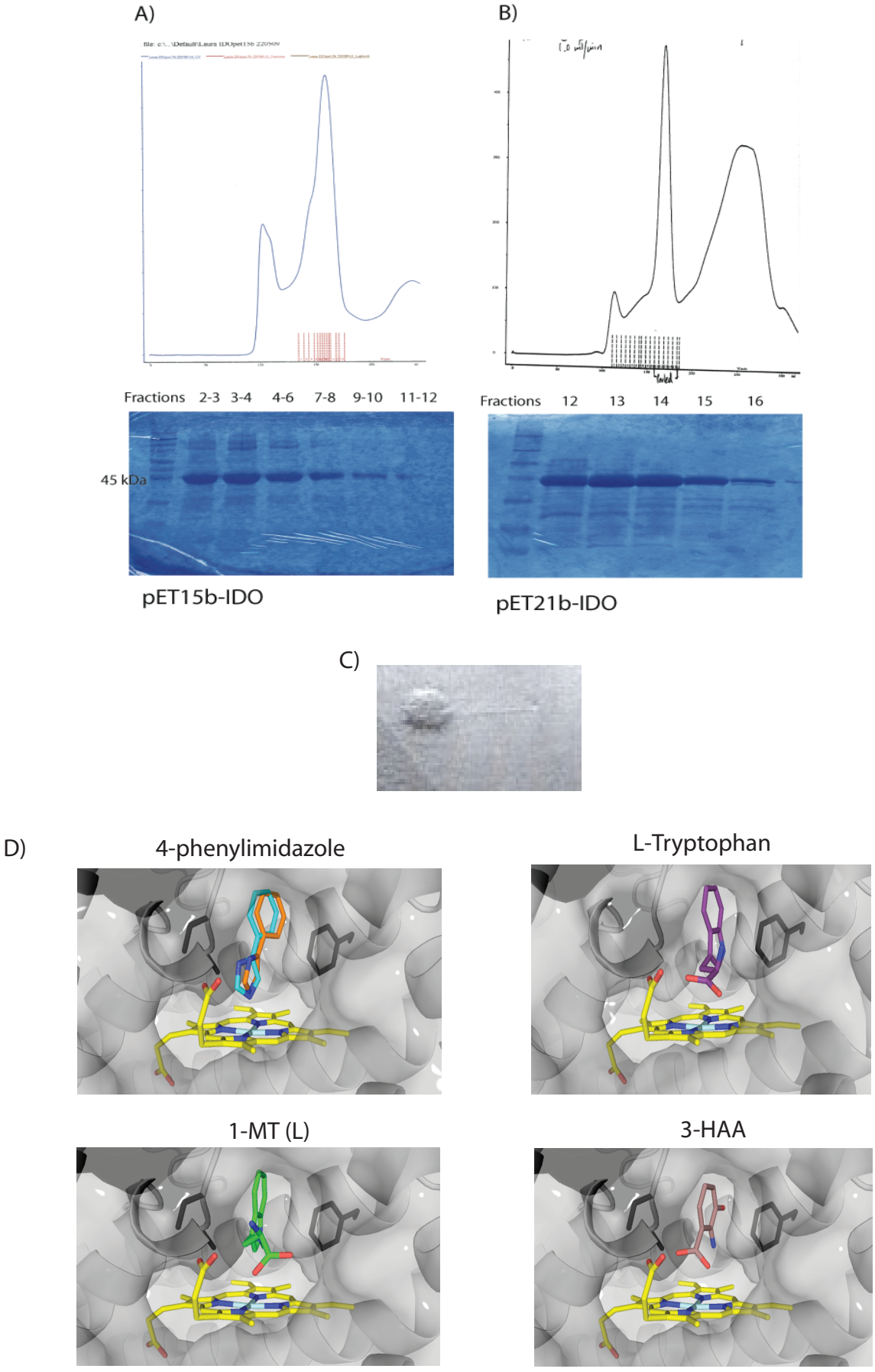

Figure 13. IDO purification, crystallisation and molecular modelling. A) Profile of protein purity when IDO expressed in pET15b, B) Profile of protein purity when IDO expressed in pET21b, C) A potential IDO crystal, too small to analyse, D) Molecular docking/modelling of IDO inhibitors and substrates.

Chapter 3: Effects of tryptophan metabolites on mTOR in T-cells and on T-cell proliferation

3.1 Introduction

Given that IDO is such a potent immunosuppressive enzyme, questions have been raised whether its mechanism of action is more related to the depletion of tryptophan or the accumulation of its metabolites.[218,219,215,220] T-lymphocytes are sensitive to the depletion of tryptophan and their proliferation is stopped by cell-cycle arrest at G1.[219] In addition to cell cycle arrest, the tryptophan starvation can result in to the down-regulation of the TCR complex ζ-chain in CD8+ T cells leading to their impairing their cytotoxic effector function.[71] The combined effects of tryptophan shortage and downstream catabolites of tryptophan can also result in naïve CD4+ CD25- T-cells becoming CD25+ T regulatory cells.[71] It has since become clear that many human tumours take advantage of this by constitutively expressing IDO, probably as one strategy to evade the host immune response.[152] Although the lack of tryptophan has a potent effect on T-cells, recently it has become evident that a few of its metabolites can also have adverse effects on the T-cells. It has been reported that 3-hydroxykynurenine suppresses CD4+ T-cell proliferation and induces T_{reg} development in a corneal transplant model.[160] It also inhibits T-cell proliferation generally in a co-culture of splenocytes and BMDCs.[221] The same study also reported L-kynurenine as capable of T-cell inhibition. 3-hydroxyanthranilic acid and quinolinic acid have also been identified as potent suppressors of T-cell proliferation as they induce apoptosis in the T-cells.[222,215] Apart from T-cells, the metabolites have various other effects on the body such as neurotoxicity and it is due to their multiple physiological roles that we decided to look at the kynurenine pathway more carefully here.

In this chapter we have studied the T-cell suppression caused by the consumption of tryptophan and confirmed that especially 3-hydroxykynurenine inhibits CD8+ T-cell proliferation either mildly or causes the cells' death. It was also the only kynurenine we found that stimulated CD25+ Foxp3+ T_{reg} development. We also examined the effect of these kynurenines on the mTOR activity of CD8+ T-cells in which 3-hydroxykynurenine caused inhibition but it was dependent on the strength of CD8+ T-cell stimulation.

3.2 Materials and methods

3.2.1 Mice

C57BL/6, OT-I (transgenic for T-cell receptor specific for ovalbumin fragment 257-264, SIINFEKL that is presented by MHC class I molecule H2-Kb) and DO11.10 (transgenic for TCR specific for ovalbumin 323-339 that is presented by the MHC class II molecule I-Ad.) mice were bred in the Biomedical Services Unit, John Radcliffe Hospital, and used for *in vitro* experiments under the authority of a U.K. Home Office Project Licence. MHC class I molecules present cytosolic peptides to cytotoxic CD8+ T-cells while the MHC class II molecule presents extracellular proteins digested in lysosomes to CD4+ (helper) T-cells.

3.2.2 Cell culture media

Cell culture media used in this chapter are

R10

RPMI 1640 (Sigma) + 10% FCS + glutamine + penicillin/streptomycin + β-mercaptoethanol (for mouse cells only)

Trp/FCS-free media (T0)

RPMI 1640 without tryptophan (Custom order from HyClone) and added FCS, contains glutamine, penicillin/streptomycin and β-mercaptoethanol

T10

RPMI 1640 without tryptophan + 10% FCS, glutamine + penicillin/streptomycin + β-mercaptoethanol

3.2.3 Amplification of kynurenine pathway enzymes from human tumour cell lines by PCR

The following human tumour cell lines were cultured in minimum essential media (Sigma) for 48h with or without 1000u/ml of human recombinant IFN-γ (Peprotech): Cervical cancer HeLa, epithelial carcinoma A431, melanoma Dx3, acute monocytic leukaemia THP1, breast cancer SKBR23, glioblastoma U87MG, pancreatic adenocarcinoma HPAF, and colon adenocarcinoma HCA7.

After 48h, cell culture media was taken off and cells lysed and RNA extracted with RNeasy kit (Qiagen). cDNA was made from an equal amount of RNA from each sample with Retroscript kit (Ambion). Each enzyme was amplified with Phusion DNA polymerase in the following reaction: Water 28µl, HF buffer 10 µl, dNTPs 0.5 µl, forward primer 5 µl, reverse primer 5 µl, cDNA 1µl, Phusion polymerase 0.5 µl. The PCR cycling was as follows: 2 min 95 ^{o}C, (30s 95 ^{o}C, 15s 57 ^{o}C, 30s 72 ^{o}C) x30, 5 min 72 ^{o}C. The following primers were used:

Enzyme	Primer sequence	Product (bp)	Accession
Indoleamine 2,3-dioxygenase (IDO)	Fwd 5' – ACC ACA AGT CAC AGC GCC -3' Rev 5' – CCC AGC AGG ACG TCA AAG -3'	618	NM_002164.5
Tryptophan 2,3 – dioxygenase (TDO)	Fwd 5' – GGC AGC GAA GAA GAC AAA TC -3' Rev 5' – GTG CAT CCG AGA AAC AAC CT -3'	285	NM_005651.2
Kynurenine arylformamidase (Afmid)	Fwd 5' – GAA GCC TTG CCT TTC TTC CTT -3' Rev 5' – TCC CTT GTT GCT TGG ATA CC -3'	216	NM_001145526

Kynurenine transaminase 1 (KATI)	Fwd 5' – TCG AAC CCT TTT TTG ACT GC -3' Rev 5' – CTG CTC CCG TTC AAA GCT CT -3'	527	NM_001122672.1
Kynurenine transaminase 2 (Aadat, KATII)	Fwd 5' – AGC TGG CAT GTT TCT ATG GA -3' Rev 5' – AAG TGG TTC AGG GAA ATT GC -3'	?	
Kynurenine hydroxylase (Kmo, KynOH)	Fwd 5'- GAC TAT TCC ACC TAA GAA CGG AGA -3' Rev 5'- ACA GGA AGA CAC AAA CTA AGG TCG -3'	530	NM_003679.3
Kynureninase (Kynase)	Fwd 5'- GAT GAG GAA GAT AAG CTG AGG C -3' Rev 5'- CTT AAG GTT TCT TCC CCC TCT -3'	500	NM_001199241.1
3-hydroxyanthranilate 3,4 –dioxygenase (3-HAO)	Fwd 5'- GAG GGC CTT CTT GGT GTG -3' Rev 5'- CAT TGA TTG GTT GTG AGT GG -3'	520	NM_012205.2
Picolinic acid carboxylase (Acmsd)	Fwd 5' – ACC ACC ATA GCC ATT TGC TC -3' Rev 5' – ACA GCT TGA GGG ACA GAG GA -3'	235	BC016018
Quinolinate phosphoribosyltransferase (QPRT)	Fwd 5'- GGT CAC AGG AGC AGC AGG -3' Rev 5'- AAG CCA GAG GAG CTG CAC -3'	?	

3.2.4 Western blotting for phospho-S6, phospho-eIF2 and β-tubulin

Cells were lysed with lysis buffer for phosphoproteins consisting of the following: 50 mM Hepes pH7.5, 100 mM NaCl, 10 mM EDTA, 1% Triton X-100, 4 mM Sodium pyrophosphate, 2 mM sodium vanadate, 10 mM sodium fluoride, ¼ Roche protease inhibitor tablet/5 ml and 1.5 mM Pefabloc (Sigma). Made up with ice cold PBS. The lysates were collected and spun for 15 min at 13000 rpm at 4 ^{o}C.

The protein content in the samples was then measured with a BCA assay and an equal amount loaded into a NuPAGE 4-12% Bis-Tris gel. The gel was run in reducing conditions (DTT 40 μM/sample, MES buffer (Invitrogen)) at 200 V for 35 min and then transferred sandwiched with a nitrocellulose membrane onto a semi-dry blotting apparatus. The protein transfer was run at 18 V for 40 min. The membrane was then blocked with 5% w/v BSA in 0.1% v/v Tween 20-PBS for 1 hour at room temperature. The membrane was then placed into a solution containing the rabbit anti-mouse pS6 antibody (Cell Signalling, 1:3000 in 5% w/v BSA, 0.1% Tween-PBS). The membrane was kept in the primary antibody on a roller overnight at 4^{o}C. Any unbound antibody was then washed off for 3x5 min with 0.1% Tween-PBS. An anti-rabbit secondary antibody with conjugated HRP was then added at 1:10000 in 5% w/v BSA, 0.1% Tween-PBS and incubated for 1 hour at room temperature. The secondary antibody was then washed off with 0.5% Tween-PBS for 5min and for 2x5 min with 0.1% Tween-PBS. The membrane was then treated with Pierce SuperSignal chemilumenescent substrate for imaging of the blot.

3.2.5 Splenocyte preparation from whole spleen

A whole spleen was mashed with the plunger end of a 1 ml syringe through a cell strainer and the strainer rinsed with R10. The cells were spun down for 5 min at 1500 rpm and the supernatant discarded. The cells were resuspended in 2 ml of red blood cell lysis buffer (Qiagen) and 8 ml of R10. The suspension was then spun down as above

and the supernatant discarded. The cells were then resuspended in the desired media and were ready to use or to be further purified.

3.2.6 Carboxyfluorescein succinimidyl ester (CFSE) -staining for cell proliferation assays

Cells were washed twice in PBS and then resuspended in PBS at 1-2x10^6/ml and 0.5 µM CFSE added. The solution was kept at room temperature for 8 min. To quench the CFSE stain, an equivalent volume of FCS was added to the solution and the cells spun down for 5 min at 1500 rpm. The supernatant was discarded and 10 ml of warm R10 added and the solution transferred to a new 15 ml Falcon tube. This was repeated twice. Finally the cells were resuspended in a desired volume of the media of choice. CFSE was purchased from eBioscience. When used in cell proliferation assays, the CFSE stain halves with every cell division making it useful in measuring cell proliferation.

3.2.7 Cell Tracker Orange (CTO) –staining

Cells were washed in R10 and resuspended in R10 at 2x10^6/ml. The CTO stain was added at 2 µM, the cells vortexed to mix the dye and incubated for 20 min at 37 ^oC. The cells were then spun down for 5 min at 1500 rpm and resuspended in fresh warm R10 and incubated for further 20 min at 37 ^oC. The suspension was then spun again and the cells washed twice in R10 and resuspended in desired volume and media. The CTO stain was purchased from Invitrogen.

3.2.8 Cell surface staining protocol

Cells were transferred into a round-bottom 96-well plate and spun down at 1500 rpm for 5 min. The supernatant was either collected or discarded and the cells washed with PBS containing 0.5% FCS or with pure PBS. The fluorescence-conjugated antibodies or

other dyes were then added at appropriate concentrations in 40 µl of PBS/sample and incubated on ice in the dark for 20 min. 150 µl of PBS was then added and the cells spun down. The cells were washed once in PBS and then resuspended in desired volume of PBS (or PBS-0.5% FCS) for FACS analysis.

3.2.9 Intracellular/intranuclear staining protocol

Cells were transferred into a round-bottom 96-well plate and spun down at 1500 rpm for 5 min. The supernatant was collected and cells washed in PBS. If cell surface staining was required, it was done at this point as in 3.2.8. If the cells were to be stained intracellularly, after the surface stain the cells were washed and resuspended in 100 µl/well of IC Fixation buffer (eBioscience) and incubated for 1 hour on ice in the dark. After fixing 100 µl/well of PBS was added and the cells spun down. Permeabilisation buffer (made up in water from 10x stock, eBioscience) was then added at 200 µl/well and the cells spun down. The antibodies for intracellular staining were then added in 50 µl of permeabilisation buffer and incubated for 20-30 min on ice in the dark. After incubation 100 µl/well of permeabilisation buffer was added and the cells spun down. The cells were then washed in 150 µl of permeabilisation buffer. If the primary intracellular antibody was not conjugated to a fluorescent dye, a secondary antibody with a dye was added at this point in 50 µl/well of permeabilisation buffer. The cells were then incubated on ice in the dark for 20-30 min and then washed in permeabilisation buffer after which they were ready for analysis. If the staining was intranuclear, it was done similarly apart from the fixation step which was instead done with Foxp3 fixation/permeabilition buffer (eBioscience) and the incubation on ice was only for 30 min. For Foxp3 staining, no secondary antibody was needed so the cells were ready to use after the primary intranuclear stain.

3.2.10 T-cell proliferation assays and FACS-based mTOR assays

Experiments were started with 200 000 splenocytes/well in 96-well plates and incubated for 72h. The SIINFEKL cognate peptide for OT-I cells had been synthesised by Katalin di Gleria in the WIMM at Oxford University. Antibodies against CD3, CD28, CD4, CD8, B220, CD25, CD69 and Foxp3 (intranuclear stain) were from eBioscience. Tryptophan metabolites were from Sigma. Antibodies against p-S6 (intracellular stain) were from Cell Signaling Technology.

3.3 Results

3.3.1 IDO activity in tumour cells inhibits CD8+ T cell proliferation and additional tryptophan can rescue it

The activity of IDO is known to suppress T cell proliferation and we wanted to confirm this by using IDO+ tumours, which should deplete the culture medium of tryptophan and produce kynurenines. In order to prevent the EL4, EG7 wild type ("EG7 WT"), EG7 GFP-transfected ("EG7 GFP") and EG7 GFP+IDO ("EG7 IDO") –transfected cells from overgrowing in the cultures and depleting the T cells from nutrients, they were irradiated for different lengths of time. The cells were then placed in 5 ml of media at $0.5x10^6$ cells/well for 48h, after which the live cells were counted and the amount of kynurenine measured in the media. Cells that had been irradiated to the maximum of six minutes stayed alive but kynurenine production stopped in cells after only 3 minutes of irradiation (Figure 1A and B). To take advantage of the maximum amount of IDO activity in the irradiated cells, we chose the one-minute time-point that was sufficient to stop the cells' proliferation.

EL4 cells that lack the OVA-peptide expression did not stimulate the OVA –specific T cell–receptor containing CD8+ T-cells within the OT-I splenocytes. EG7 WT cells stimulated the CD8+ T cells at all concentrations as did the EG7 GFP –transfected cells. IDO-transfected cells inhibited CD8+ T cell proliferation with increasing efficiency as the number of IDO+ cells increased (Figures 2A and 2B). The IDO+ cells had produced a significant amount to kynurenine and used up most of the available tryptophan (Figure 2C).

This inhibition may be due to either low levels of tryptophan or its accumulation of its metabolites ('kynurenines'), so we went on to investigate whether adding tryptophan during the assay would rescue the T-cell proliferation. Again, EL4 cells did not stimulate the CD8+ to proliferate but EG7 WT, GFP-transfected and IDO+ transfected cells did (Figures 3A and 3B). In all cases this time, the CD8+ T-cells stopped proliferating at the 5:1 EG7 to splenocyte ratio and this was probably due to a generalised nutrient

depletion as T-cells in the WT and GFP –containing samples also stopped proliferating. The addition of tryptophan partially rescued the T-cell proliferation in the GFP and IDO+ samples. All IDO+ samples had used up the available tryptophan and when it had been added, it had been consumed proportionally to the IDO+ cell content but not completely used up (Figure 3C).

3.3.2 CD8+ T cell proliferation is strongly dependent on available nutrient levels but less so on tryptophan only (FCS Trp titration)

While the T cell proliferation was partially rescued by tryptophan addition in the previous experiment, we wanted to examine how dependent it was on the foetal calf serum (FCS) concentration in the cell culture media with or without added tryptophan. When the cell culture medium does not contain any FCS, there is no CD8+ T cell proliferation even with added tryptophan (Figure 4A). Similarly at 0.5% FCS there is not enough nutrients to sustain T cell proliferation. At 1% FCS, the T cells start to proliferate and the proliferation is stronger the more tryptophan is present. The same pattern is repeated until the FCS concentration is 6% or more when the presence of extra tryptophan ceases to enhance the T cell proliferation. This is probably due to a sufficient level of tryptophan in the FCS that is now at a high enough concentration. The cell proliferation was measured quantitatively by comparing against the non-proliferated unstimulated CD8+ T cells (Figure 4B). By 6% of FCS concentration, virtually all CD8+ T cells had proliferated and the FCS/nutrient concentration was no longer limiting.

3.3.3 Kynurenine pathway enzyme expression in human tumour cell lines

As it is possible that the tryptophan metabolites (kynurenines) also inhibit T cell proliferation, we went to look at the kynurenine pathway enzyme expression pattern in various tumour lines. If any of the metabolites show T-cell inhibitory (or activatory)

activity, it would be interesting if tumour cells would preferentially express particular enzymes to enhance the production of the advantageous metabolite. We tested the following tumour derived cell lines (tissue of origin in parentheses): HeLa (cervical cancer), A431 (epithelial carcinoma), Dx3 (melanoma), THP1 (acute monocytic leukaemia), SKBR23 (breast cancer), U87MG (glioblastoma), HPAF (pancreatic adenocarcinoma), and HCA7 (colon adenocarcinoma), which all showed slightly different expression patterns from each other (Figure 5). All cell lines except SKBR23 expressed IDO after IFNγ stimulation and none of them without it. TDO was only expressed by THP1 and U87MG with and without IFNγ. Kynurenine formamidase (Afmid) that breaks down N-formyl kynurenine into kynurenine is expressed by SKBR23 and U87MG without IFNγ and weakly by SKBR23 after IFNγ treatment. Kynurenine aminotransferase I (KATI) was expressed strongly by all cell lines irrespective of IFNγ stimulation. KAT II was not expressed by any cells but this may have been due to poor primers. Kynureninase was expressed by all cel lines before and after IFNy except for SKBR23 that only expressed it after IFNy stimulation. HPAF is expressed very weakly. Kynurenine hydroxylase (KynOH) was expressed by HeLa, Dx3, and SKBR23 after IFNy treatment whereas THP1 cells expressed it strongly with or without IFNy. 3-hydroxyanthranilate 3,4 –dioxygenase (3-HAO) was expressed by A431, Dx3, and U87MG before and after IFNy and by SKBR23 only without IFNy. Picolinic acid carboxylase (Acmsd) was not expressed by any of the cell lines. The results for quinolinate phosphoribosyltransferase (QPRT) are not clear as the primers that were used did not align properly with the enzyme sequence, despite having been published before.[223]

It is possible that the differential expression pattern is beneficial to the cancer cell line, and to determine whether this relates to the inhibition of T-cell proliferation, further experiments were carried out.

3.3.4 At optimal nutrient levels, tryptophan metabolites have no significant effect on CD8+ T-cell proliferation

As there are different kynurenine pathway expression patterns in different tumour cell lines, we were interested in looking at whether any of the metabolites would affect T-cell proliferation. We first tested the effect of constant availability of kynurenine, kynurenic acid, 3-HAA, 3-HK, anthranilic acid, picolinic acid and quinolinic acid on CD8+ T-cell proliferation when the overall nutrient level is optimal. OT-I splenocytes were incubated in R10 for 72h with the addition of 25 μM of each kynurenine every 24h. This concentration was chosen as the normal RPMI 1640 media contains around 25 μM of tryptophan and 1-2 μM more when 10% of FCS is added. Therefore we hypothesised that no metabolite should accumulate to more than 25 μM within 24h. We also wanted to look whether the amount of stimulation affects the potential effect of the kynurenines, and thus had groups that had been stimulated with 10 nM, 50 nM or 100 nM of SIINFEKL peptide.

During low stimulation (10 nM) there was no significant reduction in CD8+ T-cell proliferation apart from the 3-HK and 3-HAA groups in which there was significant toxicity (Figure 6). At 25μM concentration, neither should be lethal to the cells during normal stimulation, so it is possible that the cells are more susceptible to their effects when they have not been stimulated strongly. However, it also possible that this was toxicity due to a freshly made (compared to frozen) solution that we have observed can sometimes kill the cells. During stronger stimulation (50 nM and 100 nM) there was no significant effect on the T-cell proliferation by any of the kynurenines tested (Figure 6).

3.3.5 In starvation or moderate starvation conditions 3-HK and 3-HAA mildly inhibit CD8+ T-cell proliferation

Since there was no significant effect on the tryptophan metabolites on T-cell proliferation in optimal nutrient conditions regardless of stimulation strength, we then wanted to examine whether lower nutrient levels during constant stimulation would

influence the effect of kynurenines on CD8+ T-cell proliferation. The OT-I splenocytes were incubated RPMI 1640 containing 0% FCS, 2% FCS and 4% FCS and the kynurenines added at 25 μM every 24h. The SIINFEKL peptide was added at 100nM.

Out of all the kynurenines there was only very slight inhibition of CD8+ T-cell proliferation with 3-HK and 3-HAA when the cells had been incubated in 2% FCS and 4% FCS containing RPMI (Figure 7). When the cells were starved in media containing no FCS, there was no proliferation of CD8+ T-cells and addition of kynurenines had no effect. Therefore, it appears that only 3-HK and 3-HAA have a small effect in nutrient-depleted conditions on the CD8+ T-cell proliferation but this is minor and may well be related to direct toxicity. It can be concluded therefore that if the kynurenines have any effect on CD8+ T-cells, it is not in a direct way on their proliferation at least when observed for 72h. The effect of a more sustained exposure (>72h) of these metabolites on CD8+ T-cell would be interesting to study.

3.3.6 Only 3-hydroxykynurenine of all tested kynurenines inhibits CD4+ T-cell proliferation

The kynurenines did not have an effect on CD8+ T-cell proliferation but we also wanted to see whether the same applies to CD4+ T-cells. 3-HK is known to enhance CD25+ Foxp3+ Treg generation[160] so we wanted to see whether this or any other kynurenine would affect the CD4+ T-cell proliferation. DO11.10 splenocytes were incubated with 5 μg of plated anti-CD3 and anti-CD28 in the presence of daily additions of 25 μM of the same kynurenines as in 3.3.4. Only 3-hydroxykynurenine showed minor inhibition of CD4+ B220- cell proliferation judging from the higher peak of non-proliferated cells and lower peak of the most proliferated cells (Figure 8). This agrees with the published data, and we did not find any additional kynurenines that would have this effect.

3.3.7 3-hydroxykynurenine increases CD25+ Foxp3+ T_{reg} numbers whereas other kynurenines do not affect them

As it has been previously reported that 3-hydroxykynurenine (3-HK) can increase the number of CD25+ Foxp3+ T-regulatory cells[160], we wanted to see whether any other tryptophan metabolite would have a similar effect. We also wanted to confirm the published results with our assay that 3-HK increases the CD25+ Foxp3+ Treg numbers. In our hands, there was no increase in the proliferation of CD4+ CD25+ Foxp3+ T_{reg} cells as judged from the proliferation index of these cells (Figure 9A and 9B). However, there was a slightly raised percentage of cells in samples containing 3-HK (Figure 9C). None of the other kynurenines affected the CD25+ Foxp3+ T-cell numbers significantly.

3.3.8 mTOR activity is dependent on tryptophan concentration

Tryptophan depletion is known to inhibit T-cell proliferation and their mTOR activity.[177,219] We were interested in studying whether the kynurenines tested above would have a subtler effect on the T-cells this way as they did not inhibit their proliferation (see previous results). We first wanted to confirm that mTOR is inhibited when tryptophan is depleted from the media. HeLa IDO+ cells were incubated with various amounts of tryptophan for 7h in RPMI 1640 media originally lacking tryptophan (Figure 10A). No FCS was added to the media as this would have introduced extra tryptophan to the assay. The mTOR inhibitor rapamycin was added at 20 nM to the negative control group. After 7h, the cells were lysed and a western blot made with antibodies against phospho(Ser240)S6 ("pS6") and tubulin as a loading control. There was a clear dose-dependent decrease in pS6 levels from 2 µM of tryptophan downwards but still some left when no tryptophan was present (Figure 10A). Tryptophan levels were measured from the culture media and they were depleted to unquantifiable from the sample initially containing 1 µM Trp downwards (not shown). This clearly indicates that mTOR has been inhibited and it has been due to low tryptophan levels and/or accumulation of tryptophan metabolites.

We also confirmed this effect on live cells by incubating C57BL/6 splenocytes in T0 (no tryptophan), T0 + added tryptophan, T10 (no Trp but with 10% FCS) and R10. All cells were stimulated with 5ug of plated anti-CD3 and anti-CD28 antibodies. The cells were incubated for 24h and 48h and the p-S6 level in live CD8+ B220- cells was measured. The unstimulated cells were used as a negative control. When the cells had been incubated in R10, their mTOR was fully active as the p-S6 level was high in all CD8+ cells (Figure 10B and C). The same was true for cells incubated in T10 that had high p-S6 level for all CD8+ cells. This media normally contains around 1-2 μM of tryptophan that comes from the added FCS that is completely consumed within 24h. This time the FCS batch, however, contained so much tryptophan that there was around 10 μM in the made-up T10 (measured by HPLC). This was probably the reason why the phophorylation of S6 was not inhibited during the first 24h in the CD8+ cells as the tryptophan consumption rate of stimulated splenocytes plated at those concentrations would have reduced the media tryptophan concentrations by less than 3 μM during this period (rate observations made in the laboratory by Ioannis Karydis). The cells incubated in T0 were starved of tryptophan and this was reflected in the lowered p-S6 levels. The addition of tryptophan to the T0 media reversed this and almost all cells became positive for p-S6. Interestingly, this shows that mTOR, or at least S6, is very sensitive to tryptophan since no other component of FCS was required for the almost complete phosphorylation of S6 in cells that were in T0 but received only tryptophan.

After 48h, the pattern is similar but even cells cultured in R10 have nearly exhausted the supply of nutrients other than tryptophan - if these cells were to be cultured for longer, media change would be required - that the p-S6 levels have started to come down (Figure 10B and C). The levels are similar in cells in T10 if not higher, consistent with the high tryptophan content of the FCS that was used, making any comparisons between R10 and T10 made using this batch of FCS, meaningless. Cells in T0 had a low number of cells with phosphorylated S6 and had lost the second peak (i.e. high p-S6) that was present after 24h. Interestingly, the addition of tryptophan at the beginning and after 24h into these samples kept the p-S6 levels high in the remaining CD8+ cells

but it did not enable cell proliferation (see cell numbers in 48h panel in Figure 10B). This agrees with my earlier results in Figure 4 of this chapter that tryptophan can enhance cell proliferation if sufficient other nutrition is available but is not able on its own to make cells proliferate, despite activating and keeping mTOR active.

3.3.9 Kynurenines enhance eIF2α activity in EG7 cells

T-cells sense nutrient levels by the mTORC1 pathway but also via the GCN2 pathway. The GCN2 kinase senses and is activated by uncharged t-RNAs that are present in higher concentrations when there is an amino acid deficiency in the cell. We were interested to examine whether the kynurenines would affect this pathway too since they are a sign that tryptophan is being consumed and therefore possibly depleted from the extracellular nutrient pool. We did this experiment in low tryptophan conditions to enhance any effect the metabolites may have on the pathway. In the absence of an established assay to reliably detect GCN2 activation directly – an existing phosphoantibody was withdrawn by the manufacturer in view of conflicting phosphoproteomic data – we used the proximal downstream molecule eukaryotic translation initiation factor 2A (eIF2α) as a marker for GCN2 activation. eIF2α is a subunit of a complex that senses, in addition to amino acid starvation via GCN2, also detects heme deficiency via heme-regulated kinase (HRI), viral infection via protein kinase R (PKR) and ER stress via PERK kinase.[224,225,226] It is therefore possible that production of kynurenines, may be able to influence phospho-eIF2α levels via ER stress, and thus magnify the effect of tryptophan starvation on the pathway.

EG7 IDO+ cells were incubated for 24h in Trp/FCS-free media supplemented with 1 μM of Trp. 100 μM of kynurenine, kynurenic acid, 3-HAA, anthranilic acid, and picolinic acid were added to the cultures (3-HK was also added but was toxic to the cells). Rapamycin was added at 20 nM to an additional control group to check whether inhibition of mTOR via an amino acid-independent way would cause GCN2 pathway activation. Interestingly it raised the p-eIF2α levels slightly indicating possible communication between mTOR and GCN2/eIF2α pathways (Figure 11).

3.3.10 Kynurenines do not affect mTOR activity of CD8+ T cells at low stimulation level

Similarly to the T-cell proliferation assay with low stimulation strength and added kynurenines, we did a similar assay for p-S6 levels in weakly stimulated CD8+ T-cells. OT-I splenocytes were incubated with 10 nM of SIINFEKL peptide for 2h, 9h or 21h in the presence of 25 μM of each tryptophan metabolite (kynurenine, kynurenic acid, 3-HAA, 3-HK, anthranilic acid, picolinic acid and quinolinic acid). A sample with anti-CD3 and anti-CD28 was also added as a positive control for strong stimulation. After 2h, there were no significant differences between the groups, indicating that the kynurenines cannot cause phosphorylation of S6 and in that way affect mTOR activity in mildly stimulated CD8+ T-cells (Figures 12A and 12B). At 9 hours anthranilic acid appeared to inhibit mTORC1 but this result was not reproducible in subsequent assays. After 21h 3-hydroxykynurenine appears to mildly inhibit mTORC1. This was interesting as it opened the possibility that 3-HK-mediated inhibition of CD8+ T-cell proliferation may be partially mediated through inhibition of the mTORC1 pathway.

3.3.11 3-hydroxykynurenine inhibits mTOR activity at moderate stimulation level after 24h but the effect is lost after strong stimulation

Following on from the interesting result with 3-HK in the previous experiment, we studied the effect of kynurenines on CD8+ mTORC1 pathway of CD8+ T-cells during moderate and strong stimulation under optimal nutrient conditions – i.e. culture in R10 media. The assay was done with OT-I splenocytes over 24h stimulated with 100nM and 1 μM of SIINFEKL peptide and adding 25 μM of each kynurenine to R10 media. This time CD69 levels were also measured to get an indication of the extent of CD8+ T-cell activation during the experiment. The mTOR inhibitor rapamycin lowered the amount of p-S6 at both peptide concentrations but interestingly only lowered the CD69 levels in cells that had been stimulated with 100 nM of peptide and not with 1 μM (Figure 13). Of the kynurenines, 3-HK decreased the phosphorylation of S6 when 100 nM of peptide had been used, consistent with findings from the earlier assay where 10 nM of peptide

had been used. The metabolite also lowered CD69 levels, indicating a decrease in CD8+ T-cell activation too. All this would point towards the mechanism of 3-HK –mediated T-cell inhibition to be mTOR-related. None of the metabolites had an effect on the p-S6 levels when the T-cell stimulation was strong with 1 μM of peptide. It would be interesting to see whether the same effect can be seen in the mTORC1 activity of CD4+ T-cells after 3-HK treatment.

3.4 Discussion

In this chapter we have investigated the effects of seven tryptophan metabolites on CD8+ and CD4+ T-cell proliferation and on the CD8+ T-cell mTORC1 activity in response to stimulation. We first confirmed that tryptophan depletion by IDO expressing tumour cells resulted in the inhibition of CD8+ T-cell proliferation in response to cognate peptide. This was done in an experimental system where an OVA-transfected EG7 tumour cell line acted both as a stimulator of OT-I splenocytes but also as a tryptophan scavenger (in the case of IDO transfected EG7). As this particular cell line proliferates extremely rapidly using up all the available nutrients, it was essential to irradiate the cells prior to setting them up with the splenocytes to avoid them overgrowing and depleting media prematurely of nutrients essential for T-cell growth other than tryptophan.

In the first set of experiments, the IDO+ tumours dose-dependently inhibited CD8+ T-cell proliferation, which did not happen with the IDO- cells or with the cells lacking OVA. These results proved that the depletion of tryptophan was the likely reason for the inhibition as the IDO+ cells had consumed almost all of the available tryptophan and turned it into kynurenine. To verify this result, we tried to repeat this experiment many times with the addition of tryptophan to see whether it rescues the cells, however, it was difficult to set up the assay again so that only tryptophan was consumed by the IDO+ cells and the cells would not run out of other nutrients. Therefore in the second set of EG7 OT-I experiments, there was inhibition of CD8+ cells even in the samples containing non-IDO expressing tumour. This was probably due to the tumour cells consuming most of the nutrients thus eventually inhibiting cell proliferation – in order to maintain sufficient IDO activity in irradiated cells it was impossible to completely inhibit their proliferation, and in any case they had to remain metabolically active. Nevertheless, adding tryptophan partially rescued the proliferation, and this was most obvious with the IDO+ samples that would have exhausted tryptophan from the media first: it appears that lack of this amino acid alone was responsible for a large part as they responded to its addition readily. The overall conclusion is that depletion of tryptophan by IDO+ tumours leads to inhibition of T-cell proliferation.

Since tryptophan is so important to the cell proliferation that its addition solely can rescue T-cell proliferation, we were interested in examining at what concentration its depletion started to become critical to the cells. At the same time we looked at the amount of FCS that is required as a nutrient source for cell proliferation. It was interesting to note in the context of otherwise tryptophan-free media that tryptophan cannot on its own drive T-cell proliferation when no FCS is added but it does enhance it even at minimal FCS concentration. There is also an interesting trend that at almost all FCS concentrations, it was the 10 μM concentration of tryptophan that was most effective at enhancing the proliferation (and CD8+ cell numbers) and not the highest at 25 μM. This would need to be further investigated and quantified with calibration beads, but it is possible that higher tryptophan concentrations can affect the uptake of other nutrients that are transported via the same transporter by partially blocking it.

As mentioned previously, it is not clear with regards to the mechanism of IDO related inhibition of T-cell proliferation whether it is mainly due to the depletion of tryptophan itself or whether tryptophan metabolites have a significant role as well. Several papers have reported 3-hydroxykynurenine and 3-HAA as metabolites that specifically affect CD8+ and CD4+ T-cell proliferation.[160,216,227] We were therefore interested in whether different tumour types would have differential expression of the kynurenine pathway enzymes that might result in increased production of 3-HK and 3-HAA. We did this by choosing eight human tumour cell lines and using reverse transcription -PCR to investigate the pattern of kynurenine pathway enzyme expression. We were particularly interested in the expression of kynurenine mono-oxygenase (a.k.a kynurenine hydroxylase) that makes 3-HK, kynureninase that makes 3-HAA from 3-HK and 3-HAO that breaks down 3-HAA. Interestingly kynureninase was expressed strongly by almost all of them bar SKBR23 that only expressed it under IFNγ stimulation. This would indicate that at least 3-HAA is being made, however, only HeLa, Dx3, THP1 and SKBR23 express kynurenine hydroxylase to provide 3-HK for kynureninase. There is an alternative route to 3-HAA from kynurenine via anthranilic acid if anthranilate hydroxylase is expressed (see KEGG pathway for tryptophan). This enzyme was not in our panel but if it was expressed, then it is worth noting that almost all of the tumour lines would be likely to produce significant amounts of 3-HAA due to the high

expression of kynureninase. It is therefore interesting that the enzyme responsible for breaking 3-HAA down, 3-HAO, was not expressed by HeLa, THP1, HPAF or HCA7 and only with IFNγ by U87MG. In SKBR23 cells IFNγ downregulates its expression. It is thus possible that some tumours accumulate 3-HAA and its potentially toxic by-products[228,229] by other enzymes to the detriment of any T-cells that happen to be in their vicinity. It would be interesting to look at the expression in tumour extracts and measure 3-HAA levels to see whether they use this as a method of T-cell suppression in vivo. The expression of the pathway enzymes in brain tumour lines has been studied by Miyazaki *et al*. who found that 3-HAO is not expressed in at least four glioma lines and one neuroblastoma line.[230] All of the glioma cell lines expressed kynurenine hydroxylase and kynureninase, making it possible that one of the mechanisms these tumours use to wreak havoc in the brain is by producing 3-HAA without breaking it down. 3-HAA can then form ROS and H2O2 in the brain causing damage as is the case in Alzheimer's disease.[213,231]

Although it is known that 3-HK and 3-HAA can cause T-cell inhibition, we wanted to confirm this and add five more tryptophan catabolites to investigate whether other tryptophan catabolites could affect T-cell proliferation. The assay was done over three days and using three daily additions of 25 μM of each kynurenine catabolite under optimal nutrient conditions. We also used three different concentrations of stimulatory peptide but there was no significant reduction of CD8+ T-cell proliferation apart from the lowest stimulation where 3-HK and 3-HAA killed most of the cells. It is possible that the cells were more sensitive when weakly stimulated; however this type of toxicity had also been seen intermittently with freshly made compounds so the reasons for the observed toxicity are not clear.

We did this assay also using lower nutrient levels where we could identify that 3-HK and 3-HAA do mildly inhibit CD8+ T-cell proliferation. The discrepancies between our results and other published results could be due to different read-outs as we did not specifically look for apoptosis[215] or use additional cytokines that have been reported to be needed for 3-HAA –mediated CD8+ T-cell inhibition.[216] We also did not see toxicity associated with quinolinic acid.[215] In the case of CD4+ T-cells we saw a small amount of

proliferation inhibition with 3-HK but no significant toxicity as reported by Zaher *et al*.[160] This difference may be due to us using daily 25 μM additions of 3-HK, instead of single higher doses, which may have given the cells time to adjust and metabolise some of the excess 3-HK. We also did a three-day study on Foxp3+ T_{reg} generation when the cells were co-incubated with the kynurenines. Again only 3-HK produced a somewhat higher proportion of the T_{regs} compared with the others but the lack of a clearer difference was probably due to the period of time the assay was done, which was three compared to seven when Zaher *et al*. first started to see a larger proportion of Foxp3+ T_{reg} with 3-HK and 3-HAA.[160]

We then went on to look at the effect of tryptophan and its metabolites on the mammalian target of rapamycin (mTOR). This kinase forms one of the main hubs of the mTORC1 pathways that has multiple functions, but in particular integrates information regarding intracellular nutrient, and particularly amino acid, requirements and regulates cellular growth and proliferative capacity. We were interested to see whether any of the tryptophan metabolites can affect mTOR activity, which could be one of the mechanisms how a particular metabolite such as 3-HK would inhibit CD8+ or CD4+ T-cell proliferation.

We started by confirming that low tryptophan levels in T-cells are sensed by the mTORC1 pathway. We used phosphorylation of the S6 ribosomal protein at serine 240 as a readout as this is a well established indicator of mTORC1 pathway activity. Our results clearly show a dose-dependent response of phospho-S6 levels to tryptophan starvation. In a functional assay, the lack of tryptophan resulted in lower mTORC1 activity and this was reversed by addition of tryptophan. After confirming the dependency of mTORC1 activity on tryptophan levels, we went on to investigate the effects of the tryptophan metabolites on the GCN2 kinase that heads the other major pathway known to detect intracellular amino acid depletion. This pathway is known to be activated at extreme levels of amino acid starvation. As some tryptophan metabolites are known to be toxic at high concentrations, we hypothesised that they might trigger a cellular stress response even at lower, not overtly toxic, concentrations. In turn this could conceivably feed into the GCN2-pathway at the level of eIF2α where it converges

with the ER stress related PERK-pathway, multiplying the effect of direct GCN2 activation. Alternatively GCN2 might be directly activated or become more sensitive to activation by higher levels of uncharged t-RNAs in the presence of kynurenines. We therefore looked at the phosphorylated form of eIF2α that integrates signals from both pathways. All the tested kynurenines increased the phosphorylation of eIF2α by 2-fold or more, partially confirming our hypothesis. It would be interesting to repeat this assay with a titration of the kynurenines (so that 3-HK could also be added, as it was lethal to the cells in this assay at 100μM) and with different tryptophan levels. Ideally we would like to use an antibody against phospho-GCN2 itself to clarify the way kynurenines modify this pathway.

The effect of kynurenines on mTOR was studied at different time points using varying stimulation levels. When the splenocytes were mildly stimulated using 10 nM of SIINFEKL peptide, there were no major differences from the controls. When the stimulation was stronger 3-HK emerged as a metabolite that inhibited mTOR activity in CD8+ T-cells and also the cells' activation as measured by the marker CD69. Interestingly, when the stimulation was increased further, this effect was lost. This could be down to toxicity which then decreases the mTOR activity unless rescued by a sufficiently strong activation signal. As similar results have not been reported previously it would be interesting to study this further more comprehensively by doing a time course assay with a titration of the stimulus and 3-HK to exclude direct toxicity.

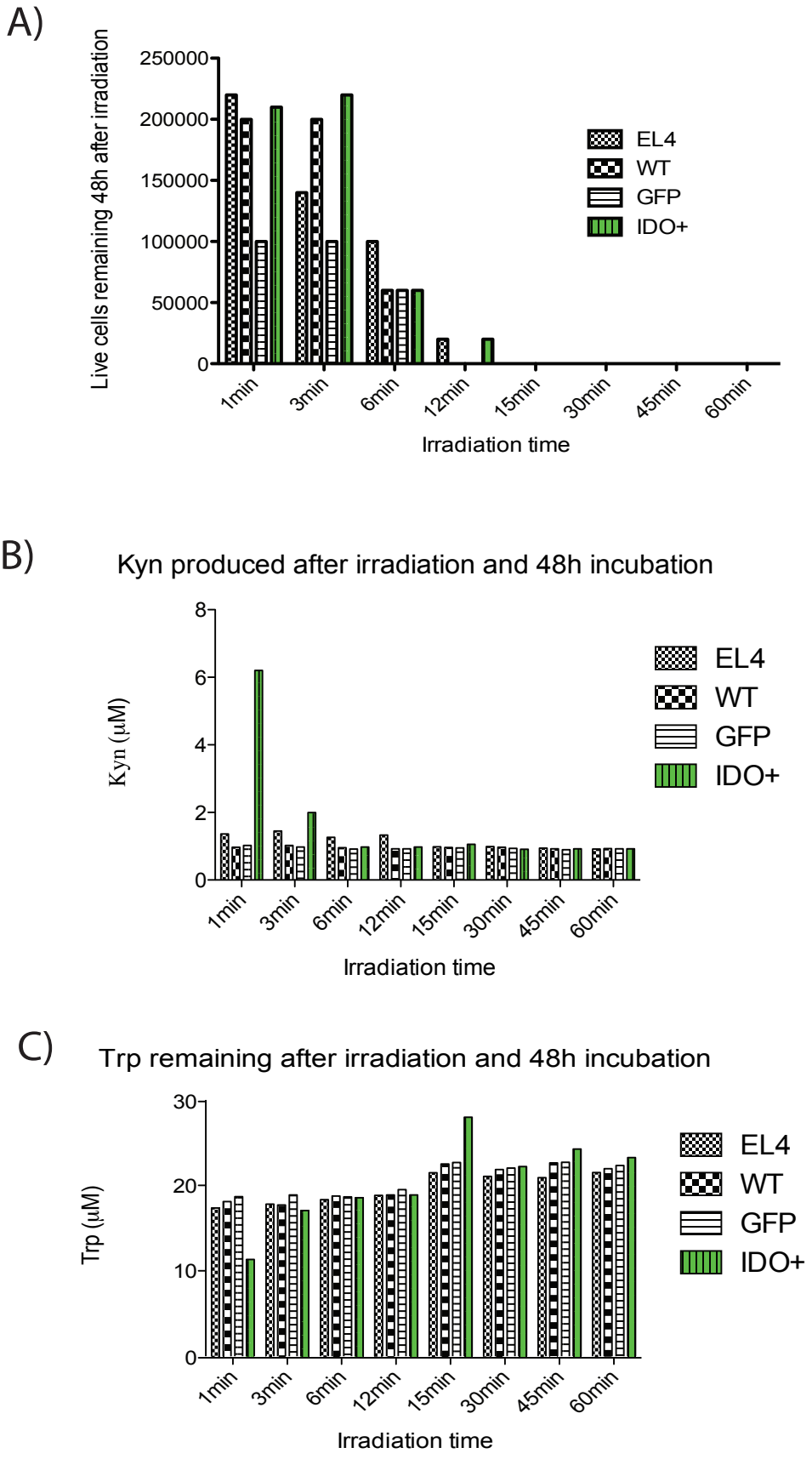

Figure 1. 1 minute of irradiation is enough to stall cell proliferation but not too much to inhibit kynurenine production. In order to establish an appropriate length of irradiation, the exposure of EL4 and EG7 to irradiation was titrated. After the irradiation, the cells were plated at 500000 cells/well in 5ml of R10 (6-well plate) for 48h after which the trypan blue negative cells were counted. A) The number of live cells of each cell type after 48h. B) Kynurenine produced by the cells during the 48h as measured from the supernatant by HPLC. C) Tryptophan remaining in the supernatant after 48h.

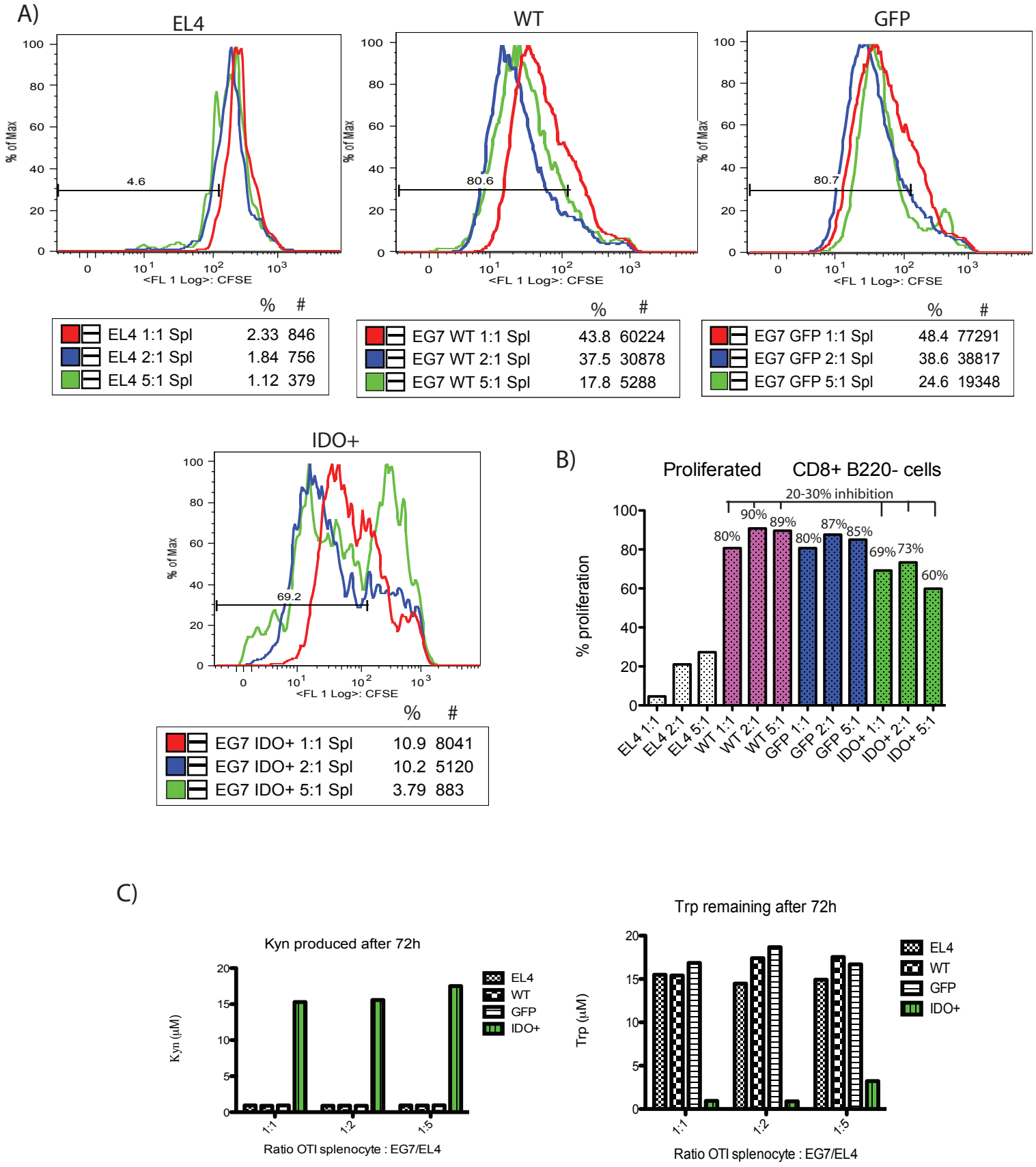

Figure 2. IDO+ cells deplete tryptophan from cell media which results in CD8+ T-cell proliferation inhibition. A) EL4, EG7 WT, EG7 GFP, EG7 IDO+ incubated in R10 with OT-I splenocytes for 72h at different concentrations. Proliferation was measured as the breakdown of CFSE and the negative control EL4 1:1 was used as a threshold. Cell numbers (#) and percentages (%) in the box refer to the number of live CD8+ B220- cells out of all live cells and the percentage of them within all live cells. B) A quantitative illustration of the proliferation measured in panel A. Each measured sample was a composite of three individual samples. C) Kynurenine produced by the cells and tryptophan remaining in culture as measured by HPLC after 72h. Representative of three separate experiments.

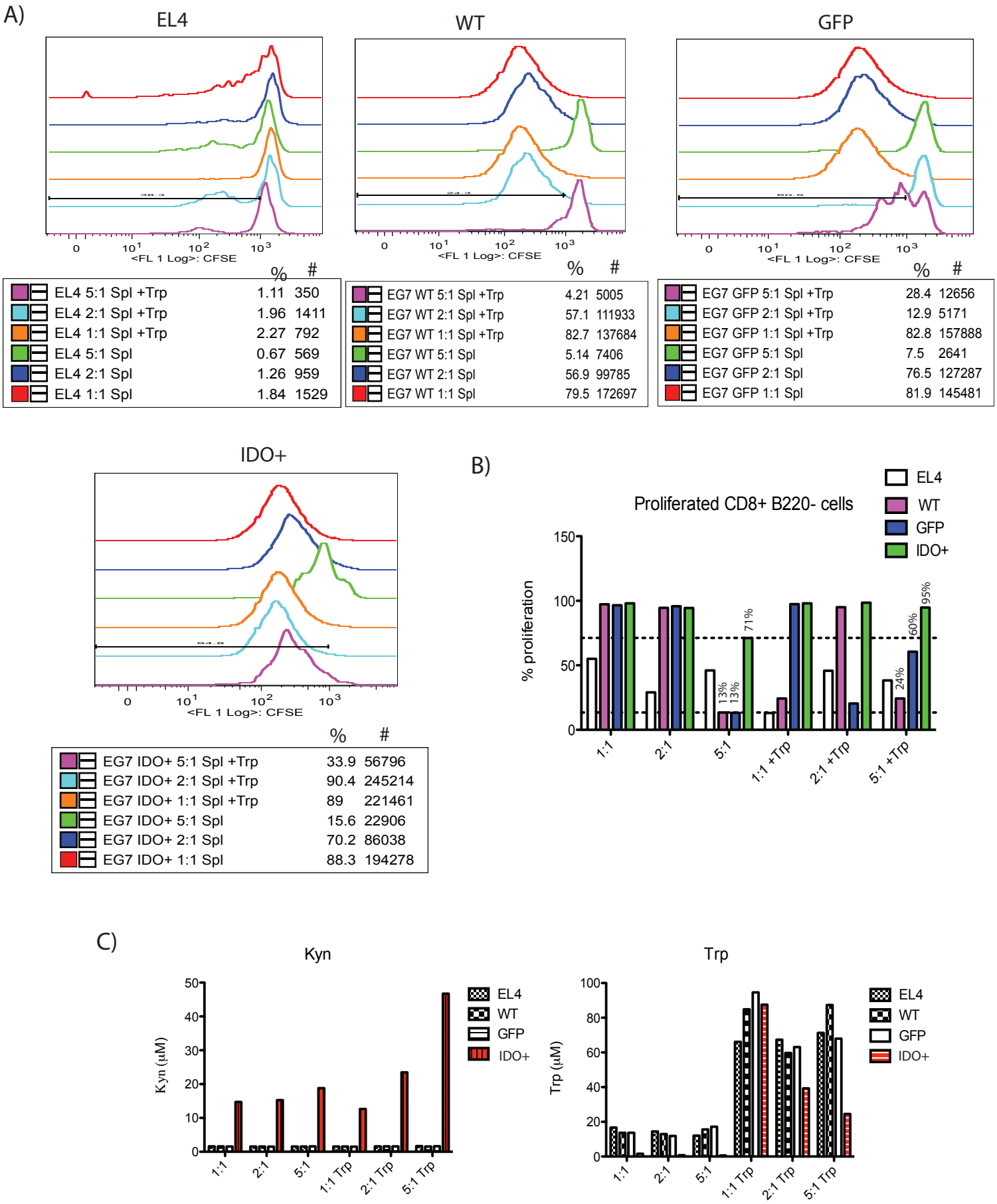

Figure 3. Addition of tryptophan partially prevents CD8+ T-cell proliferation inhibition.
A) OT-I splenocytes were incubated with different concentrations of EL4/EG7 cells for 48h. Where appropriate, tryptophan was added every 24h at 25μM. B) Percentage of proliferated CD8+ B220- cells as measured with gates in A). C) Kynurenine produced by the cells and tryptophan remaining in the media after 72h. Cell percentages (%) and numbers (#) in tables illustrate CD8+ B220- cells out of all cells. Representative of three separate experiments.

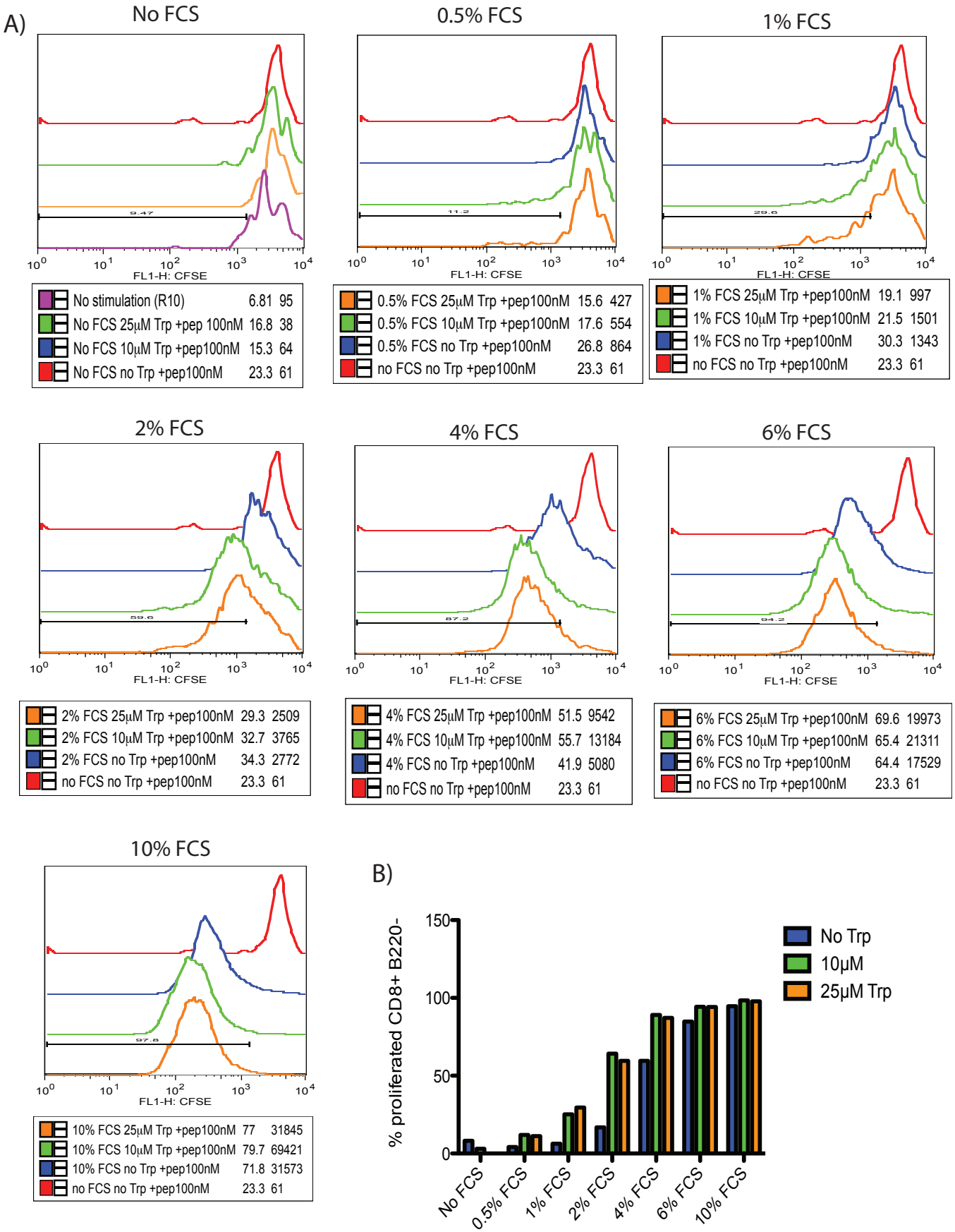

Figure 4. Effect of serum and tryptophan concentration on CD8+ T-cell proliferation.
A) Titration of FCS and tryptophan over 72h (OT-I splenocytes). Started with 200 000 cells/sample. B) Quantitative illustration of CD8+ proliferation as measured by division of CFSE. Cell numbers and percentages represent CD8+ B220- cells out all live cells. Pooled samples from triplicate wells. Peptide used was SIINFEKL.

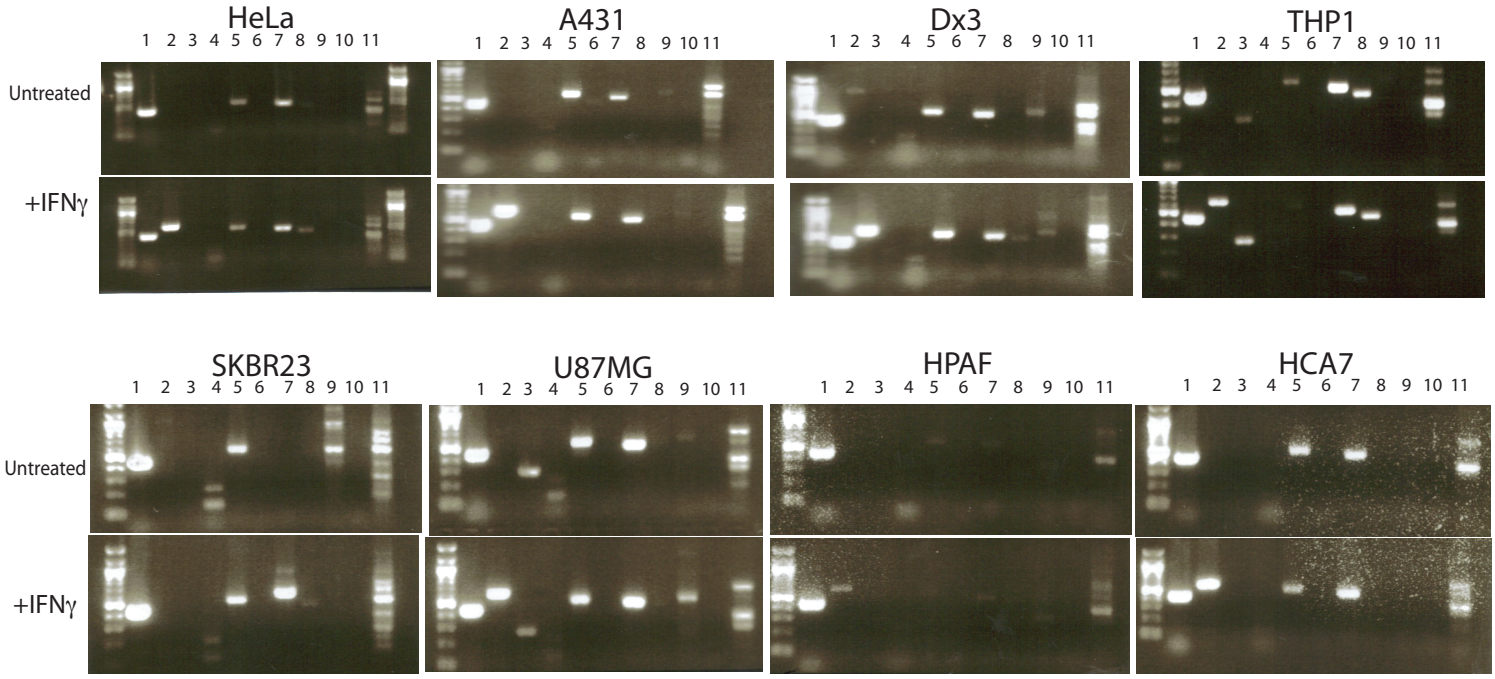

	HeLa		A431		Dx3		THP1		SKBR23		U87MG		HPAF		HCA7	
IFNγ	-	+	-	+	-	+	-	+	-	+	-	+	-	+	-	+
1. GAPDH	++	++	++	++	++	++	++	++	++	++	++	++	++	++	++	++
2. IDO	-	++	-	++	-	++	-	++	-	-	-	++	-	++	-	++
3. TDO	-	-	-	-	-	-	++	++	-	-	++	++	-	-	-	-
4. Afmid	-	-	-	-	-	-	-	-	++	-	+	-	-	-	-	-
5. KAT1	++	++	++	++	++	++	++	+	++	++	++	++	++	++	++	++
6. KAT2	-	-	-	-	-	-	-	-	-	-	-	-	-	-	-	-
7. Kynase	++	++	++	++	++	++	++	++	-	++	++	++	+	+	++	++
8. KynOH	-	+	-	-	-	++	++	++	-	+	-	-	-	-	-	-
9. 3-HAO	-	-	+	+	++	++	-	-	++	-	+	++	-	-	-	-
10. Acmsd	-	-	-	-	-	-	-	-	-	-	-	-	-	-	-	-
11. QAPT	++	++	++	++	++	++	++	++	++	++	++	++	++	++	++	++

Figure 5. Kynurenine pathway enzyme expression in human tumour cell lines. Expression of the kynurenine pathway enzymes by regular PCR. Where indicated, cells were treated with IFNγ for 48h prior to RNA extraction.

Key: IDO = Indoleamine 2,3-dioxygenase,
TDO = Tryptophan 2,3-dioxygenase
Afmid = Kynurenine (aryl)formamidase
KAT = Kynurenine transaminase/aminotransferase (I and II)
Kynase = Kynureninase
KynOH/Kmo = Kynurenine hydroxylase/mono-oxygenase
3-HAO = 3-hydroxyanthranilate 3,4-dioxygenase
Acmsd = Picolinic acid carboxylase
QAPT/QPRT = Quinolinate phosphoribosyltransferase

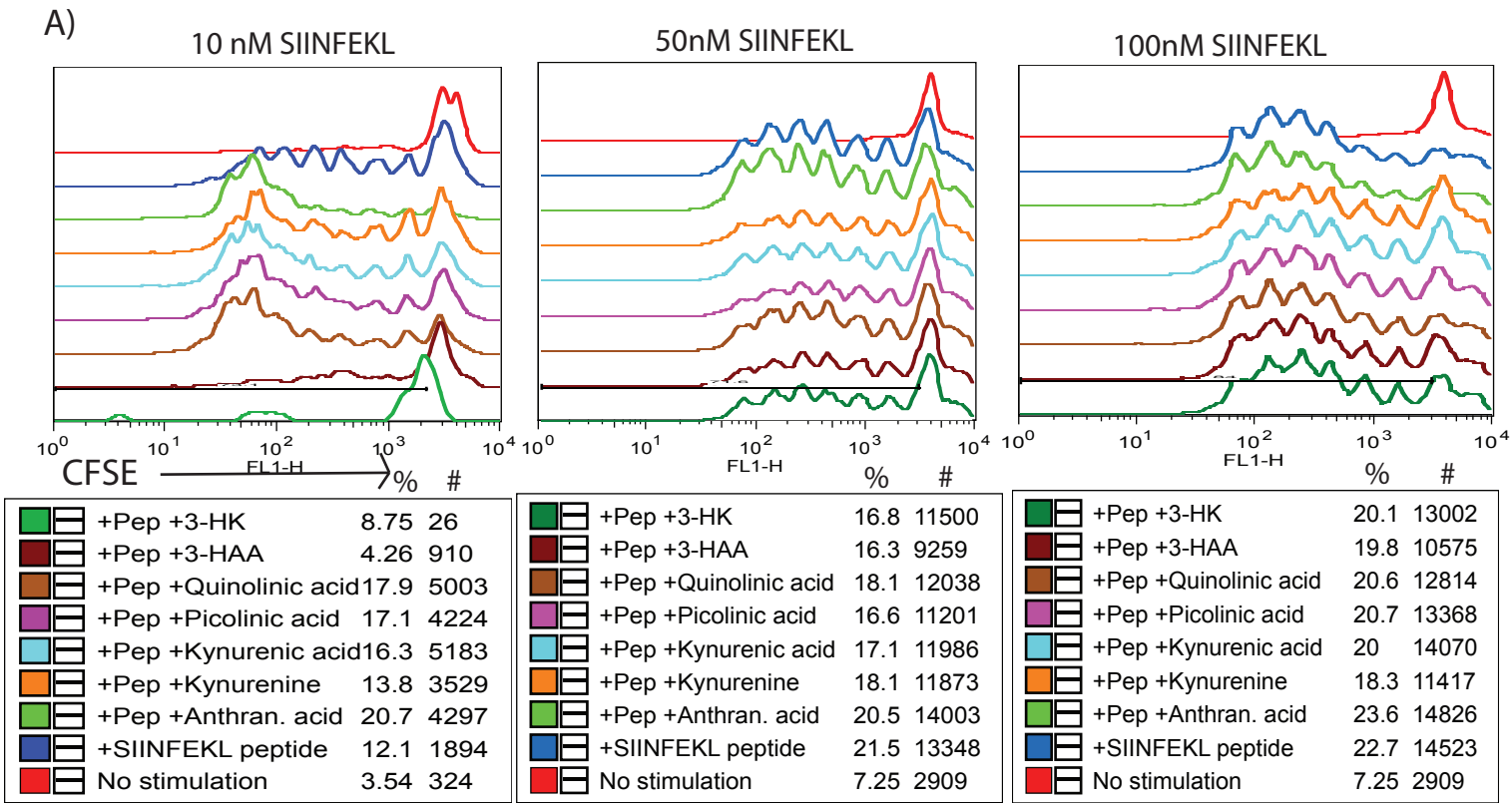

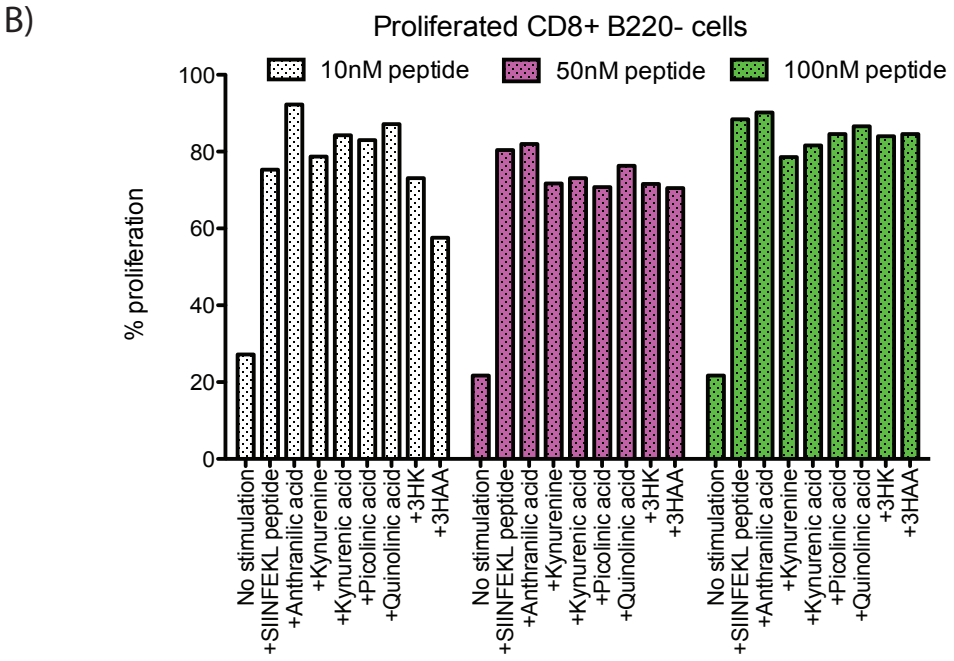

Figure 6. At optimal nutrient levels, no kynurenine has an obvious effect on CD8+ T-cell proliferation. A) 3-hydroxykynurenine ad 3-HAA showed toxic effects on the cells but this was not consistent. B) A quantitative representation of the proliferation data. The threshold used for proliferation was the "no stimulation" control. The splenocytes had been cultured in R10 for 72h with 25μM of each kynurenine added every 24h. The samples were then analysed and live CD8+ B220- cells out of all live cells are shown (# and %) with the division of CFSE on the X-axis. Samples were pooled from triplicate wells. Representative of three similar experiments.

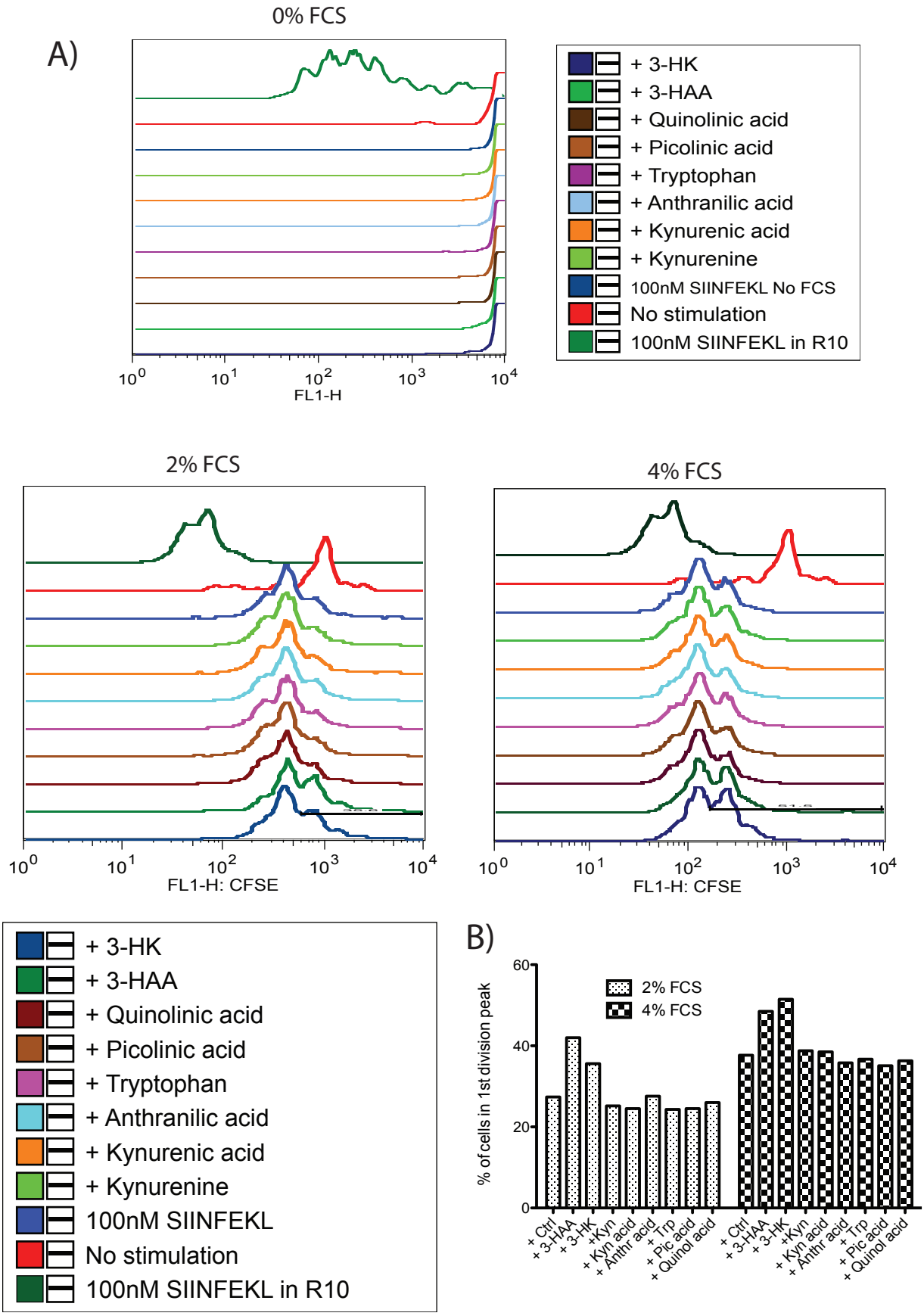

Figure 7. 3-HK and 3-HAA have a small effect on CD8+ T-cell proliferation during starvation or low nutrient availability. Total splenocytes were incubated for 72h in RPMI 1640 media with either no FCS, 2% FCS, or 4% FCS and stimulated with 100nM of SIINFEKL. Kynurenines were added every 24h at 25μM and the CFSE division of CD8+ B220- cells was measured. A) There is no effect by kynurenines on the CD8+ when the cells are starving but under low nutrient conditions 3-HAA and 3-HK inhibit their proliferation mildly. This is shown quantitatively in B) where the size of the first peak is measured indicating the percentage of less proliferated cells in the sample. Samples were pooled from triplicate wells. Representative of two experiments.

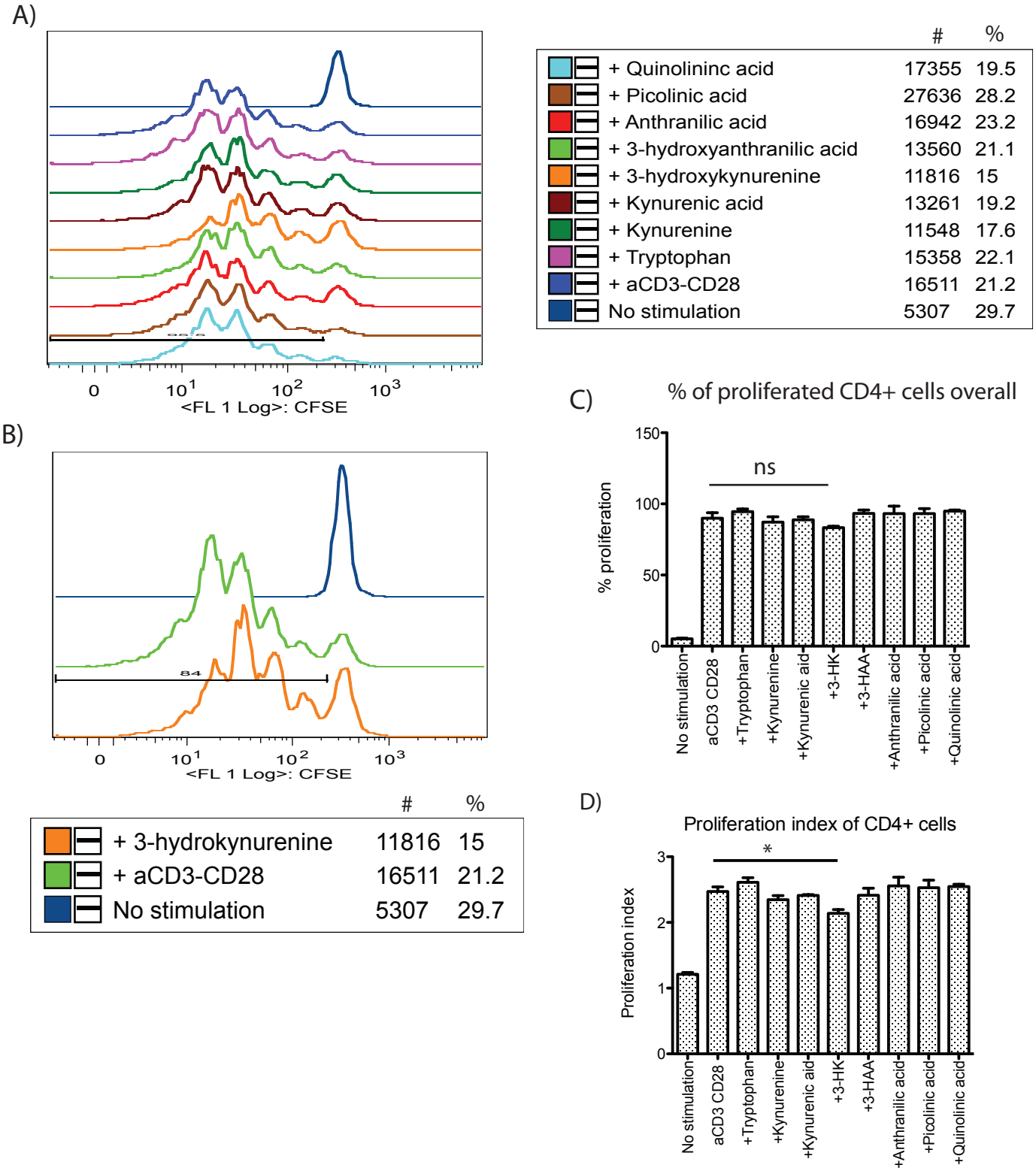

Figure 8. 3-hydroxykynurenine inhibits CD4+ T-cell proliferation marginally.
A) DO11.10 splenocytes were incubated with 3x25μM (added at the beginning of the experiment and then every 24h) of each tryptophan metabolite for 72h. Division of CFSE in CD4+ B220- cells was then measured by FACS. **B)** Close-up of the effect of 3-hydroxykynurenine on the CD4+ T-cell proliferation. **C)** Percentage of CD4+ cell proliferation when negative control used as a threshold for proliferation. When measured like this, 3-HK does not have a statistically significant effect on CD4+ proliferation when measured with 1-way ANOVA and using the Dunnett's comparison test between samples. **D)** Proliferation index of each sample. Using this parameter as a measurement of proliferation, 3-HK reduced the proliferation significantly. Statistics: 1-way ANOVA, Dunnett's multiple comparison test. * = $p<0.05$. # and % refer to number and percentage of CD4+ B220- cells out of all live cells. Figures are representative of duplicate samples and three separate experiments.

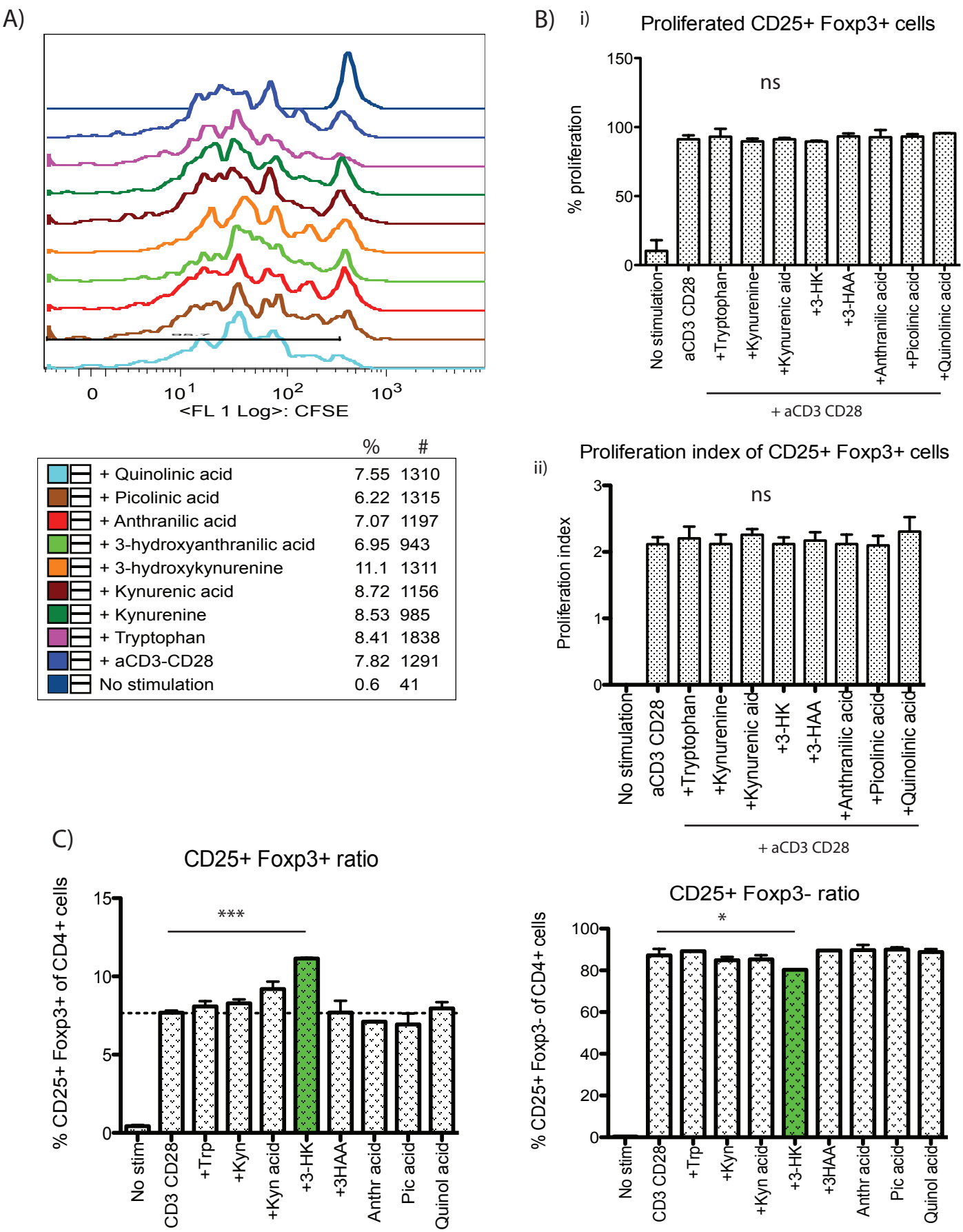

Figure 9. 3-hydroxykynurenine moderately increases CD25+ Foxp3+ Treg and reduces CD25+ Foxp3- Treg numbers and ratios but does not increase their proliferation. A) 200000 cells/sample of DO11.10 splenocytes were treated daily with 25μM of each tryptophan metabolite for 72h and CD4+ CD25+ Foxp3+ proliferation and quantities measured. B) i) Quantitative representation of proliferated CD25+ Foxp3+ when measured with the negative control as threshold. ii) Proliferation index of CD25+ Foxp3+ cells as measured by the total number of divisions divided by the the number of cells that went into division. Neither of these measurement showed significant differences between the kynurenines. C) Quantitative representation of the percentages of CD25+ Foxp3+ of all CD4+ cells. Statistics: 1-way ANOVA, *= $p<0.05$ with Dunnett's multiple comparison post test. Duplicate samples with standard deviations. Representative of two separate experiments.

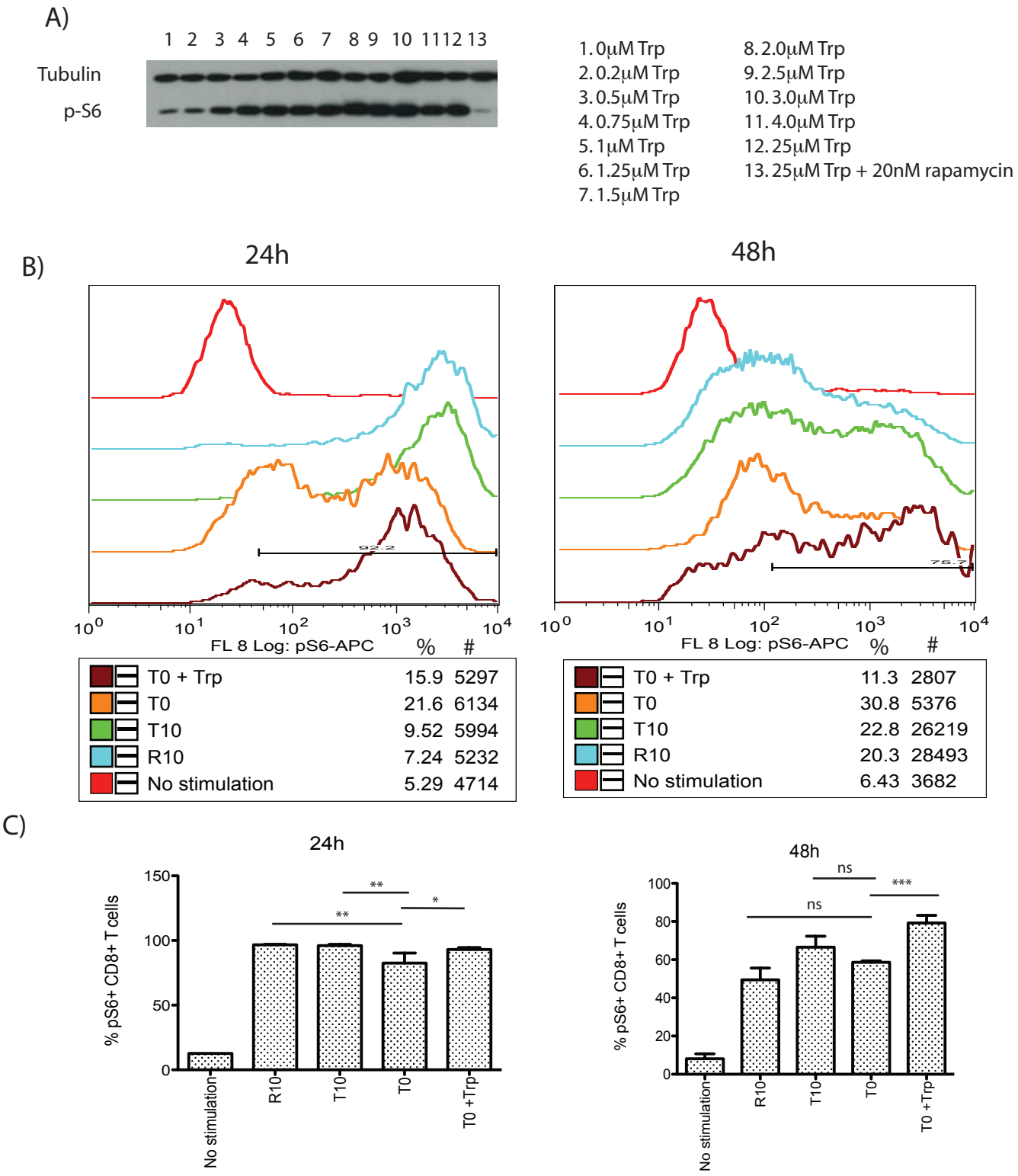

Figure 10 . Tryptophan levels affect mTOR activity in HeLa cells and CD8+ T cells.
A) mTOR activity in HeLa IDO+ after 7h with various concentrations of tryptophan as measured by amount of phosphorylated S6. B) p-S6 levels go down when tryptophan is limited in C57BL/6 CD8+ T-cells (24h and 48h) but they can be rescued by additional tryptophan. Quantitative representation of the data in B as measured by percentage of cells within marked gates. Statistics: 1-way ANOVA, $p<0.05$, triplicate samples. Stimulation with anti CD3 CD28. Cell numbers and percentages in B are the numbers of CD8+ B220- of all live cells.

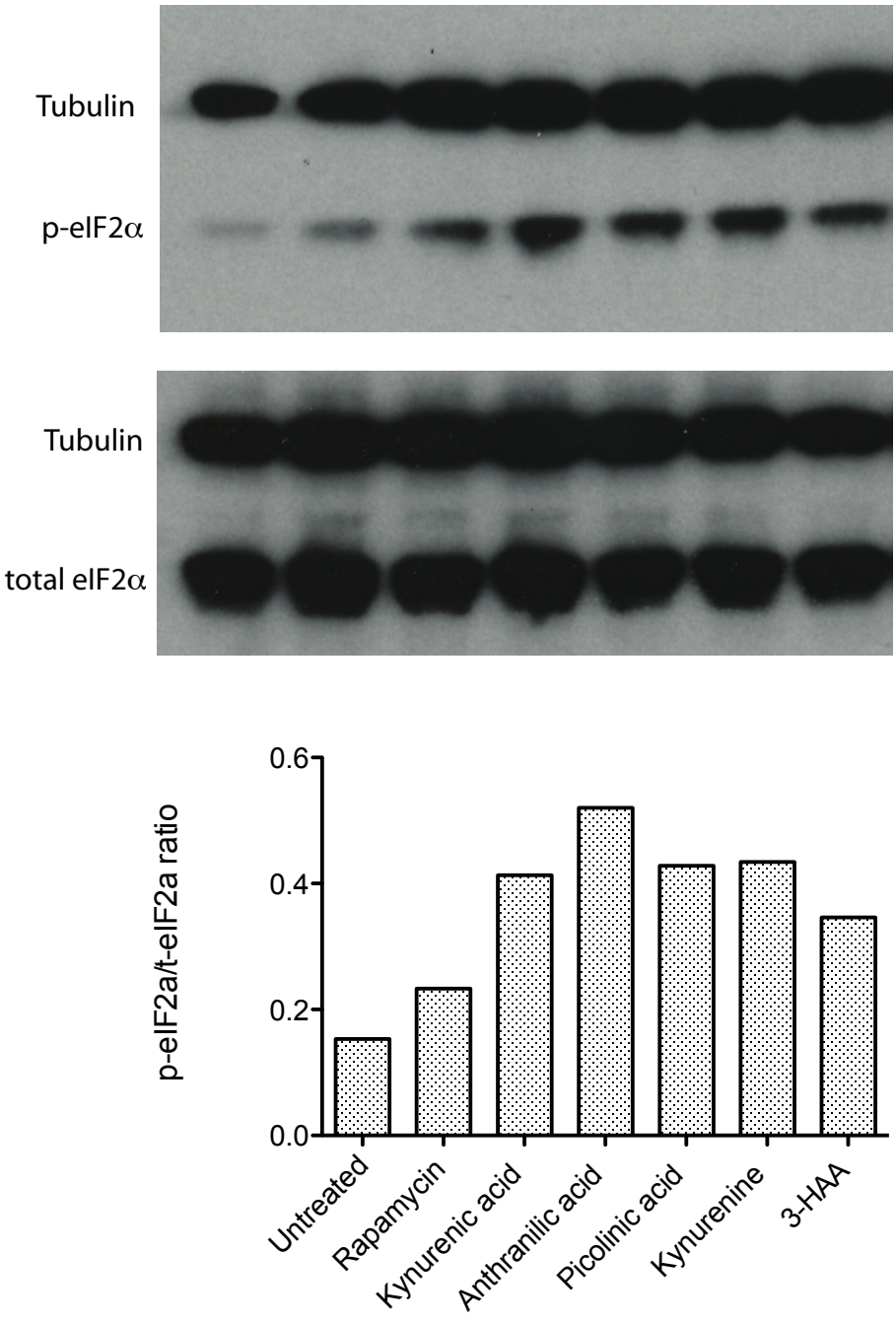

Figure 11. Phosphorylated eIF2α, located downstream of GCN2 is doubled by five kynurenines in starved cells. EG7 IDO+ cells were incubated in 1μM of Trp in Trp/FCS-free media for 24h with 100μM of each tryptophan metabolite. The pattern of the quantitative result was the same when measured against tubulin in the p-eIF2α blot or against total eIF2α. Rapamycin was used at 20nM. 3-hydroxykynurenine was omitted due to toxicity to the cells.

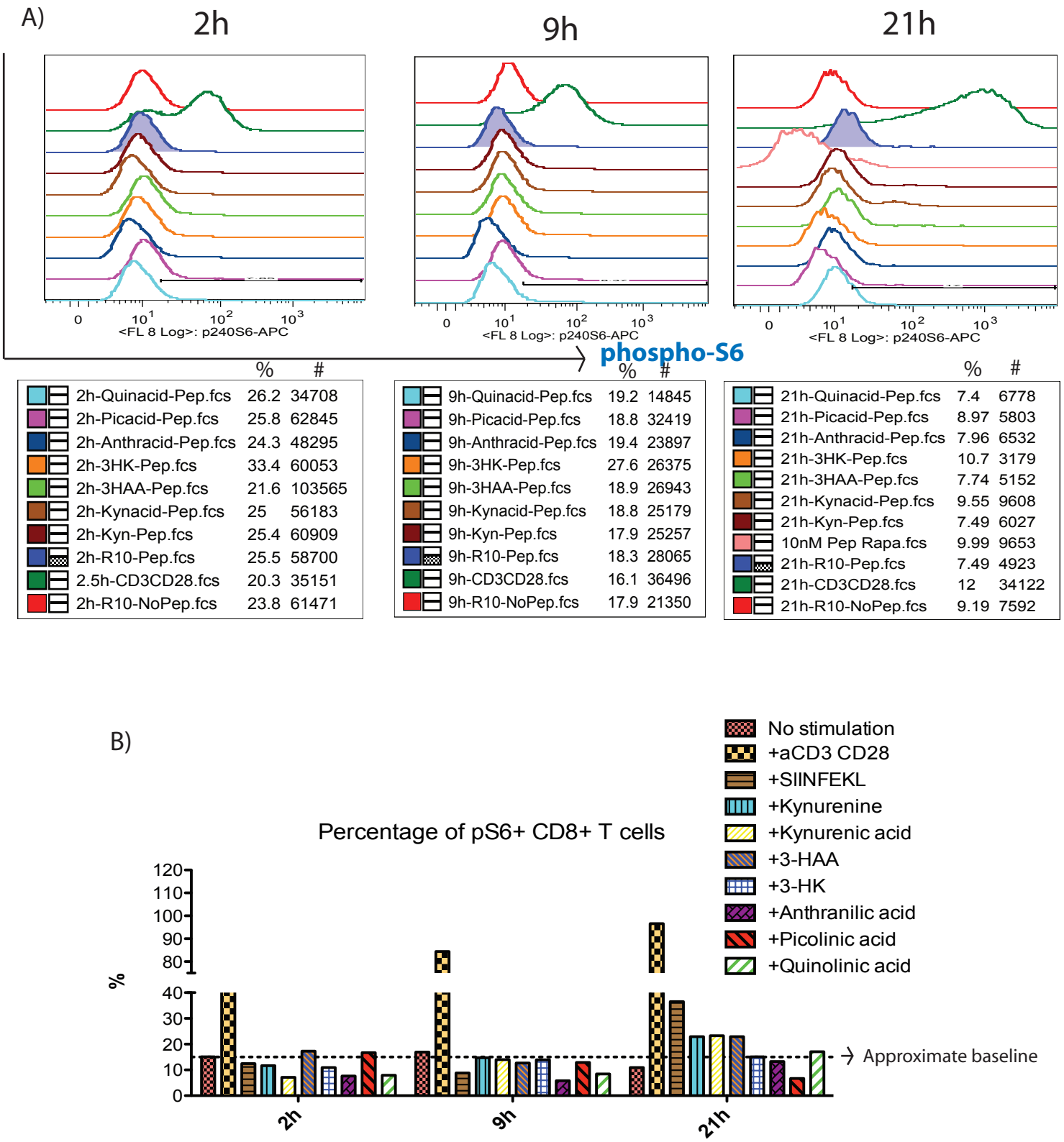

Figure 12. Kynurenines do not alter CD8+ T-cell mTOR activity significantly during low stimulation.

A) OT-I splenocytes were incubated for 2h, 9h and 21h with 25μM of each tryptophan metabolite in the presence of 10nM of SIINFEKL peptide. B) Quantitative representation of mTOR activity as measured by phosphorylated p-S6 in A. Rapamycin was used at 20nM. Analysis was done on live CD8+ B220- cells. CD69 was also measured which remained at baseline for each kynurenine at each time point (not shown). Cell percentages (#) and numbers (#) are live CD8+ B220- cells out of all live cells. Samples were pooled from duplicate wells. Representative of two experiments.

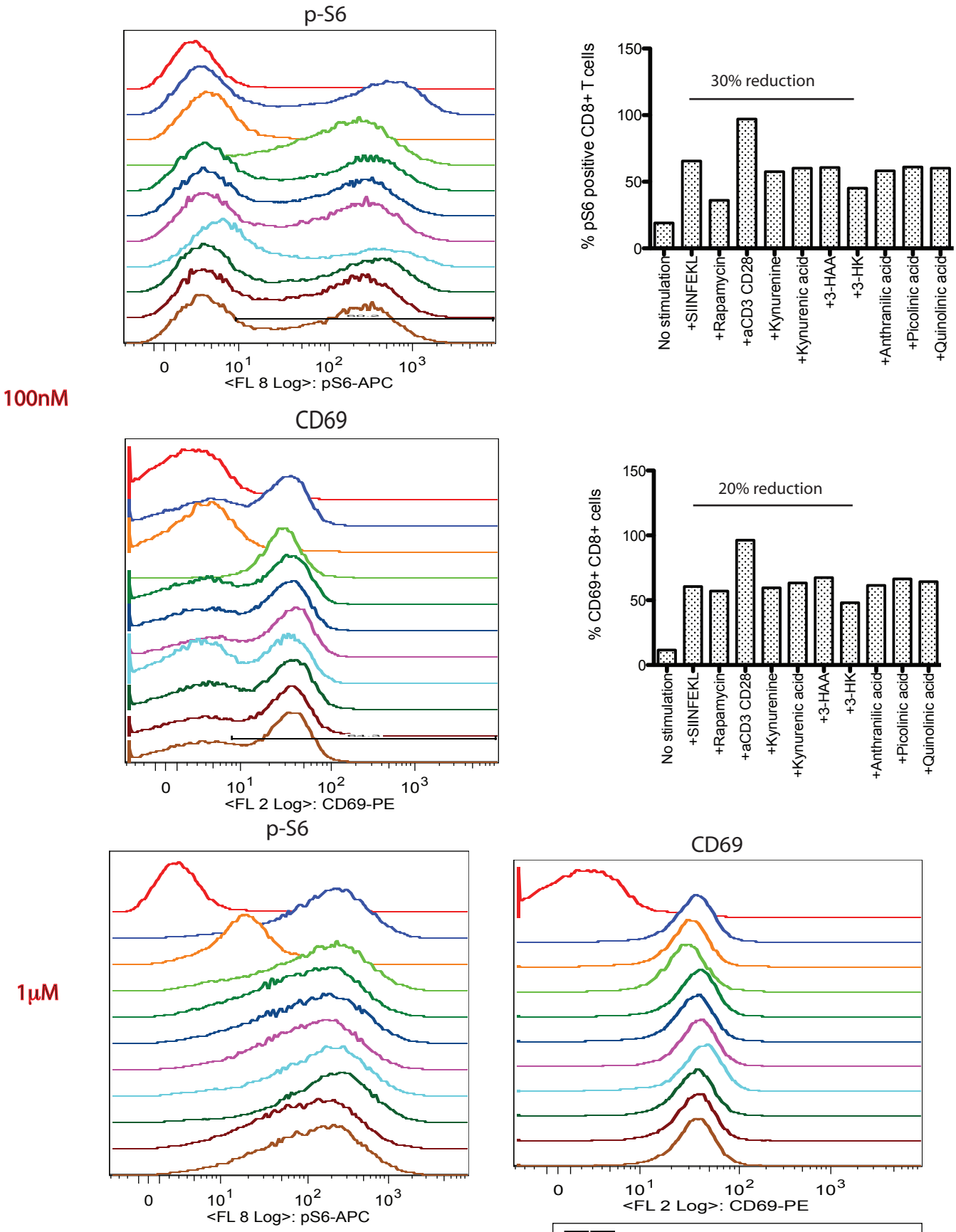

Figure 13. 3-hydroxykynurenine inhibits CD8+ T-cell mTOR and CD69 ~20-30% during moderate stimulation but the effect is lost during strong stimulation. OT-I splenocytes were incubated for 24h with 25μM of each tryptophan metabolite in the presence of either 100nM or 1μM of SIINFEKL peptide. Rapamycin was used at 20nM. Analysis for p-S6 and CD69 was done on live CD8+ B220- cells. Samples were pooled from triplicate wells. Experiment representative of at least two similar experiments.

Chapter 4: The immunoregulatory role of myeloid derived suppressor cells and the effect of amino acids on their function

4.1 Introduction

Myeloid derived suppressor cells are a heterogeneous population of cells with the ability to suppress both adaptive and innate immunity. Under normal conditions they are thought to have a role in preventing excessive immune activation and tissue damage; however in many pathological conditions, such as infections and cancer, their numbers are increased and their ability to dampen the immune response can have profoundly detrimental effects for the organism (reviewed in [232]). Known mechanisms that allow them to manipulate the immune system include the depletion of arginine and cystine/cysteine from their microenvironment. Arginine is consumed by arginase 1 and iNOS: under arginine-depleted conditions T-cells down-regulate CD3 ζ-chains thus impairing their function.[121,122] iNOS also generates nitric oxide, a potent inhibitor of T-cell proliferation [233], that further impairs T-cell function.

A more recent finding is the fact that MDSCs can act as "cysteine sinks" depleting this amino acid from their local.[127] Cystine is the disulfide-bonded dimer of two cysteine residues that can be reduced to cysteine under the right conditions. T-cells are particularly vulnerable to depletion of environmental cysteine because they do not have cystathionase that converts methionine to cysteine effectively turning this into an essential amino acid acid for them. Furthermore they do not express the xCT chain of the x_c^- transporter that transports cystine into the cell.[234] They are therefore dependent on the uptake of cysteine from the environment; under normal conditions macrophages and DCs can reduce cystine and provide a ready source for activated T-cells. When MDSCs are present, they upset this balance by taking up cystine –as they express the ASC neutral amino acid transporter that would normally allow reduced cysteine to be transported back to the extracellular space. This then leads to inhibition of T-cell proliferation. No other amino acid depletion –related inhibitory mechanism in MDSCs have so far been described in MDSCs so we decided to investigate this.

In this chapter we have studied the function of MDSCs in a DC-free system and looked at their functionality. We have also looked at the possibility that MDSC also use IDO and tryptophan depletion as an additional mechanism to augment their immunomodulatory

abilities. We have also examined the more general question of whether MDSCs deplete other essential amino acids in addition to arginine and cystine/cysteine from the local microenvironment and thereby cause any T-cells in their vicinity to undergo a proliferation arrest. Finally, we have studied the effect of MDSC and the subsequent amino acid depletion on the mTORC1 of CD8+ T-cells.

4.2 Materials and methods

4.2.1 Mice

C57BL/6, OT-1 and DO11.10 mice were bred in the Biomedical Services Unit, John Radcliffe Hospital, and used for *in vitro* experiments under the authority of a U.K. Home Office Project Licence.

4.2.2 Making of bone marrow -derived dendritic cells

Bone marrow derived DCs were obtained by *in vitro* differentiation of bone marrow monocytes. Bone marrow was flushed out from the tibias and femurs of mice with a syringe filled with R10 and 25-gauge needle. The resulting solution was then filtered through a cell strainer and any bigger particles mashed through with the plunger of a syringe. The cells were then spun down and the cells resuspended in red blood cell lysis buffer and R10 to remove the RBCs. The cells were then resuspended in R10. The cells were then resuspended in R10 containing granulocyte and macrophage –colony stimulating factor (GM-CSF) at 20 ng/ml and IL-4 at 20 ng/ml. On day 4 the medium was replaced with a fresh one containing the same amount of GM-CSF and IL-4. On day 6, the immature bone marrow cells were matured overnight with 1 μg/ml lipopolysaccharide (LPS).

4.2.3 Making and purification of myeloid derived suppressor cells

Bone marrow was extracted as above from the hind legs of mice with a syringe and the red blood cells lysed with red blood cell lysis buffer as above. The cells were then resuspended at $2x10^6$ cells/ml in R10 containing 1 ng/ml of recombinant mouse GM-CSF (Peprotech) and placed in a 6-well plate at 5 ml/well. The cells were cultured for 5-7 days and then purified with CD11c magnetic beads according to the manufacturer's

instructions (Miltenyi Biotec) (the negative fraction collected). After collecting the CD11c- fraction, the cells were labelled with a biotinylated anti-Gr1 antibody (ebioscience) for 20 min on ice. The cells were then washed with PBS/0.5%FCS and mixed with streptavidin beads according to the manufacturer's instructions (Miltenyi). The purified CD11c- Gr1+ cells were now ready to use. The usual purity of the preparations for Gr1+ cells as checked by FACS was 70-80% and in terms of strength of fluorescence for Gr1, we used both higher and middle populations together in our assays.

4.2.4 CFSE-staining of splenocytes

Cells were washed twice in PBS and then resuspended in PBS at 1-2x10^6/ml and 0.5 µM CFSE added. The solution was kept at room temperature for 8 min. To quench the CFSE stain, an equivalent volume of FCS was added to the solution and the cells spun down for 5 min at 1500 rpm. The supernatant was discarded and 10 ml of warm R10 added and the solution transferred to a new 15 ml Falcon tube. This was repeated twice. Finally the cells were resuspended in a desired volume of the media of choice. CFSE was obtained from Invitrogen. When used in cell proliferation assays, the CFSE stain halves with every cell division making it useful in measuring cell multiplication.

4.2.5 Purification of CD8+ T-cells from mixed splenocytes

The spleen was processed as above and the splenocytes resuspended in 100 µl of 0.5% FCS/PBS. Rat anti-mouse antibodies (MHC class II, CD4, CD11b and B220 at 4 µl each) were added and the mix incubated for 15 min on ice. The antibodies were then washed off and the cells resuspended in 300 µl of 0.5% FCS/PBS. The anti-rat Dynabeads (Invitrogen) used to separate the cells were prepared as follows: 300 µl of beads in a round bottom tube were rotated in magnet five times for 2 min. The supernatant was removed and 1 ml 0.5% FCS/PBS added. The suspension was rotated in the magnet

again five times for 2 min. The supernatant was removed and 1 ml of fresh FCS/PBS added and the process repeated twice. The beads were now washed and ready to use. The cells and the beads were then mixed (300 µl) and rotated at 4 ^{o}C for 30 min. The tube with the mix was then placed in the magnet and rotated a couple of times. The supernatant was collected as this was the negative fraction that contained the CD8+ cells. The cells were checked for purity by FACS and were found to be around 80% positive for CD8.

4.2.6 Arginase activity assay (colorimetric measurement)

MDSCs had been purified for CD11c- and Gr1+ and plated at 650 000 cells/well with the appropriate inhibitor at 500 µM in R10 and incubated for 48h. The cells were then lysed in 50µl/sample of lysis buffer containing 0.1% Triton X-100, 5 µl of aprotinin (stock 5-10 trypsin inhibitor units (TIU)/ml) and 5µg of antipain. Samples were then placed in a 37^{o}C heatblock for 30 min and vortexed every 10 min. Samples were then spun at 13000 rpm for 20 min and supernatant collected. Arginase was activated by the addition of 50 µl/sample of Tris-HCl (final concentration 25 mM) and 10 µl of $MnCl_2$ (final 10 mM) to the supernatant. The samples were then placed in a 56^{o}C waterbath for 10 min and then on ice. 100 µl/sample of arginine 0.5 M was then added and the samples heated in a heatblock at 37^{o}C for 30-120 min. The reaction was blocked with 800 µl of the following solution: H_2SO_4 1 part, H_3PO_4 3 parts and water 7 parts. To get the colour readout 40 µl/sample of 9% w/v di-alpha-isonitrosopropiophenone (dissolved in pure ethanol) was added to the samples and the samples heated for 30-45min at 100^{o}C. 200 µl of each sample was then placed in a flat-bottom 96-well plate and the colour intensity read at 540 nm in a cell plate reader. Standard curve was made with urea ranging from 200 µg/ml to 0.78 µg/ml. 50 µl of each standard was mixed with 50 µl of Tris-HCl and 10µl $MnCl_2$ and 100 µl of arginine 0.5 M added. Blank was 50 µl of 0.1% Triton X-100.

4.2.7 Arginase protein expression by western blot

Cells were lysed on the plate with the buffer detailed in chapter 3. The samples were pipetted up and down to dissolve all cell fragments and then spun down at 13000 rpm for 10 min. The supernatants were collected and protein content measured by a BCA assay (Pierce). The protein content was normalised across the samples so that an equal amount of protein from each sample was loaded into a NuPAGE (4-12%) Bis-Tris gel (Invitrogen). The gel was run in reducing conditions (DTT 40 μM/sample, MES buffer, (Invitrogen)) at 200 V for 35 min and then transferred sandwiched with a nitrocellulose membrane onto a semi-dry blotting apparatus. The protein transfer was run at 18 V for 40 min. The membrane was then blocked with 5% w/v BSA in 0.1% v/v Tween 20-PBS for 1 hour at room temperature. The membrane was then transferred into a tube containing the anti-arginase antibody at 1:150 (goat anti-mouse, Santa Cruz Biotechnology) in 5% BSA w/v, 0.1% Tween 20-PBS. The membrane was kept in the primary antibody on a roller overnight at 4^{o}C. Any unbound antibody was then washed off for 3x5min with 0.1% Tween-PBS. A donkey anti-goat secondary antibody with conjugated HRP was then added at 1:5000 in 5% w/v BSA, 0.1% Tween-PBS and incubated for 1 hour at room temperature. The secondary antibody was then washed off with 0.5% Tween-PBS for 5min and for 2x5min with 0.1% Tween-PBS. The membrane was then treated with Pierce SuperSignal chemiluminescent substrate for imaging of the blot.

4.2.8 IDO expression in MDSC by western blot

Purified MDSC (CD11c- Gr1+) were plated at 650 000 cells/well on a 24-well plate in R10, R10+ IFNγ (1000 u/ml, Peprotech) or in tryptophan and FCS –free RPMI and incubated for 48h. The supernatant was harvested and the cells lysed with lysis buffer for phosphoproteins (ingredients listed in chapter 3 methods). The protein content in the samples was then measured with a BCA assay and an equal amount loaded into a NuPAGE 4-12% Bis-Tris gel. The gel was run in reducing conditions (DTT 40

μM/sample, MES buffer (Invitrogen)) at 200 V for 35 min and then transferred sandwiched with a nitrocellulose membrane onto a semi-dry blotting apparatus. The protein transfer was run at 18 V for 40 min. The membrane was then blocked with 5% w/v BSA in 0.1% v/v Tween 20-PBS for 1 hour at room temperature. The membrane was then placed into a solution containing the rabbit anti-mouse IDO antibody (Santa Cruz Biotechnology, 1:150 in 5% w/v BSA, 0.1% Tween-PBS). The membrane was kept in the primary antibody on a roller overnight at 4^{o}C. Any unbound antibody was then washed off for 3x5min with 0.1% Tween-PBS. An anti-rabbit secondary antibody with conjugated HRP was then added at 1:10000 in 5% w/v BSA, 0.1% Tween-PBS and incubated for 1 hour at room temperature. The secondary antibody was then washed off with 0.5% Tween-PBS for 5min and for 2x5min with 0.1% Tween-PBS. The membrane was then treated with Pierce SuperSignal chemiluminescent substrate for imaging of the blot.

4.2.9 T-cell proliferation assays

CFSE-stained splenocytes were plated at 200 000 splenocytes/well in a 96-well (flat bottom) plate together with appropriate parts of MDSCs where relevant. The assay was run for 72h and proliferation of CD8+ B220- cells was analysed by FACS.

4.2.10 Quantitative PCR for IDO and SLC16A4

Q-PCR was performed on Applied Biosystems 7300 real-time PCR system using Quantitative CT programme with FAM-dyes and no quencher. For sequence probes we used the manufacturers (Applied Biosystems) recommendations as follows:

Human SLC16A4: Hs00190794_m1

Human IDO: Hs00158027_m1

Human ACTB: Hs99999903_m1

Human HPRT: Hs01003267_m1

Mouse SLC16A4: Mm00525195_m1

Mouse IDO: Mm00492586_m1

Mouse ACTB: Mm00607939_s1

Mouse HPRT: Mm00446968_m1

The assay was run in 96-well Q-PCR plates (Applied Biosystems) with a 20 µl sample volume. This consisted of 1 µl of probe, 10 µl of q-PCR master mix (Applied Biosystems), 4 µl of distilled water and 5 µl of cDNA mixed with distilled water (made up as 6 µl cDNA (made of 1 µg of RNA)+ 44 µl H_2O).

4.2.11 Kynurenine pathway expression in MDSC by PCR

MDSCs were purified as described in 4.3.2. The purified MDSCs (700 000 cells/sample) were cultured in R10, R10+IFNγ 1000 u/ml or in Trp/FCS –free media for 48h. After 48h, the cell culture media was taken off and cells lysed and RNA extracted with RNeasy kit (Qiagen). The RNA concentration and quality was measured with NanoDrop (Thermo Scientific). cDNA was made from an equal amount of RNA from each sample with Retroscript kit (Ambion). Each enzyme was amplified with Phusion DNA polymerase in the following reaction: Water 28 µl, HF buffer 10 µl, dNTPs 0.5 µl, forward primer 5 µl, reverse primer 5 µl, cDNA 1 µl, Phusion polymerase 0.5 µl. The PCR cycling was as follows: 2 min 95 ^{o}C, (30s 95 ^{o}C, 15s 57 ^{o}C, 30s 72 ^{o}C) x30, 5 min 72 ^{o}C. The following primers were used:

IDO (299bp):

Forward 5’ TTGAAAAGCTGCCCACACTG 3’

Reverse 5’ GTCCCCACCAGGAAATGAGA 3’

Kynureninase (325bp):

Forward 5’ ATGATGGAGCCTTCGCCTCT 3’

Reverse 5’ GGCGTTTGCCTACATCATGG 3’

Kynurenine 3-mono-oxygenase (330bp):

Forward 5’ CTGCACGTGGAAGGAGCATT 3’

Reverse 5’ CATCTCGGGGAACCTTGTCA 3’

3-hydroxyanthranilate 3,4-dioxygenase (307bp):

Forward 5’ GCAACAAGCTTATGCACCAGGA 3’

Reverse 5’ TCCTCAGTGTCCCCCACGTA 3’

Kynurenine aminotransferase (KATII) (283bp):

Forward 5’ CCTTTCCCAGTGGAAACCAG 3’

Reverse 5’ CCCTGAGGAGACGGTTTTTG 3’

Kynurenine formamidase (299bp):

Forward 5’ GTCTTCGGAGGAGCTGGAGA 3’

Reverse 5’ CCTGTGCAGTCAGTGGGTTT 3’

Picolinic acid carboxylase (327bp):

Forward 5’ TGGCTCGTAGGAATGCCATC 3’

Reverse 5’ CTGCTCGCCCAGAGGAAAG 3’

Quinolinic acid phosphoribosyltransferase (322bp):

Forward 5’ TGGCTGCTCCAAGTCACCAT 3’

Reverse 5’ GTTCCCCCAAGAGCAGGTG 3’

4.3 Results

4.3.1 Myeloid –derived suppressor cells (MDSCs) can inhibit CD8+ T-cell proliferation in vitro in response to cognate peptide presented either by matured bone marrow –derived dendritic cells (BMDCs) or by splenic antigen presenting cells

We first wanted to establish a reproducible assay to examine the effect of MDSCs on CD8+ T-cell proliferation in response to cognate peptide. In the first instance we used SIINFEKL-pulsed (100 nM for 2h at 37 ^{o}C) BMDCs that were added to the samples always at the ratio of 10 splenocytes to 1 of BMDCs. The ratio of MDSC varied from 10:1 to 1:1 (Figure 1A). T-cell proliferation was assessed using Cyan ADP-multi-colour flow cytometer by virtue of CFSE-staining as staining intensity per cell would halve for each cell division. The final analysis was done using FlowJo v8.8.6 software (© Tree Star Inc.) gating on the live CD8+ B220- cells.

The results show a MDSC –dependent inhibition of T cell proliferation with the inhibition strongest at a 1:1 splenocyte to MDSC ratio. The number and ratio of CD8+ B220- cells also go down the more MDSCs are present.

To simplify the experimental system and remove a source of potential experimental variability, we went on to repeat this assay without specially matured BMDCs, instead relying on splenic antigen presenting cells. Splenocytes and MDSC were mixed in various ratios in the presence of 100 nM of SIINFEKL peptide which showed that MDSCs started to have a visible effect when they are present at 1 part to 7 parts of splenocytes. When fewer MDSC were used, they did not inhibit the CD8+ T cell proliferation (Figure 1B). If SIINFEKL peptide was directly added to purified CD8+ T-cells alone or with MDSCs, no proliferation above baseline was detectable (data not shown). CpG is known to relieve MDSC –mediated T cell suppression in an environment where BMDCs are present.[235] In the absence of BMDCs, CpG did not relieve T-cell suppression (Figure 1C).

4.3.2 Inhibition of CD8+ and CD4+ T-cells by MDSCs is enhanced by additional IFNγ

IFNγ has been reported as essential for the inhibitory action of MDSCs.[236,237] On activation CD8+ T cells produce IFNγ that helps MDSCs to inhibit T-cells. We wanted to see whether additional IFNγ can enhance the suppression of CD8+ and CD4+ T cells. Splenocytes and MDSCs were used at a 5:1 ratio unless otherwise stated. Where relevant, the concentration of recombinant GM-CSF was 1 ng/ml. The SIINFEKL concentration in the experiment with CD8+ T-cells was 200 nM and the anti CD3 CD28 concentration in the CD4+ T cell experiment was 5 μg/ml.

MDSCs had been purified and placed in wells containing normal R10 media, R10 + IFNγ media, or tryptophan and FCS-free media. The cells were incubated for 48h and their inhibitory strength was evaluated after mixing them with CFSE-stained splenocytes. MDSCs in R10 showed stronger inhibition when given additional GM-CSF for the duration of the proliferation assay (Figure 2A). The IFNγ and GM-CSF containing samples showed the strongest suppression of CD8+ T cell proliferation of all the groups, confirming that the inhibitory function of the MDSCs is dependent on the extracellular IFNγ concentration (Figure 2B). Surprisingly, the MDSCs that had been cultured in the nutrient-deprived media prior to the proliferation experiment had not lost their functionality and still showed almost equivalent suppression of CD8+ T-cell growth to the other groups (Figure 2C).

When CD4+ T-cell proliferation was examined, the MDSCs did not cause a reduction in T-cell proliferation when no IFNγ was added (Figure 2D). This experiment also showed that for CD4+ T-cells to be suppressed more MDSCs have to be present, however this could be due to the stronger stimulation achieved with CD3 and CD28 antibodies compared to stimulation with a cognate peptide. At 5:1 ratio of splenocyte to MDSC with IFNγ present, there was minor inhibition of CD4+ T-cell proliferation but at 3:1, there was almost no growth of CD4+ T-cells. When IFNγ had not been added to the samples, the overall growth of CD4+ without MDSC was also slower. When the MDSCs were added in the absence of IFNγ, they did not show any inhibition of CD4+ T-cell

proliferation at either concentration. This suggests that IFNγ plays an important role in MDSC-mediated inhibition of both CD8+ and CD4+ T-cells.

4.3.3 MDSC –mediated CD8+ T –cell inhibition is proportional to the strength of T-cell stimulation

In view of our early results suggesting that IFNγ promotes the inhibitory function of MDSCs, we decided to investigate whether the strength of the stimulation signal also has a significant effect; we hypothesised that either excess IFNγ, other cytokines or even cell surface molecules induced by strong antigenic stimuli might affect the suppressive strength of the MDSCs.

In this experiment the ratios of splenocytes to MDSC used were 5:1 and 3:1. The SIINFEKL concentrations were 10 nM, 50 nM, 100 nM, 200 nM and 400 nM. At 5:1 ratio, there was a clear stimulation-dependent inhibition pattern, whereby stronger stimulation resulted in stronger inhibition by the MDSCs (Figure 3A). This result is also quantified in Figure 3B where the median fluorescence index (each cell has a fluorescence value and the median is the middle value in the distribution of values of all all cells) for CFSE-stained CD8+ B220- cells is higher when the SIINFEKL concentration is higher, indicating a lower rate of proliferation. The same significance of the results was also achieved by calculating the percentage of proliferated CD8+ cells (Figure 3B). At 3:1 ratio, the MDSC inhibited strongly irrespective of the strength of the T cell stimulation and this was also illustrated quantitatively (Figure 3C and D).

4.3.4 MDSCs utilise arginase and iNOS as a method to inhibit CD8+ T –cell proliferation by depleting arginine

Here we show that arginase is present in MDSC and that the known arginase and iNOS inhibitors (N-hydroxy-arginine (NHA), (Nω-hydroxy-nor-arginine (NHNA) and L-NG-monomethyl-L-arginine (L-NMMA)) do not affect its expression (Figure 4A). Arginase is expressed by MDSC cultured in R10, but not by B6 splenocytes and weakly by EG7 WT

or IDO-transfected cells (Figure 4B). The Coomassie stain of the gel after protein transfer is included in Figure 4B to show that the loading was equal even though the α-tubulin bands are not uniform in the western blot. This was a recurring problem with the MDSC western blots.

When the inhibitors were used in a functional assay in which the cells were incubated with 500 μM of each inhibitor for 48h and then pelleted for a colorimetric assay, all inhibitors showed minor inhibition of arginase, including the iNOS inhibitor L-NMMA (Figure 4C). The effect of the inhibitor was also studied in another functional assay where the readout was T-cell proliferation (CFSE division). The iNOS inhibitor L-NMMA showed statistically significant relief of MDSC-mediated suppression of T-cell proliferation at both MDSC concentrations but the dedicated arginase inhibitors did not relieve the suppression (Figures 4F, 4G, 4I). There was, however, an increase in CD8+ B220- cell numbers with both NHA and NHNA (Figures 4D and E).

We also looked into whether an addition of excess arginine can relieve the proliferation suppression and also how a media lacking arginine would affect the suppression. At both MDSC concentrations the addition of arginine brought no relief to the suppression (Figure 4E and H). Interestingly, the cells in arginine-free media proliferated considerably better than the cells in normal R10 in the presence of MDSCs (5:1) (Figures 4E, 4F, 4H, 4I). The same cannot be seen when the MDSCs are at a higher concentration (3:1).

4.3.5 IDO is expressed functionally by HeLa cells in response to IFNγ and a putative alternative tryptophan transporter SLC16A4 is up-regulated on tryptophan depletion

An alternative tryptophan transport system has been studied in our laboratory for the past couple of years.[186] It appears to be upregulated in tumour cell lines that have been either transfected with IDO or induced with IFNγ to express IDO resulting in rapid depletion of tryptophan from their culture media.

In this set of experiments we have looked at the expression of SLC16A4, which we believe to be the putative tryptophan transporter responsible for our previously obtained and published results[186], in HeLa WT cells that have been stimulated with various concentrations of IFNγ (10, 100, 500, 1000, 10000 u/ml). We have also examined what the expression level of IDO is relative to the concentration of IFNγ present, and whether the expression is sensitive to the level of available tryptophan. Both of these experiments were done for 24h and 48h, and also with added tryptophan (48h).

The expression level of SLC16A4 mRNA remained constant and low after 24h at all IFNγ concentrations, possibly because there was still free tryptophan in the media (Figure 5A and B). At 48h, when tryptophan has almost completely been consumed, SLC16A4 expression started to increase in groups stimulated with at least 100 u/ml of IFNγ. Once the expression of SLC16A4 had been up-regulated, it was not affected by additional IFNγ. Adding tryptophan after 24h of IFNγ stimulation did not prevent an increase in the levels of SLC16A4 mRNA detectable 24h later. This indicated that tryptophan starvation triggers a pathway leading to SLC16A4 up-regulation that cannot be immediately switched off. Repeat experiments using more time points and different starting tryptophan concentrations in the media will need to be performed to clarify the conditions driving SLC16A4.

IDO expression is up-regulated in many cells in response to IFNγ stimulation.[238] In parallel set of experiments we investigated whether its expression was dose-dependent and whether once initiated stayed relatively constant. In our hands the expression of IDO mRNA expression started within 24h at IFNγ concentration of 100 u/ml and the same concentrations were also required for the effect to be detectable after 48h (Figures 5C and D). Its levels also were not further raised by additional IFNγ above 100u/ml unless additional tryptophan was given after 24h which resulted in dramatic increase in the expression of IDO mRNA. Interestingly, the expression of IDO did not decrease at these time later points even when tryptophan levels were depleted. Therefore it seems that the expression of IDO is more sensitive to the tryptophan levels at the onset of IFNγ-mediated stimulation but is less dependent on it once the IDO

mRNA transcription has commenced. In the presence of non-limiting tryptophan concentrations as in the 48h samples with added tryptophan, levels of IDO mRNA expression are proportional to the strength of the IFNγ stimulus.

4.3.6 IDO is up-regulated in MDSCs after IFNγ treatment at the mRNA level but not functionally, and they do not express the alternative Trp transporter

We then went on to examine the expression of SLC16A4 and IDO in MDSCs. We were interested to see whether IDO is also one of the immunomodulatory mechanisms employed by MDSCs in tumour or inflammatory settings and whether they also accordingly employ SLC16A4 to improve their ability to take tryptophan up in a depleted environment.

We incubated purified MDSCs (CD11c- Gr1+) in R10+ IFNγ (1000 u/ml), R10 only, or kept them in Trp/FCS-free media for 48 hours with or without extra GM-CSF (1 ng/ml) during the 48h. The expression of SLC16A4 was not up-regulated against Actin or Hprt in any of the samples (not shown), and when the IFNγ or Trp/FCS-free samples were compared against the R10 sample, there was no up-regulation either but rather slight down-regulation (Figure 6A). IDO mRNA expression in the similarly treated MDSCs is, however, increased by more than 10-fold after IFNγ treatment (Figure 6B).

This led us to test by western blot the IDO protein levels in the cells after the three treatments. There was no significant increase in the IDO protein levels except for a minor one in the IFNγ –treated cells after the bands were quantified (Figure 6C). Even this small increase in IDO protein expression however is not reflected in a measurable increase in activity after IFNγ treatment, however, as there is no increase in the extracellular kynurenine levels as measured from the cell culture media by HPLC (Figure 6D).

4.3.7 The kynurenine pathway of IFNγ-treated MDSCs is expressed all the way to NAD+ synthesis and they may result in excess 3-hydroxykynurenine production

Even though up-regulation of IDO activity does not seem to contribute to MDSCs' immunomodulatory abilities, we were interested in obtaining a better overview of the kynurenine pathway in the context of MDSC metabolism, as there are several intermediate metabolites with well-established effects on the immune system e.g. driving T_{reg} development[160] and T-cell apoptosis.[159,222,215] Therefore it would be interesting to see whether any of the enzymes responsible for the production and catabolism of these metabolites are up- or downregulated in MDSCs potentially providing them with yet another immunomodulatory mechanism.

We amplified IDO, kynureninase, kynurenine mono-oxygenase, 3-hydroxyanthranilate 3,4-dioxygenase, kynurenine aminotransferase, kynurenine formamidase, picolinic acid carboxylase, and quinolinic acid phosphoribosyltransferase of the kynurenine pathway enzymes. The enzymes were amplified from purified MDSCs that had been incubated in R10, R10 + IFNγ or in Trp/FCS –free media for 48h.

In the R10-treated cells there is only a weak level of expression of IDO, 3-hydroxyanthranilate 3,4-dioxygenase and kynurenine aminotransferase so it is unlikely that the cells would preferentially make any metabolite in particularly large quantities when unstimulated (Figure 7). When the cells have been treated with IFNγ, however, the pathway is expressed all the way to the NAD+ synthesis indicating a global metabolic up-regulation during IFNγ stimulation. Kynurenine formamidase level was low but this step can take place non-enzymatically. There was a clear up-regulation of kynurenine mono-oxygenase the enzyme responsible for conversion of kynurenine into 3-hydroxykynurenine (3-HK). The latter been implicated as one of the factors promoting T_{reg} development[160] and it is possible that MDSC might make sufficient 3-HK to have an effect on any nearby T-cells. Confirmation of this hypothesis would require functional studies with quantitative measurements by Q-PCR.

MDSCs that were incubated in media lacking tryptophan and FCS, did not express the complete pathway; picolinic acid carboxylase and quinolinic acid

phosphoribosyltransferase were the only enzymes with detectable levels of mRNA expression, and therefore probably do not make excess kynurenine metabolites. MDSCs in all of these treatment groups were able to inhibit T-cell proliferation: nevertheless IFNy-treated cells seemed to have stronger inhibitory capabilities and this may be partially attributable to 3-HK production and the subsequent T_{reg} development.

4.3.8 Some essential amino acids can partially rescue CD8+ T -cell proliferation in the presence of MDSCs

Since arginine and cystine/cysteine depletion are known methods by MDSCs for their inhibitory action[122,127], we were interested in studying whether any other essential amino acids were taken up and metabolised by MDSCs to either deplete or to produce catabolites that modify T-cell function. We hypothesised that if this was the case and this process contributed to a significant extent to the MDSCs ability to inhibit T-cell proliferation in vivo, then providing an excess of the relevant amino acids should prevent this. We therefore devised a functional assay that determined the ability of individual amino acids to rescue T-cell proliferation in co-cultures with MDSCs when added every 24h into the media - we tested valine, leucine, cystine, phenylalanine, tryptophan, arginine, histidine, methionine, tyrosine, threonine, isoleucine and lysine. CFSE staining was used to provide an estimate of T-cell proliferation over 72h. The concentrations of amino acids added each day were the same as the starting concentrations in normal R10 media (valine 170 μM, leucine 380 μM, cystine 200 μM, phenylalanine 90 μM, tryptophan 25 μM, arginine 1.1 mM, histidine 97 μM, methionine 100 μM, tyrosine 130 μM, threonine 170 μM, isoleucine 380 μM and lysine 270 μM).

The daily addition of histidine, methionine, tyrosine, threonine, isoleucine and lysine did not have any effect on MDSC-mediated inhibition of T-cell proliferation either when the splenocyte to MDSC ratio was 5:1 or 3:1 (not shown). At either MDSC concentration the addition of arginine surprisingly did not have any effect on the inhibition and neither did tryptophan (Figure 8A and C). The results were also quantified by calculating the MFI and percentage of proliferated CD8+ T-cells and the differences

were not significant between the samples despite the visual appearance in the graphs (Figure 8B). A larger experiment would be warranted to achieve more certainty as to the relief of inhibition after particular amino acid addition. The result with tryptophan was expected as the MDSCs do not appear to express or up-regulate active IDO and therefore should not consume it to an extent that would affect T-cell proliferation. Cystine partially relieved the inhibition at the 5:1 ratio and enabled further T-cell proliferation, as was expected from published data which showed that MDSCs sequester cystine and do not export the converted product cysteine that T-cells would be able to utilise thus depleting them of the amino acid.[127] Therefore adding it makes more cystine available for other cells, such as macrophages, to convert for T-cells' use. Cysteine is important for T-cell activation so when there is more available, they can probably partially overcome MDSC-mediated suppression. Valine, leucine and phenylalanine at 5:1 also seemed to help to partially relieve the suppression of T-cell proliferation. At the 3:1 ratio none of the amino acids relieved the MDSC-mediated inhibition (Figure 8C).

4.3.9 Arginine, cystine, valine, leucine and phenylalanine do not appear to rescue CD4+ T-cell proliferation in response to anti-CD3 and anti-CD28 in the presence of MDSCs

We were also interested whether these findings could be extended in the CD4+ T-cell setting and proceeded with devising a similar experiment using the same amino acids as in the previously but this time focussing on CD4+ T-cells. DO11.10 splenocytes were incubated for 72h with MDSCs made from the D11.10 mouse of the same sex. Due to the lack of availability of the OVA peptide ($OVA_{323-339}$, ISQAVHAAHAEINEAGR) to stimulate the cells, we used anti-CD3 and anti-CD28 antibodies (5 µg/sample). This makes the CD8+ and CD4+ -based experiments not directly comparable but gives at least an indication as to the similarity/difference to the way the two types of T-cells react to the addition of the amino acids when MDSCs are present. We used only the amino acids that had come up "positive" for relief from the MDSC-mediated inhibition of proliferation in the CD8+ T-cell experiment. Again, the amino acids were added every 24h at the

concentration that they are normally found in the RPMI 1640 media (see 4.3.8 for concentrations). The splenocyte to MDSC ratios used were 5:1 and 3:1.

Due to the difficulty in solubilising cystine we had to dissolve it first in HCl and despite bringing its pH back to 7-7.5, it was often toxic to the cells in culture, making it difficult to study its effects in our new model system and compare results with the previous experiment. As expected tryptophan did not rescue the CD4+ T-cell proliferation and neither did arginine, in concordance with the results for CD8+ T-cells. Surprisingly, valine, leucine and phenylalanine had no effect on the T-cell proliferation even during milder suppression by the MDSCs at 5:1 (Figure 9A and 9B). Not unexpectedly, there was no effect by the amino acids on the CD4+ T-cell proliferation when the MDSC-mediated suppression was strong at 3:1 (Figure 9C).

4.3.10 MDSCs inhibit mTOR activity in CD8+ T –cells marginally after 24h but enhance it after 48h in the remaining CD8+ T –cells

Considering that MDSCs deplete at least arginine and cystine/cysteine from the extracellular amino acid pool, we were interested to see whether this has a detectable effect on the T-cell mTORC1 pathway. As mTORC1 activity is known to be inhibited when certain essential amino acids are depleted[177] and as these include arginine we would expect its depletion by MDSCs to result in mTORC1 inhibition.

Splenocytes and purified MDSCs from sex-matched C57BL/6 mice were mixed at 5:1 and 2:1 ratios and stimulated with 5 μg of anti-CD3 and CD28 antibody in R10. The cells were incubated for 24h and 48h and the live CD8+ B220- cells analysed for levels of phosphorylated S6. Three groups were included based on culture media, one of which was R10 only, one R10 + 25 μM Trp, and one R10 + Arg 1.1 mM. The amino acids were added at the beginning and also 24h into the experiment in the case of the 48h samples.

After 24h, there is a small reduction in p-S6 levels in the CD8+ T-cells in the R10 only samples and this is statistically significant albeit very minor (Figure 10A and C). Curiously when either tryptophan or arginine was added, it decreased the pS6 levels

somewhat in the samples where MDSCs were not present. If they were present, the addition of either amino acid made no difference when compared to the p-S6 levels in the samples without MDSCs but with the amino acid (Figure 10A and C). The results were even more unexpected after 48h. Instead of the MDSCs inhibiting the p-S6 levels in the CD8+ T-cells, they were raised in the cells. These results were statistically significant in all samples, with or without added tryptophan or arginine (Figure 10B and D). The MDSCs had inhibited the T-cell proliferation during the 48h as judged from the cell numbers in Figure 10 but it appears that the remaining cells increased their mTORC1 activity as expressed by increased levels of S6 phosphorylation.

4.4 Discussion

In this chapter we have looked at another immunosuppressive mechanism involved in cancer that has relatively recently been described. Myeloid derived suppressor cells are a heterogeneous population consisting of mature and immature myeloid cells, and they are found in most patients with cancer.[239] One of the mechanisms MDSCs use to inhibit T-cell proliferation is by depleting the amino acids arginine and cystine/cysteine from their microenvironment.[127,240,125]

Arginine depletion is one of the most well characterised mechanisms. L-arginine is the substrate for two enzymes; arginase that converts it to urea and L-ornithine, and iNOS that produces nitric oxide (NO).[233,241] The effects of arginine shortage in the T-cell microenvironment include the down-regulation of the T-cell CD3ζ co-receptor and decrease of the expression of the cell cycle regulators cyclin D3 and cyclin-dependent kinase 4 (CDK4).[242,243,121] By producing NO, iNOS in turn suppresses T-cell function by inhibiting the phosphorylation of JAK3 and STAT5 in T-cells.[123] Other mechanisms include the inhibition of MHC class II expression in APCs and the induction of apoptosis.[124,244] We were interested in looking whether MDSCs can use any other amino acids for this purpose, how they affect the mTOR signalling of CD8+ T-cells and how dependent their inhibitory ability is on the strength of activation of effector cells.

We started by looking at mouse MDSCs and whether their inhibitory capability in vitro was influenced by the presence of matured BMDCs. Most studies involving MDSCs so far have been in vivo or have used BMDCs to act as APCs to the effector T-cells. We wanted to see whether a simpler in vitro assay could be used for studies in which we evaluated what the effect of different amino acid concentrations in the media had on the function of either MDSCs or effector cells in the same sample. By not having additional BMDCs in the cultured samples, we could ignore any effect matured BMDCs may have on the media and remove an additional source of variability as they would have had to be derived from a different animal than the one providing the effector cells.

The control assay involving BMDCs showed an MDSC dose-dependent inhibition of CD8+ T-cell proliferation with the strongest inhibition observed at a ratio of 1:1 of

purified CD8+ to MDSC. We then went on to show that without BMDCs, using unseparated splenocytes instead to provide both the APCs and the T-cells, the ratio of whole splenocytes to MDSC needed for almost complete inhibition of CD8+ T-cells was between 5:1 or 7:1. As the CD8+ T-cells would have constituted between 10 to 15 % of the unseparated splenocyte population, this indicates that somewhat higher amounts of MDSCs were necessary to obtain similar levels of inhibition. Whether this was due to impaired cell-cell contact secondary to the increased number of non-effector non-MDSC cells in the well, or to the lack if mature BMDCs or to some other factor remains to be established. In any case we can conclude that MDSCs can inhibit CD8+ T-cell proliferation in the absence of mature BMDCs albeit with reduced efficacy.

CpG was also used as a control to inhibit the MDSC activity as has been reported, although we saw no inhibition when mature BMDC were not used.[235,245] This lack of inhibition of MDSC activity is not surprising, though in the light of results showing that CpG-mediated inhibition of MDSC activity is due to the activation of TLR9 on DCs (particularly plasmacytoid DCs (pDCs)).[235] On engagement of TLR9 the pDCs produce IFNα that enables the maturation of MDSCs into macrophages that do not suppress T-cell proliferation.[235] In the absence of mature BMDCs able to respond to CpG no IFNα will be produced and as a result the suppressive activity of MDSCs is not affected.

We chose to use the 5:1 ratio of whole splenocytes to MDSCs, and in subsequent experiments this is what was used unless otherwise mentioned. We went to confirm that IFNγ is needed for the inhibitory activity of MDSC since its addition clearly enhanced it. Its effect was even more pronounced in inhibiting CD4+ T-cell proliferation as they would not normally secrete as high levels of IFNγ as CD8+ T-cells. There was no inhibition of CD4+ T-cell proliferation without IFNγ even at the highest concentration of MDSCs (3:1). This dependency of MDSCs inhibitory ability on IFNγ has been documented by others too [237,246] and it has been suggested that it is required for the activation of iNOS in the MDSC [247] or the induction of IL-4 and IL-13 production by MDSC that then induce arginase I expression.[246] However, our results for CD4+ cells were conducted in the presence of CD3 CD28 antibodies, and not the cognate peptide and this may have had an effect on the sensitivity of the cells to IFNγ. In our experience

the cells respond very strongly to the antibodies and subtle differences with added IFNγ may therefore go unnoticed. Therefore any future work for comparison should be performed with the cognate peptide in order to achieve equal stimulation.

Next we wanted to look at the dependency of MDSC activity on the strength of CD8+ T-cell stimulation. We used OT-I splenocytes and MDSC for this experiments and titrated the SIINFEKL cognate peptide to see whether this could affect the MDSC function. We saw that the MDSCs inhibited more strongly at higher peptide concentrations but this was only clearly visible when the MDSC concentration was at 5:1. This was not due to exhaustion of the T-cells by the stronger stimulation as without MDSCs they proliferated normally. The effect was not as clear anymore at higher MDSC concentrations – where inhibition might have been maximal in any case. All groups were supplemented with an equal amount of IFNγ at the beginning of the experiment but it is possible that the effect could be due to increased amounts of IFNγ secreted by the CD8+ T-cells in response to the stronger stimulation. Alternatively the increase in stimulation might have led to increased production of reactive oxygen species or nitrogen species along the increase in stimulation. It is also possible that the inhibitory function of MDSCs requires reaching a certain threshold of T-cell activation before they become functionally inhibitory. There may be a higher 'licensing' signal that is required before the MDSCs can become inhibitory as a safety mechanism to prevent inhibition in environments that have low inflammation. Further investigations will have to be done to establish the cause and it would also be interesting to repeat this assay using a trans-well plate that allow physical separation of the splenocytes and MDSCs preventing cell-cell contact. This would give an indication as to whether the inhibition is contact-dependent or mediated by soluble factors. In any case, these results further enhance the notion that the function of MDSCs is strongest when they are present in an inflammatory environment as suggested by Haverkamp *et al*. [237] and it is not dependent on DCs.

We then moved on to investigate the amino acid aspect of MDSC-mediated inhibition, and proceeded to confirm the expression of arginase in MDSCs. We could not see marked inhibition of MDSC activity with the arginase inhibitors we used; only some

with the iNOS inhibitor L-NMMA suggesting that iNOS activity in MDSCs is more potent as an inhibitory mechanism than arginase activity. We could not give all the inhibitors together at the same concentration due to toxicity to the cells. Interestingly it turned out that the MDSCs did not suppress well in assays that lacked arginine completely. This raises the possibility that the presence of arginine itself is not as important to the T-cells and it is the arginine metabolites that actually inhibit the T-cell proliferation. At higher MDSC concentration (3:1), other MDSC-mediated suppression mechanisms probably override the benefit of not having arginine-derived metabolites around as T-cell proliferation was almost completely abolished.

Our research group recently discovered that IDO+ tumour cells can increase their uptake of tryptophan by up-regulating an additional tryptophan transporter.[186] This enables cancer cells to take up tryptophan from the environment more efficiently than T-cells that do not express it. Combined with IDO expression by tumour cells, the up-regulation of the additional transporter results in rapid depletion of tryptophan, conferring a significant disadvantage to T-cells as they are forced to use less efficient transporters, such as System L. Although this transporter has not yet been conclusively identified, data from experiments in our laboratory suggest the monocarboxylate transporter 5 (SLC16A4) as a strong candidate for this role.

We have shown the upregulation of the transporter here in IFNγ-stimulated HeLa cells which up-regulate it under low tryptophan conditions within 48h. IDO mRNA was also up-regulated but more rapidly -within 24h. At this point tryptophan had not yet been completely consumed so SLC16A4 expression was low. As soon as tryptophan in the media ran out the expression of the transporter went up. Interestingly IDO mRNA expression is not reduced when tryptophan is depleted within the time-frame we used.

Since MDSCs are able to survive within a tumour microenvironment, and are known to use amino acid-depleting mechanisms, it is conceivable that they might also express IDO when stimulated by IFNγ and take advantage of the high affinity tryptophan transport system in a tryptophan-low setting. Somewhat surprisingly then, while MDSCs express IDO mRNA after IFNγ stimulation, they do not produce the functional protein. They also do not up-regulate the SLC16A4 in a tryptophan-low environment. Therefore it does not

look like MDSCs utilise IDO in their repertoire to inhibit T-cells or SLC16A4 as an aide with which to survive in the tumour microenvironment. They up-regulate IDO mRNA but this does not seem to translate into enzymatic activity at least within the time scale we have looked at.

Although IDO itself does not appear to be up-regulated by the MDSCs, this did not preclude the possibility that other tryptophan breakdown products might be produced and accumulated via changes in expression of other members of the tryptophan catabolic pathway. We therefore proceeded to examine the expression of the kynurenine pathway enzymes in the MDSC. There was a generalised up-regulation of the pathway in the IFNγ -treated cells that would appear to lead to NAD+ synthesis, and this was consistent with what we would expect to see in a cell with increased metabolic demands due to interferon stimulation. We did detect, however, proportionally stronger up-regulation of kynurenine mono-oxygenase –the enzyme responsible for 3-HK production, so it is conceivable that this metabolite could accumulate in amounts sufficient to cause T-cell inhibition. These results were not quantitative, however, so expression levels would have to be confirmed by quantitative PCR.

Since IDO and tryptophan depletion were not additional mechanisms that MDSCs employ to inhibit T-cells, we looked at the possibility that other essential amino acids could be taken up by MDSCs similarly to arginine and cystine/cysteine. We tested many amino acids and discovered that addition of valine, leucine and phenylalanine suppressed MDSC activity slightly *in vitro*. While these results were not statistically significant as the strength of relief varied from experiment to experiment they do, however, show an interesting phenomenon and illustrate that other amino acids have the potential to alter MDSC-mediated T-cell inhibition. For valine this effect may be due to the fact that it is a known arginase inhibitor[248] in high concentrations, which then partially inhibits the arginase function of the MDSCs. Leucine in turn inhibits arginine transport via the transport system y^+L in Xenopus oocytes[249] and may have the same effect in mouse cells thus partially blocking arginine depletion employed by the MDSCs. The effect of phenylalanine can possibly be attributed to a similar phenomenon as it

shares its transporter with arginine in oocytes[250] and therefore may prevent arginine uptake also in mouse MDSCs.

It is noteworthy that these effects were not seen in CD4+ T-cells demonstrating an interesting difference between the T-cell subtypes. Although MDSCs do inhibit CD4+ T-cell proliferation, it is clear that processes such as increased ROS production play a much more significant role than amino acid depletion. CD8+ T-cells on the other hand seem more dependent on amino acid availability and are therefore more receptive to the addition of amino acids during the experiment. Again, however, these experiments would have to be carried out with the cognate peptide as stimulation to provide a fair comparison.

Lastly we studied the effect of MDSCs on the mTORC1 signalling pathway of activated CD8+ T-cells. Since MDSCs deplete arginine and cystine/cysteine from their micro-environment, we hypothesised that starvation of these amino acids should result in detectable inhibition of the mTORC1 axis in T-cells. We could indeed see slight inhibition of mTOR after 24h but significant activation after 48h. There had been clear inhibition of proliferation of the CD8+ T-cells but it appeared that the remaining cells had increased their mTOR activity. This is an interesting result and would be consistent with recent studies that have demonstrated reactivation of the mTORC1 pathway under conditions of prolonged starvation to limit autophagic processes.[251,252] The addition of tryptophan or arginine did not relieve the mTOR inhibition, however, indicating that the other toxic effects of MDSCs such as NO and ROS, were likely responsible for the effects on the mTORC1 pathway and further experiments – including shorter time courses and inhibitors of iNOS would be needed to establish the cause and significance of the effects on mTORC1. These experiments were done with anti CD3 and CD28 stimulation and it would be interesting to see whether there was a difference if the T-cells were stimulated with the cognate (SIINFEKL) peptide. The signalling cascade between these two methods is different and may affect how much the MDSC are able to inhibit the T-cells. The ability of the MDSC to affect the mTOR (e.g. timescale and strength) in T-cells could therefore be different due to the different stimulation state of the T-cell.

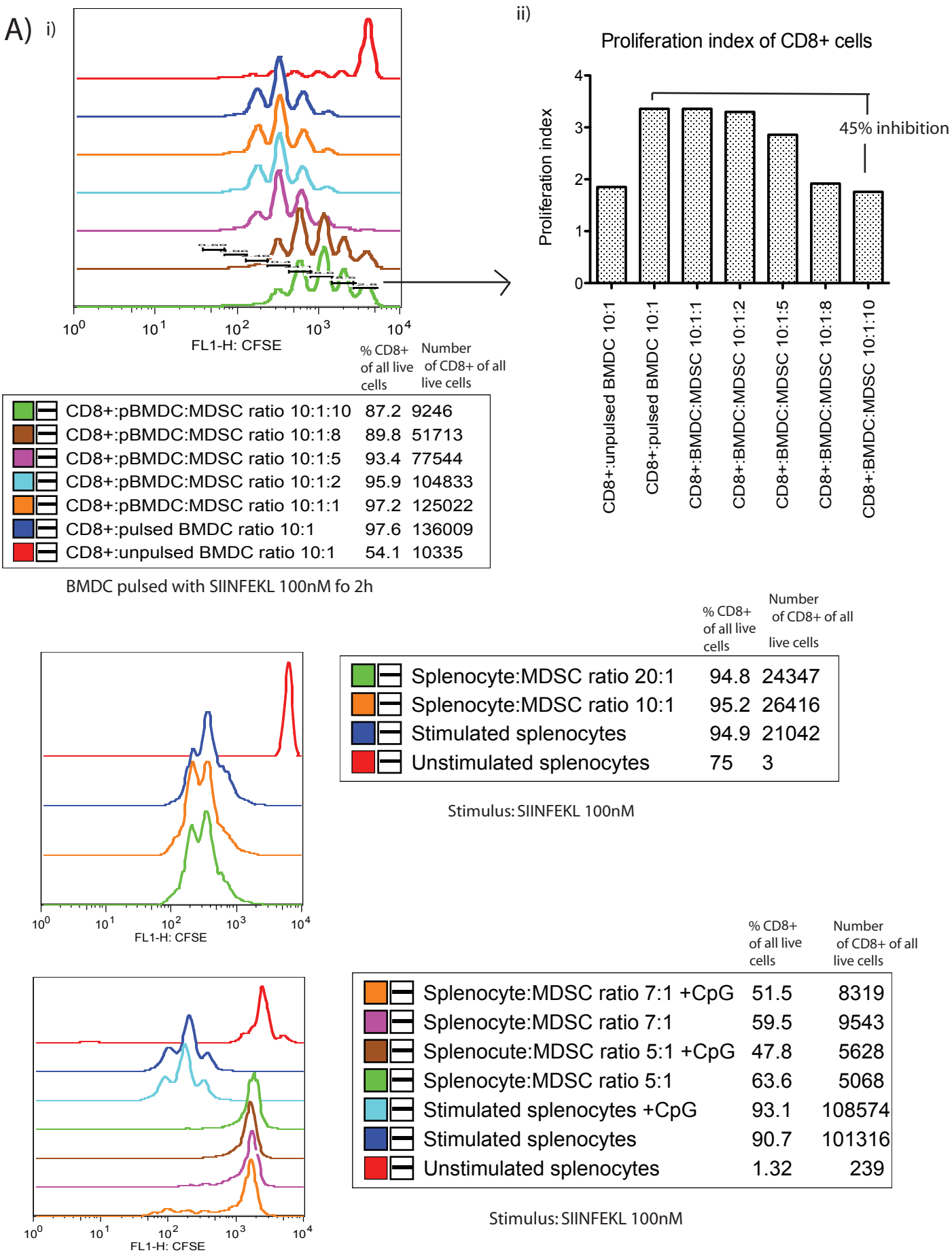

Figure 1. Inhibition of mouse CD8+ B220- splenocyte proliferation by myeloid derived suppressor cells. A) i) MDSCs inhibit DC-stimulated CD8+ T-cells proportionally. ii) A quantitative representation of the proliferation. The proliferation index was calculated as the total number of divisions divided by the the number of cells that went into division. B) Low concentration of MDSCs in the absence of DCs do not inhibit OT-I splenocyte proliferation. C) Higher concentrations of MDSC inhibit OT-I proliferation but CpG does not rescue it in the absence of DCs. Results are representative of at least two separate experiments.

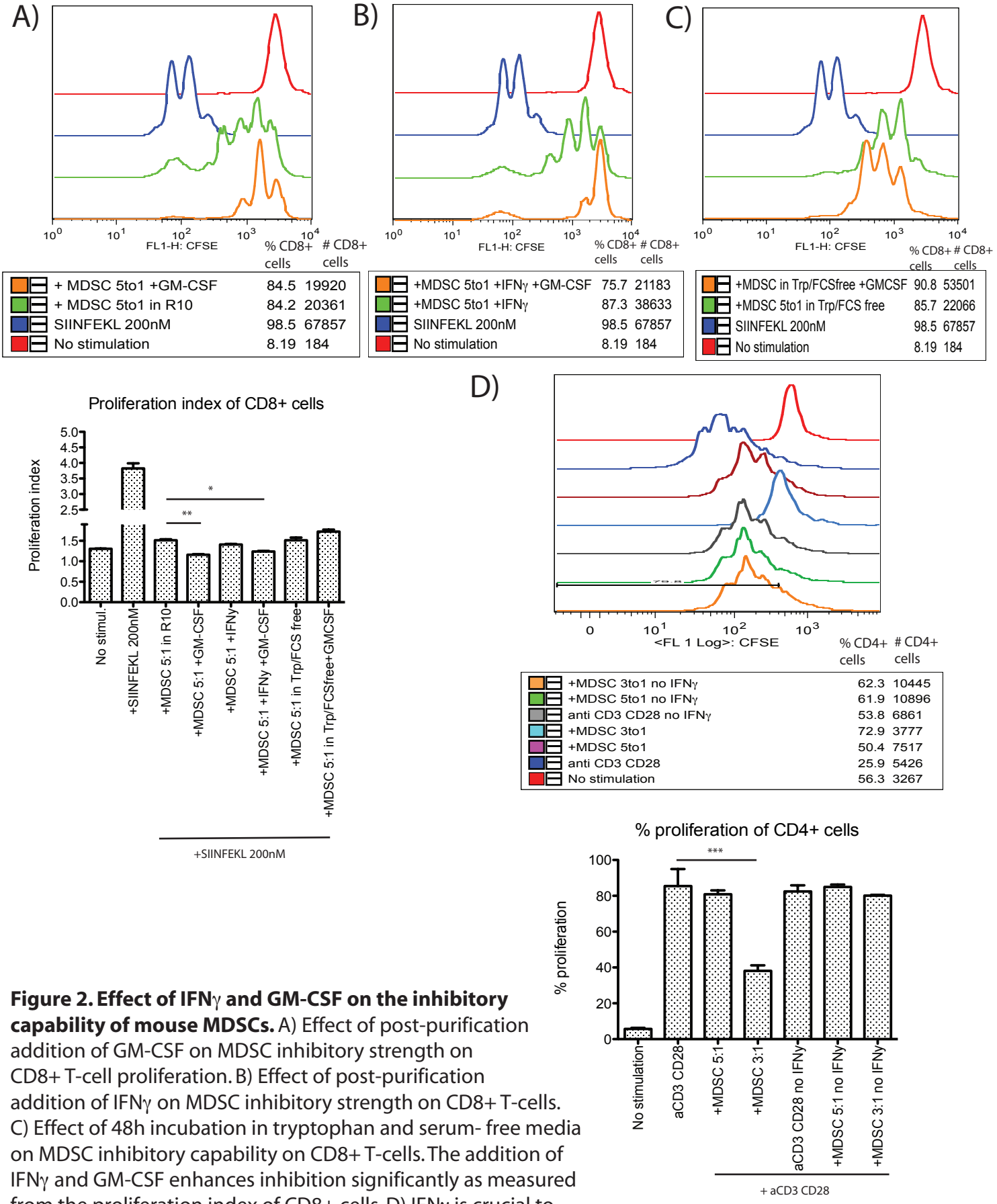

Figure 2. Effect of IFNγ and GM-CSF on the inhibitory capability of mouse MDSCs. A) Effect of post-purification addition of GM-CSF on MDSC inhibitory strength on CD8+ T-cell proliferation. B) Effect of post-purification addition of IFNγ on MDSC inhibitory strength on CD8+ T-cells. C) Effect of 48h incubation in tryptophan and serum- free media on MDSC inhibitory capability on CD8+ T-cells. The addition of IFNγ and GM-CSF enhances inhibition significantly as measured from the proliferation index of CD8+ cells. D) IFNγ is crucial to MDSC inhibition of CD4+ T-cell proliferation too. Duplicate samples with statistics with 1-way ANOVA and Dunnett's post test. In D all samples stimulated with anti CD3 CD28 unless legend says "no stimulation".

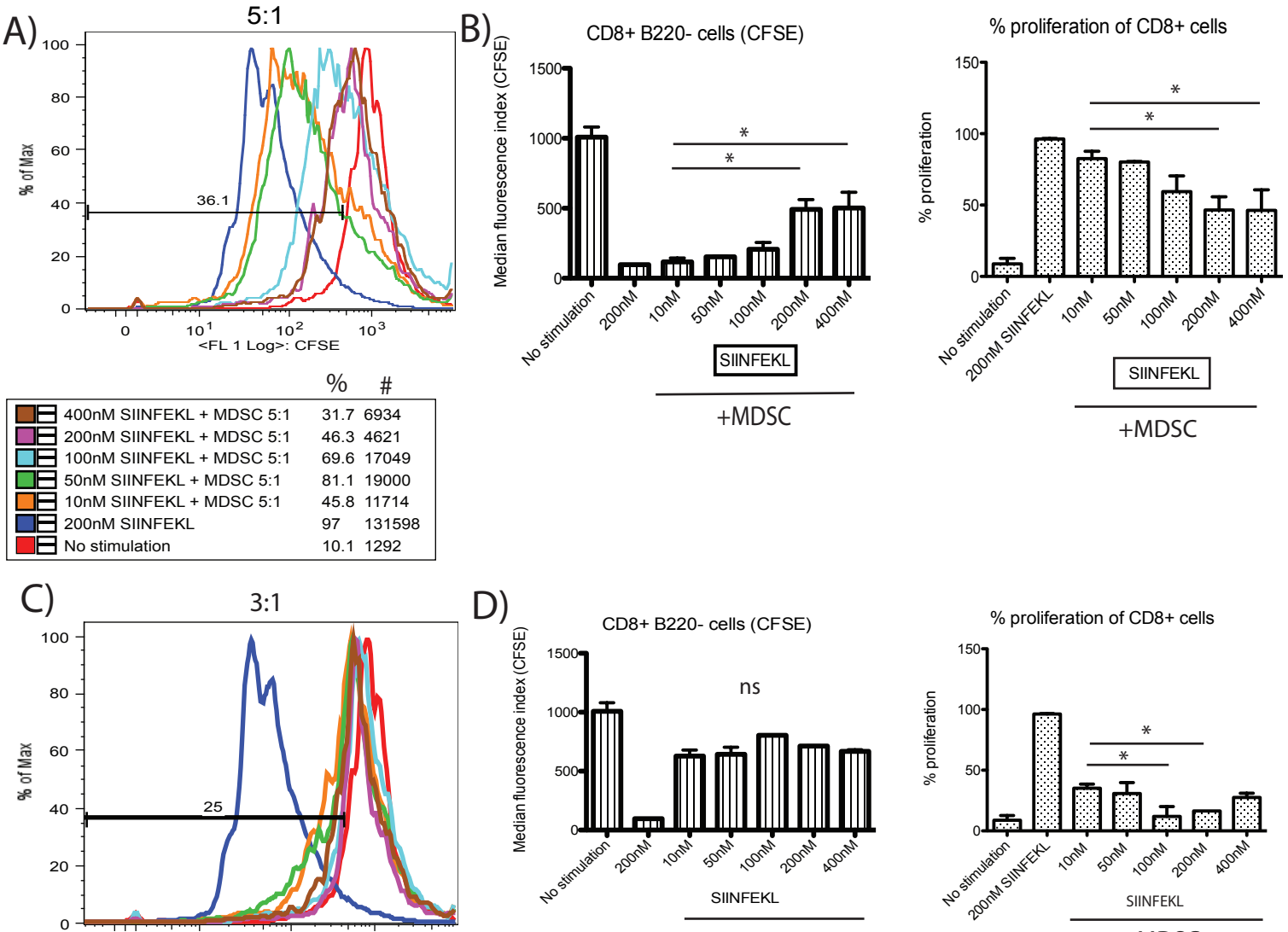

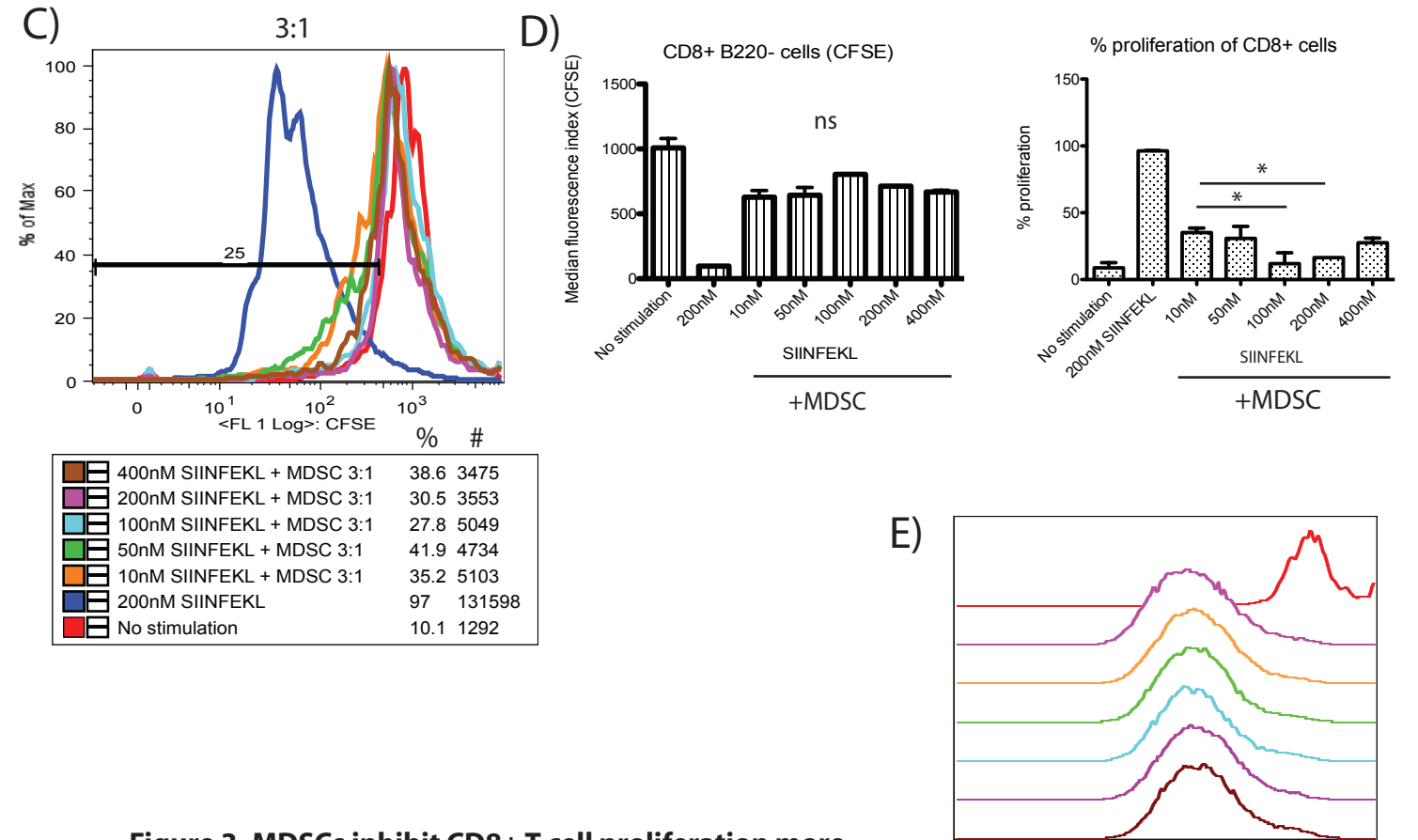

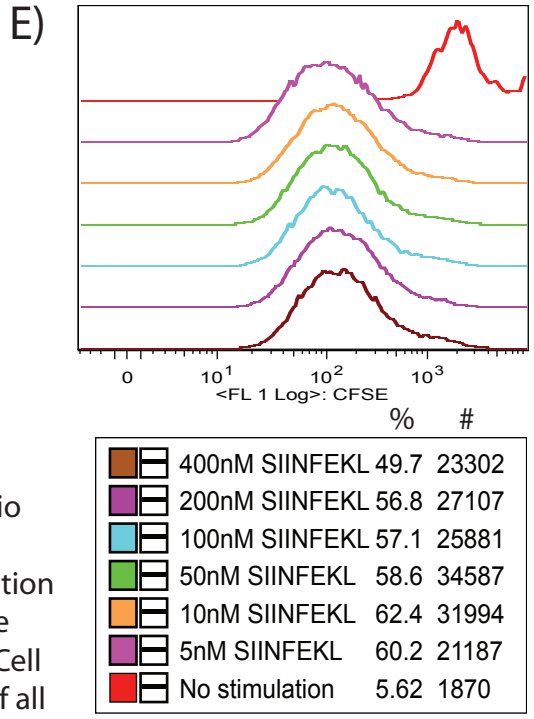

Figure 3. MDSCs inhibit CD8+ T cell proliferation more strongly when T-cell stimulation is stronger. A) CD8+ T-cell proliferation when splenocyte to MDSC ratio 5:1. Inhibition is stronger when stimulation is stronger. B) Quantitative representation of the data in A. C) When splenocyte to MDSC ratio is 3:1, the effect is mostly lost. D) Quantitative representation of the data in C, which shows a significant effect of stronger stimulation for proliferation. E) Without MDSCs CD8+ T-cell proliferate to the same extent within 72h regardless of the strength of stimulation. Cell numbers (#) and percentages (%) represent CD8+ B220- cells out of all live cells. Statistics: 1-way ANOVA of duplicate samples, $p<0.05$ with Dunnett's post test.

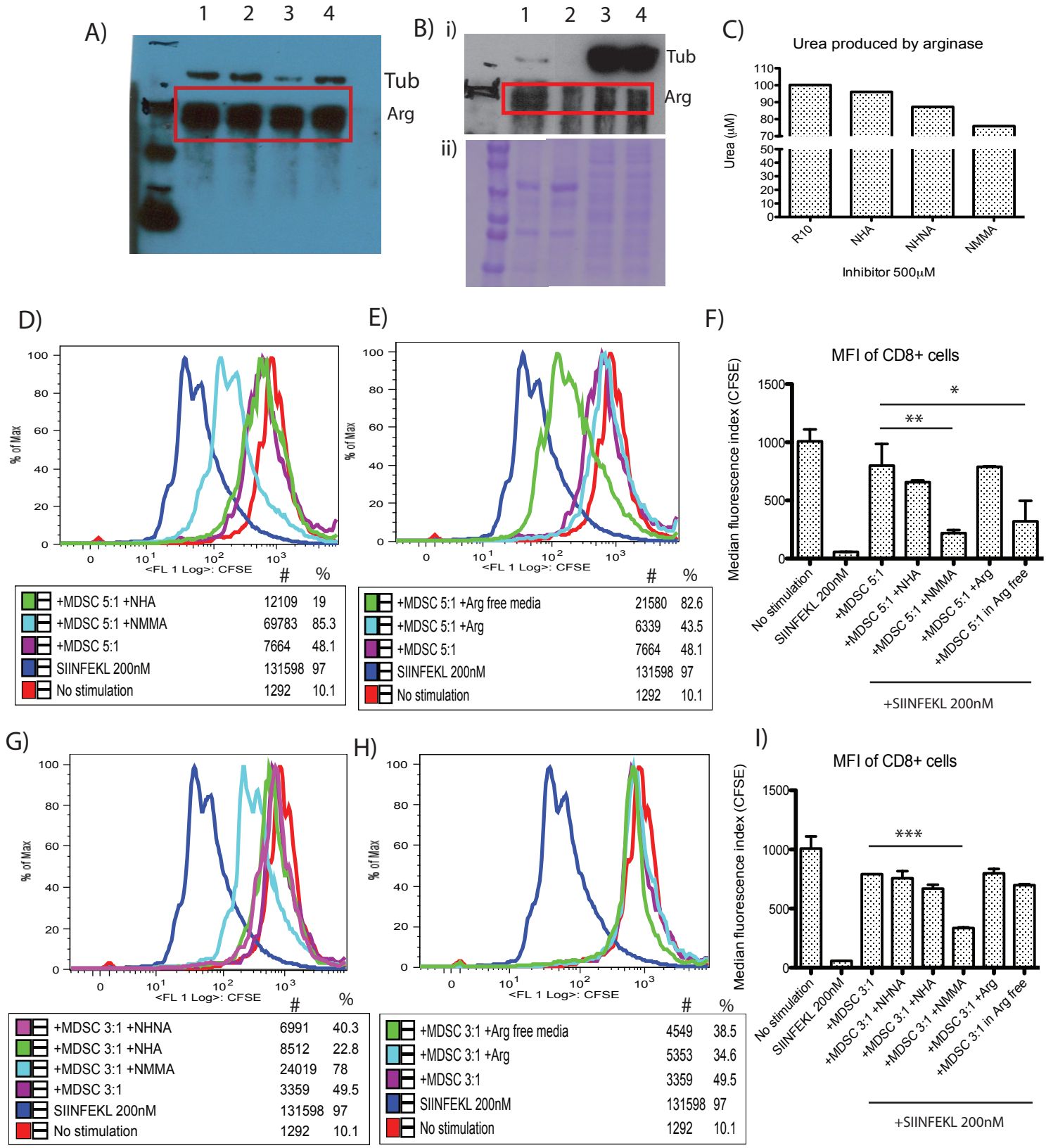

Figure 4. Arginase expression and its effect on MDSC inhibitory ability. A) Arginase expression (red frame) is not affected by arginase inhibitors; 1. MDSC (DO11.10) in R10 (48h), 2. NHA, 3. NHNA, 4. NMMA. B) i) Arginase (two bands in the red frame) is expressed in MDSC (1) but not in B6 splenocytes (2) and weakly in EG7 WT (3) and EG7 IDO+ (4) , ii) Coomassie stain showing equal loading of protein (MDSCs and spenocytes have a different protein pattern to EG7 cells, C) Arginase is weakly inhibited by arginase inhibitors in an enzymatic assay, D) and E) Arginase inhibition does not greatly enhance CD8+ T-cell proliferation, F) Quantitative representation of median fluorescence index that shows that only NMMA and Arginine-free media have a significant effect on MDSC-mediated CD8+ inhibition. G) and H) Only NMMA relieves CD8+ inhibition at 3:1 MDSC concentration. Arginase-free media decreases MDSC- mediated CD8+ T -cell inhibition, but the effect is lost when MDSC concentration is higher (3:1) (I). Quantitative representation showing that only NMMA relieved CD8+ inhibition. FACS samples are representative of duplicate samples. # and % refer to live CD8+ B220- cells out of all live cells.

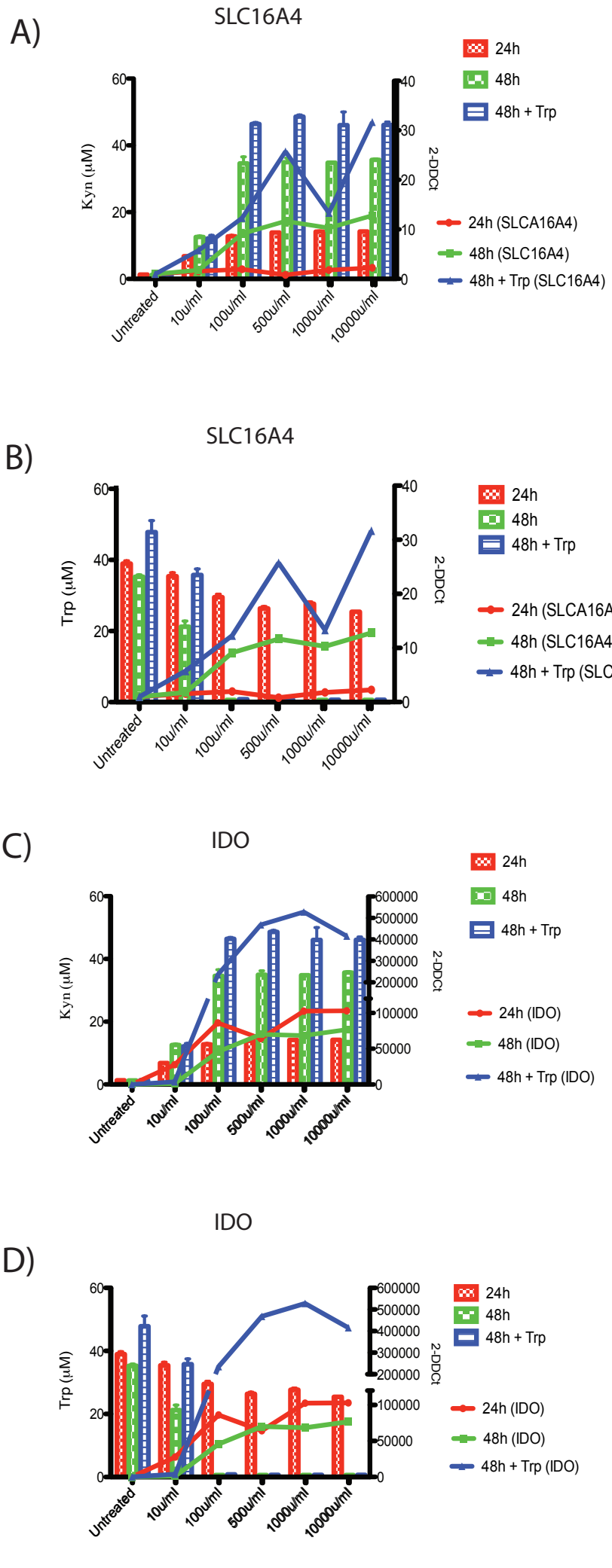

Figure 5. Alternative Trp-transporter SLC16A4 is up-regulated on tryptophan depletion but IDO expression remains unaffected by it and by the increase in IFNγ. A) SLC16A4 expression in HeLa WT cells after stimulation with IFNγ. Plotted also against kynurenine and tryptophan concentrations in the cell culture (A and B). C) and D) IDO expression in the same cells, plotted against kynurenine and tryptophan in the cell culture after 24h and 48h. The samples were in triplicate and the error bars are standard deviations.

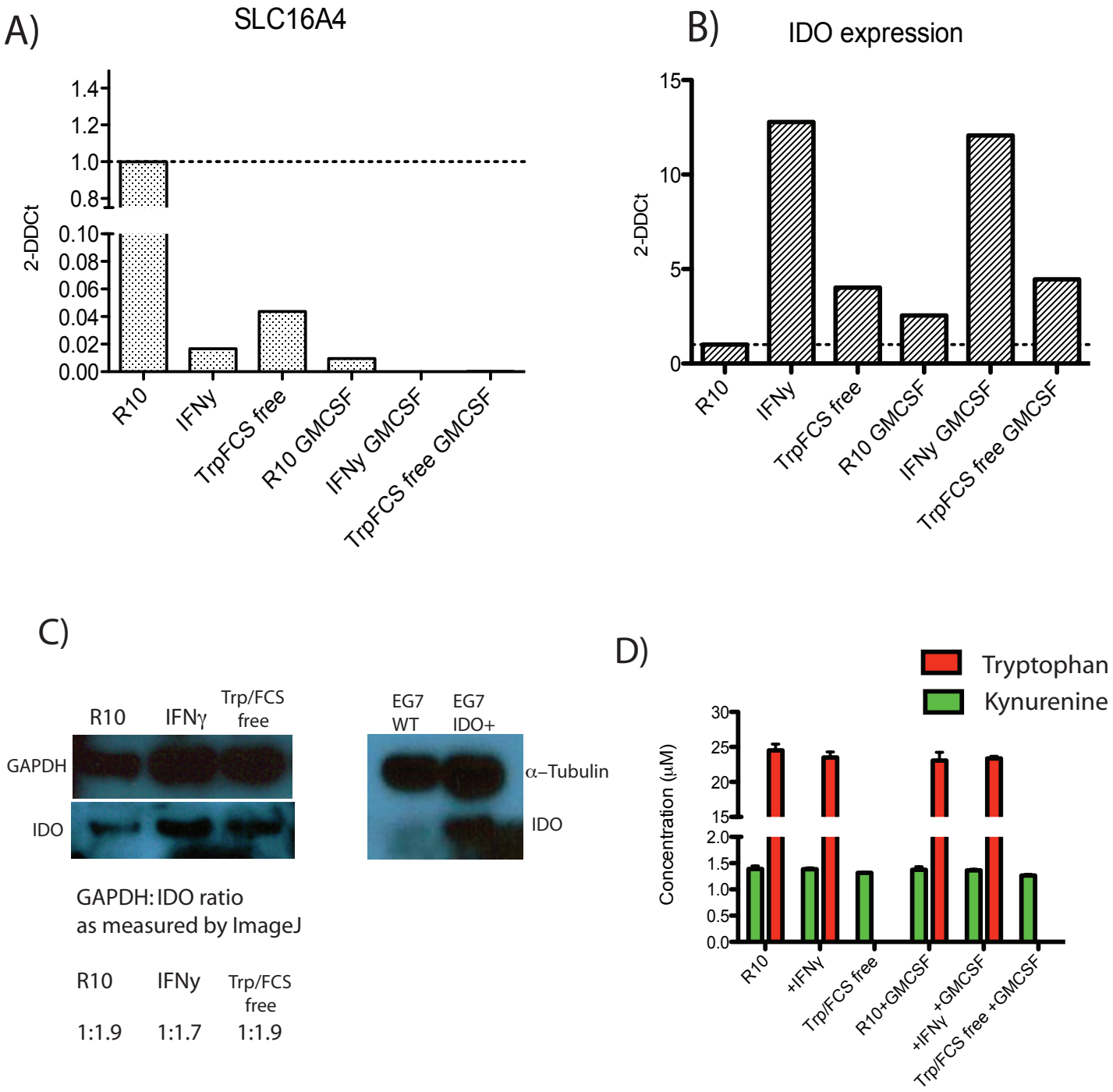

Figure 6. SLC16A4 and IDO expression in mouse MDSC.
A) SLC16A4 mRNA expression in MDSC cells treated in various ways for 48h as measured by Q-PCR. B) IDO mRNA expression in the same MDSCs as in A as measured by Q-PCR. C) IDO protein expression in MDSCs after different treatments for 48h as measured by western blot. IFNγ-treated sample has a slightly higher amount of IDO . D) Kynurenine and tryptophan concentration in the MDSC cell culture media after 48h. In D samples are in triplicate, and errors represent standard deviations.

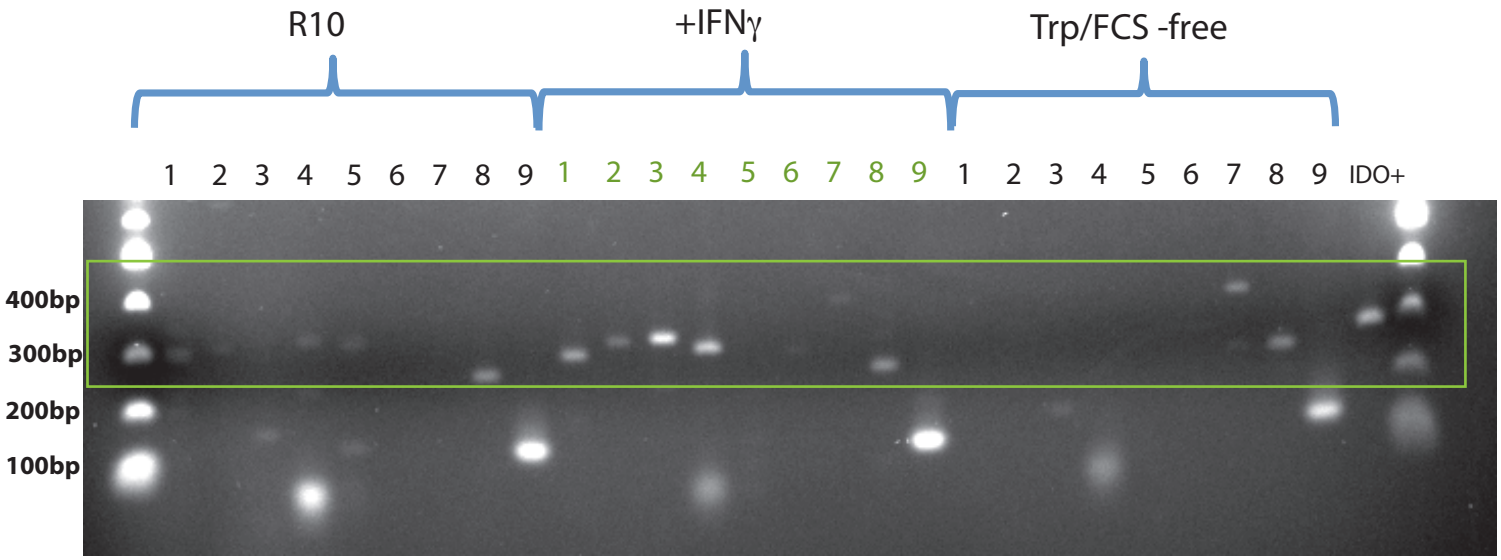

1. IDO (299bp), 2. Kynureninase (325bp), 3. Kynurenine 3-mono-oxygenase (330bp),
4. 3-hydroxyanthranilate 3,4-dioxygenase (307bp), 5. Kynurenine aminotransferase (283bp),
6. Kynurenine formamidase (299bp), 7. Picolininc acid carboxylase (327bp),
8. Quinolinic acid phosphoribosyltransferase (322bp), 9. GAPDH (130bp), IDO+ : EG7 IDO+.

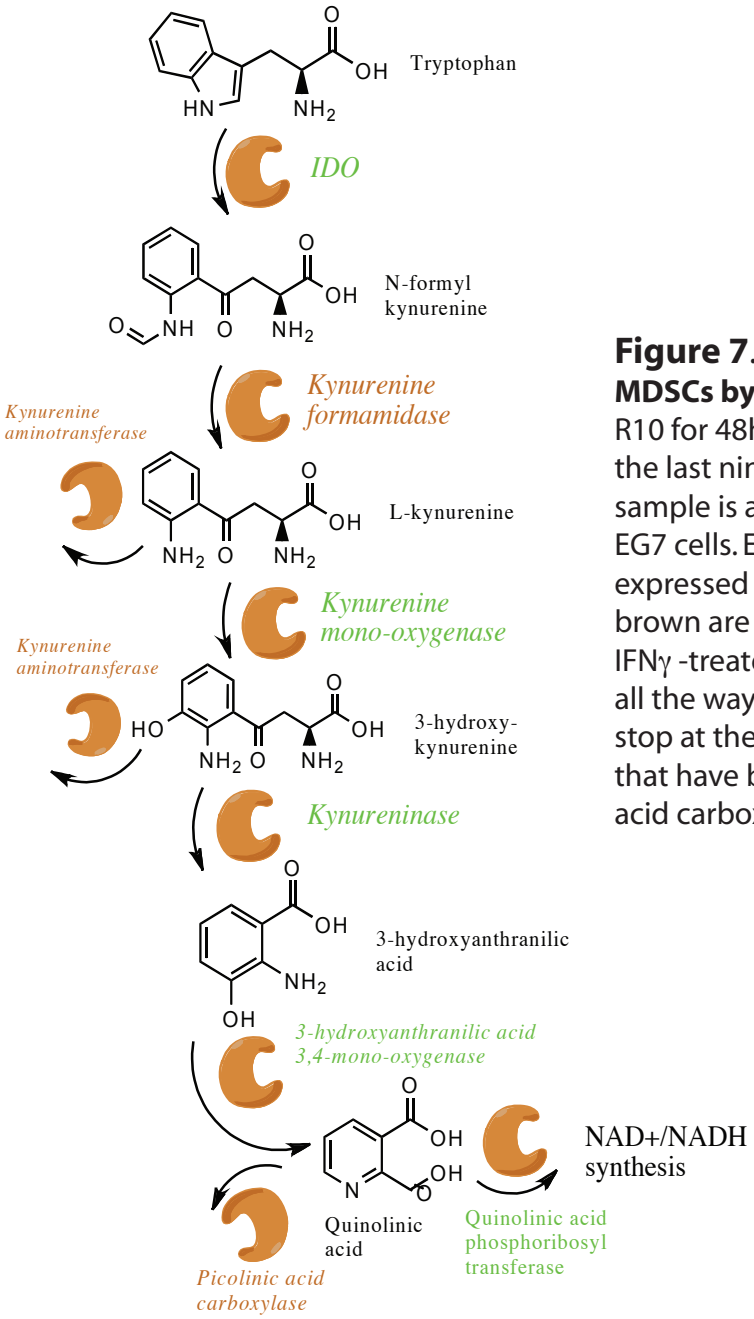

Figure 7. Kynurenine pathway expression in MDSCs by PCR. The first nine samples had been incubated in R10 for 48h, the second nine with added IFNγ (1000u/ml), and the last nine in media lacking tryptophan and FCS. The last sample is a positive control for IDO from IDO- transfected EG7 cells. Enzymes in green in the diagram are strongly expressed in MDSCs treated with IFNγ whereas enzymes in brown are expressed more weakly or not at all. IFNγ -treated MDSCs express the kynurenine pathway all the way to NAD+ synthesis, whereas untreated cells (R10) stop at the kynurenine to 3-hydroxykynurenine step. MDSC that have been in Trp/FCS -free media only express picolinic acid carboxylase and quinolinic acid phosphoribosyltransferase.

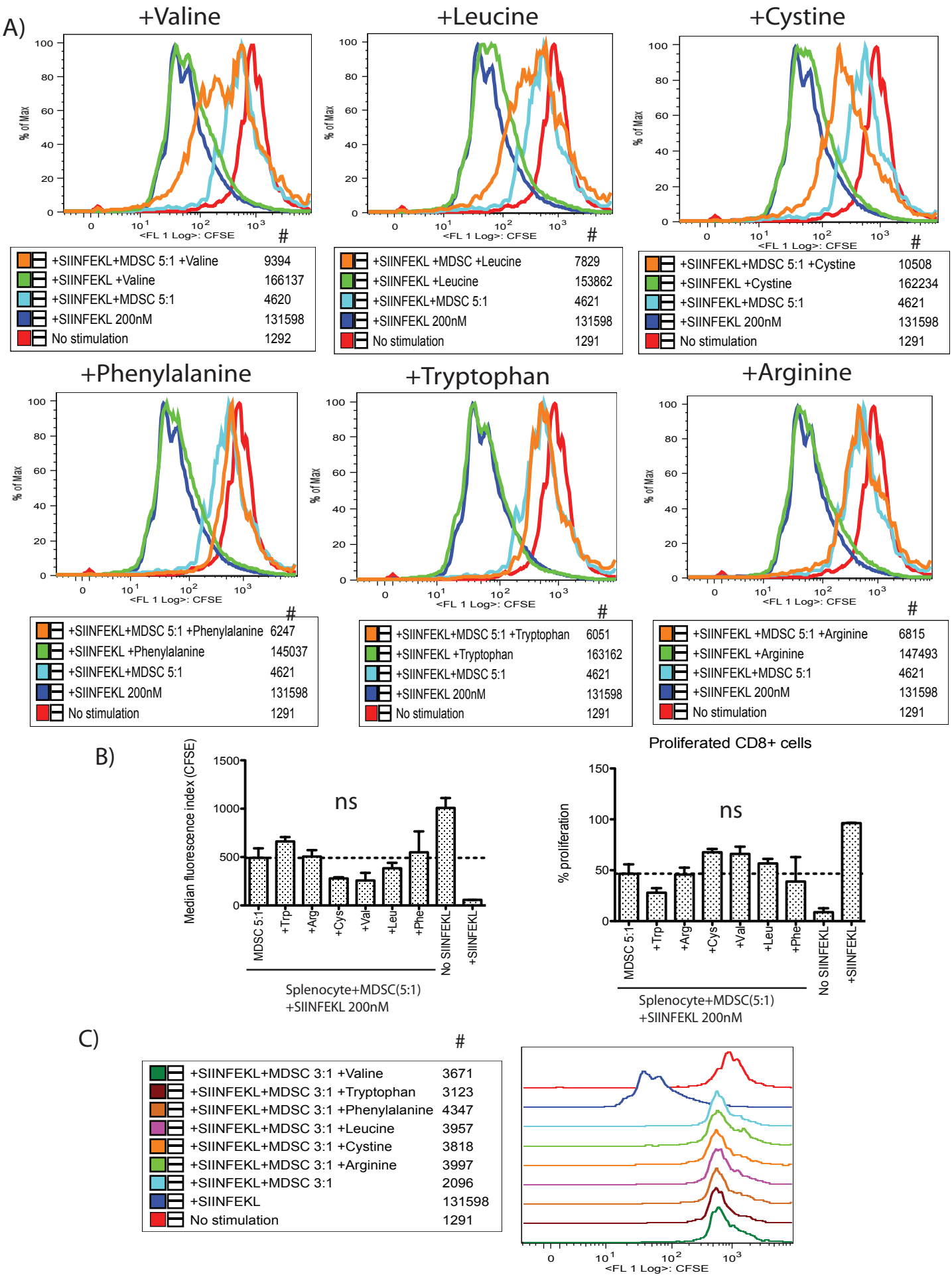

Figure 8. Valine, leucine, and cystine do not relieve MDSC-mediated CD8+ T-cell proliferation inhibition significantly even though they do provide a weak relief.

A) Splenocyte to MDSC ratio 5:1 where relief can be seen, B) Quantitative illustrations of A showing median fluorescence and proliferation of CD8+ cells when - control is the threshold. There is no significant relief of MDSC-mediated suppression when the amino acids are added, although there is a consistent visual difference. C) at a higher MDSC concentration no relief is seen (3:1), Statistics: duplicate samples, errors are standard deviations, 1-way ANOVA $p<0.05$. In FACS legends, cell numbers represent number of CD8+ B220- cells out of all live cells.

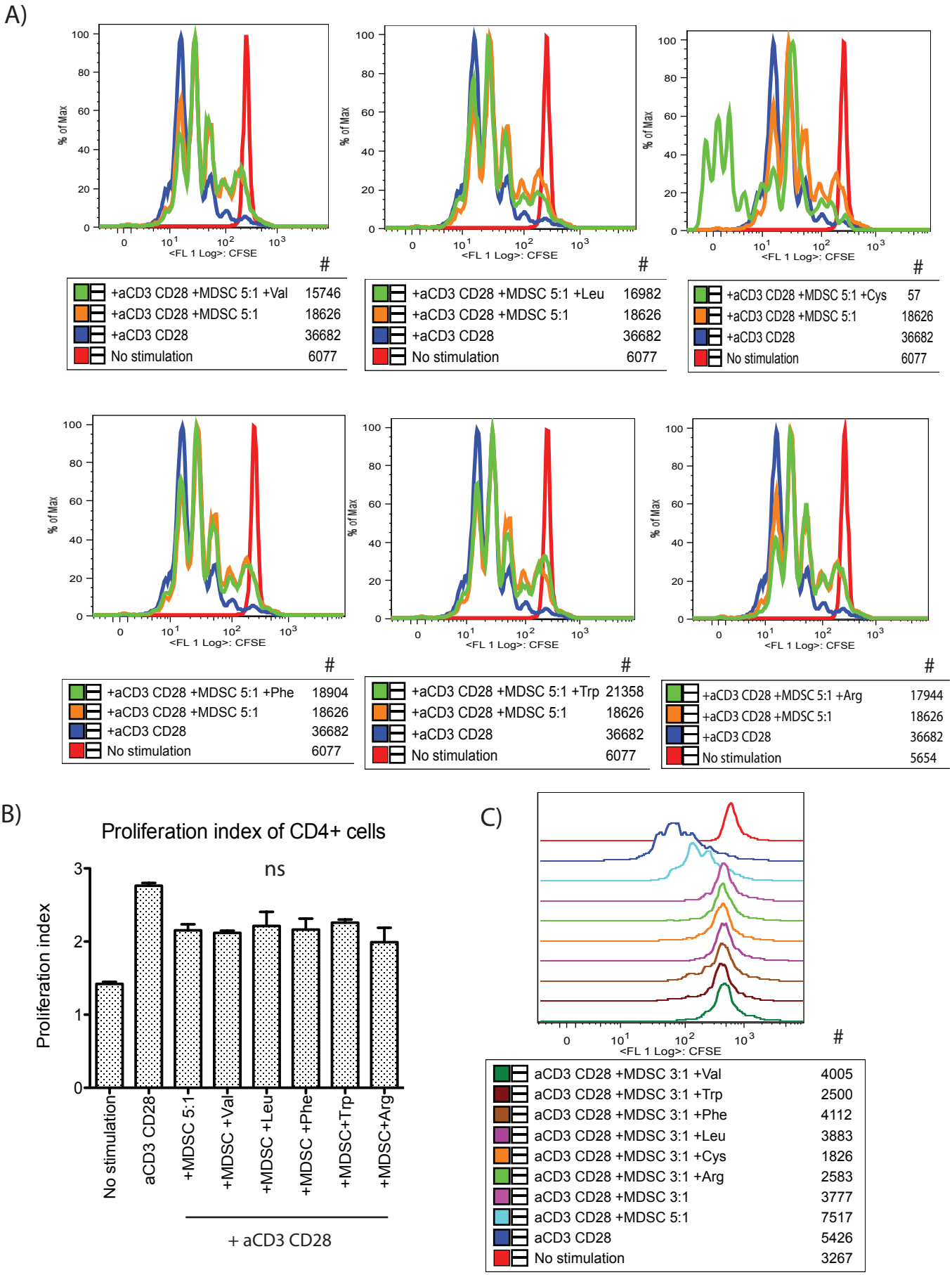

Figure 9. Addition of amino acids does not relieve inhibition of CD4+ T-cell proliferation. A) DO11.10 splenocyte to MDSC ratio 5:1. None of the amino acids that relieved CD8+ T-cell inhibition, relieved CD4+ T-cell proliferation, B) Proliferation index of CD4+ cells when the splenocyte:MDSC ratio is 5:1. There are no significant differences between the added amino acids indicating that they cannot relieve MDSC-mediated inhibition in this setting. Cystine is not included because it was not possible to calculate its proliferation index due to low cell numbers. C) Splenocyte to MDSC ratio 3:1. No relief of inhibition by amino acids. Cell numbers (#) represent CD4+ B220- cells out of all live cells. Duplicate samples statistically analysed with 1-way ANOVA and Dunnett's post test. $p<0.05$. Figures representative of two separate experiments.

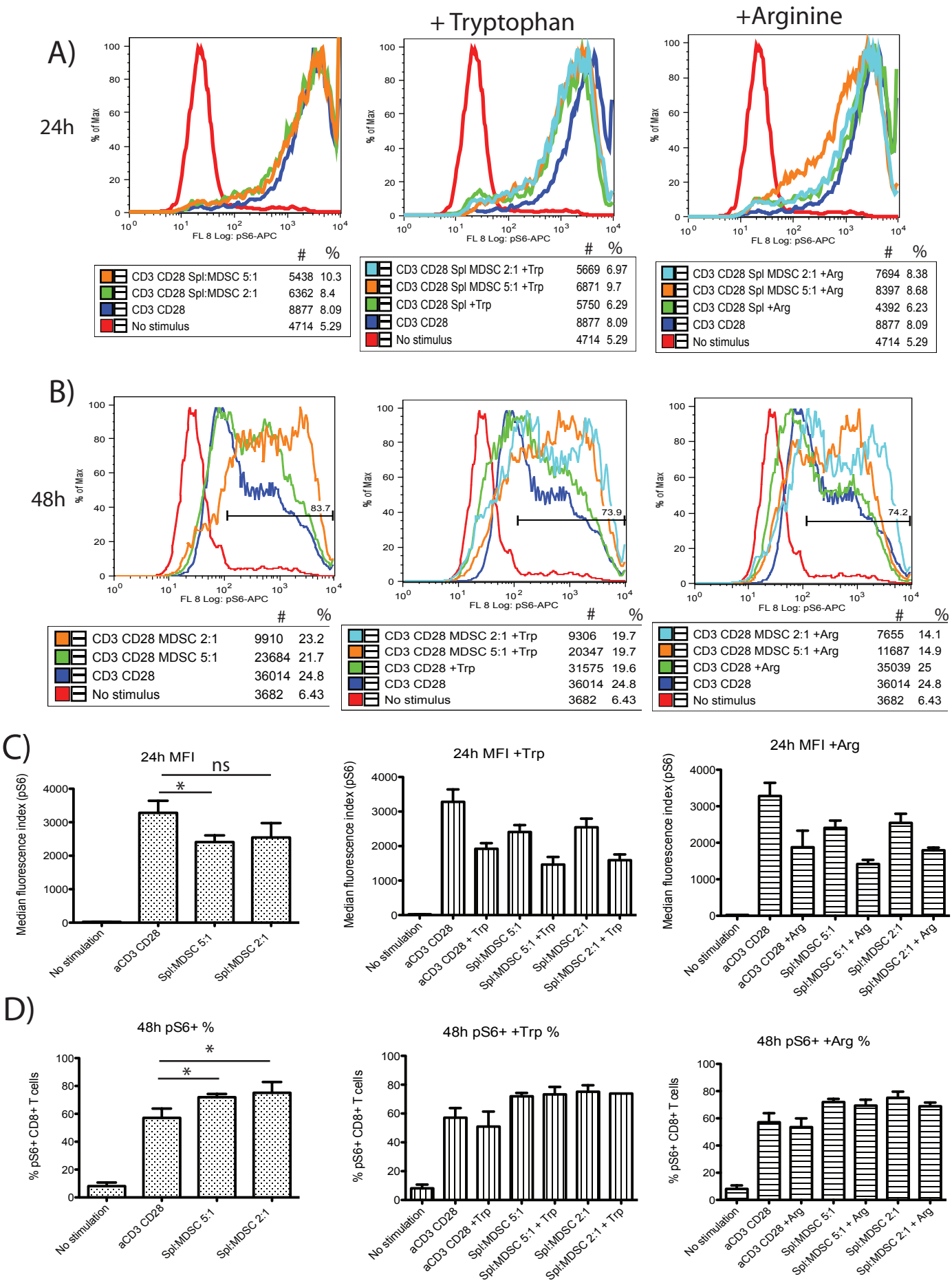

Figure 10. MDSCs inhibit mTOR activity in CD8+ T-cells after 24h but increase it after 48h in the remaining cells. Addition of neither tryptophan or arginine can enhance mTOR activity. The T-cells were stimulated with CD3 CD28 antibodies. A) and B) CD8+ B220- cells (% and # of all live cells) were analysed for p-S6 levels after 24h and 48h with and without added tryptophan and arginine. C) For 24h samples the quantitative analysis was done using the median fluorescence index (MFI, measuring the fluorescence intensity of the population of cells) as the peaks were fairly unimodal. D) For 48h samples the analysis was done using the percentage of p-S6+ CD8+ B220- cells. Statistical analysis ($p<0.05$) was 1-way ANOVA. Error bars shown are standard deviations of triplicate samples.

Chapter 5: Concluding remarks and future directions

In recent years, it has become apparent that IDO and tryptophan metabolites that are formed along the kynurenine pathway play a significant role in the process of tumour evasion adding to the repertoire available to cancer cells for circumventing detection and/or destruction.

The role of tryptophan metabolites is an emerging area in tumour immunology. In the course of this project we identified 3-HAA as a molecule that at first glance appeared to have potential as the basis for a clinically useful IDO inhibitor. While this proved not to be the case, we came across its previously possibly unappreciated physiological role in the self-regulation of the tryptophan pathway. It would be interesting to further examine whether H_2O_2 is normally produced to any significant extent in cells in which the kynurenine pathway is particularly active. Tumour cells in particular would be an interesting target if their kynurenine pathway is only active up to the production of 3-HAA. It would be illuminating to examine whether this is another mechanism by which the tumour cells can affect the effector T-cells, or other immune cells, around them. This could possibly be achievable by measuring the H_2O_2 levels directly in the culture media. The expression of kynurenine pathway enzymes could be analysed quantitatively by Q-PCR. So far, we have only done this by reverse transcription PCR.

We went on to carry out a detailed study of the effects of different kynurenines on activated T-cells in the mouse system. While the results were not conclusive they did provide useful pointers for future research projects in particular with regards to potential involvement of a putative mTORC1-GCN2 axis. In order to achieve comparable results between the CD4+ and CD8+ T-cells, the experiments with CD4+ T-cells would have to be repeated with their cognate peptide as activation stimulus. Here we have only used CD3 and CD28 antibodies, which produce strong activation, which may override subtle differences that could be seen with the cognate peptide stimulus. In addition, when CD4+ were exposed to the kynurenines when looking at the development of T_{regs}, the cells were only cultured for 3 days. Therefore in order to obtain more reliable results for T_{reg} development, the assay would have to be repeated and extended to at least seven days, as published reports have done. It would probably be beneficial to do a side-by-side comparison at same time with the two different

stimuli, CD3 CD28 antibodies and the cognate peptide, to see whether this matters in terms of T_{reg} development. One of the more interesting results is definitely the potential of the kynurenines to affect the GCN2 pathway. More work in this area would definitely be warranted as it would provide a new angle on how at least tryptophan starvation is detected, and how tumour cells can exploit this by first inhibiting protein synthesis via mTOR and then by GCN2 too. To start with, these experiments could be done by titrating the different kynurenines to see whether the response is dose-dependent, but also to look at the levels of the active (phosphorylated) GCN2 directly by western blot or immunoprecipitation to see whether the effect of the kynurenines comes from the GCN2 or whether it is a stress signal via e.g. the PERK-pathway. These alternative pathways could also be looked at by e.g. western blot or immunocytochemistry.

Finally we looked into more detail in the mechanisms employed by MDSCs to achieve inhibition of T-cell proliferation. In particular, we investigated whether amino-acid depletion-orientated processes played a significant role and succeeded in excluding IDO expression from the list of potential methods used. Moreover in our assays the effect of replenishing amino-acids such as arginine, whose depletion is widely believed to be one of the main mediators of MDSCs' inhibitory capacity, did not rescue proliferation to the expected extent. Intriguingly, carrying out the assay in arginine-free media actually impeded the inhibitory capacity of MDSCs suggesting a significant role for arginine catabolites such as NO. In this chapter we looked at both CD8+ and CD4+ T-cells and again, in order for the results to be directly comparable, the experiments with CD4+ would have to be repeated with the cognate peptide as stimulus. Interesting results were obtained with CD8+ T-cells and MDSC when the the T-cells were stimulated with a range of cognate peptide concentrations. The fact that the stronger the stimulus, the stronger the inhibition by MDSCs, is an intriguing one. It would be worth investigating this more by trying to find the source for these results. A quick way would be to look by ELISA at the concentration of IFNγ in the media, that is, whether by giving the T-cells a stronger activation signal, they produce more of the cytokine, which in turn is required by the MDSC to function effectively. Another way, would be to look at the levels of ROS production and see whether with a stronger activation signal, the MDSC are 'encouraged' by the T-cells to produce more of these radicals, leading to dampening of

T-cell proliferation. Also, it would be interesting to do the original assay in a transwell-plate to ascertain whether the reaction is contact-dependent or mediated by soluble factors.

The amplification of kynurenine pathway enzymes in MDSCs should also be repeated by doing Q-PCR since our results indicated the possibility that after IFNγ exposure the cells seem to express more kynurenine mono-oxygenase that produces 3-hydroxykynurenine. If the results showed more of this enzyme, it could be another mechanism to cause T-cell toxicity. Although the results with T-cells and MDSCs with the addition of certain amino acids to relieve MDSC-mediated inhibition were not conclusive, it would be exciting to confirm the results we obtained by competitive transport assays in MDSCs, to see whether leucine and phenylalanine really compete with arginine transport as suggested by research in oocytes.

Overall we believe our results demonstrate the importance of amino acid catabolic pathways in the process of immune evasion and provide useful starting points for research towards concrete clinical applications in the fight against cancer.

Appendices

```
mouse               1 MALSKISPTEGSRRILEDHHIDEDVGFALPHPLVELPDAYSPWVLVARNL     50
                      .....|.|..|.:::||||:||||||:|...|||.|:.|:.:|::|
human               1 ----MAHAMENSWTISKEYHIDEEVGFALPNPQENLPDFYNDWMFIAKHL     46

mouse              51 PVLIENGQLREEVEKLPTLSTDGLRGHRLQRLAHLALGYITMAYVWNRGD    100
                      |.|||:|||||.||||..||.|.|..|:.||||.|.||.|||||||.:|.
human              47 PDLIESGQLRERVEKLNMLSIDHLTDHKSQRLARLVLGCITMAYVWGKGH     96

mouse             101 DDVRKVLPRNIAVPYCELSEKLGLPPILSYADCVLANWKKKDPNGPMTYE    150
                      .|||||||||||||:||:||.|||||.|||||||||||||||.|:|||
human              97 GDVRKVLPRNIAVPYCQLSKKLELPPILVYADCVLANWKKKDPNKPLTYE    146

mouse             151 NMDILFSFPGGDCDKGFFLVSLLVEIAASPAIKAIPTVSSAVERQDLKAL    200
                      |||:||||..|||.|||||||||||||:.|||.||||..|::.|:...|
human             147 NMDVLFSFRDGDCSKGFFLVSLLVEIAAASAIKVIPTVFKAMQMQERDTL    196

mouse             201 EKALHDIATSLEKAKEIFKRMRDFVDPDTFFHVLRIYLSGWKCSSKLPEG    250
                      .|||.:||:.||||.::|.::.|.|:|..||.||||||||||.:.:|.:|
human             197 LKALLEIASCLEKALQVFHQIHDHVNPKAFFSVLRIYLSGWKGNPQLSDG    246

mouse             251 LLYEGVWDTPKMFSGGSAGQSSIFQSLDVLLGIKHEAGKESPAEFLQEMR    300
                      |:|||.|:.||.|:|||||||:||..||||||:..||....|:|||:||
human             247 LVYEGFWEDPKEFAGGSAGQSSVFQCFDVLLGIQQTAGGGHAAQFLQDMR    296

mouse             301 EYMPPAHRNFLFFLESAPPVREFVISRHNEDLTKAYNECVNGLVSVRKFH    350
                      .||||||||||..|||.|.|||||:|:.:..|.:||:.||..|||:|.:|
human             297 RYMPPAHRNFLCSLESNPSVREFVLSKGDAGLREAYDACVKALVSLRSYH    346

mouse             351 LAIVDTYIMKPSKKKPTDGDKSEEPSNVESRGTGGTNPMTFLRSVKDTTE    400
                      |.||..||:.|:.::|.:...||:||.:|::|||||:.|.||::|:.|||
human             347 LQIVTKYILIPASQQPKENKTSEDPSKLEAKGTGGTDLMNFLKTVRSTTE    396

mouse             401 KALLSWP    407
                      |:||...
human             397 KSLLKEG    403


    Length: 407
    # Identity:     247/407 (60.7%)
    # Similarity:   306/407 (75.2%)
    # Gaps:           4/407 (1.0%)
    # Score: 1274.0
```

Appendix I. Sequence identity between mouse and human IDO proteins. Analysis performed with Needle pairwise alignment using the following IDO sequences: mouse NM_008324.1, human NM_002164.5.

Bibliography

1. Hoebe, K., Janssen, E. & Beutler, B. The interface between innate and adaptive immunity. *Nat. Immunol.* **5**, 971-974 (2004).
2. Thiel, S. Complement activating soluble pattern recognition molecules with collagen-like regions, mannan-binding lectin, ficolins and associated proteins. *Mol. Immunol.* **44**, 3875-3888 (2007).
3. Medzhitov, R. & Janeway, C.A., Jr Innate immunity: impact on the adaptive immune response. *Curr. Opin. Immunol.* **9**, 4-9 (1997).
4. Medzhitov, R. & Janeway, C.A., Jr Innate immunity: the virtues of a nonclonal system of recognition. *Cell* **91**, 295-298 (1997).
5. Jiang, Y., Oliver, P., Davies, K.E. & Platt, N. Identification and characterization of murine SCARA5, a novel class A scavenger receptor that is expressed by populations of epithelial cells. *J. Biol. Chem.* **281**, 11834-11845 (2006).
6. Kawai, T. & Akira, S. Toll-like receptors and their crosstalk with other innate receptors in infection and immunity. *Immunity* **34**, 637-650 (2011).
7. Kolev, M., Towner, L. & Donev, R. Complement in Cancer and Cancer Immunotherapy. *Archivum Immunologiae Et Therapiae Experimentalis* (2011).doi:10.1007/s00005-011-0146-x
8. Kemper, C., Atkinson, J.P. & Hourcade, D.E. Properdin: emerging roles of a pattern-recognition molecule. *Annu. Rev. Immunol.* **28**, 131-155 (2010).
9. Lambrecht, B.N. Alveolar macrophage in the driver's seat. *Immunity* **24**, 366-368 (2006).
10. Lumeng, C.N., Bodzin, J.L. & Saltiel, A.R. Obesity induces a phenotypic switch in adipose tissue macrophage polarization. *J. Clin. Invest.* **117**, 175-184 (2007).
11. Gordon, S. & Taylor, P.R. Monocyte and macrophage heterogeneity. *Nat. Rev. Immunol.* **5**, 953-964 (2005).
12. Benoit, M., Desnues, B. & Mege, J.-L. Macrophage Polarization in Bacterial Infections. *The Journal of Immunology* **181**, 3733 -3739 (2008).
13. Porcheray, F. *et al.* Macrophage activation switching: an asset for the resolution of inflammation. *Clin. Exp. Immunol.* **142**, 481-489 (2005).
14. Dinapoli, M.R., Calderon, C.L. & Lopez, D.M. The altered tumoricidal capacity of macrophages isolated from tumor-bearing mice is related to reduce expression of the inducible nitric oxide synthase gene. *J. Exp. Med.* **183**, 1323-1329 (1996).
15. Pollard, J.W. Tumour-educated macrophages promote tumour progression and metastasis. *Nat. Rev. Cancer* **4**, 71-78 (2004).
16. Condeelis, J. & Pollard, J.W. Macrophages: obligate partners for tumor cell migration, invasion, and metastasis. *Cell* **124**, 263-266 (2006).
17. Sica, A., Schioppa, T., Mantovani, A. & Allavena, P. Tumour-associated macrophages are a distinct M2 polarised population promoting tumour progression: potential targets of anti-cancer therapy. *Eur. J. Cancer* **42**, 717-727 (2006).
18. Mantovani, A., Cassatella, M.A., Costantini, C. & Jaillon, S. Neutrophils in the activation and regulation of innate and adaptive immunity. *Nat. Rev. Immunol.* **11**, 519-531 (2011).

19. van Gisbergen, K.P.J.M., Ludwig, I.S., Geijtenbeek, T.B.H. & van Kooyk, Y. Interactions of DC-SIGN with Mac-1 and CEACAM1 regulate contact between dendritic cells and neutrophils. *FEBS Lett.* **579**, 6159-6168 (2005).
20. Fridlender, Z.G. *et al.* Polarization of tumor-associated neutrophil phenotype by TGF-beta: "N1" versus "N2" TAN. *Cancer Cell* **16**, 183-194 (2009).
21. Paust, S. & von Andrian, U.H. Natural killer cell memory. *Nat. Immunol.* **12**, 500-508 (2011).
22. Bryceson, Y.T. *et al.* Molecular mechanisms of natural killer cell activation. *J Innate Immun* **3**, 216-226 (2011).
23. Sun, J.C. & Lanier, L.L. NK cell development, homeostasis and function: parallels with CD8(+) T cells. *Nat. Rev. Immunol.* **11**, 645-657 (2011).
24. Anfossi, N. *et al.* Human NK cell education by inhibitory receptors for MHC class I. *Immunity* **25**, 331-342 (2006).
25. Paust, S. *et al.* Critical role for the chemokine receptor CXCR6 in NK cell-mediated antigen-specific memory of haptens and viruses. *Nat. Immunol.* **11**, 1127-1135 (2010).
26. Sun, J.C., Beilke, J.N. & Lanier, L.L. Adaptive immune features of natural killer cells. *Nature* **457**, 557-561 (2009).
27. Faget, J. *et al.* Early Detection of Tumor Cells by Innate Immune Cells Leads to Treg Recruitment through CCL22 Production by Tumor Cells. *Cancer Res.* **71**, 6143-6152 (2011).
28. Bonnet, M., Ferrier, P. & Spicuglia, S. Molecular genetics at the T-cell receptor beta locus: insights into the regulation of V(D)J recombination. *Adv. Exp. Med. Biol.* **650**, 116-132 (2009).
29. Chen, Z.W. Immune biology of Ag-specific γδ T cells in infections. *Cell. Mol. Life Sci.* **68**, 2409-2417 (2011).
30. Godfrey, D.I., Stankovic, S. & Baxter, A.G. Raising the NKT cell family. *Nat. Immunol.* **11**, 197-206 (2010).
31. Sakaguchi, S., Yamaguchi, T., Nomura, T. & Ono, M. Regulatory T cells and immune tolerance. *Cell* **133**, 775-787 (2008).
32. Sakaguchi, S., Miyara, M., Costantino, C.M. & Hafler, D.A. FOXP3+ regulatory T cells in the human immune system. *Nat. Rev. Immunol.* **10**, 490-500 (2010).
33. Curiel, T.J. *et al.* Specific recruitment of regulatory T cells in ovarian carcinoma fosters immune privilege and predicts reduced survival. *Nat. Med.* **10**, 942-949 (2004).
34. Coombes, J.L. *et al.* A functionally specialized population of mucosal CD103+ DCs induces Foxp3+ regulatory T cells via a TGF-beta and retinoic acid-dependent mechanism. *J. Exp. Med.* **204**, 1757-1764 (2007).
35. Walker, M.R., Carson, B.D., Nepom, G.T., Ziegler, S.F. & Buckner, J.H. De novo generation of antigen-specific CD4+CD25+ regulatory T cells from human CD4+CD25- cells. *Proc. Natl. Acad. Sci. U.S.A.* **102**, 4103-4108 (2005).
36. Tran, D.Q., Ramsey, H. & Shevach, E.M. Induction of FOXP3 expression in naive human CD4+FOXP3 T cells by T-cell receptor stimulation is transforming growth factor-beta dependent but does not confer a regulatory phenotype. *Blood* **110**, 2983-2990 (2007).
37. Baecher-Allan, C., Brown, J.A., Freeman, G.J. & Hafler, D.A. CD4+CD25high regulatory cells in human peripheral blood. *J. Immunol.* **167**, 1245-1253 (2001).
38. Taams, L.S. *et al.* Antigen-specific T cell suppression by human CD4+CD25+ regulatory T cells. *Eur. J. Immunol.* **32**, 1621-1630 (2002).

39. Levings, M.K., Sangregorio, R. & Roncarolo, M.G. Human cd25(+)cd4(+) t regulatory cells suppress naive and memory T cell proliferation and can be expanded in vitro without loss of function. *J. Exp. Med.* **193**, 1295-1302 (2001).
40. Jonuleit, H. *et al.* Identification and functional characterization of human CD4(+)CD25(+) T cells with regulatory properties isolated from peripheral blood. *J. Exp. Med.* **193**, 1285-1294 (2001).
41. Dieckmann, D., Plottner, H., Berchtold, S., Berger, T. & Schuler, G. Ex vivo isolation and characterization of CD4(+)CD25(+) T cells with regulatory properties from human blood. *J. Exp. Med.* **193**, 1303-1310 (2001).
42. Baecher-Allan, C., Viglietta, V. & Hafler, D.A. Inhibition of human CD4(+)CD25(+high) regulatory T cell function. *J. Immunol.* **169**, 6210-6217 (2002).
43. Kushwah, R. & Hu, J. Complexity of dendritic cell subsets and their function in the host immune system. *Immunology* **133**, 409-419 (2011).
44. Heath, W.R. & Carbone, F.R. Dendritic cell subsets in primary and secondary T cell responses at body surfaces. *Nat. Immunol.* **10**, 1237-1244 (2009).
45. Reis e Sousa, C. Toll-like receptors and dendritic cells: for whom the bug tolls. *Semin. Immunol.* **16**, 27-34 (2004).
46. Ni, K. & O'Neill, H.C. The role of dendritic cells in T cell activation. *Immunol. Cell Biol.* **75**, 223-230 (1997).
47. Villadangos, J.A., Schnorrer, P. & Wilson, N.S. Control of MHC class II antigen presentation in dendritic cells: a balance between creative and destructive forces. *Immunol. Rev.* **207**, 191-205 (2005).
48. Abbas, A.K., Murphy, K.M. & Sher, A. Functional diversity of helper T lymphocytes. *Nature* **383**, 787-793 (1996).
49. Ehrlich, P. Ueber den jetzigen Stand der Karzinomforschung. *Ned. Tijdschr. Geneeskd* **5**, 273-290 (1909).
50. Stutman, O. Tumor development after 3-methylcholanthrene in immunologically deficient athymic-nude mice. *Science* **183**, 534-536 (1974).
51. Hayday, A.C. [gamma][delta] cells: a right time and a right place for a conserved third way of protection. *Annu. Rev. Immunol.* **18**, 975-1026 (2000).
52. Shinkai, Y. *et al.* RAG-2-deficient mice lack mature lymphocytes owing to inability to initiate V(D)J rearrangement. *Cell* **68**, 855-867 (1992).
53. Shankaran, V. *et al.* IFNgamma and lymphocytes prevent primary tumour development and shape tumour immunogenicity. *Nature* **410**, 1107-1111 (2001).
54. Boon, T. & van der Bruggen, P. Human tumor antigens recognized by T lymphocytes. *J. Exp. Med.* **183**, 725-729 (1996).
55. Panelli, M.C. *et al.* Phase 1 study in patients with metastatic melanoma of immunization with dendritic cells presenting epitopes derived from the melanoma-associated antigens MART-1 and gp100. *J. Immunother.* **23**, 487-498 (2000).
56. Cresswell, P., Ackerman, A.L., Giodini, A., Peaper, D.R. & Wearsch, P.A. Mechanisms of MHC class I-restricted antigen processing and cross-presentation. *Immunol. Rev.* **207**, 145-157 (2005).
57. Chen, Y.-T. *et al.* Multiple cancer/testis antigens are preferentially expressed in hormone-receptor negative and high-grade breast cancers. *PLoS ONE* **6**, e17876 (2011).

58. Shi, Y., Evans, J.E. & Rock, K.L. Molecular identification of a danger signal that alerts the immune system to dying cells. *Nature* **425**, 516-521 (2003).
59. Groh, V. *et al.* Broad tumor-associated expression and recognition by tumor-derived gamma delta T cells of MICA and MICB. *Proc. Natl. Acad. Sci. U.S.A.* **96**, 6879-6884 (1999).
60. Coudert, J.D. & Held, W. The role of the NKG2D receptor for tumor immunity. *Semin. Cancer Biol.* **16**, 333-343 (2006).
61. Steinman, R.M., Hawiger, D. & Nussenzweig, M.C. Tolerogenic dendritic cells. *Annu. Rev. Immunol.* **21**, 685-711 (2003).
62. Lee, P.P. *et al.* Characterization of circulating T cells specific for tumor-associated antigens in melanoma patients. *Nat. Med.* **5**, 677-685 (1999).
63. Willimsky, G. & Blankenstein, T. Sporadic immunogenic tumours avoid destruction by inducing T-cell tolerance. *Nature* **437**, 141-146 (2005).
64. Overwijk, W.W. *et al.* Tumor regression and autoimmunity after reversal of a functionally tolerant state of self-reactive CD8+ T cells. *J. Exp. Med.* **198**, 569-580 (2003).
65. Ochsenbein, A.F. *et al.* Immune surveillance against a solid tumor fails because of immunological ignorance. *Proc. Natl. Acad. Sci. U.S.A.* **96**, 2233-2238 (1999).
66. Otten, G.R. & Germain, R.N. Split anergy in a CD8+ T cell: receptor-dependent cytolysis in the absence of interleukin-2 production. *Science* **251**, 1228-1231 (1991).
67. Cuenca, A. *et al.* Extra-lymphatic solid tumor growth is not immunologically ignored and results in early induction of antigen-specific T-cell anergy: dominant role of cross-tolerance to tumor antigens. *Cancer Res.* **63**, 9007-9015 (2003).
68. Maeda, A. *et al.* The expression of co-stimulatory molecules and their relationship to the prognosis of human acute myeloid leukaemia: poor prognosis of B7-2-positive leukaemia. *Br. J. Haematol.* **102**, 1257-1262 (1998).
69. Hersey, P., Si, Z., Smith, M.J. & Thomas, W.D. Expression of the co-stimulatory molecule B7 on melanoma cells. *Int. J. Cancer* **58**, 527-532 (1994).
70. Koneru, M., Schaer, D., Monu, N., Ayala, A. & Frey, A.B. Defective proximal TCR signaling inhibits CD8+ tumor-infiltrating lymphocyte lytic function. *J. Immunol.* **174**, 1830-1840 (2005).
71. Fallarino, F. *et al.* The combined effects of tryptophan starvation and tryptophan catabolites down-regulate T cell receptor zeta-chain and induce a regulatory phenotype in naive T cells. *J. Immunol* **176**, 6752-6761 (2006).
72. Zea, A.H. *et al.* L-Arginine modulates CD3zeta expression and T cell function in activated human T lymphocytes. *Cell. Immunol.* **232**, 21-31 (2004).
73. Leach, D.R., Krummel, M.F. & Allison, J.P. Enhancement of antitumor immunity by CTLA-4 blockade. *Science* **271**, 1734-1736 (1996).
74. van Elsas, A., Hurwitz, A.A. & Allison, J.P. Combination immunotherapy of B16 melanoma using anti-cytotoxic T lymphocyte-associated antigen 4 (CTLA-4) and granulocyte/macrophage colony-stimulating factor (GM-CSF)-producing vaccines induces rejection of subcutaneous and metastatic tumors accompanied by autoimmune depigmentation. *J. Exp. Med.* **190**, 355-366 (1999).
75. Phan, G.Q. *et al.* Cancer regression and autoimmunity induced by cytotoxic T lymphocyte-associated antigen 4 blockade in patients with metastatic melanoma. *Proc. Natl. Acad. Sci. U.S.A.* **100**, 8372-8377 (2003).

76. Blank, C. & Mackensen, A. Contribution of the PD-L1/PD-1 pathway to T-cell exhaustion: an update on implications for chronic infections and tumor evasion. *Cancer Immunol. Immunother.* **56**, 739-745 (2007).
77. Freeman, G.J. *et al.* Engagement of the PD-1 immunoinhibitory receptor by a novel B7 family member leads to negative regulation of lymphocyte activation. *J. Exp. Med.* **192**, 1027-1034 (2000).
78. Iwai, Y. *et al.* Involvement of PD-L1 on tumor cells in the escape from host immune system and tumor immunotherapy by PD-L1 blockade. *Proc. Natl. Acad. Sci. U.S.A.* **99**, 12293-12297 (2002).
79. Latchman, Y. *et al.* PD-L2 is a second ligand for PD-1 and inhibits T cell activation. *Nature Immunology* **2**, 261-268 (2001).
80. Sica, G.L. *et al.* B7-H4, a molecule of the B7 family, negatively regulates T cell immunity. *Immunity* **18**, 849-861 (2003).
81. Wang, X. *et al.* B7-H4 Treatment of T Cells Inhibits ERK, JNK, p38, and AKT Activation. *PLoS ONE* **7**, e28232 (2012).
82. Krambeck, A.E. *et al.* B7-H4 expression in renal cell carcinoma and tumor vasculature: associations with cancer progression and survival. *Proc. Natl. Acad. Sci. U.S.A.* **103**, 10391-10396 (2006).
83. Kryczek, I. *et al.* B7-H4 expression identifies a novel suppressive macrophage population in human ovarian carcinoma. *J. Exp. Med.* **203**, 871-881 (2006).
84. Kuss, I., Hathaway, B., Ferris, R.L., Gooding, W. & Whiteside, T.L. Decreased absolute counts of T lymphocyte subsets and their relation to disease in squamous cell carcinoma of the head and neck. *Clin. Cancer Res.* **10**, 3755-3762 (2004).
85. Hoffmann, T.K. *et al.* Spontaneous apoptosis of circulating T lymphocytes in patients with head and neck cancer and its clinical importance. *Clin. Cancer Res.* **8**, 2553-2562 (2002).
86. Andreola, G. *et al.* Induction of lymphocyte apoptosis by tumor cell secretion of FasL-bearing microvesicles. *J. Exp. Med.* **195**, 1303-1316 (2002).
87. Wong, R.S.Y. Apoptosis in cancer: from pathogenesis to treatment. *J. Exp. Clin. Cancer Res.* **30**, 87 (2011).
88. Danial, N.N. & Korsmeyer, S.J. Cell death: critical control points. *Cell* **116**, 205-219 (2004).
89. Raffo, A.J. *et al.* Overexpression of bcl-2 protects prostate cancer cells from apoptosis in vitro and confers resistance to androgen depletion in vivo. *Cancer Res.* **55**, 4438-4445 (1995).
90. Fulda, S., Meyer, E. & Debatin, K.-M. Inhibition of TRAIL-induced apoptosis by Bcl-2 overexpression. *Oncogene* **21**, 2283-2294 (2002).
91. Miquel, C. *et al.* Role of bax mutations in apoptosis in colorectal cancers with microsatellite instability. *Am. J. Clin. Pathol.* **123**, 562-570 (2005).
92. Goolsby, C., Paniagua, M., Tallman, M. & Gartenhaus, R.B. Bcl-2 regulatory pathway is functional in chronic lymphocytic leukemia. *Cytometry B Clin Cytom* **63**, 36-46 (2005).
93. Tian, F. *et al.* Expression of c-FLIP in malignant melanoma, and its relationship with the clinicopathological features of the disease. *Clin. Exp. Dermatol.* (2011).doi:10.1111/j.1365-2230.2011.04238.x
94. Wolf, B.B. *et al.* Defective cytochrome c-dependent caspase activation in ovarian cancer cell lines due to diminished or absent apoptotic protease activating factor-1 activity. *J. Biol. Chem.* **276**, 34244-34251 (2001).

95. Keane, M.M., Ettenberg, S.A., Lowrey, G.A., Russell, E.K. & Lipkowitz, S. Fas expression and function in normal and malignant breast cell lines. *Cancer Res.* **56**, 4791-4798 (1996).
96. Wei, Y., Fan, T. & Yu, M. Inhibitor of apoptosis proteins and apoptosis. *Acta Biochim. Biophys. Sin. (Shanghai)* **40**, 278-288 (2008).
97. Lopes, R.B., Gangeswaran, R., McNeish, I.A., Wang, Y. & Lemoine, N.R. Expression of the IAP protein family is dysregulated in pancreatic cancer cells and is important for resistance to chemotherapy. *Int. J. Cancer* **120**, 2344-2352 (2007).
98. Ashhab, Y., Alian, A., Polliack, A., Panet, A. & Ben Yehuda, D. Two splicing variants of a new inhibitor of apoptosis gene with different biological properties and tissue distribution pattern. *FEBS Lett.* **495**, 56-60 (2001).
99. Vucic, D., Stennicke, H.R., Pisabarro, M.T., Salvesen, G.S. & Dixit, V.M. ML-IAP, a novel inhibitor of apoptosis that is preferentially expressed in human melanomas. *Curr. Biol.* **10**, 1359-1366 (2000).
100. Owen-Schaub, L., Chan, H., Cusack, J.C., Roth, J. & Hill, L.L. Fas and Fas ligand interactions in malignant disease. *Int. J. Oncol.* **17**, 5-12 (2000).
101. Gordon, N. *et al.* Fas expression in lung metastasis from osteosarcoma patients. *J. Pediatr. Hematol. Oncol.* **27**, 611-615 (2005).
102. Liu, K., Caldwell, S.A. & Abrams, S.I. Immune selection and emergence of aggressive tumor variants as negative consequences of Fas-mediated cytotoxicity and altered IFN-gamma-regulated gene expression. *Cancer Res.* **65**, 4376-4388 (2005).
103. Liu, K., Caldwell, S.A., Greeneltch, K.M., Yang, D. & Abrams, S.I. CTL adoptive immunotherapy concurrently mediates tumor regression and tumor escape. *J. Immunol.* **176**, 3374-3382 (2006).
104. Kortylewski, M. *et al.* Inhibiting Stat3 signaling in the hematopoietic system elicits multicomponent antitumor immunity. *Nat. Med.* **11**, 1314-1321 (2005).
105. Wang, T. *et al.* Regulation of the innate and adaptive immune responses by Stat-3 signaling in tumor cells. *Nat. Med.* **10**, 48-54 (2004).
106. Thomas, D.A. & Massagué, J. TGF-beta directly targets cytotoxic T cell functions during tumor evasion of immune surveillance. *Cancer Cell* **8**, 369-380 (2005).
107. Li, M.O., Wan, Y.Y., Sanjabi, S., Robertson, A.-K.L. & Flavell, R.A. Transforming growth factor-beta regulation of immune responses. *Annu. Rev. Immunol.* **24**, 99-146 (2006).
108. Harizi, H., Juzan, M., Grosset, C., Rashedi, M. & Gualde, N. Dendritic cells issued in vitro from bone marrow produce PGE(2) that contributes to the immunomodulation induced by antigen-presenting cells. *Cell. Immunol.* **209**, 19-28 (2001).
109. Vakkila, J. & Lotze, M.T. Inflammation and necrosis promote tumour growth. *Nat. Rev. Immunol.* **4**, 641-648 (2004).
110. España, L. *et al.* Overexpression of Bcl-xL in human breast cancer cells enhances organ-selective lymph node metastasis. *Breast Cancer Res. Treat.* **87**, 33-44 (2004).
111. Jung, Y.-J., Kim, J.-Y. & Park, J.-H. TGF-beta1 inhibits Fas-mediated apoptosis by regulating surface Fas and cFLIPL expression in human leukaemia/lymphoma cells. *Int. J. Mol. Med.* **13**, 99-104 (2004).
112. Terabe, M. *et al.* NKT cell-mediated repression of tumor immunosurveillance by IL-13 and the IL-4R-STAT6 pathway. *Nat. Immunol.* **1**, 515-520 (2000).

113. Terabe, M. *et al.* Transforming growth factor-beta production and myeloid cells are an effector mechanism through which CD1d-restricted T cells block cytotoxic T lymphocyte-mediated tumor immunosurveillance: abrogation prevents tumor recurrence. *J. Exp. Med.* **198**, 1741-1752 (2003).
114. Pastuła, A. & Marcinkiewicz, J. Myeloid-derived suppressor cells: a double-edged sword? *Int J Exp Pathol* **92**, 73-78 (2011).
115. Cripps, J.G., Wang, J., Maria, A., Blumenthal, I. & Gorham, J.D. Type 1 T helper cells induce the accumulation of myeloid-derived suppressor cells in the inflamed Tgfb1 knockout mouse liver. *Hepatology* **52**, 1350-1359 (2010).
116. Bronte, V. & Zanovello, P. Regulation of immune responses by L-arginine metabolism. *Nat. Rev. Immunol.* **5**, 641-654 (2005).
117. Youn, J.-I., Nagaraj, S., Collazo, M. & Gabrilovich, D.I. Subsets of myeloid-derived suppressor cells in tumor-bearing mice. *J. Immunol.* **181**, 5791-5802 (2008).
118. Gabrilovich, D.I. & Nagaraj, S. Myeloid-derived suppressor cells as regulators of the immune system. *Nat. Rev. Immunol.* **9**, 162-174 (2009).
119. Bunt, S.K. *et al.* Reduced inflammation in the tumor microenvironment delays the accumulation of myeloid-derived suppressor cells and limits tumor progression. *Cancer Res.* **67**, 10019-10026 (2007).
120. Pan, P.-Y. *et al.* Reversion of immune tolerance in advanced malignancy: modulation of myeloid-derived suppressor cell development by blockade of stem-cell factor function. *Blood* **111**, 219-228 (2008).
121. Rodriguez, P.C., Quiceno, D.G. & Ochoa, A.C. L-arginine availability regulates T-lymphocyte cell-cycle progression. *Blood* **109**, 1568-1573 (2007).
122. Rodriguez, P.C. *et al.* Arginase I production in the tumor microenvironment by mature myeloid cells inhibits T-cell receptor expression and antigen-specific T-cell responses. *Cancer Res* **64**, 5839-5849 (2004).
123. Bingisser, R.M., Tilbrook, P.A., Holt, P.G. & Kees, U.R. Macrophage-derived nitric oxide regulates T cell activation via reversible disruption of the Jak3/STAT5 signaling pathway. *J. Immunol.* **160**, 5729-5734 (1998).
124. Harari, O. & Liao, J.K. Inhibition of MHC II gene transcription by nitric oxide and antioxidants. *Curr. Pharm. Des.* **10**, 893-898 (2004).
125. Kusmartsev, S., Nefedova, Y., Yoder, D. & Gabrilovich, D.I. Antigen-specific inhibition of CD8+ T cell response by immature myeloid cells in cancer is mediated by reactive oxygen species. *J. Immunol* **172**, 989-999 (2004).
126. Nagaraj, S. *et al.* Altered recognition of antigen is a mechanism of CD8+ T cell tolerance in cancer. *Nat. Med.* **13**, 828-835 (2007).
127. Srivastava, M.K., Sinha, P., Clements, V.K., Rodriguez, P. & Ostrand-Rosenberg, S. Myeloid-derived suppressor cells inhibit T-cell activation by depleting cystine and cysteine. *Cancer Res* **70**, 68-77 (2010).
128. Movahedi, K. *et al.* Identification of discrete tumor-induced myeloid-derived suppressor cell subpopulations with distinct T cell-suppressive activity. *Blood* **111**, 4233-4244 (2008).

129. Huang, B. *et al.* Gr-1+CD115+ immature myeloid suppressor cells mediate the development of tumor-induced T regulatory cells and T-cell anergy in tumor-bearing host. *Cancer Res.* **66**, 1123-1131 (2006).
130. Brady, F.O. Inhibition of rabbit intestinal indoleamine 2,3-dioxygenase by copper chelators. *FEBS Lett.* **57**, 237-240 (1975).
131. Brady, F.O. Tryptophan 2,3-dioxygenase: a review of the roles of the heme and copper cofactors in catalysis. *Bioinorg Chem* **5**, 167-182 (1975).
132. Ozaki, Y., Edelstein, M.P. & Duch, D.S. The actions of interferon and antiinflammatory agents of induction of indoleamine 2,3-dioxygenase in human peripheral blood monocytes. *Biochem. Biophys. Res. Commun.* **144**, 1147-1153 (1987).
133. Yoshida, R., Imanishi, J., Oku, T., Kishida, T. & Hayaishi, O. Induction of pulmonary indoleamine 2,3-dioxygenase by interferon. *Proc. Natl. Acad. Sci. U.S.A.* **78**, 129-132 (1981).
134. Mellor, A.L. & Munn, D.H. IDO expression by dendritic cells: tolerance and tryptophan catabolism. *Nat. Rev. Immunol.* **4**, 762-774 (2004).
135. Hirata, F., Nomiyama, S. & Hayaishi, O. Indoleamine 2,3-dioxygenase. Note I. Catalytic and molecular properties. *Acta Vitaminol. Enzymol.* **29**, 288-290 (1975).
136. Habara-Ohkubo, A., Takikawa, O. & Yoshida, R. Cloning and expression of a cDNA encoding mouse indoleamine 2,3-dioxygenase. *Gene* **105**, 221-227 (1991).
137. Dai, W. & Gupta, S.L. Molecular cloning, sequencing and expression of human interferon-gamma-inducible indoleamine 2,3-dioxygenase cDNA. *Biochem. Biophys. Res. Commun.* **168**, 1-8 (1990).
138. Chauhan, N. *et al.* Reassessment of the reaction mechanism in the heme dioxygenases. *J. Am. Chem. Soc* **131**, 4186-4187 (2009).
139. Sugimoto, H. *et al.* Crystal structure of human indoleamine 2,3-dioxygenase: catalytic mechanism of O2 incorporation by a heme-containing dioxygenase. *Proc. Natl. Acad. Sci. U.S.A* **103**, 2611-2616 (2006).
140. Röhrig, U.F. *et al.* Rational design of indoleamine 2,3-dioxygenase inhibitors. *J. Med. Chem.* **53**, 1172-1189 (2010).
141. Macchiarulo, A., Nuti, R., Bellocchi, D., Camaioni, E. & Pellicciari, R. Molecular docking and spatial coarse graining simulations as tools to investigate substrate recognition, enhancer binding and conformational transitions in indoleamine-2,3-dioxygenase (IDO). *Biochim. Biophys. Acta* **1774**, 1058-1068 (2007).
142. Vottero, E. *et al.* Cytochrome b(5) is a major reductant in vivo of human indoleamine 2,3-dioxygenase expressed in yeast. *FEBS Lett.* **580**, 2265-2268 (2006).
143. Carlin, J.M., Ozaki, Y., Byrne, G.I., Brown, R.R. & Borden, E.C. Interferons and indoleamine 2,3-dioxygenase: role in antimicrobial and antitumor effects. *Experientia* **45**, 535-541 (1989).
144. Bonney, E.A. & Matzinger, P. Much IDO about pregnancy. *Nat. Med.* **4**, 1128-1129 (1998).
145. Munn, D.H. *et al.* Prevention of allogeneic fetal rejection by tryptophan catabolism. *Science* **281**, 1191-1193 (1998).
146. Alexander, A.M. *et al.* Indoleamine 2,3-dioxygenase expression in transplanted NOD Islets prolongs graft survival after adoptive transfer of diabetogenic splenocytes. *Diabetes* **51**, 356-365 (2002).

147. Gorczynski, R.M., Hadidi, S., Yu, G. & Clark, D.A. The same immunoregulatory molecules contribute to successful pregnancy and transplantation. *Am. J. Reprod. Immunol.* **48**, 18-26 (2002).
148. Kwidzinski, E. *et al.* Indolamine 2,3-dioxygenase is expressed in the CNS and down-regulates autoimmune inflammation. *FASEB J.* **19**, 1347-1349 (2005).
149. Sakurai, K., Zou, J.-P., Tschetter, J.R., Ward, J.M. & Shearer, G.M. Effect of indoleamine 2,3-dioxygenase on induction of experimental autoimmune encephalomyelitis. *J. Neuroimmunol.* **129**, 186-196 (2002).
150. Potula, R. *et al.* Inhibition of indoleamine 2,3-dioxygenase (IDO) enhances elimination of virus-infected macrophages in an animal model of HIV-1 encephalitis. *Blood* **106**, 2382-2390 (2005).
151. Yoshida, R., Park, S.W., Yasui, H. & Takikawa, O. Tryptophan degradation in transplanted tumor cells undergoing rejection. *J. Immunol.* **141**, 2819-2823 (1988).
152. Uyttenhove, C. *et al.* Evidence for a tumoral immune resistance mechanism based on tryptophan degradation by indoleamine 2,3-dioxygenase. *Nat. Med* **9**, 1269-1274 (2003).
153. Munn, D.H. Indoleamine 2,3-dioxygenase, Tregs and cancer. *Curr. Med. Chem.* **18**, 2240-2246 (2011).
154. Zádori, D., Klivényi, P., Toldi, J., Fülöp, F. & Vécsei, L. Kynurenines in Parkinson's disease: therapeutic perspectives. *Journal of Neural Transmission (Vienna, Austria: 1996)* (2011).doi:10.1007/s00702-011-0697-3
155. Guidetti, P. *et al.* Elevated brain 3-hydroxykynurenine and quinolinate levels in Huntington disease mice. *Neurobiol. Dis.* **23**, 190-197 (2006).
156. Myint, A.M. *et al.* Reversal of imbalance between kynurenic acid and 3-hydroxykynurenine by antipsychotics in medication-naïve and medication-free schizophrenic patients. *Brain, Behavior, and Immunity* (2011).doi:10.1016/j.bbi.2011.05.005
157. Forrest, C.M. *et al.* Purine, kynurenine, neopterin and lipid peroxidation levels in inflammatory bowel disease. *J. Biomed. Sci.* **9**, 436-442 (2002).
158. Topczewska-Bruns, J., Pawlak, D., Tankiewicz, A., Chabielska, E. & Buczko, W. Kynurenine metabolism in central nervous system in experimental chronic renal failure. *Adv. Exp. Med. Biol.* **527**, 177-182 (2003).
159. Morita, T. *et al.* 3-Hydroxyanthranilic acid, an L-tryptophan metabolite, induces apoptosis in monocyte-derived cells stimulated by interferon-gamma. *Ann. Clin. Biochem* **38**, 242-251 (2001).
160. Zaher, S.S., Germain, C., Fu, H., Larkin, D.F.P. & George, A.J.T. 3-hydroxykynurenine suppresses CD4+ T-cell proliferation, induces T-regulatory-cell development, and prolongs corneal allograft survival. *Invest. Ophthalmol. Vis. Sci* **52**, 2640-2648 (2011).
161. Laplante, M. & Sabatini, D.M. mTOR signaling at a glance. *Journal of Cell Science* **122**, 3589 - 3594 (2009).
162. Peterson, T.R. *et al.* DEPTOR is an mTOR inhibitor frequently overexpressed in multiple myeloma cells and required for their survival. *Cell* **137**, 873-886 (2009).
163. Wang, L., Harris, T.E., Roth, R.A. & Lawrence, J.C. PRAS40 Regulates mTORC1 Kinase Activity by Functioning as a Direct Inhibitor of Substrate Binding. *Journal of Biological Chemistry* **282**, 20036 -20044 (2007).

164. Sarbassov, D.D. *et al.* Prolonged rapamycin treatment inhibits mTORC2 assembly and Akt/PKB. *Mol. Cell* **22**, 159-168 (2006).
165. Jacinto, E. *et al.* Mammalian TOR complex 2 controls the actin cytoskeleton and is rapamycin insensitive. *Nat. Cell Biol.* **6**, 1122-1128 (2004).
166. Hosokawa, N. *et al.* Nutrient-dependent mTORC1 Association with the ULK1–Atg13–FIP200 Complex Required for Autophagy. *Molecular Biology of the Cell* **20**, 1981 -1991 (2009).
167. DeYoung, M.P., Horak, P., Sofer, A., Sgroi, D. & Ellisen, L.W. Hypoxia regulates TSC1/2–mTOR signaling and tumor suppression through REDD1-mediated 14–3–3 shuttling. *Genes & Development* **22**, 239 -251 (2008).
168. Hara, K. *et al.* Amino acid sufficiency and mTOR regulate p70 S6 kinase and eIF-4E BP1 through a common effector mechanism. *J. Biol. Chem.* **273**, 14484-14494 (1998).
169. Sancak, Y. *et al.* The Rag GTPases Bind Raptor and Mediate Amino Acid Signaling to mTORC1. *Science* **320**, 1496 -1501 (2008).
170. Zhang, Y.-J. *et al.* mTOR signaling pathway is a target for the treatment of colorectal cancer. *Ann. Surg. Oncol.* **16**, 2617-2628 (2009).
171. Chapuis, N. *et al.* Perspectives on inhibiting mTOR as a future treatment strategy for hematological malignancies. *Leukemia* **24**, 1686-1699 (2010).
172. Zhang, Y.-J., Duan, Y. & Zheng, X.F.S. Targeting the mTOR kinase domain: the second generation of mTOR inhibitors. *Drug Discov. Today* **16**, 325-331 (2011).
173. Tsang, C.K., Qi, H., Liu, L.F. & Zheng, X.F.S. Targeting mammalian target of rapamycin (mTOR) for health and diseases. *Drug Discov. Today* **12**, 112-124 (2007).
174. Guertin, D.A. & Sabatini, D.M. Defining the role of mTOR in cancer. *Cancer Cell* **12**, 9-22 (2007).
175. Zeng, Z. *et al.* Rapamycin derivatives reduce mTORC2 signaling and inhibit AKT activation in AML. *Blood* **109**, 3509-3512 (2007).
176. Rao, R.R., Li, Q., Odunsi, K. & Shrikant, P.A. The mTOR kinase determines effector versus memory CD8+ T cell fate by regulating the expression of transcription factors T-bet and Eomesodermin. *Immunity* **32**, 67-78 (2010).
177. Cobbold, S.P. *et al.* Infectious tolerance via the consumption of essential amino acids and mTOR signaling. *Proc. Natl. Acad. Sci. U.S.A* **106**, 12055-12060 (2009).
178. Hey, S.J., Byrne, E. & Halford, N.G. The interface between metabolic and stress signalling. *Ann. Bot.* **105**, 197-203 (2010).
179. Hinnebusch, A.G. Translational regulation of GCN4 and the general amino acid control of yeast. *Annu. Rev. Microbiol.* **59**, 407-450 (2005).
180. Ye, J. *et al.* The GCN2-ATF4 pathway is critical for tumour cell survival and proliferation in response to nutrient deprivation. *EMBO J* **29**, 2082-2096 (2010).
181. Lageix, S. *et al.* Arabidopsis eIF2alpha kinase GCN2 is essential for growth in stress conditions and is activated by wounding. *BMC Plant Biol.* **8**, 134 (2008).
182. Kudo, Y. & Boyd, C.A. Characterisation of L-tryptophan transporters in human placenta: a comparison of brush border and basal membrane vesicles. *J. Physiol. (Lond.)* **531**, 405-416 (2001).

183. Fukasawa, Y. *et al.* Identification and characterization of a Na(+)-independent neutral amino acid transporter that associates with the 4F2 heavy chain and exhibits substrate selectivity for small neutral D- and L-amino acids. *J. Biol. Chem.* **275**, 9690-9698 (2000).
184. Devés, R. & Boyd, C.A. Transporters for cationic amino acids in animal cells: discovery, structure, and function. *Physiol. Rev.* **78**, 487-545 (1998).
185. Hediger, M.A., Kanai, Y., Lee, W.S. & Wells, R.G. Identification of a new family of proteins involved in amino acid transport. *Soc. Gen. Physiol. Ser.* **48**, 301-314 (1993).
186. Silk, J.D. *et al.* IDO Induces Expression of a Novel Tryptophan Transporter in Mouse and Human Tumor Cells. *The Journal of Immunology* **187**, 1617 -1625 (2011).
187. Okamoto, A. *et al.* Indoleamine 2,3-dioxygenase serves as a marker of poor prognosis in gene expression profiles of serous ovarian cancer cells. *Clin. Cancer Res* **11**, 6030-6039 (2005).
188. Brandacher, G. *et al.* Prognostic value of indoleamine 2,3-dioxygenase expression in colorectal cancer: effect on tumor-infiltrating T cells. *Clin. Cancer Res* **12**, 1144-1151 (2006).
189. Ino, K. *et al.* Indoleamine 2,3-dioxygenase is a novel prognostic indicator for endometrial cancer. *Br. J. Cancer* **95**, 1555-1561 (2006).
190. Pan, K. *et al.* Expression and prognosis role of indoleamine 2,3-dioxygenase in hepatocellular carcinoma. *J. Cancer Res. Clin. Oncol* **134**, 1247-1253 (2008).
191. Hou, D.-Y. *et al.* Inhibition of indoleamine 2,3-dioxygenase in dendritic cells by stereoisomers of 1-methyl-tryptophan correlates with antitumor responses. *Cancer Res* **67**, 792-801 (2007).
192. Muller, A.J., DuHadaway, J.B., Donover, P.S., Sutanto-Ward, E. & Prendergast, G.C. Inhibition of indoleamine 2,3-dioxygenase, an immunoregulatory target of the cancer suppression gene Bin1, potentiates cancer chemotherapy. *Nat. Med* **11**, 312-319 (2005).
193. Muller, A.J. & Prendergast, G.C. Marrying immunotherapy with chemotherapy: why say IDO? *Cancer Res* **65**, 8065-8068 (2005).
194. Eguchi, N., Watanabe, Y., Kawanishi, K., Hashimoto, Y. & Hayaishi, O. Inhibition of indoleamine 2,3-dioxygenase and tryptophan 2,3-dioxygenase by beta-carboline and indole derivatives. *Arch. Biochem. Biophys* **232**, 602-609 (1984).
195. Cady, S.G. & Sono, M. 1-Methyl-DL-tryptophan, beta-(3-benzofuranyl)-DL-alanine (the oxygen analog of tryptophan), and beta-[3-benzo(b)thienyl]-DL-alanine (the sulfur analog of tryptophan) are competitive inhibitors for indoleamine 2,3-dioxygenase. *Arch. Biochem. Biophys* **291**, 326-333 (1991).
196. Lob, S. *et al.* Levo- but not dextro-1-methyl tryptophan abrogates the IDO activity of human dendritic cells. *Blood* **111**, 2152 -2154 (2008).
197. Munn, D.H. *et al.* Expression of indoleamine 2,3-dioxygenase by plasmacytoid dendritic cells in tumor-draining lymph nodes. *J. Clin. Invest* **114**, 280-290 (2004).
198. Peterson, A. C., Migawa, M. T. et al*Medicinal Chemistry Research* **4**, 531-544 (1994).
199. Kudo, Y. & Boyd, C.A. The role of L-tryptophan transport in L-tryptophan degradation by indoleamine 2,3-dioxygenase in human placental explants. *J. Physiol. (Lond.)* **531**, 417-423 (2001).
200. Yang, H.-J. *et al.* A combination of the metabolic enzyme inhibitor APO866 and the immune adjuvant L-1-methyl tryptophan induces additive antitumor activity. *Exp. Biol. Med. (Maywood)* **235**, 869-876 (2010).

201. Yi, Y.-M. *et al.* A new tumor vaccine: FAPτ-MT elicits effective antitumor response by targeting indolamine2,3-dioxygenase in antigen presenting cells. *cbt* **11**, 866-873 (2011).
202. Opitz, C.A. *et al.* The indoleamine-2,3-dioxygenase (IDO) inhibitor 1-methyl-D-tryptophan upregulates IDO1 in human cancer cells. *PLoS ONE* **6**, e19823 (2011).
203. Brastianos, H.C. *et al.* Exiguamine A, an indoleamine-2,3-dioxygenase (IDO) inhibitor isolated from the marine sponge Neopetrosia exigua. *J. Am. Chem. Soc* **128**, 16046-16047 (2006).
204. Pereira, A., Vottero, E., Roberge, M., Mauk, A.G. & Andersen, R.J. Indoleamine 2,3-dioxygenase inhibitors from the Northeastern Pacific Marine Hydroid Garveia annulata. *J. Nat. Prod* **69**, 1496-1499 (2006).
205. Carr, G., Chung, M.K.W., Mauk, A.G. & Andersen, R.J. Synthesis of indoleamine 2,3-dioxygenase inhibitory analogues of the sponge alkaloid exiguamine A. *J. Med. Chem* **51**, 2634-2637 (2008).
206. Kumar, S. *et al.* Indoleamine 2,3-dioxygenase is the anticancer target for a novel series of potent naphthoquinone-based inhibitors. *J. Med. Chem* **51**, 1706-1718 (2008).
207. Yue, E.W. *et al.* Discovery of potent competitive inhibitors of indoleamine 2,3-dioxygenase with in vivo pharmacodynamic activity and efficacy in a mouse melanoma model. *J. Med. Chem* **52**, 7364-7367 (2009).
208. Koblish, H.K. *et al.* Hydroxyamidine inhibitors of indoleamine-2,3-dioxygenase potently suppress systemic tryptophan catabolism and the growth of IDO-expressing tumors. *Mol. Cancer Ther* **9**, 489-498 (2010).
209. Stone, T.W. & Darlington, L.G. Endogenous kynurenines as targets for drug discovery and development. *Nat Rev Drug Discov* **1**, 609-620 (2002).
210. Jones, G., Willett, P., Glen, R.C., Leach, A.R. & Taylor, R. Development and validation of a genetic algorithm for flexible docking. *J. Mol. Biol* **267**, 727-748 (1997).
211. Schüttelkopf, A.W. & van Aalten, D.M.F. PRODRG: a tool for high-throughput crystallography of protein-ligand complexes. *Acta Crystallogr. D Biol. Crystallogr* **60**, 1355-1363 (2004).
212. Poljak, A. *et al.* Inhibition of indoleamine 2,3 dioxygenase activity by H2O2. *Arch. Biochem. Biophys* **450**, 9-19 (2006).
213. Dykens, J.A., Sullivan, S.G. & Stern, A. Oxidative reactivity of the tryptophan metabolites 3-hydroxyanthranilate, cinnabarinate, quinolinate and picolinate. *Biochem. Pharmacol* **36**, 211-217 (1987).
214. Buettner, G.R., Doherty, T.P. & Bannister, T.D. Hydrogen peroxide and hydroxyl radical formation by methylene blue in the presence of ascorbic acid. *Radiat Environ Biophys* **23**, 235-243 (1984).
215. Fallarino, F. *et al.* T cell apoptosis by tryptophan catabolism. *Cell Death Differ* **9**, 1069-1077 (2002).
216. Weber, W.P. *et al.* Differential effects of the tryptophan metabolite 3-hydroxyanthranilic acid on the proliferation of human CD8+ T cells induced by TCR triggering or homeostatic cytokines. *Eur. J. Immunol* **36**, 296-304 (2006).
217. López, A.S. *et al.* Effect of 3-hydroxyanthranilic acid in the immunosuppressive molecules indoleamine dioxygenase and HLA-G in macrophages. *Immunol. Lett* **117**, 91-95 (2008).
218. Attwood, J.T. & Munn, D.H. Macrophage suppression of T cell activation: a potential mechanism of peripheral tolerance. *Int. Rev. Immunol* **18**, 515-525 (1999).

219. Munn, D.H. *et al.* Inhibition of T cell proliferation by macrophage tryptophan catabolism. *J. Exp. Med* **189**, 1363-1372 (1999).
220. Frumento, G. *et al.* Tryptophan-derived catabolites are responsible for inhibition of T and natural killer cell proliferation induced by indoleamine 2,3-dioxygenase. *J. Exp. Med* **196**, 459-468 (2002).
221. Dai, X. & Zhu, B.T. Suppression of T-cell response and prolongation of allograft survival in a rat model by tryptophan catabolites. *Eur. J. Pharmacol.* **606**, 225-232 (2009).
222. Lee, S.-M. *et al.* Tryptophan metabolite 3-hydroxyanthranilic acid selectively induces activated T cell death via intracellular GSH depletion. *Immunol. Lett* **132**, 53-60 (2010).
223. Heyes, M.P., Chen, C.Y., Major, E.O. & Saito, K. Different kynurenine pathway enzymes limit quinolinic acid formation by various human cell types. *Biochem. J* **326 (Pt 2)**, 351-356 (1997).
224. Moretti, L., Cha, Y.I., Niermann, K.J. & Lu, B. Switch Between Apoptosis and Autophagy: Radiation-Induced Endoplasmic Reticulum Stress? *Cell Cycle* **6**, 793-798 (2007).
225. Kim, J.H., Park, S.M., Park, J.H., Keum, S.J. & Jang, S.K. eIF2A mediates translation of hepatitis C viral mRNA under stress conditions. *EMBO J.* **30**, 2454-2464 (2011).
226. Chen, J.-J. Regulation of protein synthesis by the heme-regulated eIF2alpha kinase: relevance to anemias. *Blood* **109**, 2693-2699 (2007).
227. Yan, Y. *et al.* IDO upregulates regulatory T cells via tryptophan catabolite and suppresses encephalitogenic T cell responses in experimental autoimmune encephalomyelitis. *J. Immunol* **185**, 5953-5961 (2010).
228. Hiramatsu, R. *et al.* Cinnabarinic acid generated from 3-hydroxyanthranilic acid strongly induces apoptosis in thymocytes through the generation of reactive oxygen species and the induction of caspase. *J. Cell. Biochem* **103**, 42-53 (2008).
229. Brennan, R.J. & Schiestl, R.H. Aniline and its metabolites generate free radicals in yeast. *Mutagenesis* **12**, 215-220 (1997).
230. Miyazaki, T. *et al.* Indoleamine 2,3-dioxygenase as a new target for malignant glioma therapy. Laboratory investigation. *J. Neurosurg* **111**, 230-237 (2009).
231. Bonda, D.J. *et al.* Indoleamine 2,3-dioxygenase and 3-hydroxykynurenine modifications are found in the neuropathology of Alzheimer's disease. *Redox Rep.* **15**, 161-168 (2010).
232. Nagaraj, S. *et al.* Regulatory Myeloid Suppressor Cells in Health and Disease. *Cancer Research* **69**, 7503 -7506 (2009).
233. Bronte, V., Serafini, P., Mazzoni, A., Segal, D.M. & Zanovello, P. L-arginine metabolism in myeloid cells controls T-lymphocyte functions. *Trends Immunol* **24**, 302-306 (2003).
234. Gmünder, H., Eck, H.P. & Dröge, W. Low membrane transport activity for cystine in resting and mitogenically stimulated human lymphocyte preparations and human T cell clones. *Eur. J. Biochem* **201**, 113-117 (1991).
235. Zoglmeier, C. *et al.* CpG blocks immunosuppression by myeloid-derived suppressor cells in tumor-bearing mice. *Clin. Cancer Res* **17**, 1765-1775 (2011).
236. Meyer, C. *et al.* Chronic inflammation promotes myeloid-derived suppressor cell activation blocking antitumor immunity in transgenic mouse melanoma model. *Proceedings of the National Academy of Sciences of the United States of America* (2011).doi:10.1073/pnas.1108121108

237. Haverkamp, J.M., Crist, S.A., Elzey, B.D., Cimen, C. & Ratliff, T.L. In vivo suppressive function of myeloid-derived suppressor cells is limited to the inflammatory site. *Eur. J. Immunol* **41**, 749-759 (2011).
238. Wilke, C.M. *et al.* Dual biological effects of the cytokines interleukin-10 and interferon-γ. *Cancer Immunology, Immunotherapy: CII* (2011).doi:10.1007/s00262-011-1104-5
239. Almand, B. *et al.* Increased production of immature myeloid cells in cancer patients: a mechanism of immunosuppression in cancer. *J. Immunol* **166**, 678-689 (2001).
240. Wu, G. & Morris, S.M., Jr Arginine metabolism: nitric oxide and beyond. *Biochem. J* **336 (Pt 1)**, 1-17 (1998).
241. Mazzoni, A. *et al.* Myeloid suppressor lines inhibit T cell responses by an NO-dependent mechanism. *J. Immunol.* **168**, 689-695 (2002).
242. Kropf, P. *et al.* Arginase activity mediates reversible T cell hyporesponsiveness in human pregnancy. *Eur. J. Immunol.* **37**, 935-945 (2007).
243. Rodriguez, P.C. *et al.* Regulation of T cell receptor CD3zeta chain expression by L-arginine. *J. Biol. Chem.* **277**, 21123-21129 (2002).
244. Rivoltini, L. *et al.* Immunity to cancer: attack and escape in T lymphocyte-tumor cell interaction. *Immunol. Rev.* **188**, 97-113 (2002).
245. De Santo, C. *et al.* Invariant NKT cells reduce the immunosuppressive activity of influenza A virus-induced myeloid-derived suppressor cells in mice and humans. *J. Clin. Invest* **118**, 4036-4048 (2008).
246. Gallina, G. *et al.* Tumors induce a subset of inflammatory monocytes with immunosuppressive activity on CD8+ T cells. *J. Clin. Invest* **116**, 2777-2790 (2006).
247. Kusmartsev, S.A., Li, Y. & Chen, S.H. Gr-1+ myeloid cells derived from tumor-bearing mice inhibit primary T cell activation induced through CD3/CD28 costimulation. *J. Immunol* **165**, 779-785 (2000).
248. Lerzynski, G., Suschek, C.V. & Kolb-Bachofen, V. In hepatocytes the regulation of NOS-2 activity at physiological L-arginine levels suggests a close link to the urea cycle. *Nitric Oxide* **14**, 300-308 (2006).
249. Wells, R.G., Lee, W.S., Kanai, Y., Leiden, J.M. & Hediger, M.A. The 4F2 antigen heavy chain induces uptake of neutral and dibasic amino acids in Xenopus oocytes. *J. Biol. Chem* **267**, 15285-15288 (1992).
250. Peter, G.J. *et al.* Multiple components of arginine and phenylalanine transport induced in neutral and basic amino acid transporter-cRNA-injected Xenopus oocytes. *Biochem. J* **318 (Pt 3)**, 915-922 (1996).
251. Yu, L. *et al.* Termination of autophagy and reformation of lysosomes regulated by mTOR. *Nature* **465**, 942-946 (2010).
252. Rong, Y. *et al.* Spinster is required for autophagic lysosome reformation and mTOR reactivation following starvation. *Proc. Natl. Acad. Sci. U.S.A* **108**, 7826-7831 (2011).